UNITED STATES DEPARTMENT OF THE INTERIOR

GEOLOGICAL SURVEY

OFFICE OF EARTHQUAKE STUDIES

NUCLEAR EVENT TIME HISTORIES AND COMPUTED SITE TRANSFER FUNCTIONS FOR LOCATIONS IN THE LOS ANGELES REGION

Open-File Report 80-1173

U.S. Geological Survey
Denver Federal Center
Denver, CO 80225

Any use of trade names and trademarks in this publication is for descriptive purposes only and does not constitute endorsement by the U.S. Geological Survey.

This report is preliminary and has not been edited or reviewed for conformity with Geological Survey standards and nomenclature.

1980

This page intentionally left blank

NUCLEAR EVENT TIME HISTORIES AND COMPUTED SITE TRANSFER FUNCTIONS FOR LOCATIONS IN THE LOS ANGELES REGION

By A. M. Rogers, P. A. Covington,
R. B. Park, R. D. Borcherdt, and D. M. Perkins

Open-File Report 80-1173

This report is preliminary and has not been edited or reviewed for conformity with U.S. Geological Survey standards and nomenclature.

Table of Contents

Page

Introduction

Data Collection and Processing..... 1

Spectral Analysis of the Signal..... 16

Spectral Analysis of the Noise..... 18

Computation of the Site Transfer Function..... 21

Acknowledgments..... 29

References Cited..... 30

Appendix A: Examination of tranfer function statistics..... 31

Appendix B: Nuclear-event time histories ordered alphabetically by nuclear event..... 38

Appendix C: Site transfer functions ordered alphabetically by nuclear event.....132

Illustrations

Figure 1.--Map of station locations in the greater Los Angeles region. Insert is shown in Figure 2..... 2

Figure 2.--Map of station locations in downtown Los Angeles..... 3

Figure 3.--Map of station locations in the San Bernadino and Santa Ana regions..... 4

Figure 4.--Map of station locations in the Oxnard-Ventura region..... 5

Figure 5.--Map of station locations in the Lake Hughes region..... 6

Figures 6-10.--Graphs of $\hat{X}$ and ${}_j\sigma_k^i$ 23

Figure A1.--The distribution of the synthetic STF-LR..... 35

Figure A2.--The distribution of observed values, ${}_jY_k^{GMB}$ 36

Figure A3.--Normal probability plot of ${}_jY_k^{GMB}$ 36

Tables

Page

Table 1.--Table of station names, station coordinates, and nuclear events recorded at each station..... 7

Table 2.--Table of station addresses..... 11

Table 3.--Table of nuclear event names, detonation times, coordinates, and magnitudes..... 15

Table 4.--A list of pooled standard deviations, $\bar{\sigma}$ computed for those station-components recorded for 3 or more nuclear events.... 28

INTRODUCTION

This report presents a collection of Nevada Test Site (NTS) nuclear explosion recordings obtained at sites in the greater Los Angeles, Calif., region. The report includes ground velocity time histories, as well as, derived site transfer functions. These data have been collected as part of a study to evaluate the validity of using low-level ground motions to predict the frequency-dependent response of a site during an earthquake.

For this study 19 nuclear events were recorded at 98 separate locations. Some of these sites have recorded more than one of the nuclear explosions, and, consequently, there are a total of 159, three-component station records. The location of all the recording sites are shown in figures 1-5, the station coordinates and abbreviations are given in table 1. The station addresses are listed in table 2, and the nuclear explosions that were recorded are listed in table 3. The recording sites were chosen on the basis of three criteria: (1) that the underlying geological conditions were representative of conditions over significant areas of the region, (2) that the site was the location of a strong-motion recording of the 1971 San Fernando earthquake, or (3) that more complete geographical coverage was required in that location.

DATA COLLECTION AND PROCESSING

The data in this report were recorded using L-7 seismograph systems which are owned by the Nevada Operations Office of the U.S. Department of Energy. The L-7 is a wide-band three-component seismograph that records on magnetic-tape with a flat velocity response for ground motion periods in the range 0.03 seconds to 10 seconds. Station tapes were dubbed to produce one or more event tapes containing the records for all stations for a given nuclear event. In

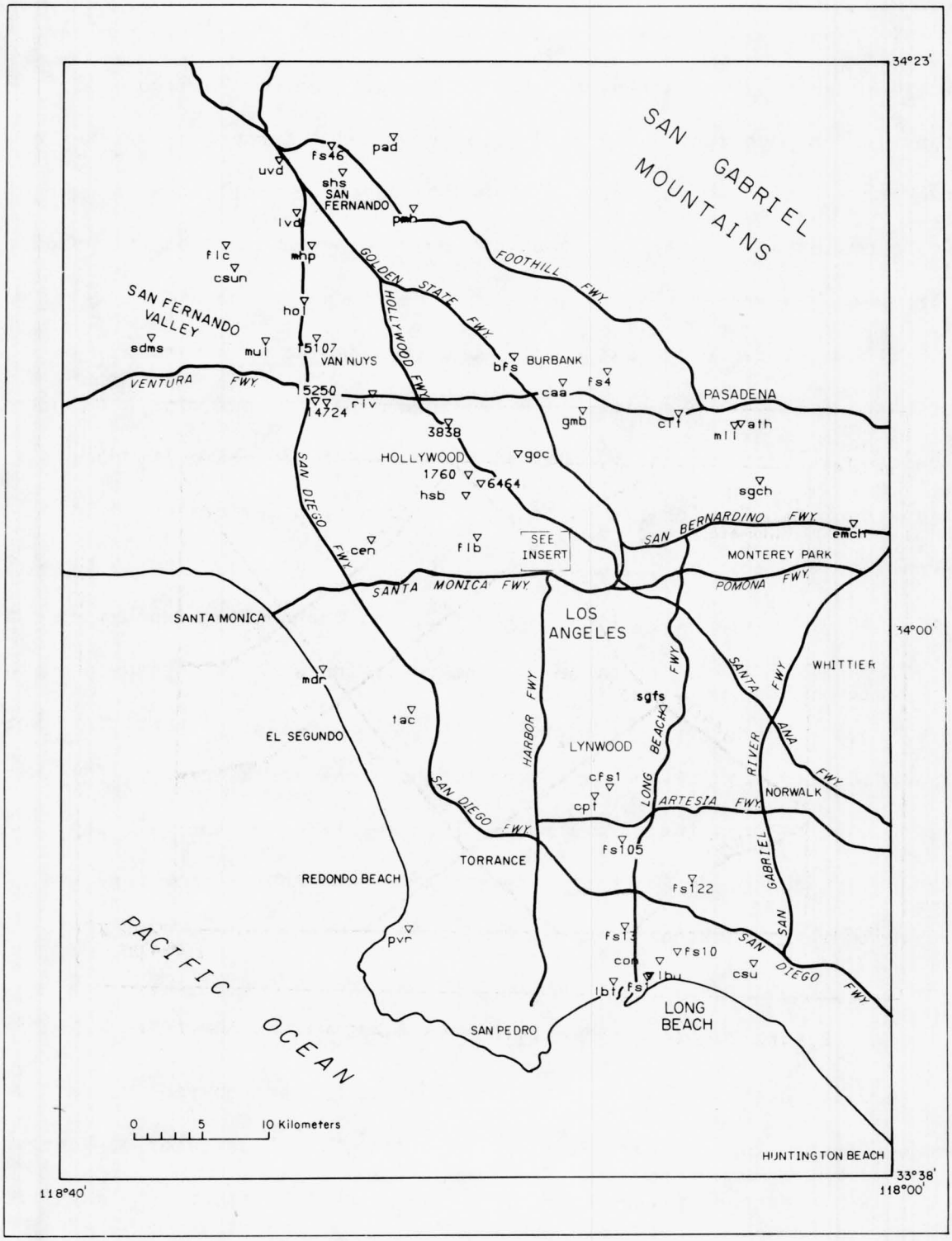

Figure 1.--Station locations in the greater Los Angeles region. Insert is shown in Figure 2.

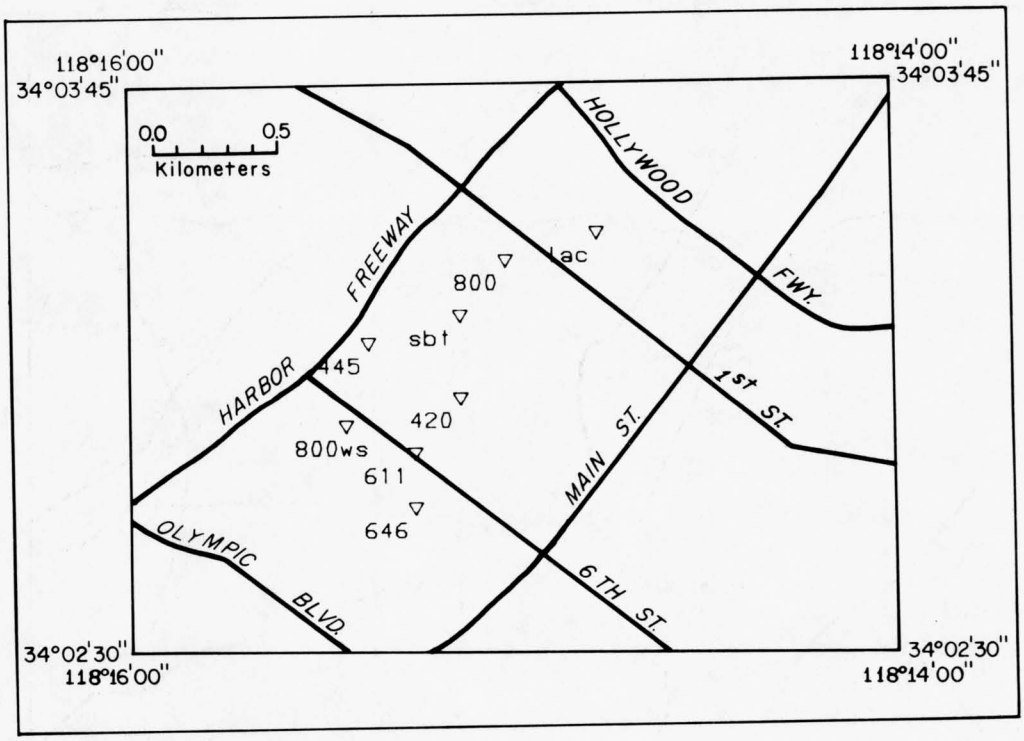

Figure 2.--Station locations in downtown Los Angeles.

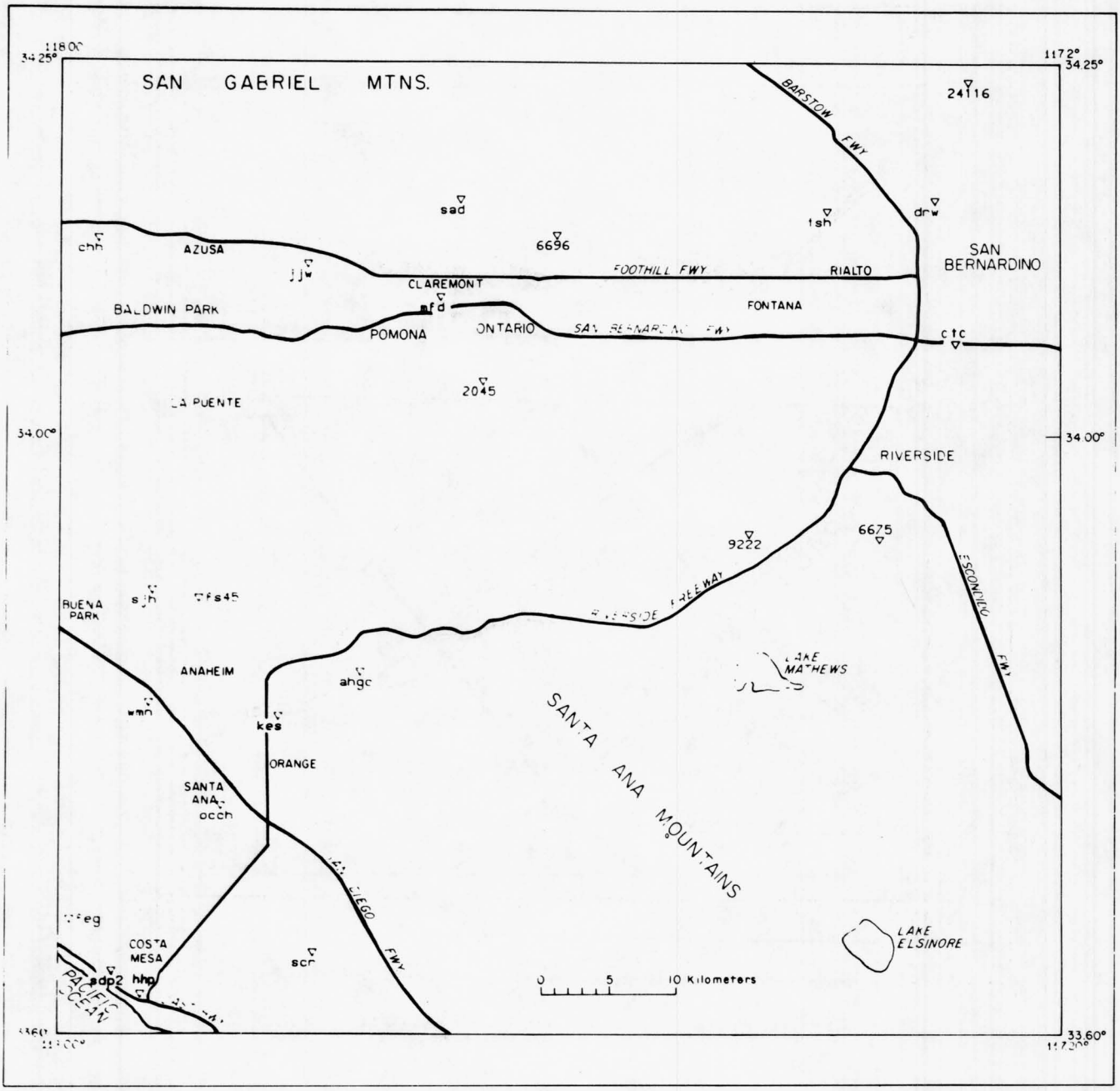

Figure 3.--Station locations in the San Bernadino and Santa Ana regions.

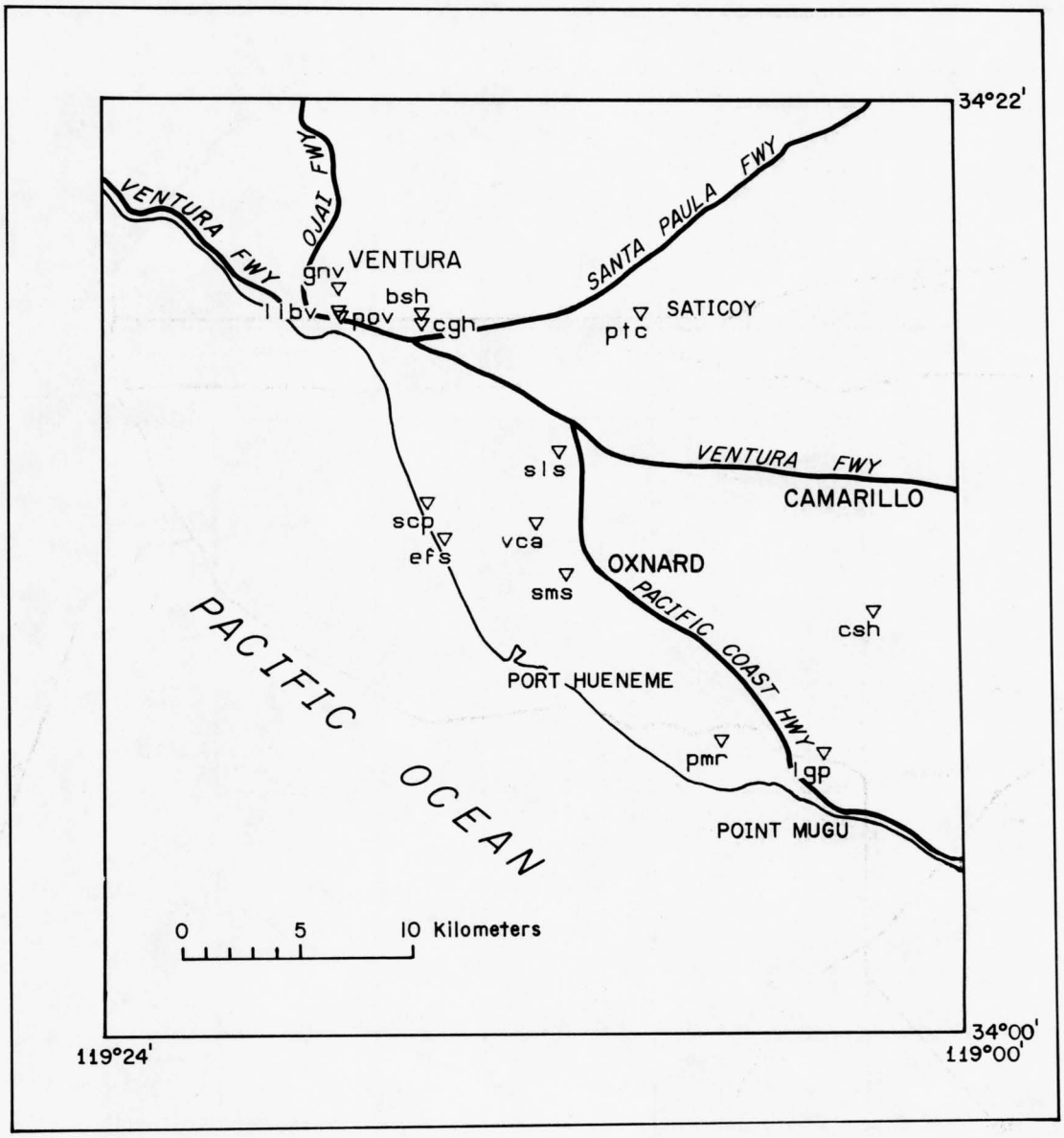

Figure 4.--Station locations in the Oxnard-Ventura region.

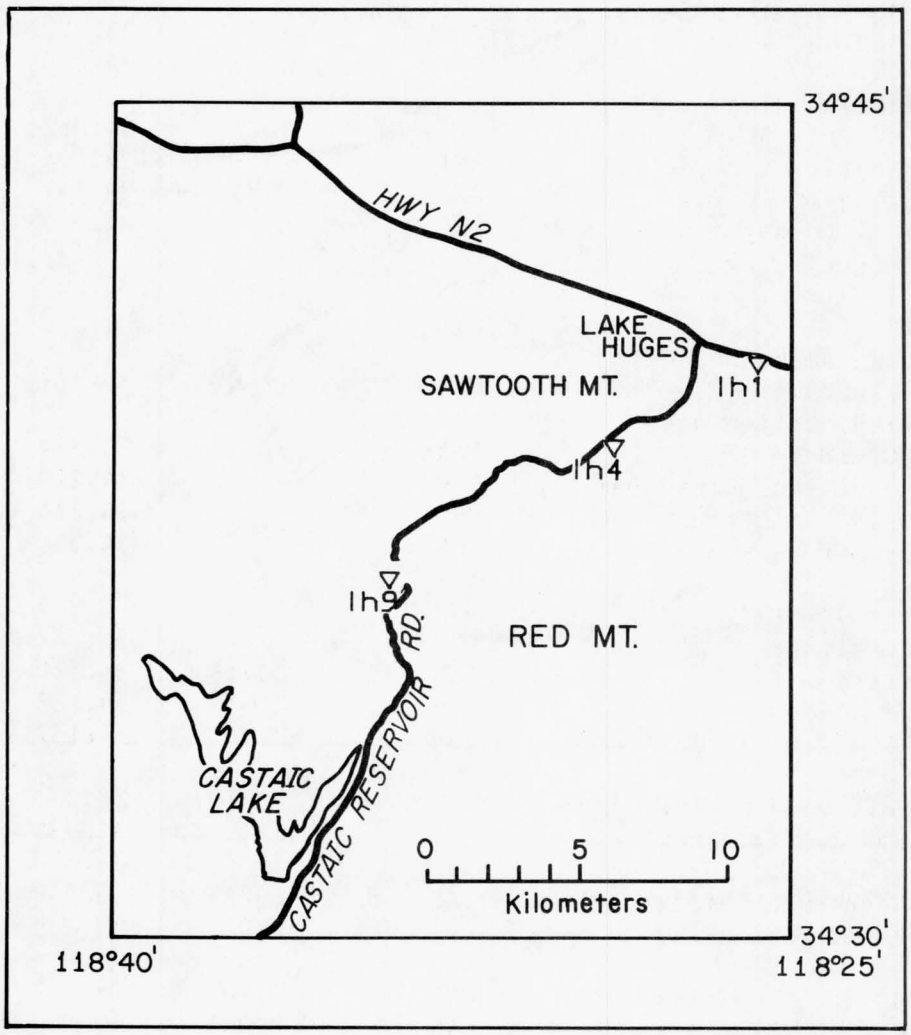

Figure 5.--Station locations in the Lake Hughes region.

Table 1.--Stations in Los Angeles that Recorded NTS Explosions

Shot(s)	Name	Abbrev.	Cal. Tech. ID	Lat. N.	Long. W.
1	L.A. County F.S.1.	FS1	0204*	33.768	118.196
1	St. Mary's Convent	CON	-	33.779	118.186
1	L.A. County F.S. 10	FS10	-	33.785	118.172
1	L.A. County F.S. 13	FS13	-	33.802	118.214
1-6,8-19	Cal. Tech. Seism. Lab.	CIT	G106	34.145	118.170
2	L.A. County F.S. 122	FS122	-	33.834	118.160
2	L.A. County F.S. 105	FS105	-	33.860	118.216
2	Compton Airport	CPT	-	33.889	118.238
2	Compton F.S. H.Q.1	CFS1	-	33.895	118.226
3,4,15	Holiday Inn	HOI	C048	34.220	118.471
3	Farmer's Ins. Bldg.	FIB	E072	34.062	118.331
3	Security Bank Tower	SBT	892+	34.054	118.252
3,4,15,16,17	Glendale Mun. Bldg.	GMB	F088	34.147	118.247
3	L.A. County Courthouse	LAC	-	34.057	118.246
3	Century City, 1901 Ave. of the Stars	CEN	R249	34.060	118.417
4,16,17	Casa Adobe School, Glendale	CAA	-	34.166	118.263
4	Fire Station 46, Glendale	FS46	-	34.324	118.449
4	Lower Van Norman Dam	LVD	-	34.279	118.477
5,6	Upper Van Norman Dam	UVD	-	34.314	118.491
5,6	Sylmar High School	SHS	-	34.306	118.440
5,6	Mission Hills P.O.	MHP	-	34.257	118.465
5,6,15	Pacoima Mem. Hospital	PMH	-	34.282	118.383
5,6	Pacoima Dam	PAD	C041*	34.330	118.399
7,8,15	Athenaeum	ATH	G107	34.138	118.120
7,8,15	Millikan Library	MIL	G108	34.137	118.125
7,11	Hollywood Storage bsmt.	HSB	D057	34.090	118.341
8	800 W. First BH Towers	800	Q241	34.056	118.250
9,10	Long Beach Ter. Island	LBT	0205	33.756	118.223
9,10	Long Beach Utility Bldg.	LBU	0204	33.769	118.194
9,10,11	Palos Verdes Estates	PVR	N191	33.800	118.387
11,15	Griffith Observatory	GOC	0198	34.118	118.299
11	646 S. Olive Street	646	F098	34.047	118.254
11	1760 Orchid Street Holiday Inn	1760	Q236	34.104	118.339
11,15	3838 Lankershime Blvd.	3838	L166	34.139	118.355
11	14724 Ventura Blvd.	14724	Q233	34.152	118.453

Table 1.--Stations in Los Angeles that Recorded NTS Explosions (Continued)

Shot(s)	Name	Abbrev.	Cal. Tech. ID	Lat. N.	Long. W.
11	15250 Ventura Blvd.	15250	H115	34.153	118.462
11	6464 Sunset Blvd.	6464	R246	34.098	118.329
11	420 S. Grand	420	K157	34.051	118.252
11	445 Figueroa Street	445	C054	34.053	118.256
11	611 W. Sixth Street	611	G112	34.049	118.254
11	800 W. Sixth Street	800WS		34.050	118.257
11	Lake Hughes #4	LH4	J142	34.648	118.481
11	Lake Hughes #1	LH1	J141	34.673	118.429
11	Lake Hughes #9	LH9	J143	34.608	118.562
11	Cal. State Univ. Long Beach	CSU	N196	33.777	118.111
11	Tishman Airport Ctr.	TAC	S267	33.947	118.385
11	15107 Vanowen Street	15107	J145	34.195	118.461
12	226 Ridgeline	226		33.985	117.820
12	Chino Airport	CHA		33.977	117.640
12	10670 54th	10670		33.990	117.517
12	6675 Allessandro Blvd.	6675		33.932	117.347
12	Condosta Tractor Company	CTC		34.061	117.286
12,15	3595 Hurst	DRW		34.156	117.302
12	6696 Eastwood Street	6696		34.133	117.604
12	2045 Cypress	2045		34.036	117.663
12	9222 Colorado Avenue	9222		33.935	117.451
12	24116 Crestforest Drive	24116		34.235	117.275
12	Montclair Fire Dept.	MFD		34.092	117.697
12	San Antonio Dam	SAD		34.157	117.681
13,16,17	Laguna Peak	LGP		34.108	119.064
13	Petroseed Company, Saticoy	PTC		34.280	119.148
13	Generating Station, Ventura	GNV		34.290	119.290
13	Bard Sanitarium	BSH		34.280	119.251
13	County General Hosp., Ventura	CGH		34.276	119.251

Table 1.--Stations in Los Angeles that Recorded NTS Explosions (Continued)

Shot(s)	Name	Abbrev.	Cal. Tech. ID	Lat. N.	Long. W.
13	Post Office, Ventura	POV		34.279	119.289
13	Library, Ventura	LIBV		34.281	119.290
13	Camarillo State Hospital	CSH		34.163	119.040
13,19	School District Maintenance Shop	SDMS		34.195	118.594
13	Mulholland Jr. High Sch.	MUL		34.193	118.502
13	Cal. State University, Northridge	CSUN		34.242	118.527
13,15	Riverside Dr. School, Van Nuys	RIV		34.158	118.416
13	CIT Financial Loan Company	FLC		34.257	118.534
13	So. California Power Plant	SCP		34.206	119.249
13	San Miguel School	SMS		34.178	119.184
13	Sierra Linda School	SLS		34.226	119.187
13	Ventura County Airport	VCA		34.198	119.198
14	South Gate Fire Station	SGFS		33.948	118.183
14	Hoag Hospital	HHP		33.625	117.932
14	Sewage Disposal Plant #2	SDP2		33.640	117.955
14	Free Evangel. Church	FEG		33.674	117.989
14	Katella Elem. School	KES		33.811	117.825
14	Walnut Manor	WMN		33.819	117.928
14	Anaheim Hills Golf Course	AHGC		33.841	117.760
14	Sand Canyon Reservoir	SCR		33.654	117.796
14	St. Jude Hospital	SJH		33.894	117.926
14	Orange County Court House	OCCH		33.751	117.870
15,16,17	Fire Station 4, Glendale	FS4		34.173	118.227
15	Burbank Fire Station, Central Hdqtrs.	BFS		34.183	118.302

Table 1.--Stations in Los Angeles that Recorded NTS Explosions (Continued)

Shot(s)	Name	Abbrev.	Cal. Tech. ID	Lat. N.	Long. W.
15	Equestrian Center	EQC		33.982	117.820
15	Trapp School	TSH		34.149	117.388
16,17	5219 Whitecap St.	EFS		34.192	119.241
16,17	Pacific Missile Range	PMR		34.113	119.112
16,17,19	Fire Station 145, Rowland Heights	FS45		33.889	117.889
16,17,19	El Monte City Hall, Police Hdqtrs.	EMCH		34.071	118.030
16,17	235 E. Gladstone	JJW		34.114	117.803
16,17	City of Hope Hospital	CHH		34.130	117.970
16,17	San Gabriel Comm. Hospital	SGCH		34.100	118.105
18	Marina Del Rey	MDR		33.974	118.456

*Indicates nuclear recording near-by strong motion station.
+Strong motion station - no record.

Table 2.--Stations in Los Angeles that Recorded NTS Explosions

Abbrev.	Name and Addresses
FS1	L. A. County, Fire Station 1 (F.S.), 100 Magnolia, Los Angeles, CA.
CON	St. Mary's Convent, 10th and Linden, Long Beach, CA.
FS10	L. A. County F. S. 10, 1417 Peterson, Los Angeles, CA.
FS13	L. A. County F. S. 13, 2475 Adriatic, Los Angeles, CA
CIT	Cal. Tech. Old Seism. Lab., Cal. Tech., Pasadena, CA.
FS122	L. A. County F. S. 122, 2600 Green Meadow Rd., Lakewood, CA.
FS105	L. A. County F. S. 105, 18915 S. Santa Fe Ave., Compton, CA.
CPT	Compton Airport, 901 W. Alondra Blvd., Compton, CA.
CFS1	Compton F.S.H.Q. 1, 201 S. Acacia, Compton, CA.
HOI	Holiday Inn, 8244 Orion Blvd., Van Nuys, CA.
FIB	Farmer's Ins. Bldg., 4680 Wilshire Blvd., Los Angeles, CA.
SBT	Security Bank Tower, 333 S. Hope, Los Angeles, CA.
GMB	Glendale Municipal Bldg., 633 E. Broadway, Glendale, CA.
LAC	L. A. County Courthouse, Olive & First St., Los Angeles, CA.
CEN	Century City, 1901 Avenue of the Stars, Los Angeles, CA.
CAA	Casa Adobe School, 1330 Dorothy Drive, Glendale, CA.
FS46	Fire Station 46, 14425 Olive View Dr., Sylmar, CA.
LVD	Lower Van Norman Dam, Sub Station, San Fernando, CA.
UVD	Upper Van Norman Dam, San Fernando, CA.
SHS	Sylmar High School, Sylmar, CA.
MHP	Mission Hills Post Office, Mission Hills, CA.
PMH	Pacoima Memorial Hospital, 1160 Eldridge Avenue, Pacoima, CA.
PAD	Pacoima Dam, San Fernando, CA.
ATH	Athenaeum, Cal. Tech., Pasadena, CA.
MIL	Millikan Library, Cal. Tech., Pasadena, CA.
HSB	Bekins Hollywood storage basement, 1025 Highland Avenue, Hollywood, CA.
800	800 W. First B. H. Towers, Los Angeles, CA.
LBT	Long Beach Ter. Island, S. California Edison Power Plant, Long Beach, CA.
LBU	Long Beach Utility Bldg., 216 W. Broadway, Long Beach, CA.
PVR	Palos Verdes Estates, 2516 Via Tejon, Long Beach, CA.
GOC	Griffith Observatory, Griffith Park, Box 27787, Los Angeles, CA.
646	Donovan Jewelry, Athletic Club Garage, 646 S. Olive Street, Los Angeles, CA.
TAC	Tishman Airport Center, 5250 Century Blvd. Los Angeles, CA.
420	Pacific Telephone, 420 S. Grand, Los Angeles, CA.

Table 2.--Stations in Los Angeles that Recorded NTS Explosions (continued)

Abbrev.	Name and Addresses
445	Union Bank Square, 445 S. Figueroa Street, Los Angeles, CA.
1760	Holiday Inns, Inc., 1760 Orchid Street, Hollywood, CA.
3838	Sheraton Universal Hotel, 3838 Lankershime Blvd., Los Angeles, CA.
14724	Certified Life Tower, 14724 Ventura Blvd., Los Angeles, CA.
15250	Bank of California Bldg., 15250 Ventura Blvd., Los Angeles, CA.
15107	Valley Presbyterian Hospital, 15107 Vanowen Street, Van Nuys, CA.
800WS	Security Pacific Financial Center, 800 West 6th Street, Los Angeles, CA.
611	Crocker Bank Plaza, 611 West 6th Street, Los Angeles, CA.
6464	Stanley Folb Bldg., 6464 Sunset Blvd., Los Angeles, CA.
LH1	Lake Hughes #1, Fire Station 78, West Lake Elizabeth, Lake Road, Lake Hughes, CA.
LH9	Lake Hughes #9, Warm Springs Camp, Lake Hughes, CA.
LH4	Lake Hughes #4, Elizabeth Lake Canyon, CA.
CSU	Cal. State University, Humanities Bldg., Long Beach, CA.
226	226 Ridgeline, Diamond Bar, Ca.
CHA	Chino Airport, Chino, CA.
10670	10670 54th Mira Loma, Ca.
6675	6675 Allessandro Blvd., Riverside, CA.
CTC	Condosta Tractor Co., 10617 Hunts Lane, Riverside, CA.
DRW	3595 Hurst, San Bernadino, CA.
6696	6696 Eastwood Street, Alta Loma, CA.
2045	2045 Cypress Avenue, Ontario, CA.
9222	9222 Colorado Avenue, Riverside, CA.
24116	24116 Crestforest Drive, Crestline, CA.
MFB	Montclair Fire Dept., corner of Arrow Highway and Monte Verde Avenue, Montclair, CA.
SAD	San Antonio Dam, Upland, CA.
LGP	Laguna Peak, Point Mugu, CA.
PTC	Petroseed Company, Saticoy, CA.
GNV	Ventura Generating Station, Grant Memorial Park, Ventura, CA.
BSH	Bard Sanitarium, Ventura, CA.
CGH	County General Hospital, Loma Vista Road and Agnus Drive, Ventura, CA.
POV	Ventura Post Office, Corner Santa Clara Street and Fir Street Ventura, CA.
LIBV	Ventura Library, 651 E. Main Street, Ventura, CA.
CSH	Camarillo State Hospital, Main Bldg., Lewis Road, Camarillo, CA.
SDMS	School District Maintenance Shop, Corner Eaton Avenue and Vanowen Street, Canoga Park, CA.
MUL	Mulholland Jr. High School, Vanowen Street and Balboa Blvd, Reseda, CA.

Table 2.--Stations in Los Angeles that recorded NTS Explosions (Continued)

Abbrev.	Name and Addresses
CSUN	Cal State University, Northridge, Engineering Bldg., Northridge, CA.
RIV	Riverside Drive School, Corner of Ethel Avenue and Riverside Drive, Van Nuys, CA.
FLC	CIT Financial Loan Company, 10242 Reseda Blvd. Northridge, CA.
SCP	Southern California Power Plant, Mandalay Beach, Oxnard, CA.
SMS	San Miguel School, 2400 S. Jay Street, Oxnard, CA.
SLS	Sierra Linda School, 2201 N. Jasmine Street, Oxnard, CA.
VCA	Ventura County Airport, Valenti Aviation Bldg., West Fifth Street, Oxnard, CA.
SGFS	South Gate Fire Station, South Gate Park, Southern Avenue and Vossler, South Gate, CA.
HHP	Hoag Hospital, 301 Newport Blvd., Newport Heights, CA.
SDP2	Sewage Disposal Plant #2, Brookhurst Street, Huntington Beach, CA.
FEG	Free Evangelical Church, Florida Street and Utica Avenue, Huntington Beach, CA.
KES	Katella Elementary School, Corner of Katella Ave. and Hardy Street, Orange, CA.
WMN	Walnut Manor, Lutheran Home, Corner of Walnut Street and Ball Road, Anaheim, CA.
AHGC	Anaheim Hills Golf Course, Walnut Canyon Road, Anaheim, CA.
SCR	Sand Canyon Reservoir, 610 Newport Center Drive, Irvine, CA.
SJH	St. Jude Hospital, Balboa Road, Fullerton, CA.
OCCH	Orange County Court House, Engineering Addition Bldg., across the street from Court House, 8th Street and Birch Street, Santa Ana, CA.
FS4	Glendale Fire Station 4, 1734 N. Canada Blvd., Glendale, CA.
BFS	Burbank Fire Station, Central Headquarters, 353 E. Olive Avenue, Burbank, CA.
EQC	Equestrian Center, 22615 Lazy Meadows, Diamond Bar, CA.
TSH	Trapp School, Riverside Avenue, Rialto, CA.
EFS	5219 Whitecap Street, Oxnard, CA.
PMR	Pacific Missile Range, Bldg. 375, Navy Astronautics Group, Point Mugu, CA.
FS45	Rowland Heights Fire Station 145, 1525 S. Nogales Avenue, Rowland Heights, CA.
EMCH	El Monte City Hall, Police Headquarters, 11323 Valley Blvd., El Monte, CA.

Table 2.--Stations in Los Angeles that Recorded NTS Explosions (Continued)

Abbrev.	Name and Address
JJW	235 E. Gladstone, San Dimas, CA.
CHH	City of Hope Hospital, 1500 E. Duarte, City of Hope, CA.
SGCH	San Gabriel Community Hospital, 218 S. Santa Anita Street, San Gabriel, CA.
MDR	Marina Del Rey, 75 m northeast of the intersection of Marina and Tahiti Way.

Table 3.--Nuclear Event Names, Detonation Times, Coordinates, and m_b Magnitudes obtained from: "Preliminary Determination of Epicenters."

Shot	Name	Date	Time (GMT) hr	min	sec	Lat. N.	Long. W.	m_b
1	Mast	19 June 75	13	00	0.09	37.351	116.320	6.1
2	Camembert	26 June 75	12	30	0.16	37.279	116.369	6.2
3	Chiberta	20 Dec 75	20	00	0.16	37.144	116.062	5.7
4	Muenster	03 Jan 76	19	15	0.16	37.297	116.333	6.2
5	Fontina	12 Feb 76	14	45	0.16	37.271	116.488	6.3
6	Cheshire	14 Feb 76	11	30	0.16	37.242	116.420	6.0
7	Estuary	09 Mar 76	14	00	0.09	37.310	116.364	6.0
8	Colby	14 Mar 76	12	30	0.16	37.306	116.471	6.3
9	Pool	17 Mar 76	14	15	0.09	37.256	116.329	6.1
10	Strait	17 Mar 76	14	45	0.09	37.107	116.053	5.8
11	Billet	27 July 76	20	30	0.07	37.075	116.044	5.3
12	Rudder	28 Dec 76	18	00	0.07	37.101	116.036	5.5
13	Crewline	25 May 77	17	00	0.07	37.094	116.045	5.3
14	Scantling	19 Aug 77	17	55	0.07	37.110	116.054	5.6
15	Iceberg	23 Mar 78	16	30	0.00	37.102	116.051	5.6
16	Fondutta	11 Apr 78	15	30	0.16	37.300	116.327	5.3
17	Backbeach	11 Apr 78	17	45	0.07	37.234	116.368	5.5
18	Pepato	11 June 79	14	00	0.17	37.290	116.455	5.7
19	Fajy	28 Jun 79	14	44	0.17	37.143	116.088	5.1

most cases, each station record contains several hundred seconds of signal preceeded by at least 20 seconds of ambient noise. The analog tape data were processed using an EAI 690-640 analog-digital computer system. The time histories were corrected to ground velocity and band-pass filtered using filter corners at 0.1 and 40.0 Hz. The filter slopes were 12 and 24 db/oct, respectively. The resulting time histories were then digitized at 100 samples per second, and a digital 7-track tape was recorded. The data processing system and the L-7 seismograph are discussed in greater detail by Park and Hays (1977).

Because it was determined that NTS nuclear explosions recorded in Los Angeles on the L-7 contained little or no energy above 10 Hz, the digital time histories were further low-pass filtered using a filter corner frequency of 10 Hz with a slope of 18 db/oct. Subsequent reduction to 50 samples per second reduced the storage requirements. These time histories are shown in Appendix B.

SPECTRAL ANALYSIS OF THE SIGNAL

Before spectral analysis any DC offset is removed from the data, and a data window is applied as suggested by Bingham and others (1967). This window tapers the leading and trailing ten percent of the data using a cosine bell:

$$\omega(t) = \begin{cases} 0.5(1-\cos(\pi t/0.1T)) & 0 \leq t < 0.1T \\ 1.0 & 0.1T \leq t \leq 0.9T \\ 0.5(1-\cos((T-t)/0.1T)) & 0.9T < t \leq T \end{cases}$$

where T = data window length. This operation has the effect of reducing intermodulation distortion as well as reducing the effects of discontinuities at the ends of the time history on the resulting spectra. When required, the

windowed time function is padded with zeros to 16,384 points for uniform input to the Fast Fourier Transform (FFT).

Application of the FFT produces the Fourier coefficients

$$a_k = \frac{1}{N} \sum_{j=0}^{2N-1} X_j \cos \frac{\pi kj}{N} \quad k=0,\ldots N$$

$$b_k = \frac{1}{N} \sum_{j=0}^{2N-1} X_j \sin \frac{\pi kj}{N} \quad k=1,\ldots N-1$$

and the power spectral density is computed from

$$P_k = [a_k^2 + b_k^2].$$

In order to obtain stable spectral estimates the spectral values are smoothed with the following triangular operator (Singleton and Poulter, 1967):

$$P'_k = \frac{1}{m^2} \sum_{j=-m+1}^{m-1} (m - |j|) P_{k+j}$$

where m = 25 was chosen for the signal analysis. The width of this triangle is $2m\Delta f$ Hz.

The stability of the smoothed power spectrum estimates can be approximately determined from

$$R_x \simeq 25(k - 1)^{-1/2}$$

where R_x is the range in db that contains the actual and estimated spectral value with a probability of 96 percent, and k is the the number of degrees of freedom (Blackman and Tukey, 1958). In the signal analysis case N=16,384

$f_{nyquist} = 1/2\Delta t = 25$ Hz
$\Delta f = 1/T = 1/(327.68 \text{ Sec}) = .003052$
$N_f = 25/\Delta f = 8192$

Since there are 2m-1 points in each smoothed spectral estimate, where 2m-1 = 49, there are $k \simeq 60$ degrees of freedom (Appendix A). Therefore,

$$R_x = 3.2\text{db}$$

where 10db equals a factor of 10 for power spectra. This range is approximately centered around the true mean power spectrum. Since the amplitude spectrum ${}_sS_k$ (proportional to the square root of the power spectrum) is used to compute transfer functions, this value of R_x implies that ${}_sS_k$ is within a factor of 1.2 times the true value 96 percent of the time. Although this R_x underestimates the actual spectral range because the calculation is based on the assumption that the time histories are Gaussian noise samples, the measure is useful to show that the stability achieved by smoothing is good in the ideal case.

SPECTRAL ANALYSIS OF THE NOISE

The noise power spectral density ${}_nP'_k$, is calculated by the same procedure that is used for the signal (${}_sP'_k$), although a shorter duration time history is used. The noise time history is 20 seconds (1024 points) long producing a frequency spacing of unsmoothed spectral estimates equal to 0.0488 Hz. In order to achieve approximately the same smoothed spectral resolution used in the signal case (0.15 Hz) the noise must be smoothed by a 3-point triangular operator (m=2). The stability of ${}_nP'_k$ is not as good as it is for ${}_sP'_k$ because

the smoothing operator is shorter. In this case R_x equals 14db indicating that the amplitude spectrum S_k is within a factor of 2 times the true value 96 percent of the time.

Signal-to-noise (SNR) ratios and site transfer functions are computed using the unnormalized spectrum

$$ {}_sS_k = \Delta t N \, (P'_k)^{1/2} $$

because ${}_sS_k$ is unaffected by the length of the signal data window as long as the window includes all significant portions of the signal. The noise spectrum (${}_nS_k$), however, is dependent on the length of the noise data window, and, thus, ${}_nS_k$ must be adjusted to an equivalent noise data window length equal to the signal data window length before the SNR can be computed. The required adjustment can be obtained as follows. From Parseval's theorem we have:

$$ rms^2 = \frac{1}{2N} \sum_{t=0}^{2N-1} x_t^2 = \sum_{k=0}^{2N-1} |X_k|^2 $$

where x_t is the discrete time history,

$$ |X_k|^2 = \frac{1}{4} (a_k^2 + b_k^2) $$
$$ = \frac{1}{4} P_k \quad , $$

and rms = root-mean-square of the time history. Therefore,

$$\mathrm{rms}^2 = \frac{1}{4} \sum_{k=0}^{2N-1} P_k \simeq \frac{N\,\overline{P}}{2}$$

$$\overline{P} \simeq \frac{2\ \mathrm{rms}^2}{N} .$$

For stationary noise, rms is constant and, therefore, the power spectral density is inversely proportional to the length of the data window. The mean unnormalized spectrum is therefore:

$$_n\overline{S}_k \simeq \sqrt{2}\,\Delta t\ N^{1/2}\ \mathrm{rms}.$$

This result implies that the unnormalized noise spectrum for an equivalent data window equal to the signal data window can be obtained by scaling the noise spectrum as follows:

$$_nS'_k = (N_s/N_n)^{1/2}\ {}_nS_k.$$

The SNR is then computed from

$$\mathrm{SNR} = \frac{{}_sS_k^{\,2}}{{}_nS'_k}$$

and if SNR ≤ 2, ${}_sS_k$ is rejected at that period. Because ${}_nS_k$ is known to within about a factor of two, as shown above, this procedure will occasionally reject good data or accept poor data, but on the average will produce a ${}_sS_k$ that is

uncontaminated by bands of noise. Practically, the presence of noise is indicated by setting the spectral and site transfer functions (STF) values equal to 1×10^{-38} at those periods where the criteria is not met. During plotting of the STF, the plot pen is lifted for those periods where the STF values equal 1×10^{-38}. This procedure produces what might be described as "drop out" in the STF plots shown in Appendix C.

COMPUTATION OF THE SITE TRANSFER FUNCTION

The crystalline rock site CIT, which was used as a base station and recorded all the nuclear events except one, was used to form the STF for all stations. Rogers and others, (1979) have discussed the basis for computing the STF in this manner. The STF is given by:

$$ {}_jSTF_k^i = \frac{{}_jS_k^i}{{}_jS_k^0} \qquad \begin{array}{ll} k = 0,\ldots n & \text{(period)} \\ i = 1,\ldots m & \text{(stations)} \\ j = v,\ t,\ r & \text{(components).} \end{array} $$

In order to determine the stability of the STF, we have reoccupied station pairs to record several nuclear events. In cases where three or more nuclear events were recorded it was possible to compute the geometric mean and associated standard deviation from:

$$ {}_j\hat{X}_k^i = 10^{\left[\frac{1}{t} \sum_{q=1}^{t} \mathrm{Log}_{10}\left({}_jSTF_k^{iq}\right)\right]} \qquad \text{for t nuclear events} $$

$$ {}_j\sigma_k^i = 10^{\left[\frac{1}{t-1} \sum_{q=1}^{t} \left[\mathrm{Log}_{10}({}_jSTF_k^{iq}) - \mathrm{Log}_{10}(\hat{X})\right]\right]**0.5} . $$

The basis for assuming the STF to be log-normally distributed is given in Appendix A. Figures 6 through 10 show $\hat{X}$ and $\hat{X}*\sigma$, $\hat{X}/\sigma$ for those stations and components where they could be computed. Assuming that the samples at each period are drawn from a population with a common variance, we can compute the pooled variance from:

$$ {}_j\bar{\sigma}^i = 10^{\left[\frac{1}{n} \sum_{k=1}^{n} \left(\mathrm{Log}_{10}({}_j\sigma_k^i)^2\right)\right]**0.5} . $$

Table 4 gives $\bar{\sigma}$ for each of the station components shown in figure 6 through 10. For the cases where $\bar{\sigma}$ could be computed, it ranged between 1.3-1.7 with a mean value of 1.38. This range corresponds to approximately a factor of 1.9 for the 96 percent probability level. This result indicates the transfer functions have a high degree of stability.

Some irregularities that are present in the time histories and STF of Appendix B and C should be discussed. For instance, for event BILLET, the long-period ground motion on this record that preceeds and overlaps the nuclear event signal is due to the Tang-shan earthquake that occurred in northeastern China just prior to the nuclear event. In a few cases time histories contain unusual bursts of noise that occur prior to the signal. In all cases such bursts were excluded from data used to compute either the noise or signal spectra. Occasionally, it was impossible to obtain a segment of noise of sufficient duration preceeding the signal. In these cases a noise segment was chosen from the end of the record. For event ESTUARY the

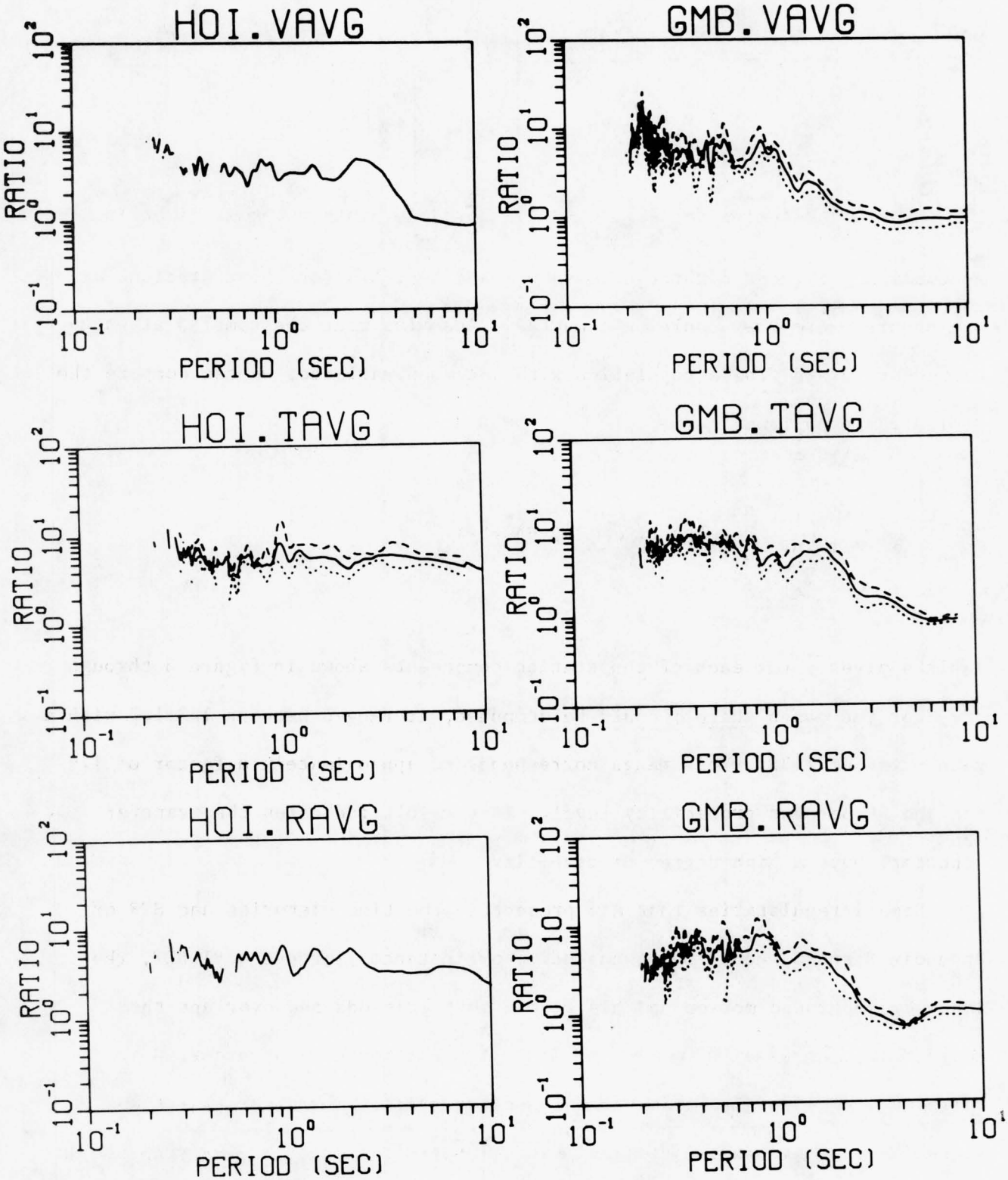

Figure 6.--Graphs of $\hat{X}$ (solid line) and ${}_j\sigma_k^i$ (dashed and dotted lines) vs. period. Nomenclature such as GMB.VAVG indicates the average vertical component STF at Station GMB.

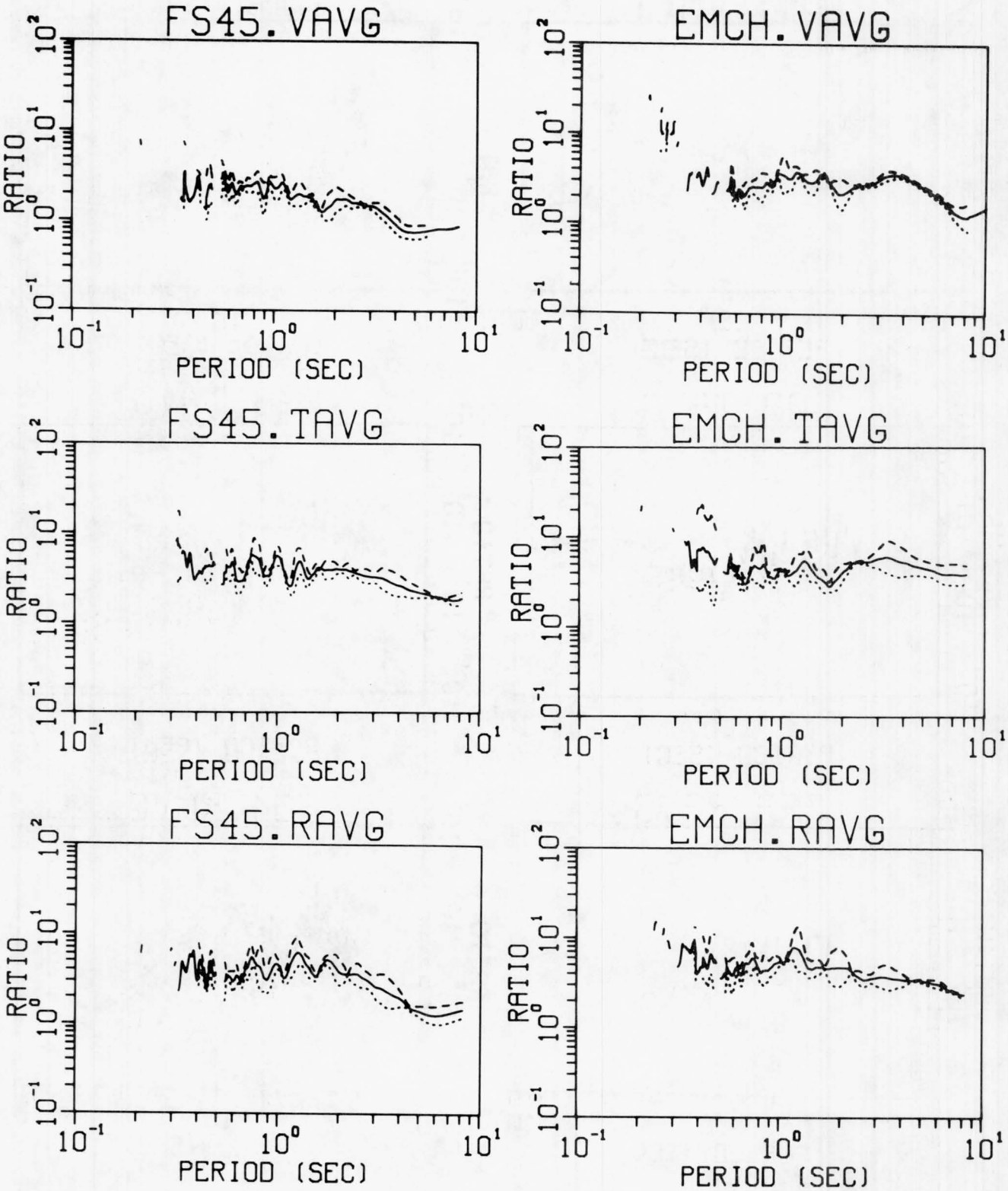

Figure 7.--Graphs of $\hat{X}$ (solid line) and ${}_j\sigma_k^i$ (dashed and dotted lines) vs. period. Nomenclature such as GMB.VAVG indicates the average vertical component STF at Station GMB.

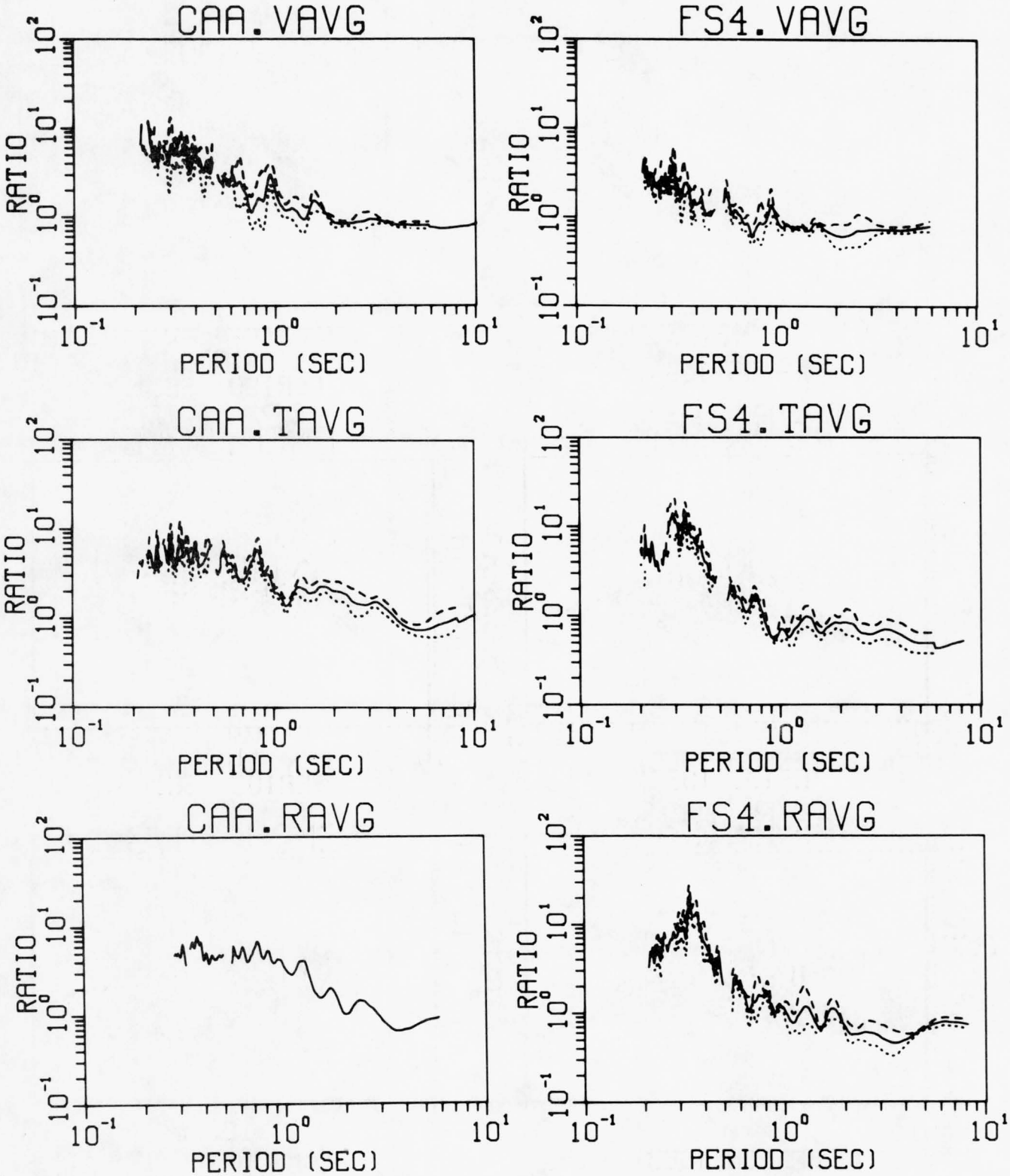

Figure 8.--Graphs of $\hat{X}$ (solid line) and ${}_j\sigma_k^i$ (dashed and dotted lines) vs. period. Nomenclature such as GMB.VAVG indicates the average vertical component STF at Station GMB.

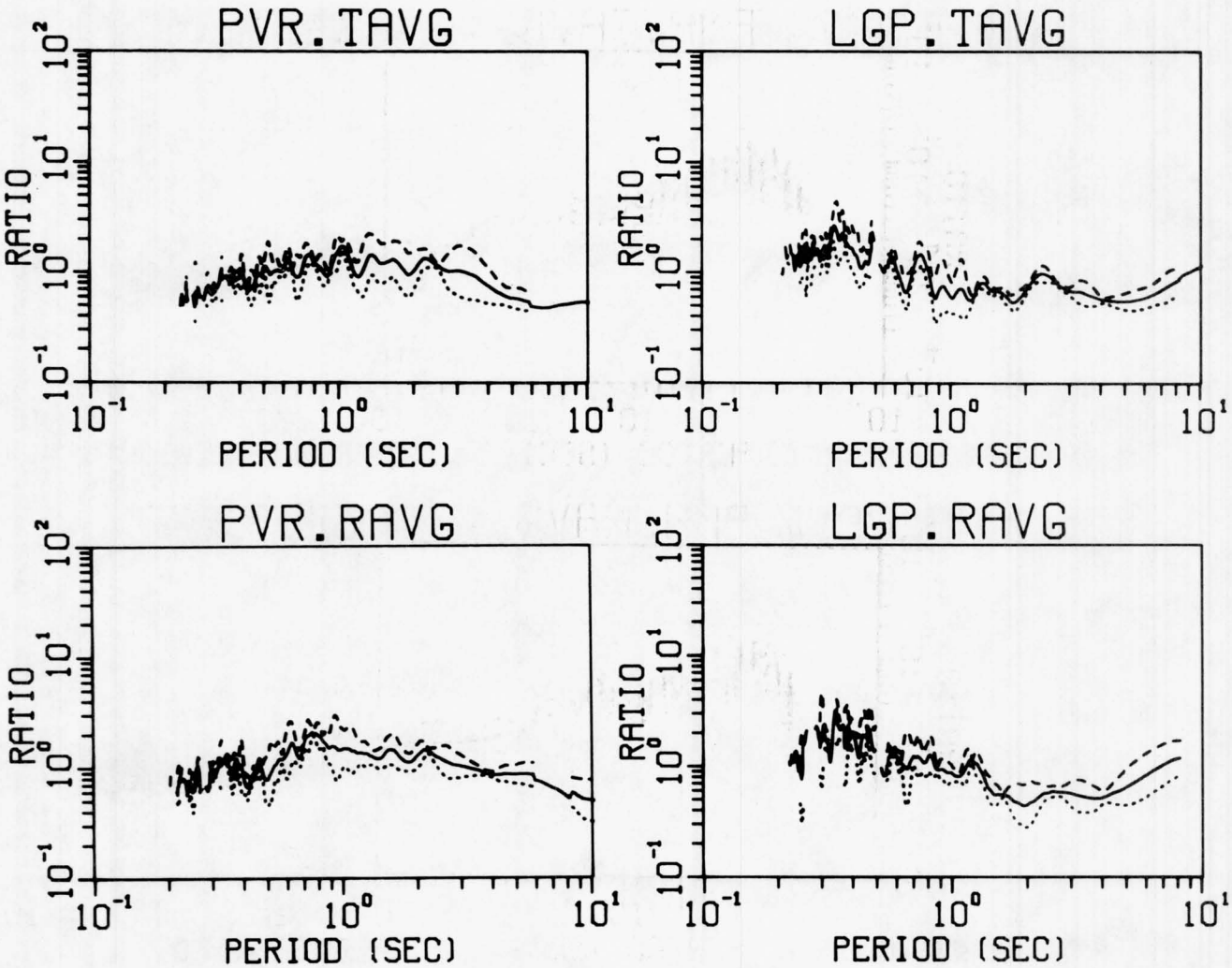

Figure 9.--Graphs of $\hat{X}$ (solid line) and ${}_j\sigma_k^i$ (dashed and dotted lines) vs. period. Nomenclature such as GMB.VAVG indicates the average vertical component STF at Station GMB.

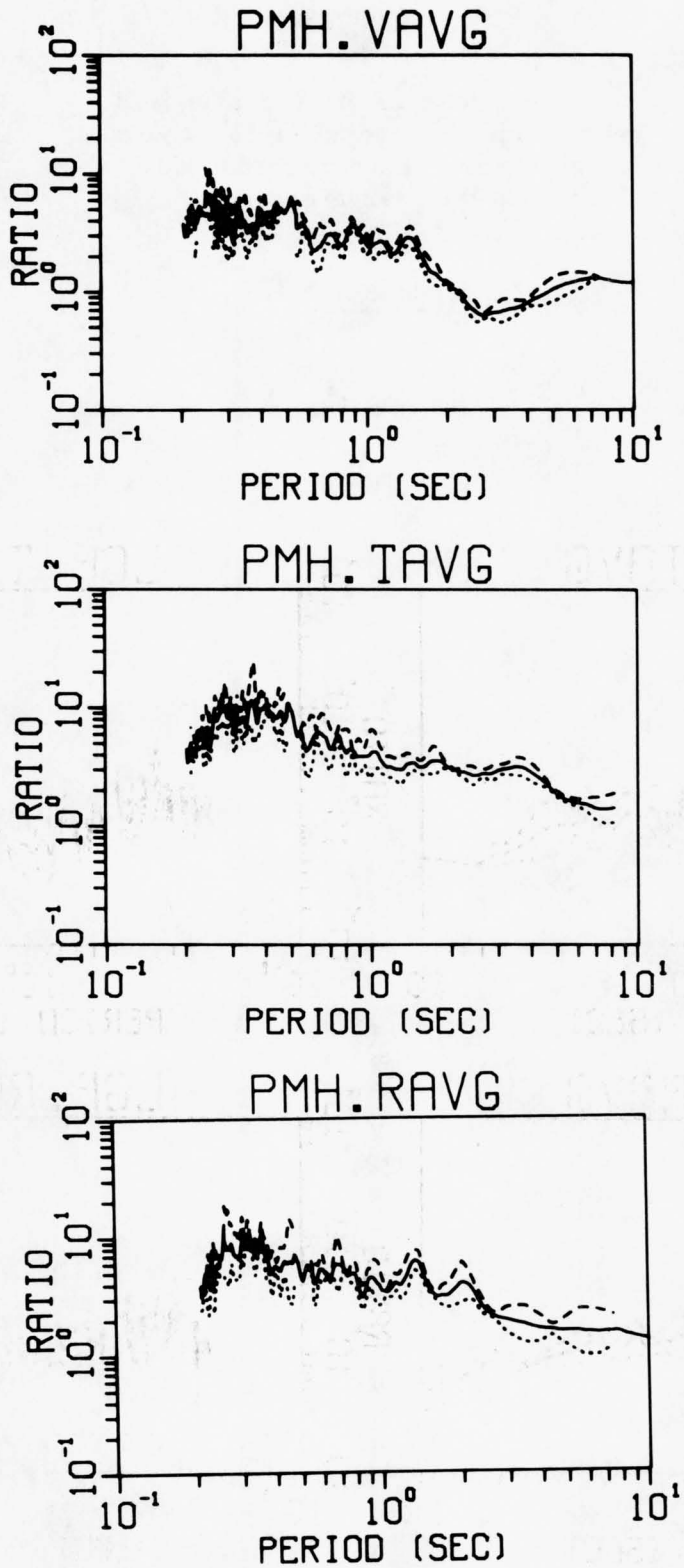

Figure 10.--Graphs of $\hat{X}$ (solid line) and ${}_j\sigma_k^i$ (dashed and dotted lines) vs. period. Nomenclature such as GMB.VAVG indicates the average vertical component STF at Station GMB.

Table 4.--A list of pooled standard deviations, $\bar{\sigma}$, computed for those station-components recorded for 3 or more nuclear events.

Station	Component	$\bar{\sigma}$
GMB	V	1.46
	T	1.33
	R	1.40
PMH	V	1.36
	T	1.37
	R	1.40
LGP	V	---
	T	1.40
	R	1.50
FS4	V	1.34
	T	1.33
	R	1.32
FS45	V	1.33
	T	1.36
	R	1.30
EMCH	V	1.27
	T	1.69
	R	1.39
HOI	V	---
	T	1.33
	R	---
CAA	V	1.45
	T	1.29
	R	---
PVR	V	---
	T	1.36
	R	1.35

instrument at CIT failed, and, therefore, no STF could be computed. The records at ATH for event COLBY contain intermittant noise bursts throughout the record produced by the tape recording device. In processing these data the noise segment included one of the bursts. The very high STF values for station HOI and event ICEBERG in the period range 0.2-0.3 seconds are due to noise in the signal portion of HOI record and are not representative of the site amplification at those periods. This problem also exists for the following event; station-components: event CREWLINE; PTC (station name alone indicates all components), SCP, POV-vertical and transverse, FLC-vertical and transverse, MUL-, SDMS-, VCA-, SMS-, GNV-vertical; event SCANTLING; SGFS, SGP2-vertical; event FONDUTTA; EMCH, EFS; event BACKBEACH; EMCH; event ICEBERG; RIV-vertical. In all other cases the noise discriminant appears to work satisfactorily.

ACKNOWLEDGMENTS

The field work was accomplished with the help principally of Gene Sembera, Ray Bradley, Ted Barnhard, John German, Garron Woodruff, and Ken King. Duane Dobbs wrote the computer programs that transferred data from the analog-digital computer to the DEC-10 and Honeywell computers. John Tinsley aided in the selection of the sites by providing geological data at proposed recording locations. We were greatly assisted by Liz Ordahl in the preparation of many of the figures.

We are grateful to the Nevada Operations of the U.S. Department of Energy for providing the seismograph systems that were used in this study and, particularly, to P. N. Halstead of that office who helped in coordinating the usage of these instruments.

REFERENCES CITED

Bingham, C., Godfrey, M. D., and Tukey, J. W., 1967, Modern techniques of power spectrum estimation: IEEE Transactions on Audio and Electroacoustics, AU-15, p. 56-66.

Blackman, R. B., and Tukey, J. W., 1958, The measurement of power spectra: New York, Dover Publications, 190 p.

Croxton, F. E., 1959, Elementary statistics, with applications in medicine and biological sciences: New York, Dover Publications, 376 p.

Jenkins, G. M. and Watts, D. G., 1968, Spectral analysis and its applications: San Francisco, California, Holden-Day, 525 p.

Otnes, R. K. and Enochson, Loren, 1972, Digital time series analysis: New York, John Wiley and Sons, 467 p.

Park, R. B, and Hays, W. W., 1977, Use of a hybrid computer in engineering seismology research, U.S. Geological Survey Journal of Research 5, p. 651-661.

Rogers, A. M., Tinsley, J. C., Hays, W. W., and King, K. W., 1979, Evaluation of the relation between near-surface geologic units and ground response in the vicinity of Long Beach, California: Bulletin of the Seismological Society of America 69, p. 1603-1622.

Singleton, R. C. and Poulter, T. C., 1967, Spectral analysis of the call of the male killer whale: IEEE Transactions on Audio and Electroacoustics, AU-15, p. 104-113.

Tukey, J. W., 1967, An introduction to the calculations of numerical spectrum analysis, in Harris B., Ed., Spectral analysis of time series: New York, John Wiley and Sons, p. 25-46.

APPENDIX A

Examination of transfer function statistics.

In order to establish that the underlying distribution of the STF is log-normal, we compute several realizations of the distribution of the spectra that are used to determine STF, then compute a STF realization using the spectra and test its distribution against the hypothesis that it is log-normally distributed.

We start from the assumption that the time series values are random samples drawn from a Gaussian population. In actuality this assumption is not valid, but none the less it serves as a useful starting point to establish the statistical properties of time series in the ideal case. Unsmoothed spectra computed from these time series are distributed as χ^2 random variables with 2 degrees of freedom (Jenkins and Watts, 1968). The smoothed spectral estimates are χ^2_n random variables with n degrees of freedom given by (Otnes and Enochson, 1972):

$$n = 2\ B_f T$$

where B_f = final effective spectral bandwidth,

T = data window length.

The bandwidth is evaluated from:

$$B = 1/\left[\int_{-\infty}^{\infty} |W(f)|^2 df\right] \qquad (1)$$

where $w(f) = F.\ T.\ \{w(t)\}$. The bandwidth may also be evaluated from:

$$B = 1/\left[\int_{-\infty}^{\infty} w^2(t)dt\right]$$

(Jenkins and Watts, 1968),

where $w(t)$ = the data window function.

When using the data window of this study, that is, the modified cosine window with 10 percent tapering on each end, it can be shown that the bandwidth of each estimate is approximately $B_e = 1/T$. If ℓ of these estimates are averaged, the bandwidth becomes $B_e' = \ell\ B_e$, and the resulting spectral window is trapezoidal in shape. In this study we have multiplied this trapezoid by a triangular function; thus, the final bandwidth (B_f) is B_e' multiplied by the effective bandwidth of the triangular window. Using equation (1) when

$$W(f) = \begin{matrix} f/M^2 & 0 \leq f < M \\ (2M-f)/M^2 & M \leq f \leq 2M \end{matrix}$$

it is found that the effective bandwidth of the triangular window, B, is

$$B = 0.75 \quad \text{and}$$
$$B_f = 0.75\ell/T \quad .$$

Therefore,

$$n = 2B_fT = (2)(0.75)(\ell)$$
$$= 1.5\ell \quad .$$

In this study $\ell = 49$

$$n = 73 \ .$$

Tukey (1967) suggests the following approximate method of evaluating the degrees of freedom:

$$n = HN_T/N_f$$

where H = number of elementary frequency bands averaged

N_T = number of time samples minus padded zeros and the number of points tapered.

N_f = number of spectral estimates between 0 and f_{nyq}.

In this study H should be replaced by 0.75H to account for the loss in degrees of freedom by smoothing with a triangular spectral window:

$$n = \frac{(0.75)(49)\ (16384-3277)}{8192} \simeq 60 \quad .$$

This value of n is assumed in the following simulations.

Two thousand χ^2_{60} random variables were generated with 60 degrees of freedom using a digital computer for two separate realizations, ${}^1\chi^2_{60}$ and ${}^2\chi^2_{60}$. The random variable LR was computed as a simulation of the transfer function random variable. LR is given by:

$$LR = \mathrm{Log}_{10}[({}^1\chi^2_{60} / {}^2\chi^2_{60})^{1/2}] \quad .$$

Square roots are taken because the STF is computed using the square root of the power spectrum. The distribution of LR is shown in figure A1. This distribution can be fit by a normal curve because calculations of skewness ($\beta_1 = 3.2 \times 10^{-5}$) and kurtosis ($\beta_2 = 3.16$) do not differ significantly from the values of 0 and 3 for a normal curve (Croxton, 1959). Therefore, we assume that in the ideal case the STF follows a log-normal distribution.

In order to study an observed STF distribution, the data from station GMB are employed because five estimates of the STF for this site are available. We compute the random variable y from:

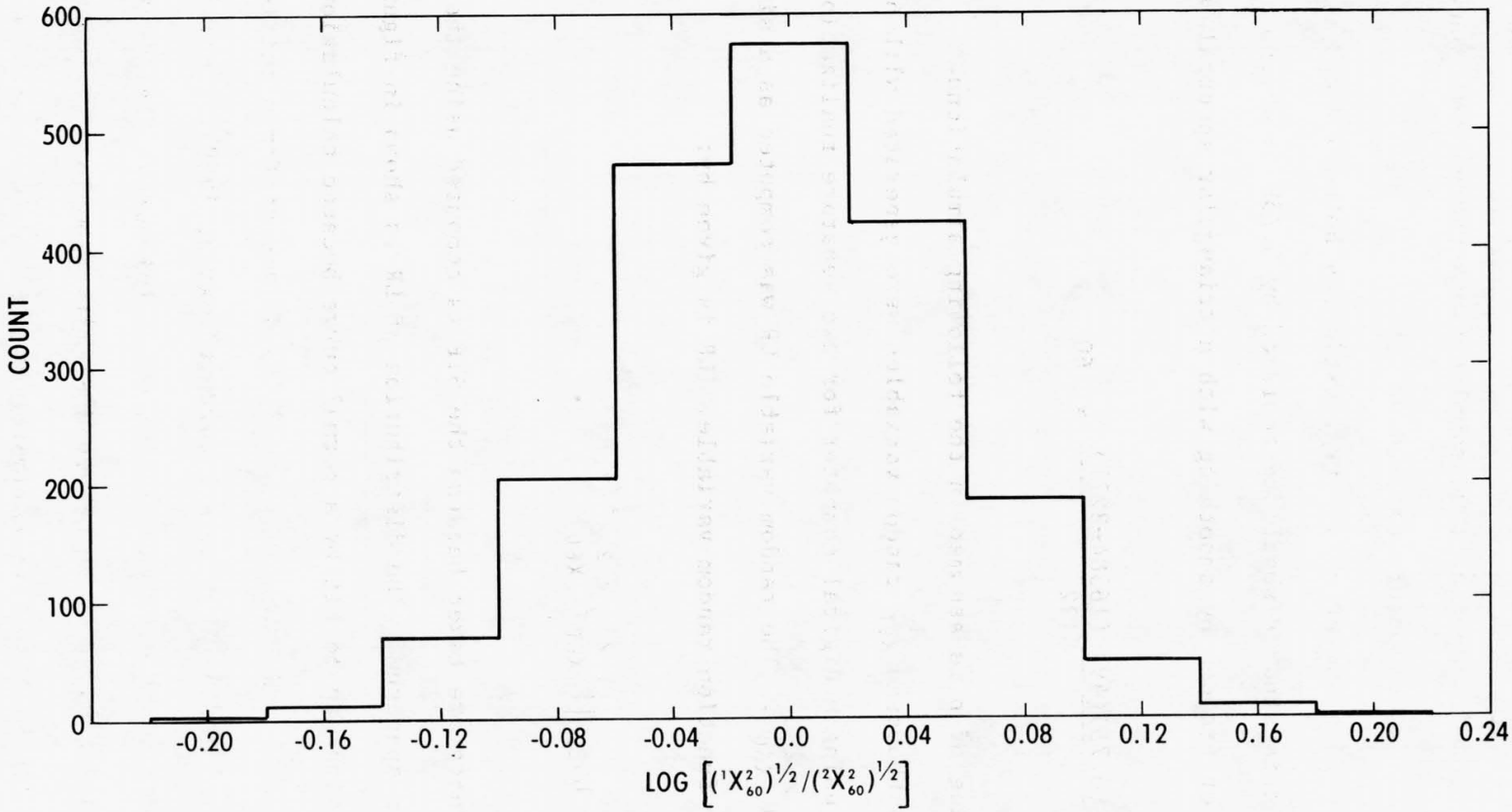

Figure A1.--The distribution of the synthetic STF-LR.

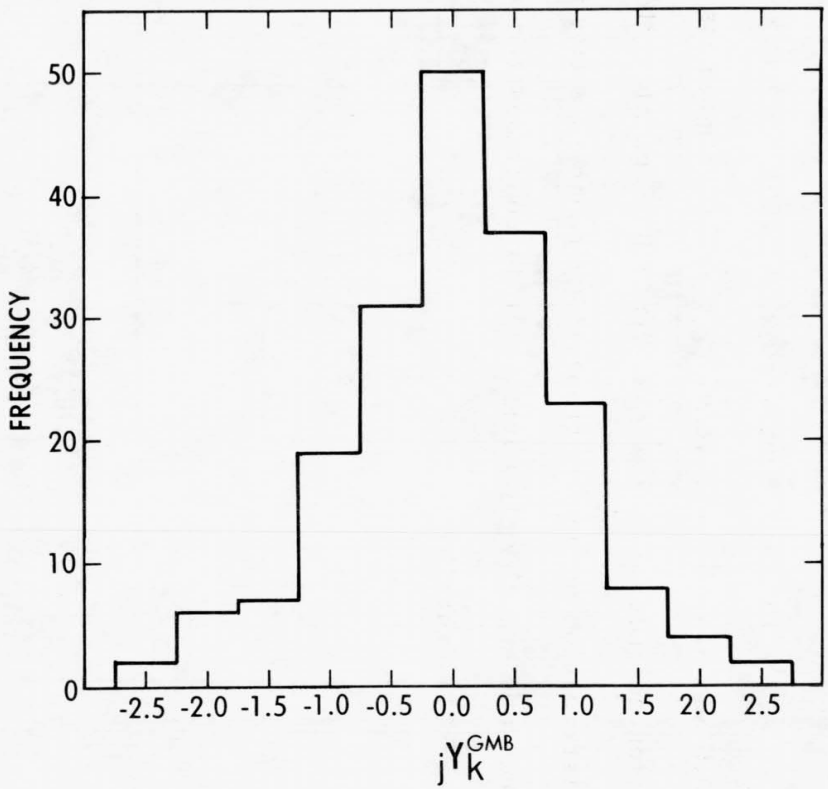

Figure A2.--The distribution of observed values, $_jY_k^{GMB}$.

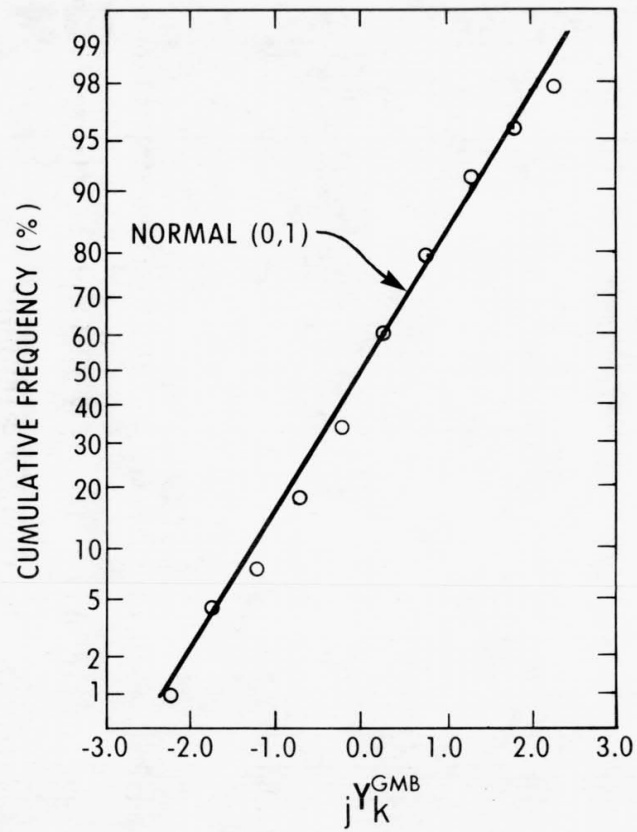

Figure A3.--Normal probability plot of $_jY_k^{GMB}$.

$$ {}_jY_k^{GMB} = [\mathrm{Log}_{10}({}_jSTF_k^{GMB}) - \mathrm{Log}_{10}({}_j\hat{X}_k^{GMB})]/SD $$

where

$SD = \mathrm{Log}_{10}\ 1.38$ (see table 4, and text above),

and $\hat{X}$ is defined above.

If it can be shown that y is distributed as n(0,1) then STF follows a log-normal distribution. The distribution of y is shown in figure A2, and the mean and standard deviation for these data are:

$$\mu = 1.7 \times 10^{-5}$$

$$\sigma = 0.943$$

$$n = \text{number of values} = 191$$

The skewness ($\beta_1 = 6.7 \times 10^{-2}$)and kurtosis ($\beta_2 = 3.55$) are not significantly different than 0.0 and 3.0, respectively. A χ^2-test of goodness-of-fit to the normal distribution can not be rejected at the 5 percent significance level. A plot of the distribution on normal probability paper is shown in figure A3 and indicates the data are closely normal. It is concluded then that observed STF's are log-normally distributed.

APPENDIX B

Nuclear-event time histories listed alphabetically by nuclear event.

VERTICAL COMPONENT
EVENT BACKBEACH

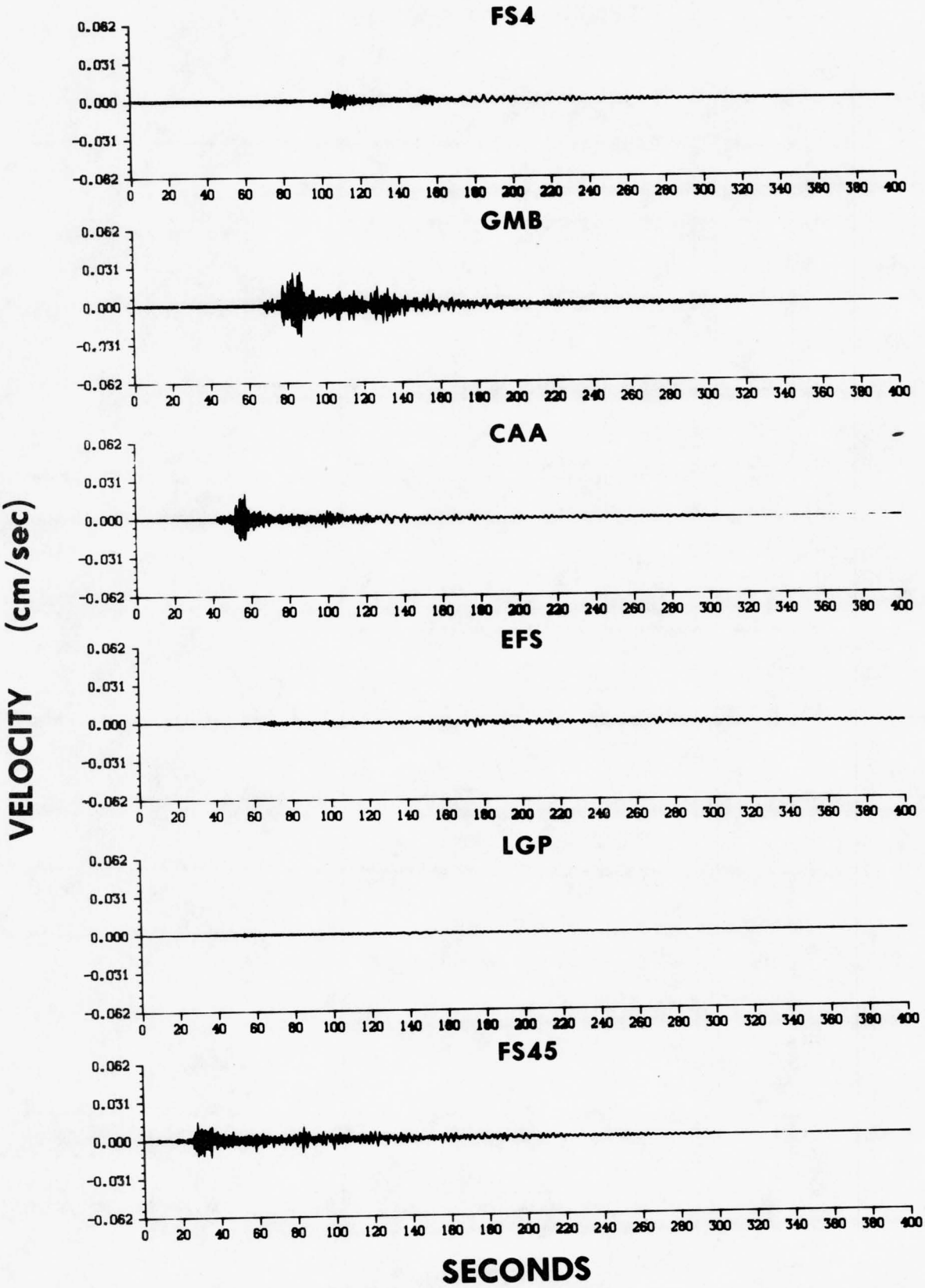

VERTICAL COMPONENT
EVENT BACKBEACH

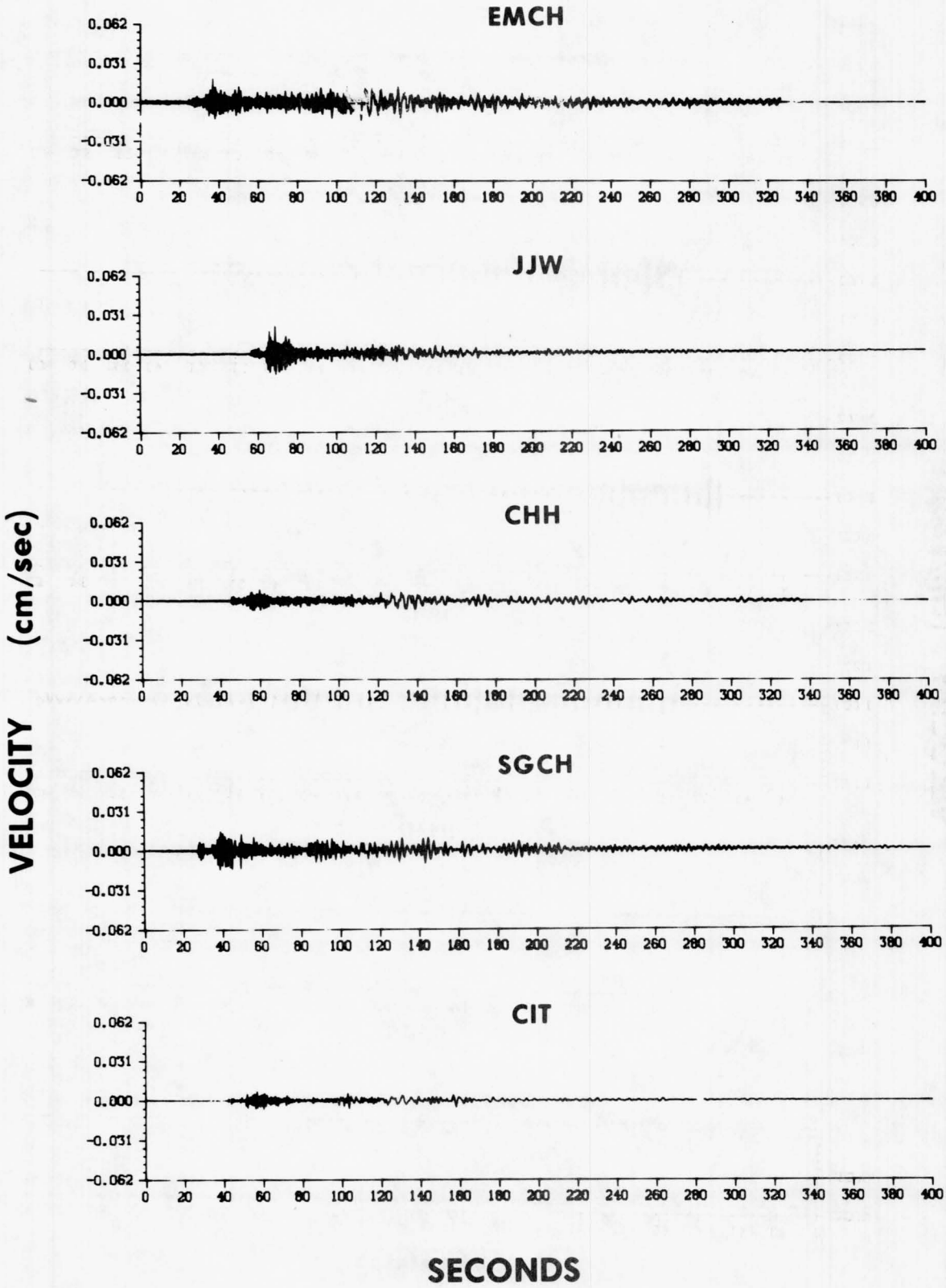

TRANSVERSE COMPONENT
EVENT BACKBEACH

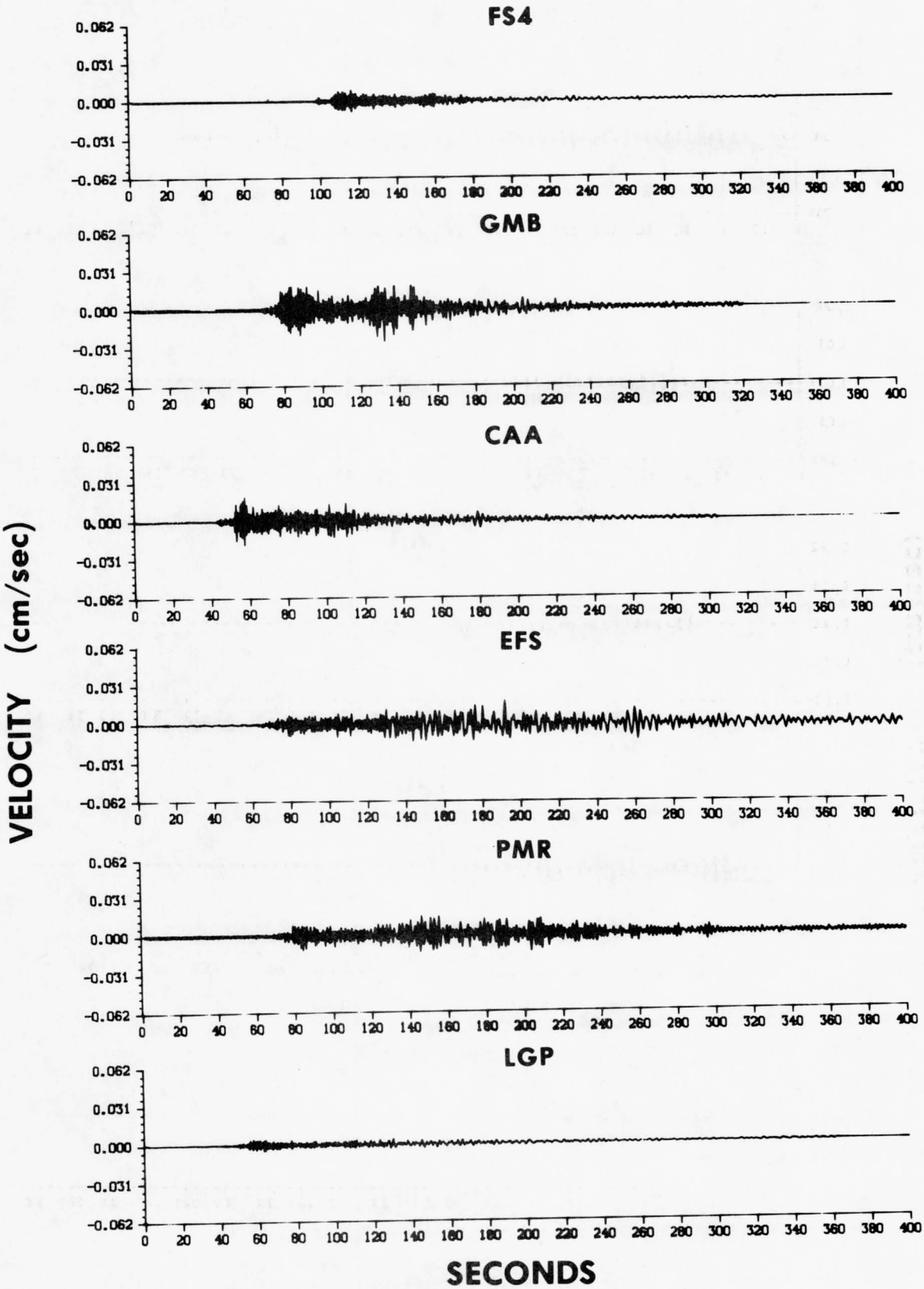

TRANSVERSE COMPONENT
EVENT BACKBEACH

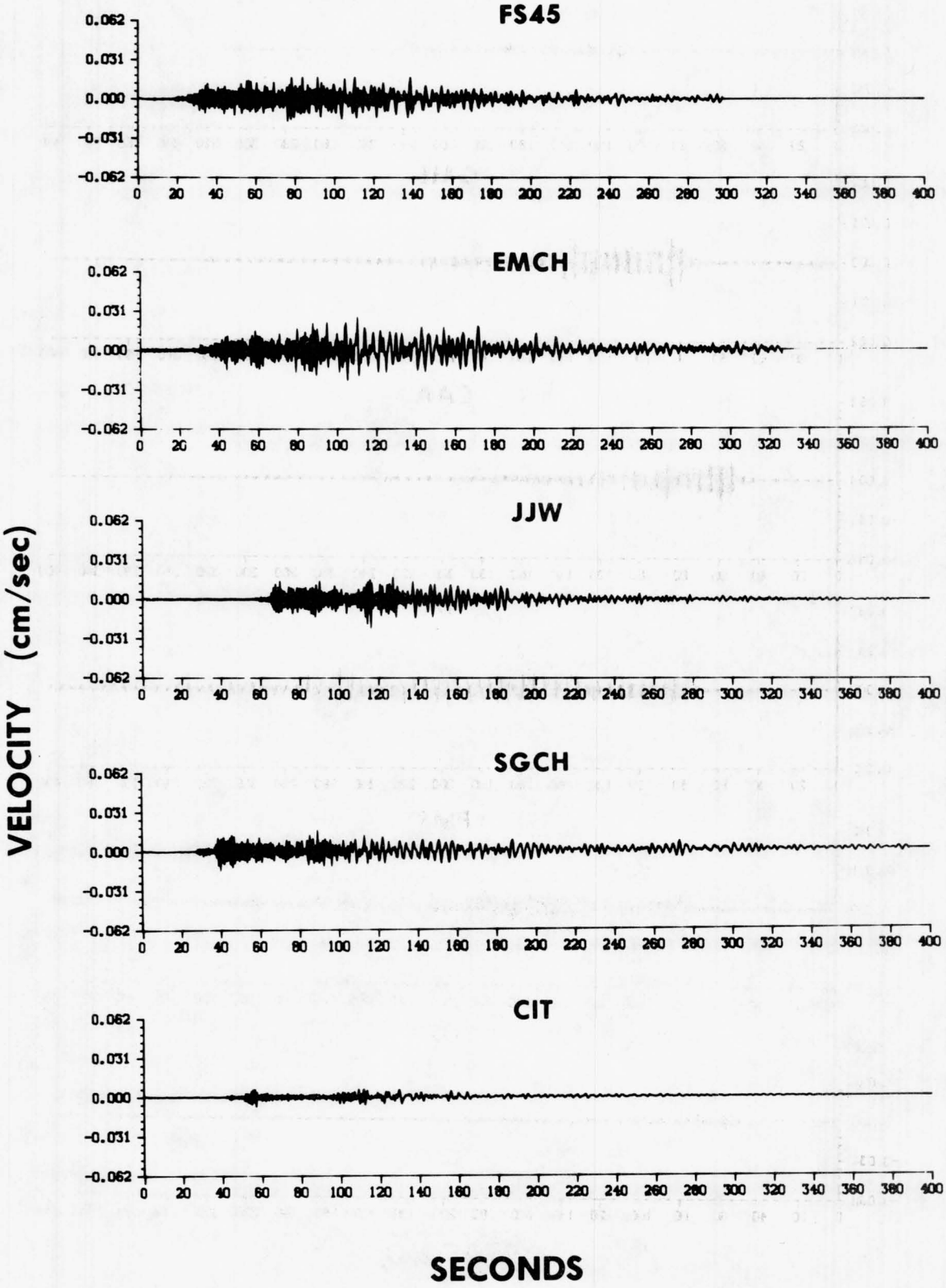

RADIAL COMPONENT
EVENT BACKBEACH

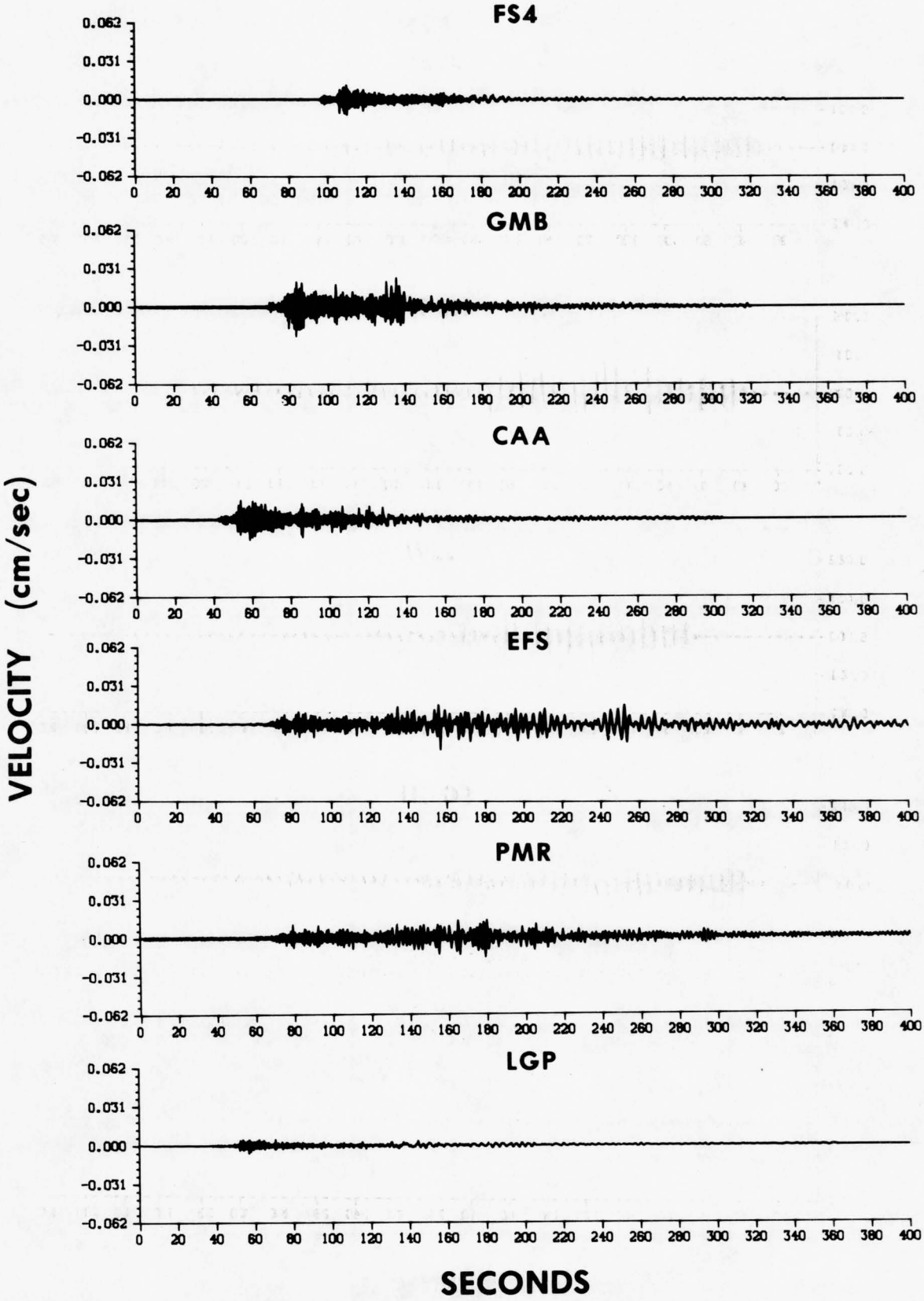

RADIAL COMPONENT
EVENT BACKBEACH

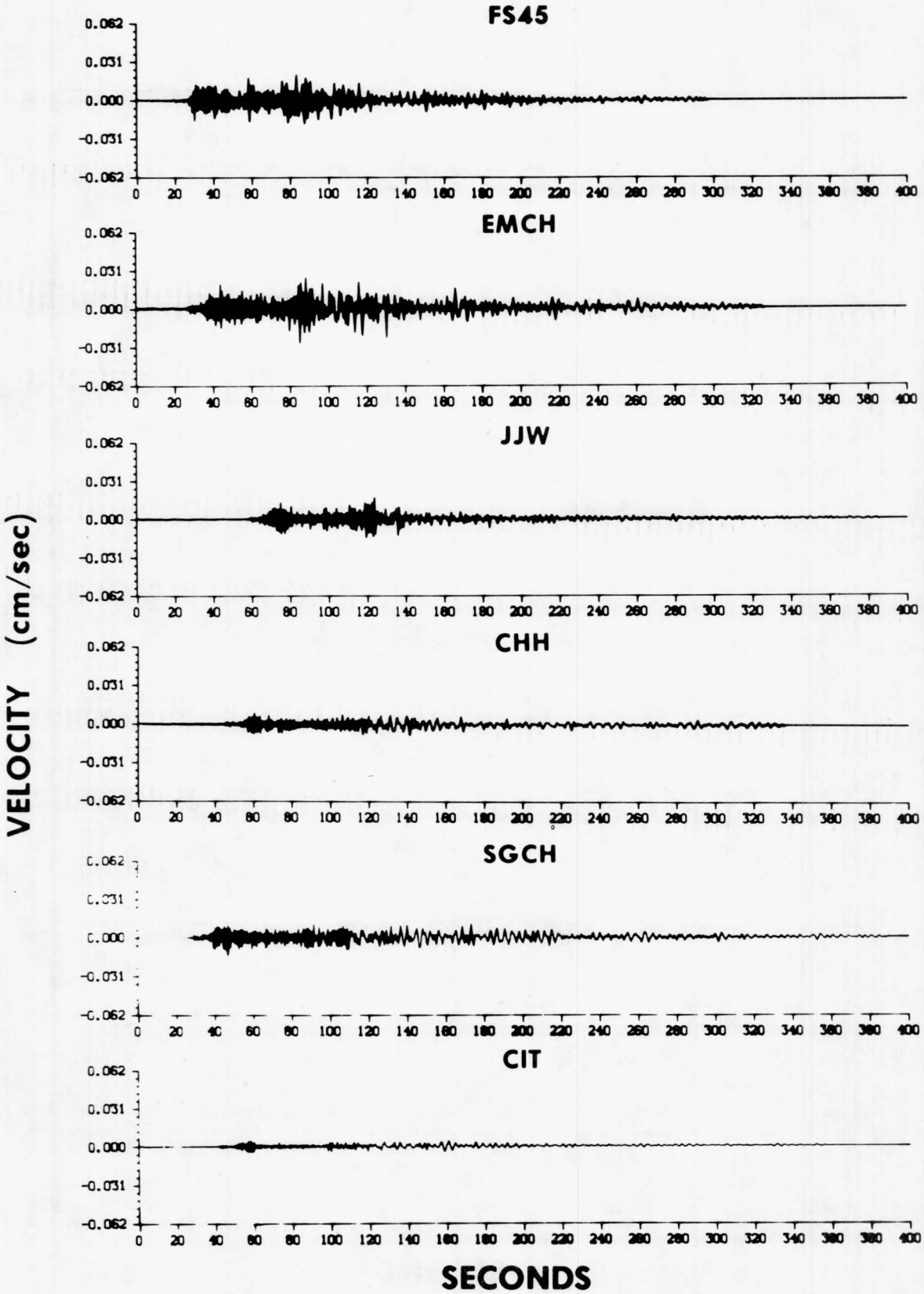

VERTICAL COMPONENT
EVENT BILLET

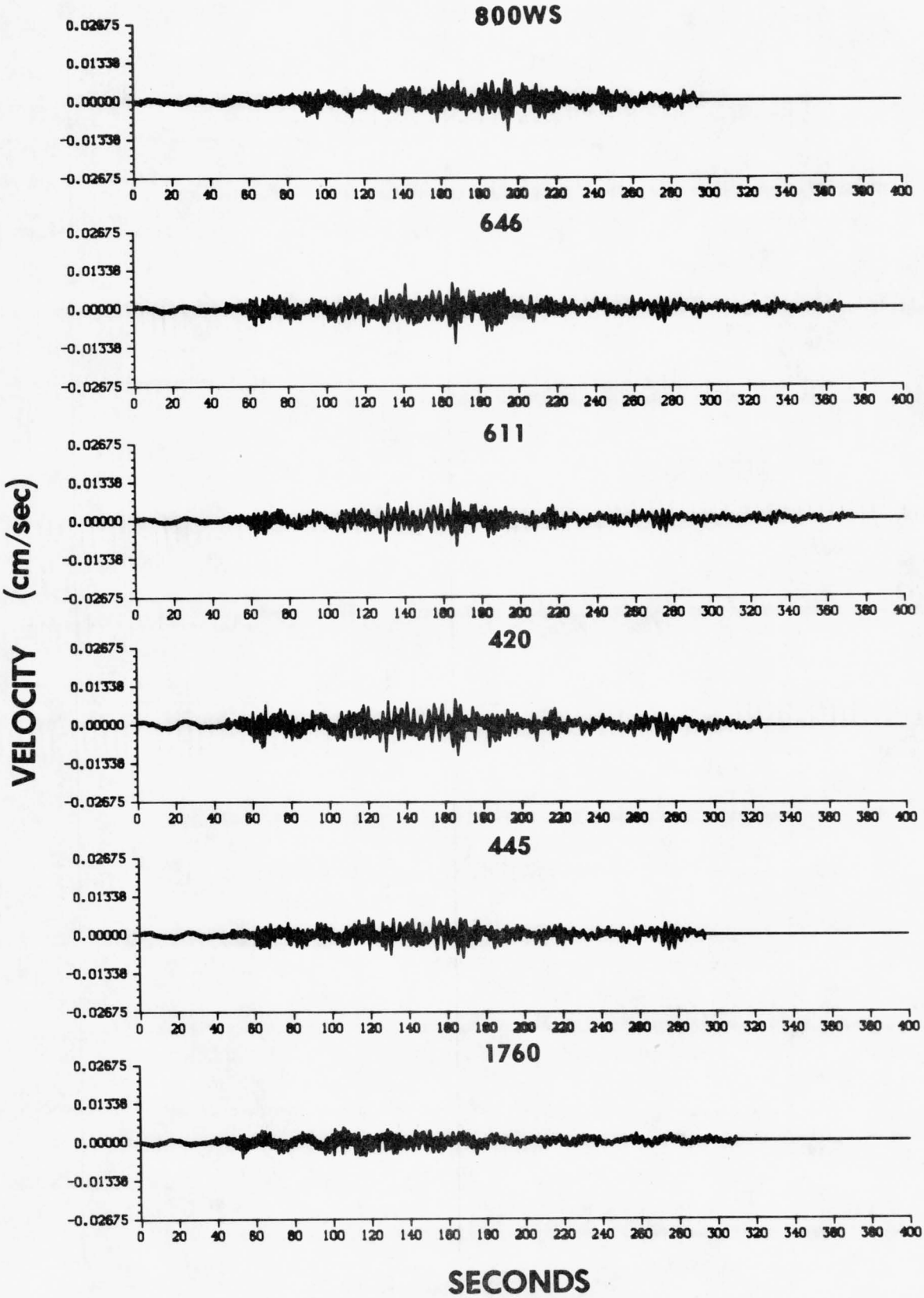

VERTICAL COMPONENT
EVENT BILLET

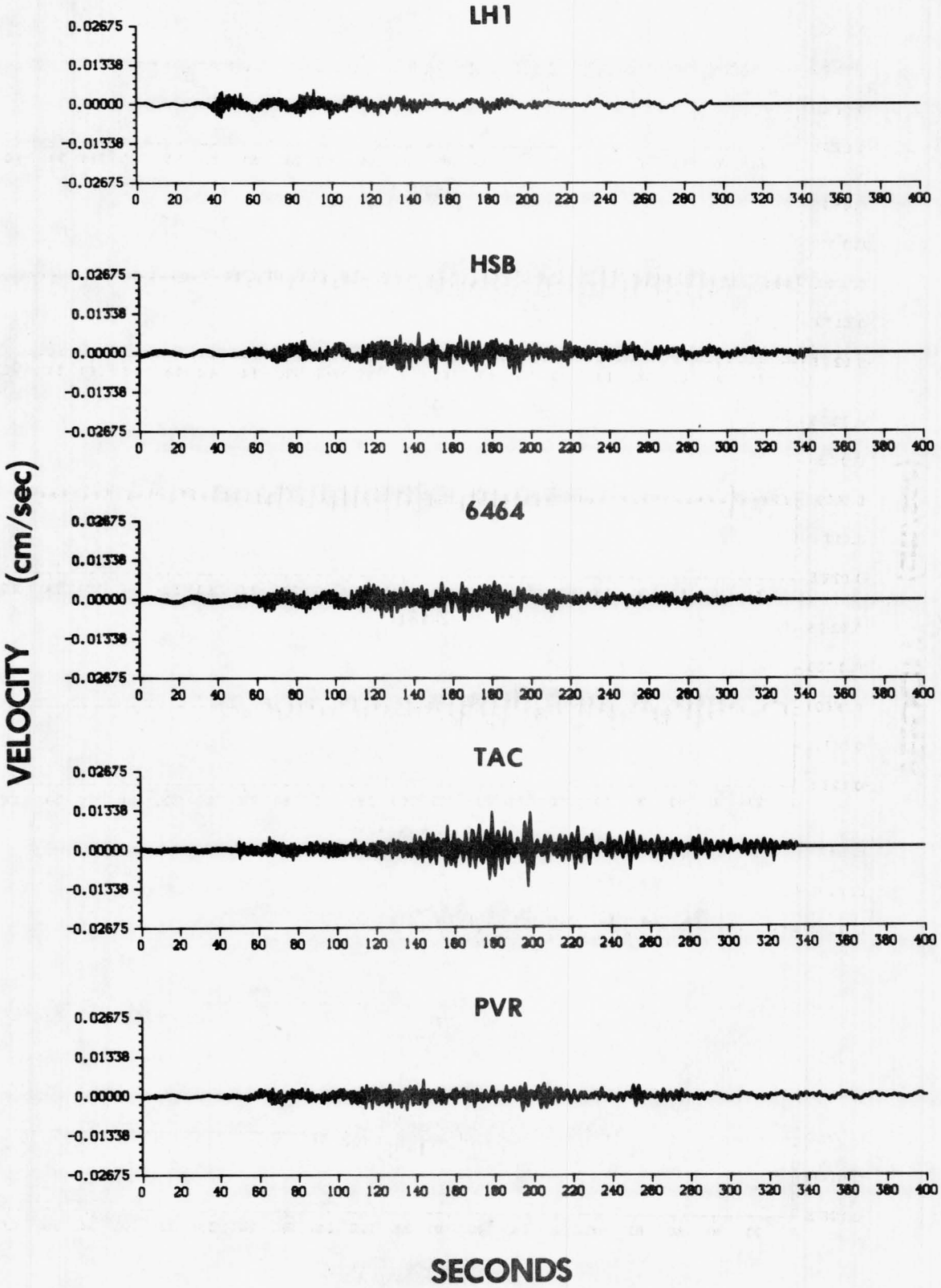

VERTICAL COMPONENT
EVENT BILLET

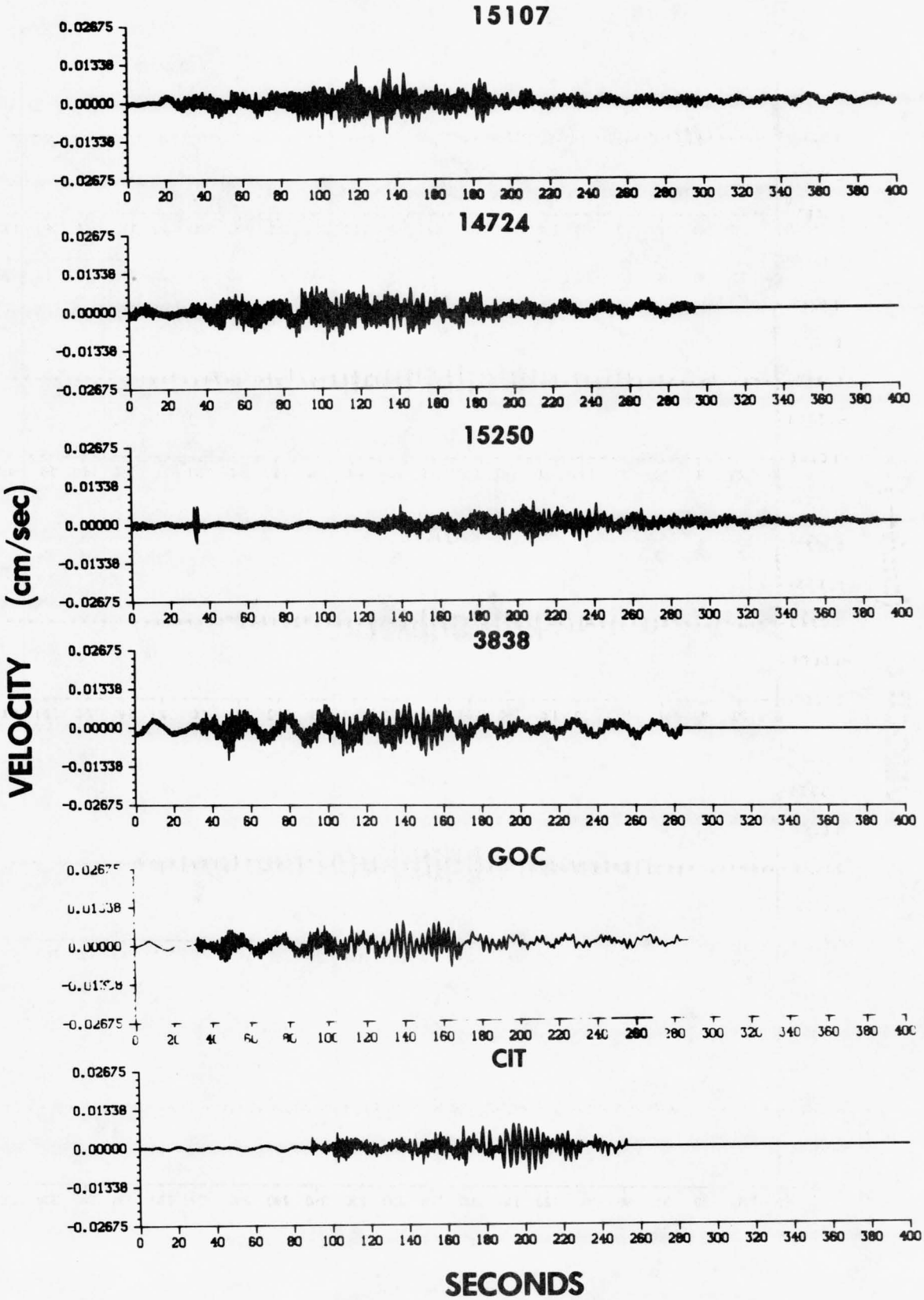

VERTICAL COMPONENT
EVENT BILLET

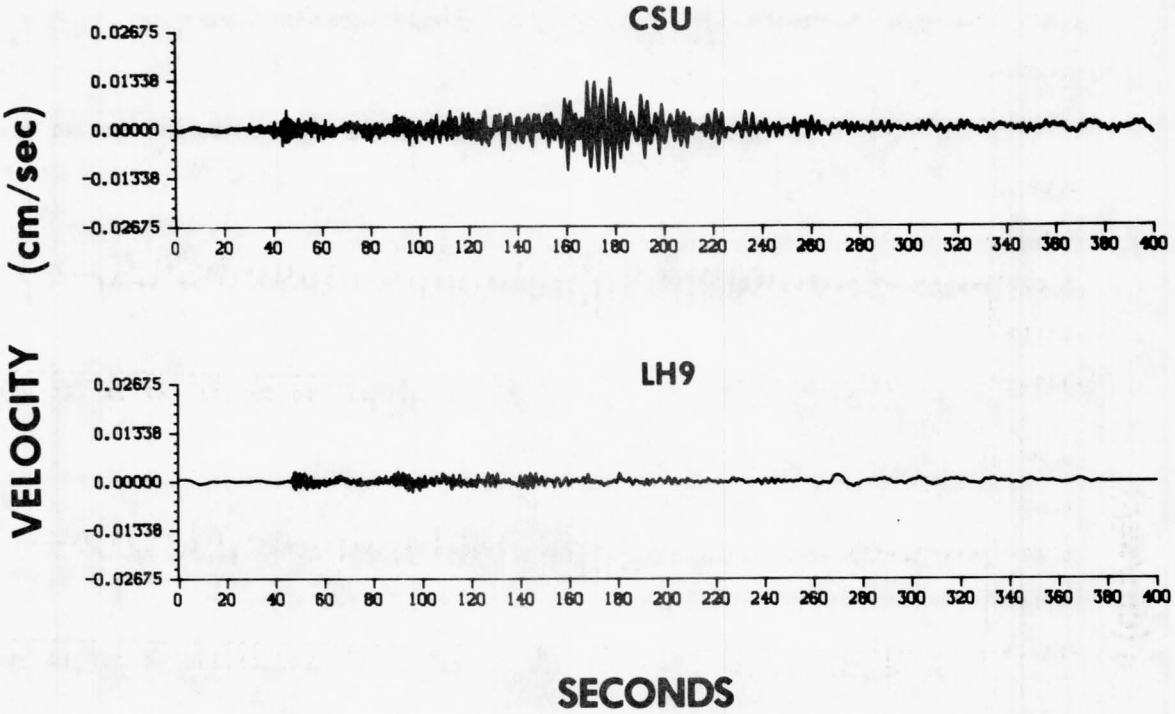

TRANSVERSE COMPONENT
EVENT BILLET

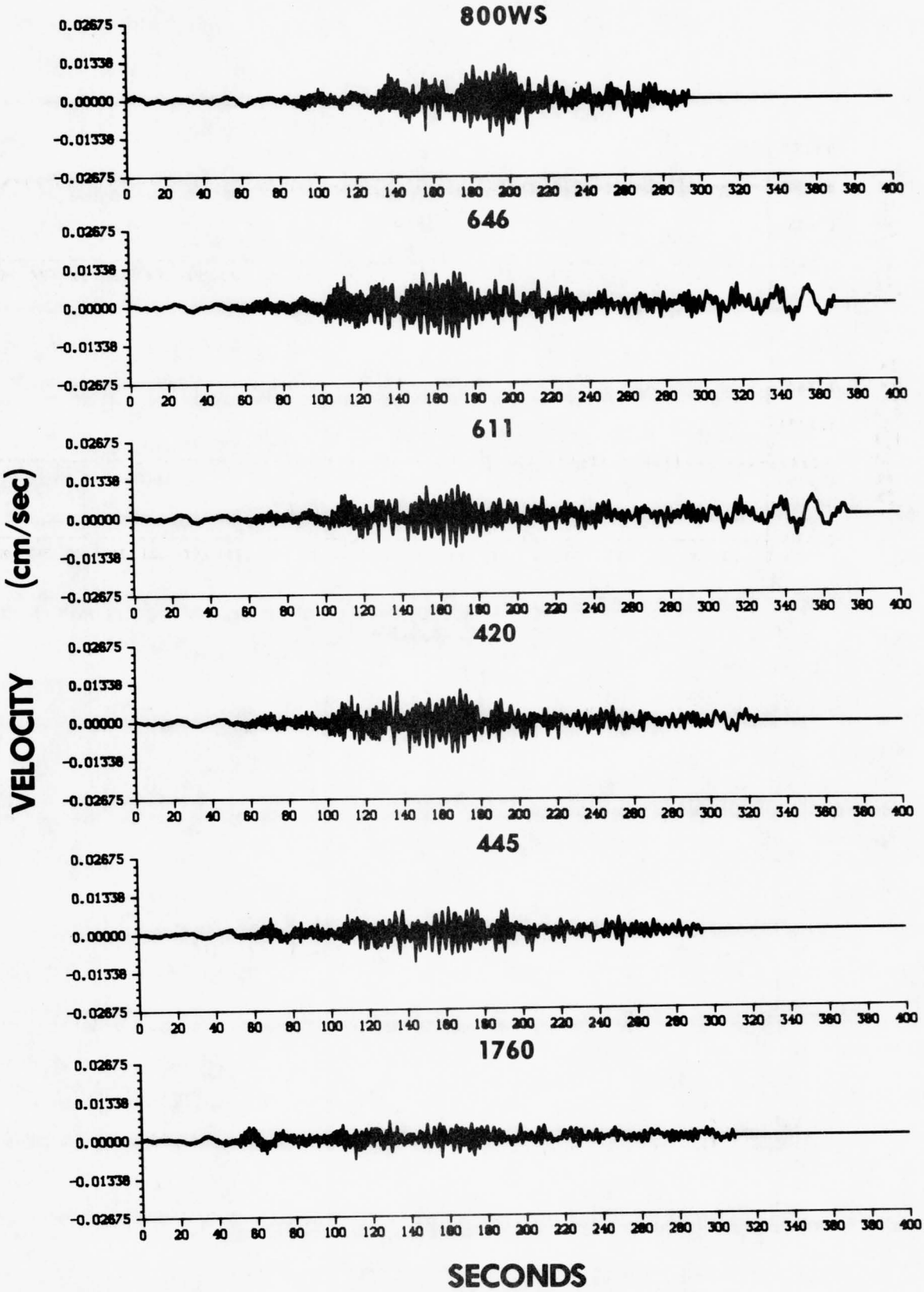

TRANSVERSE COMPONENT
EVENT BILLET

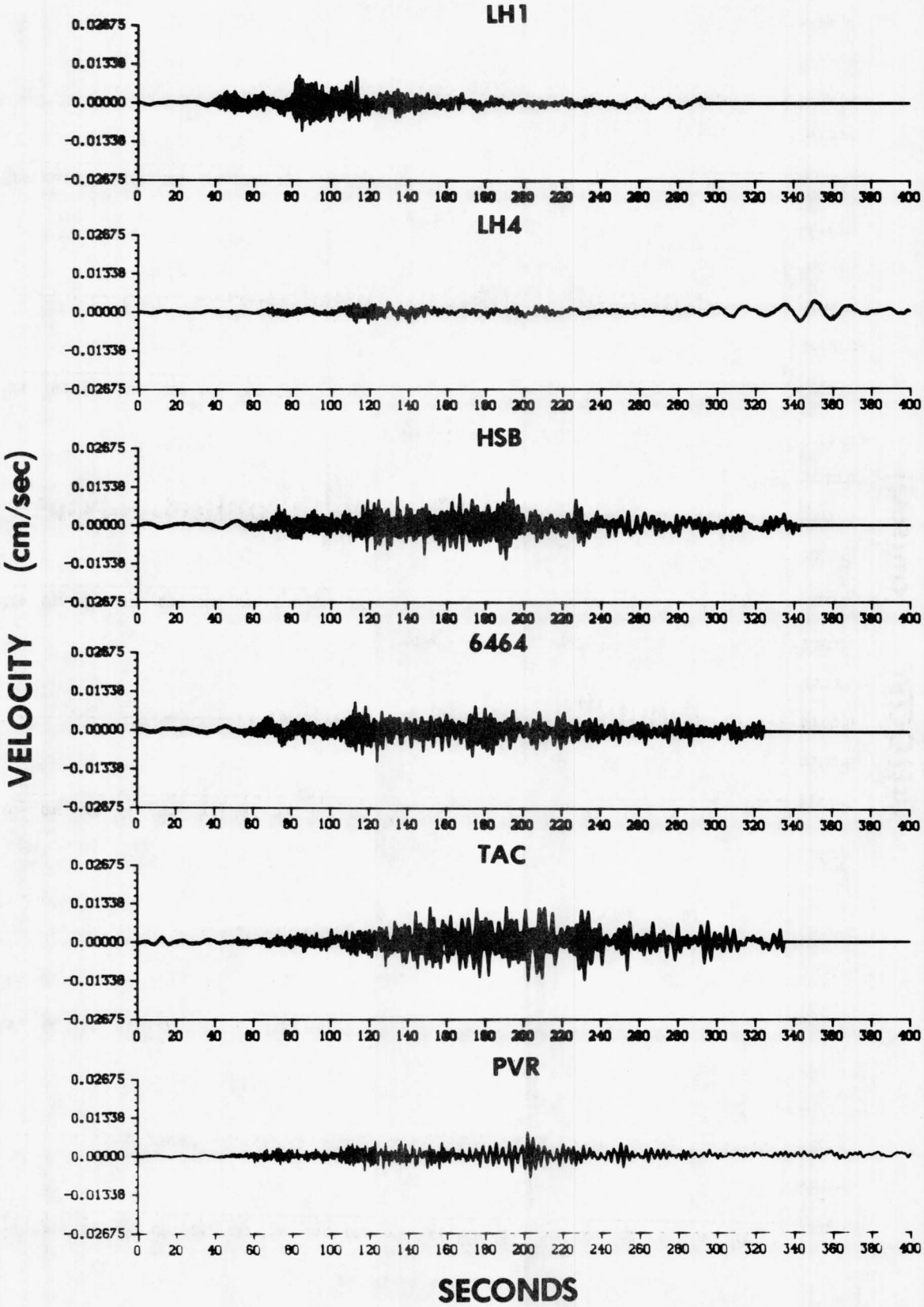

TRANSVERSE COMPONENT

EVENT BILLET

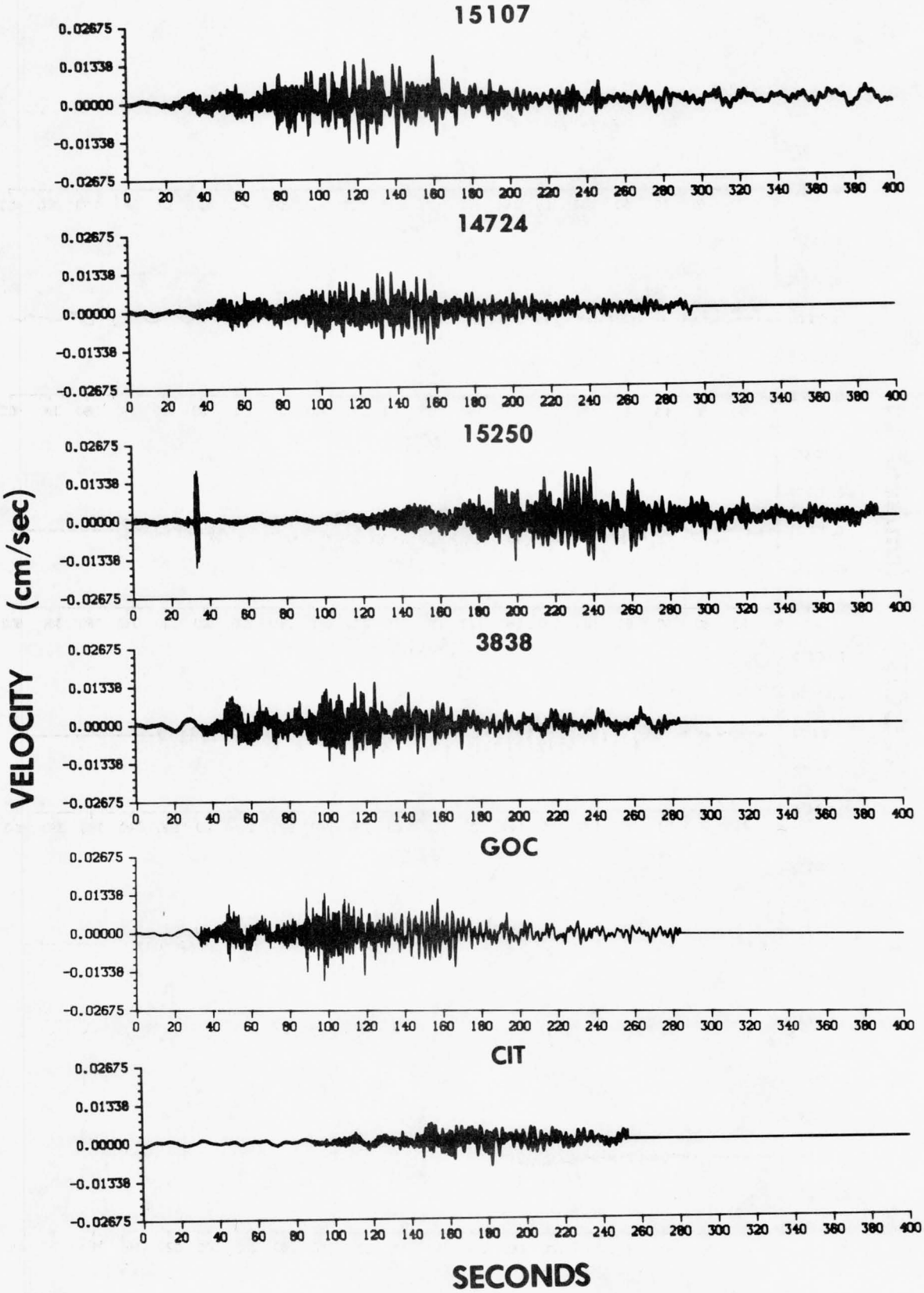

TRANSVERSE COMPONENT
EVENT BILLET

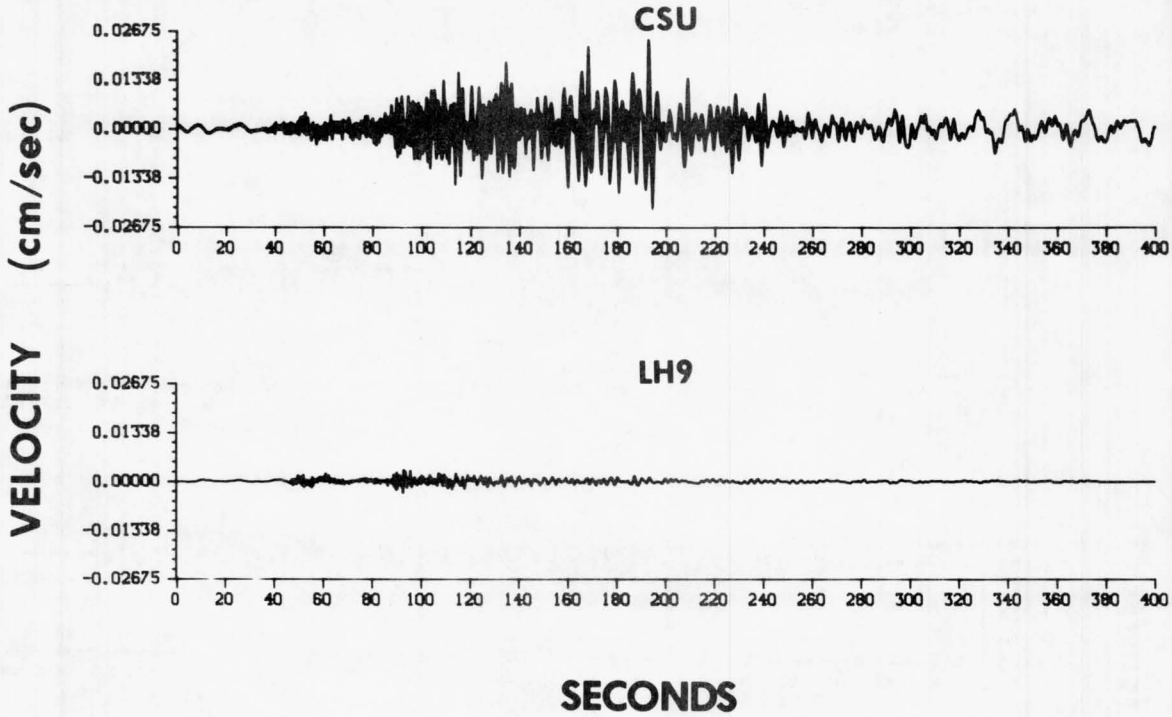

RADIAL COMPONENT
EVENT BILLET

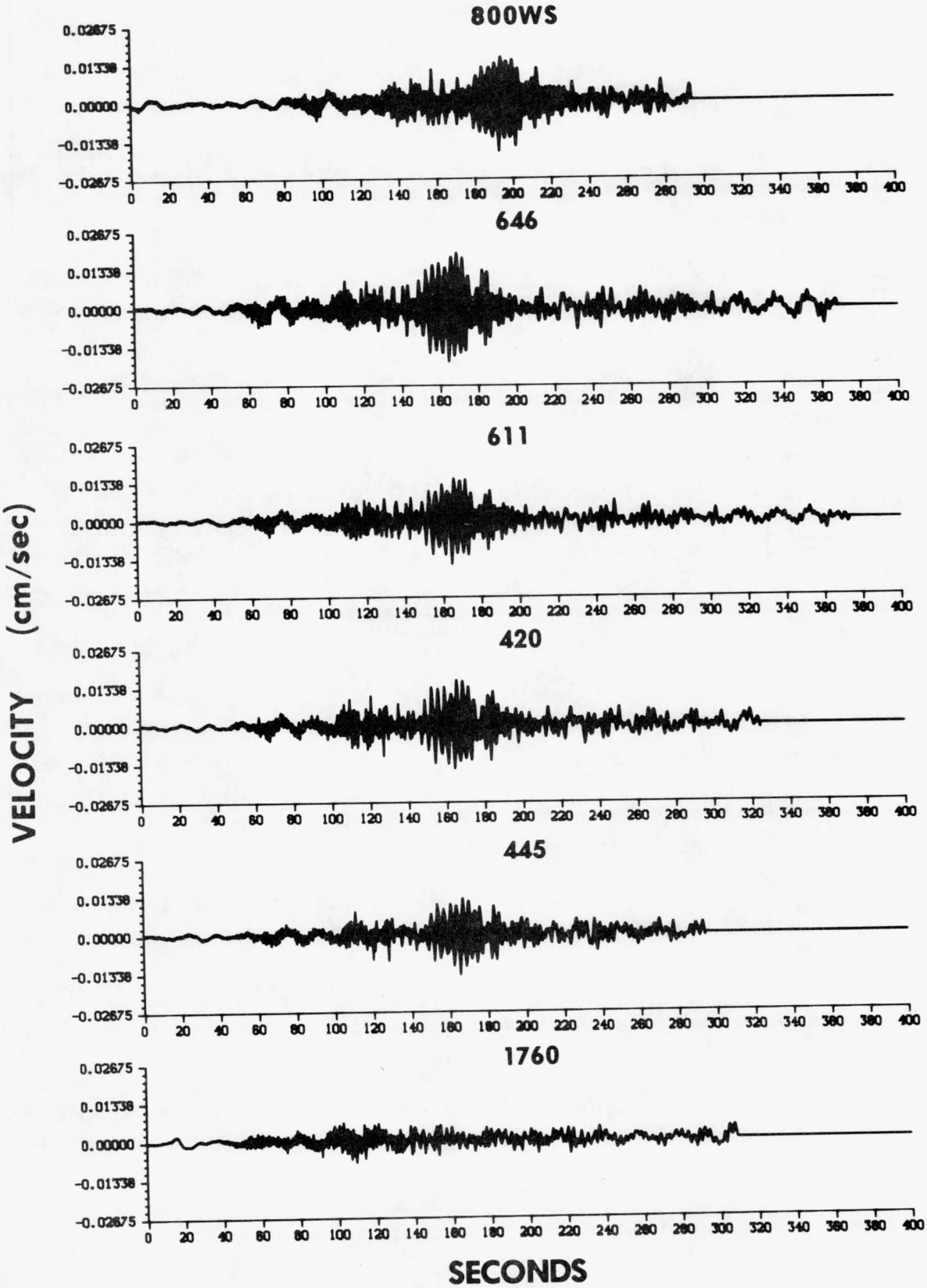

RADIAL COMPONENT
EVENT BILLET

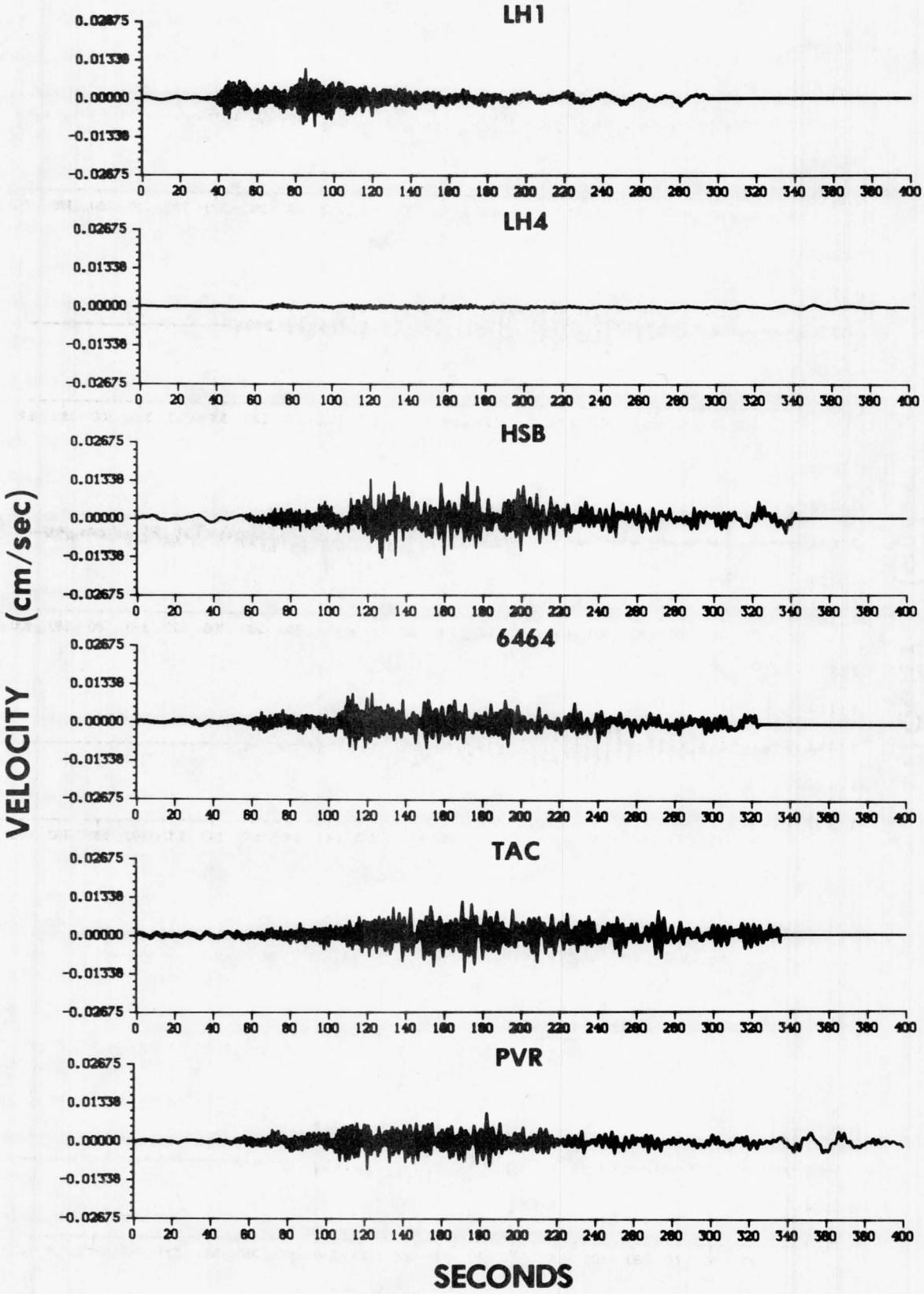

RADIAL COMPONENT
EVENT BILLET

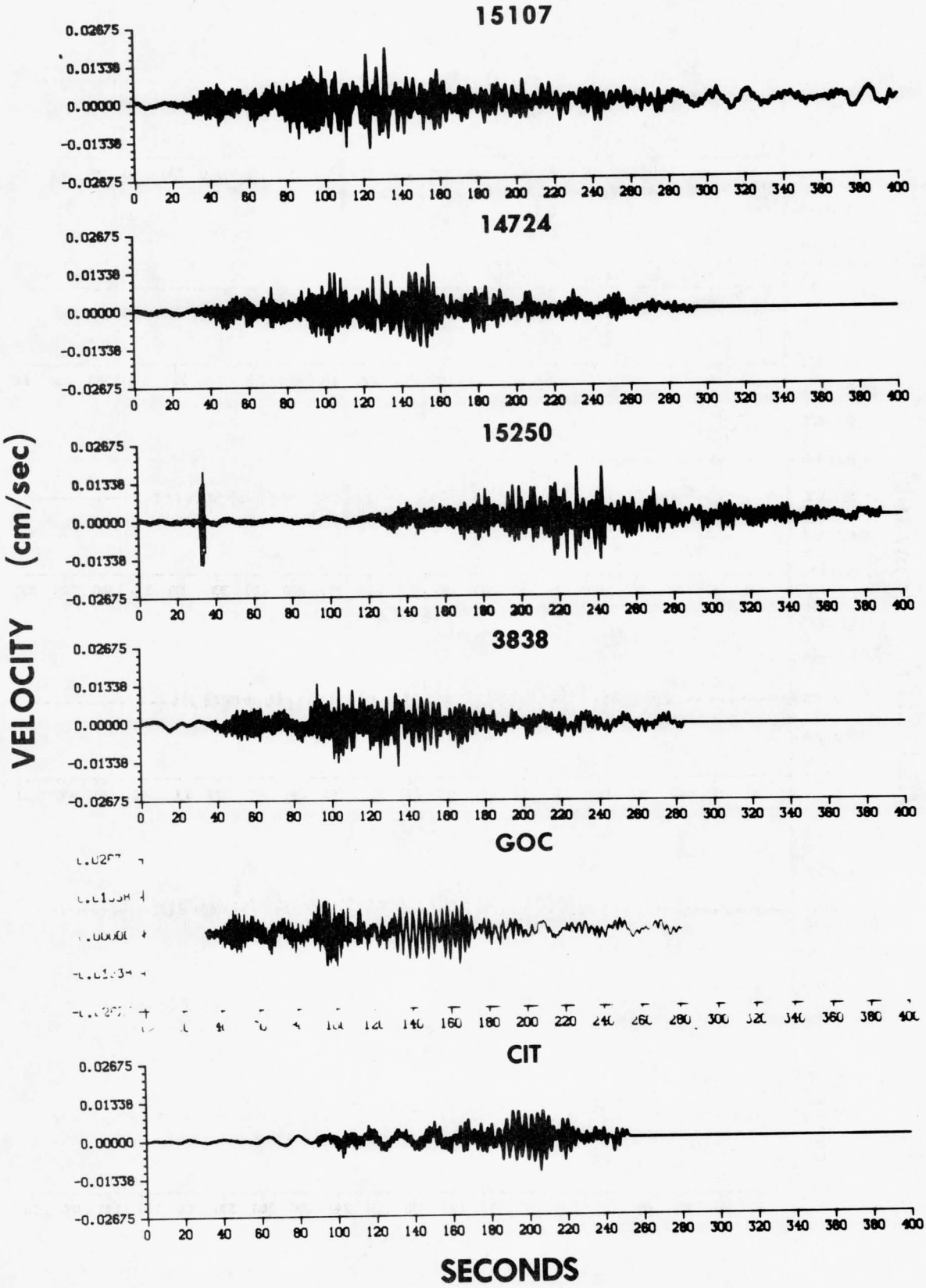

RADIAL COMPONENT
EVENT BILLET

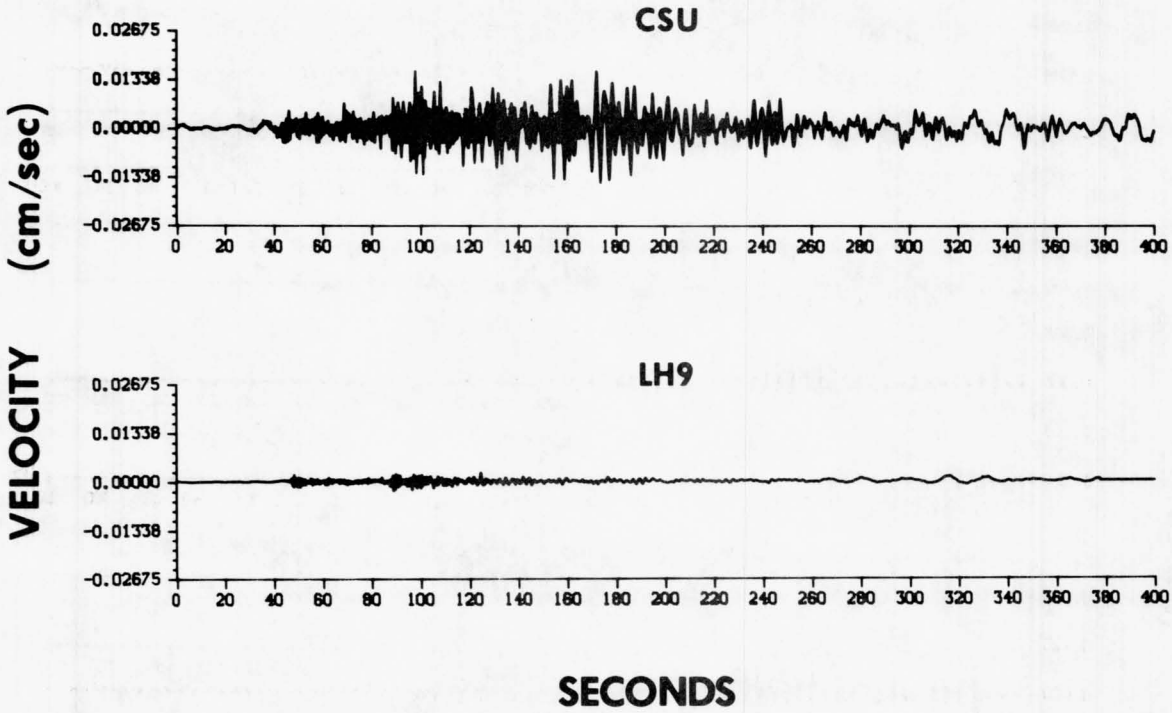

VERTICAL COMPONENT
EVENT CAMEMBERT

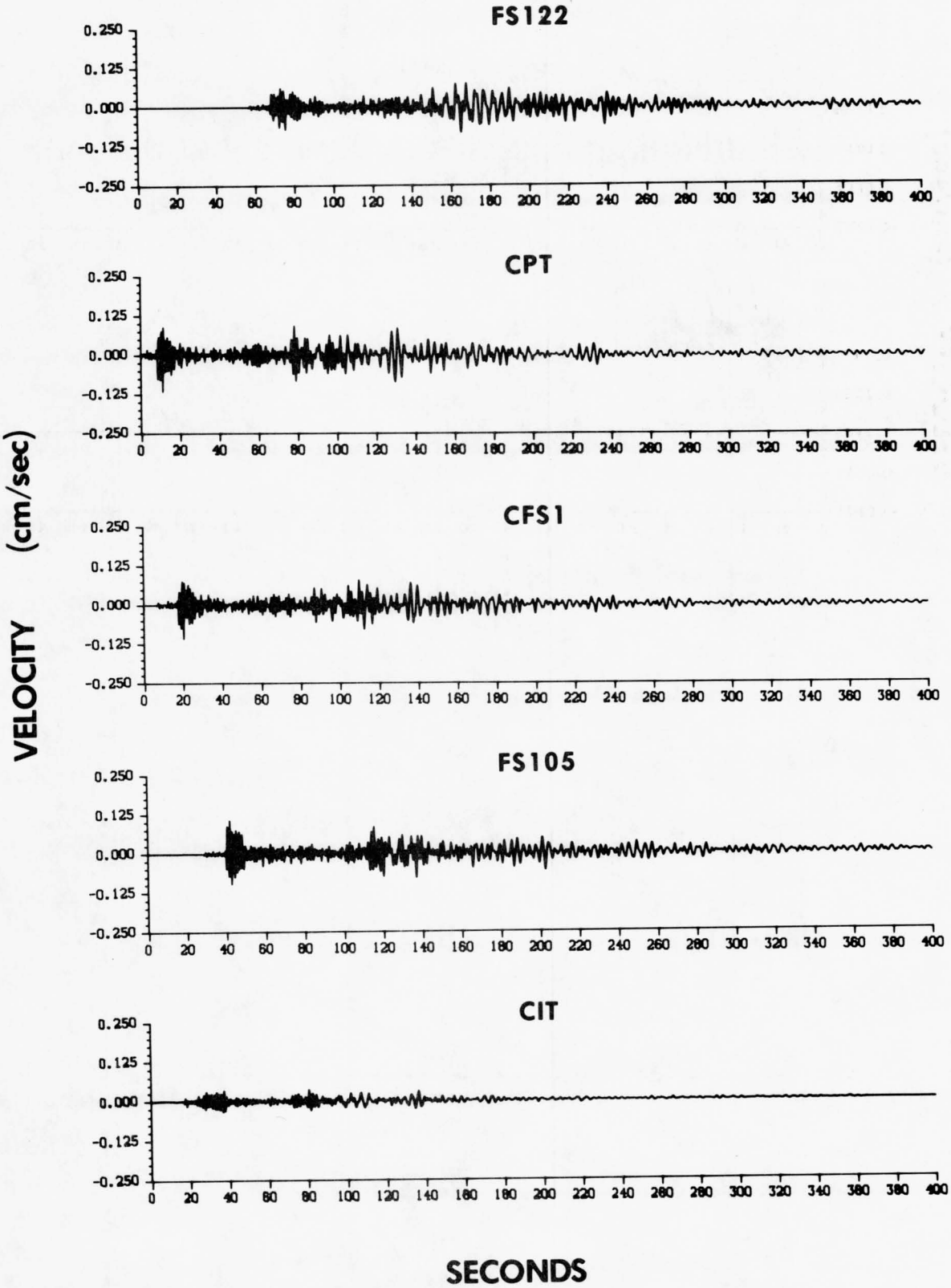

TRANSVERSE COMPONENT
EVENT CAMEMBERT

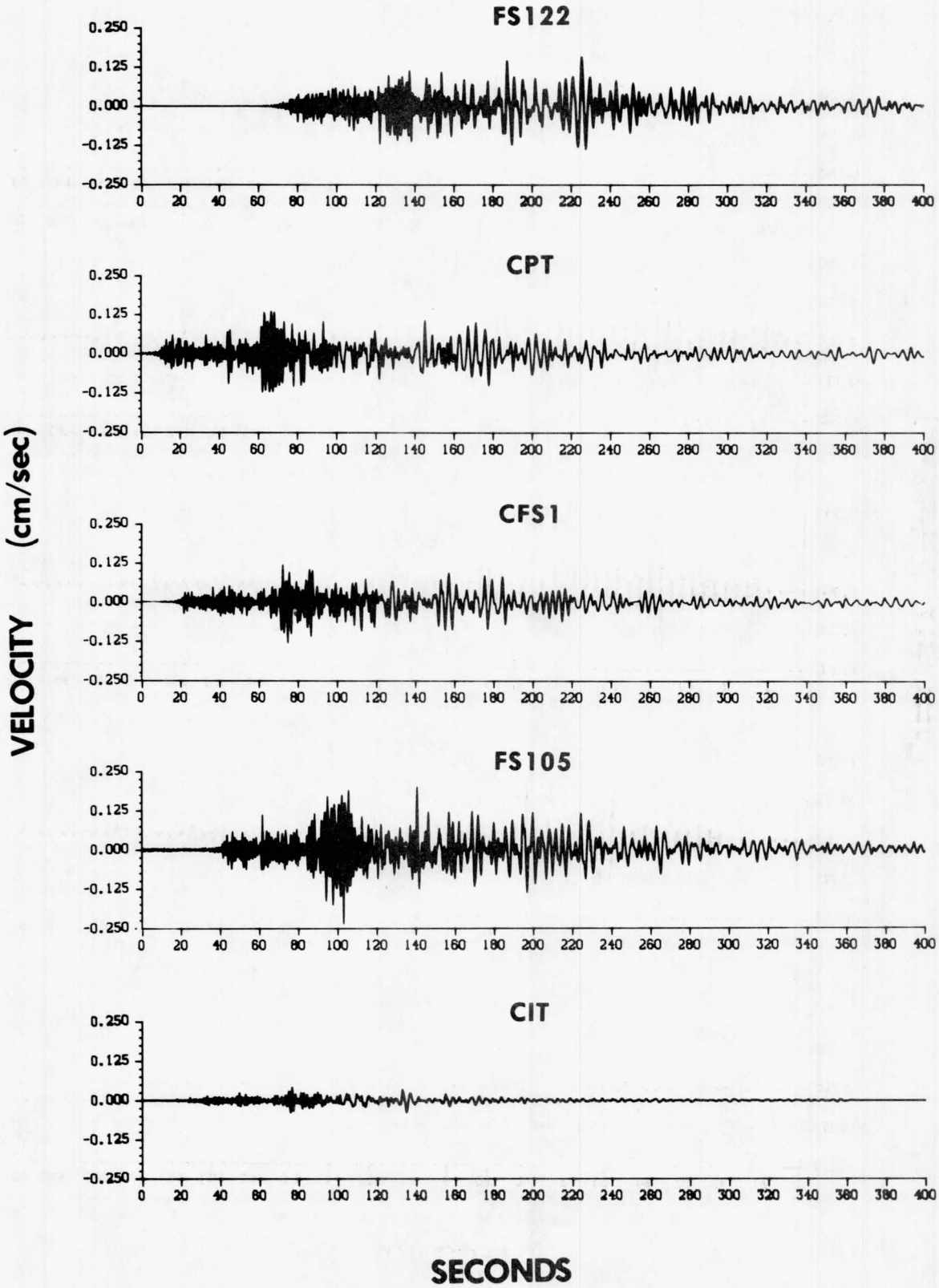

RADIAL COMPONENT
EVENT CAMEMBERT

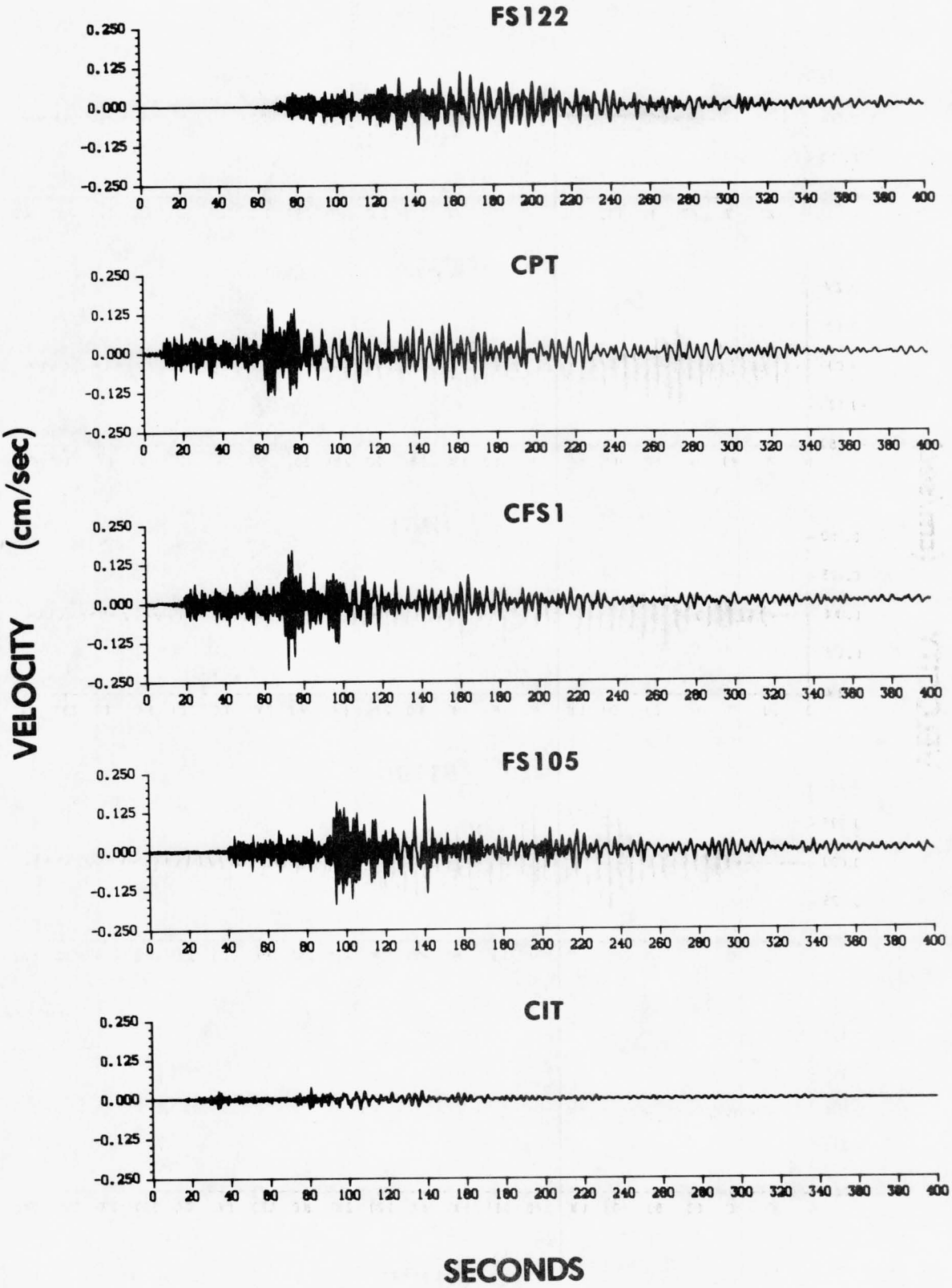

VERTICAL COMPONENT
EVENT CHESIRE

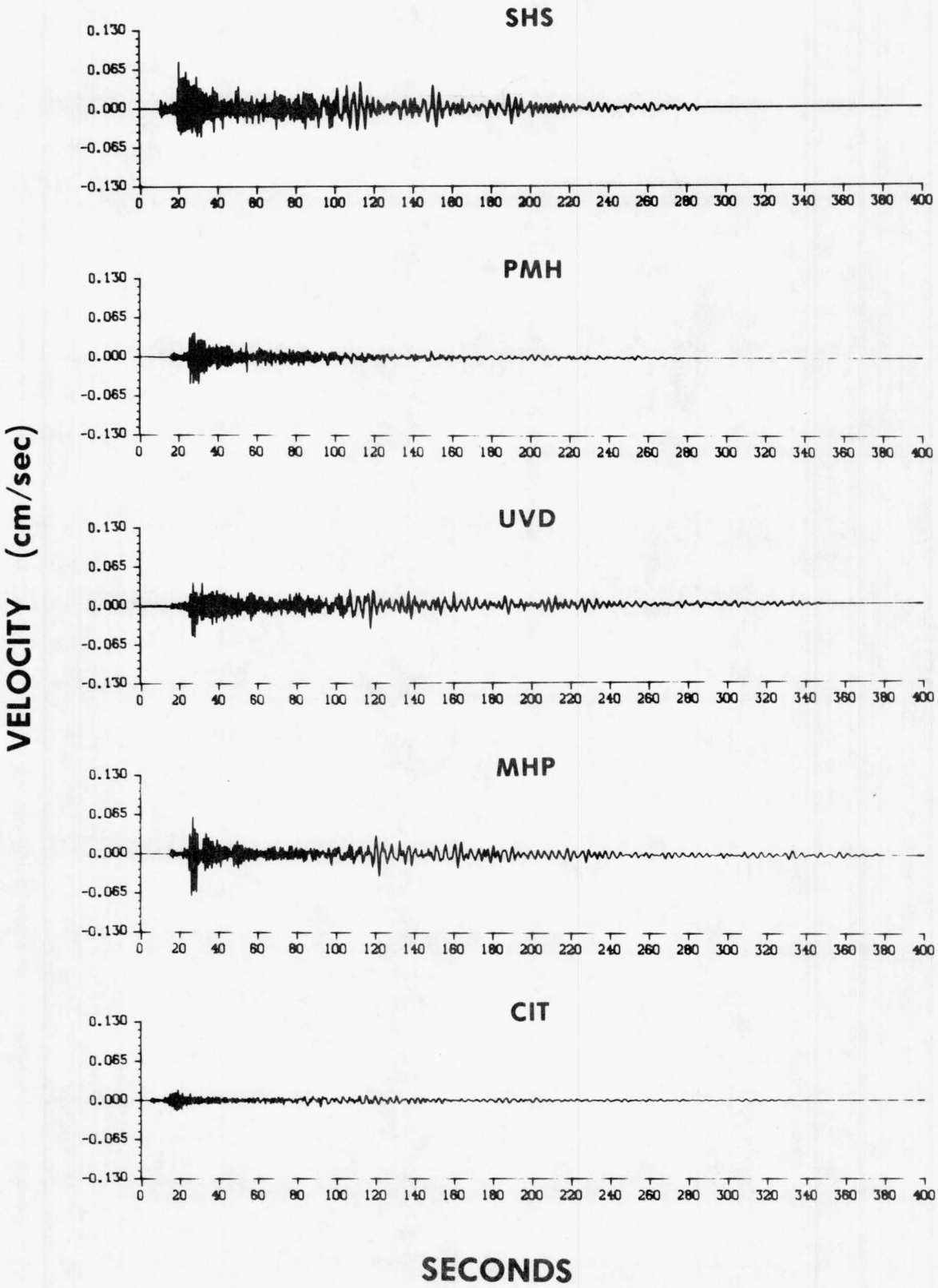

TRANSVERSE COMPONENT
EVENT CHESIRE

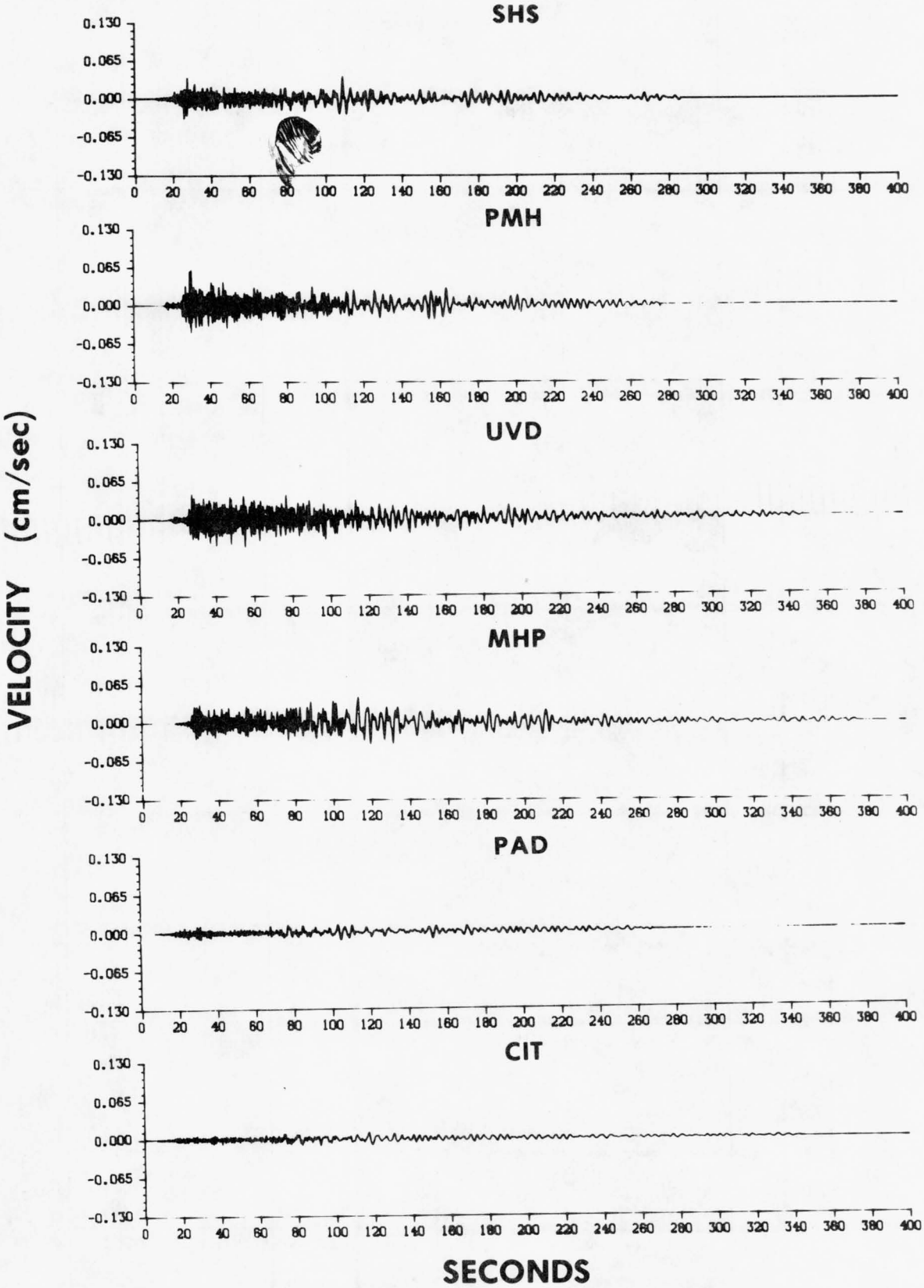

RADIAL COMPONENT
EVENT CHESIRE

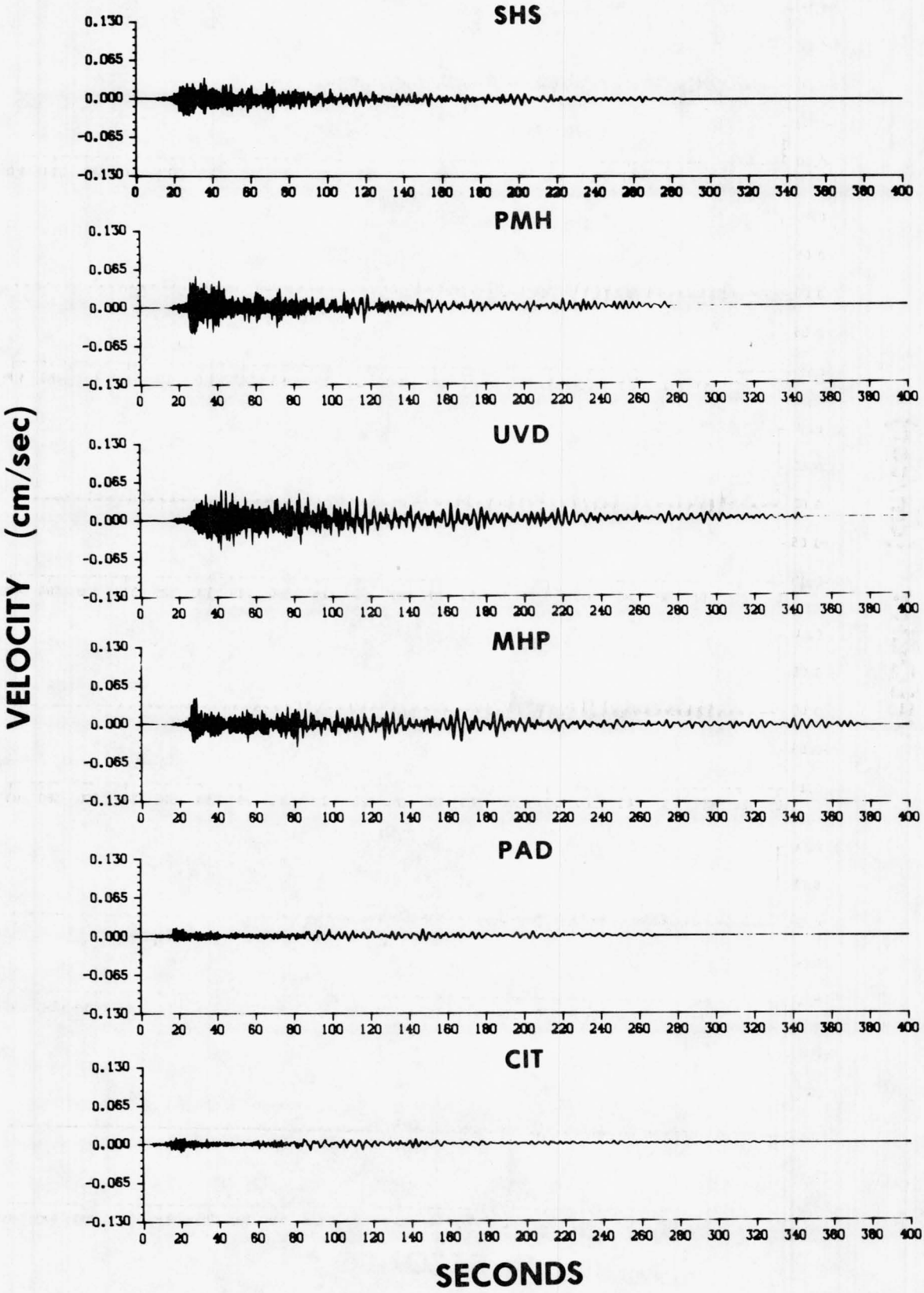

VERTICAL COMPONENT
EVENT CHIBERTA

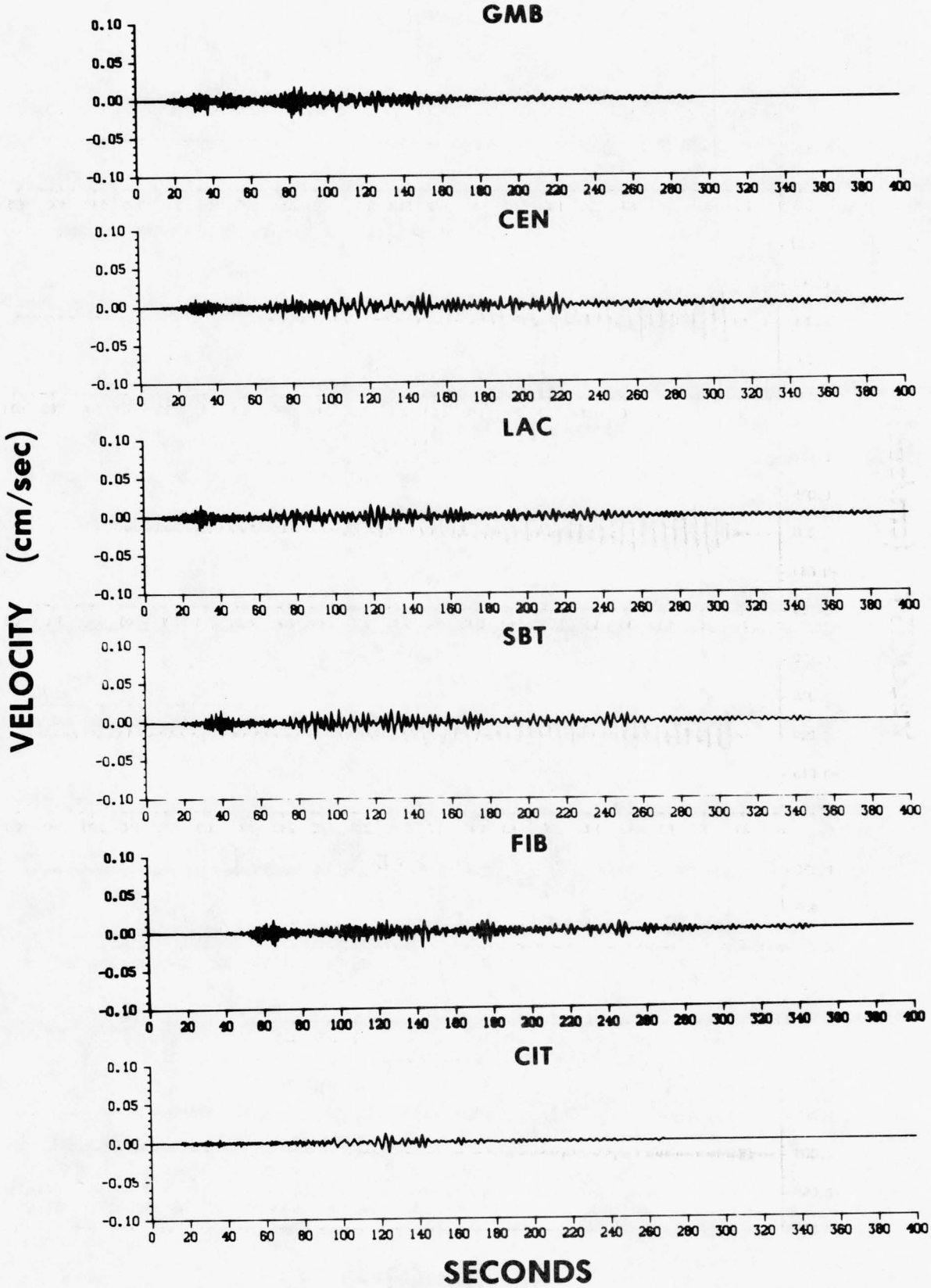

TRANSVERSE COMPONENT
EVENT CHIBERTA

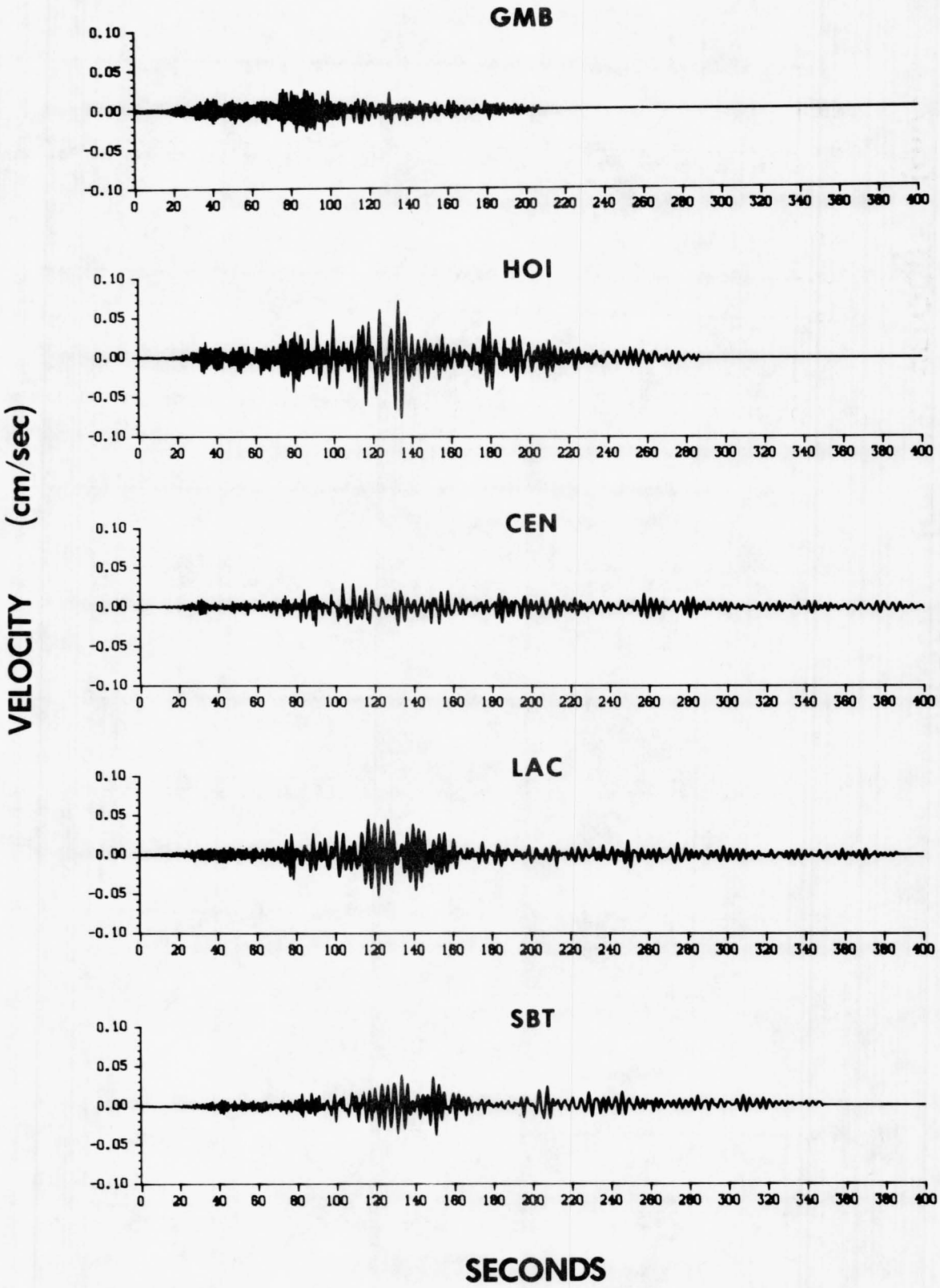

TRANSVERSE COMPONENT
EVENT CHIBERTA

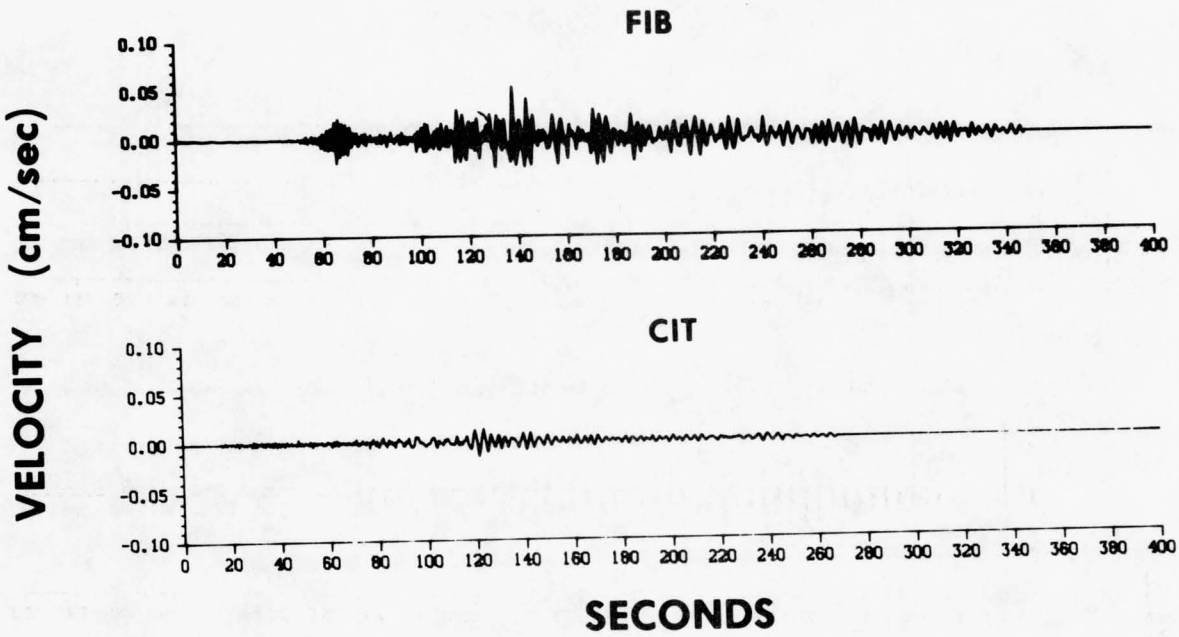

RADIAL COMPONENT
EVENT CHIBERTA

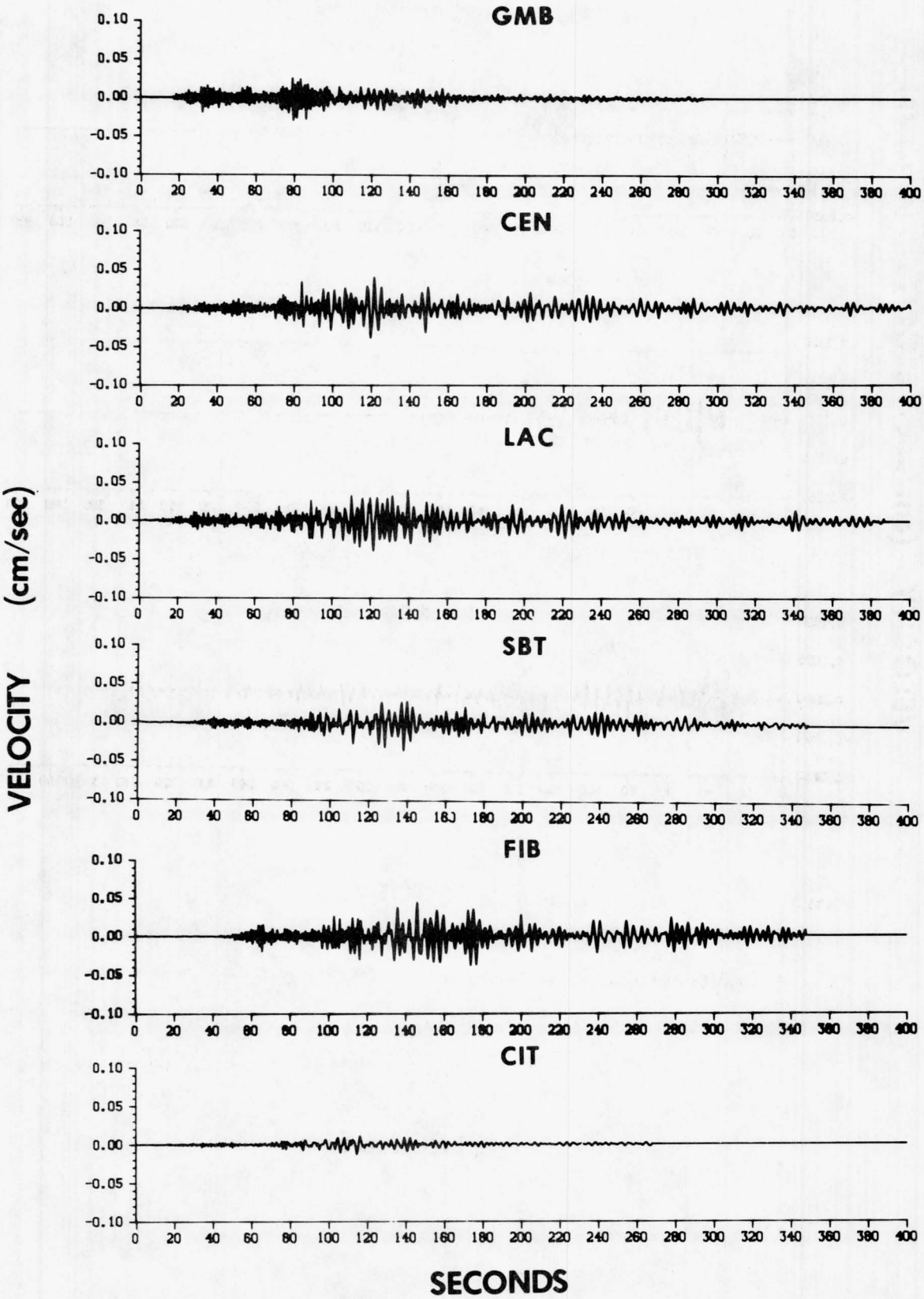

VERTICAL COMPONENT
EVENT COLBY

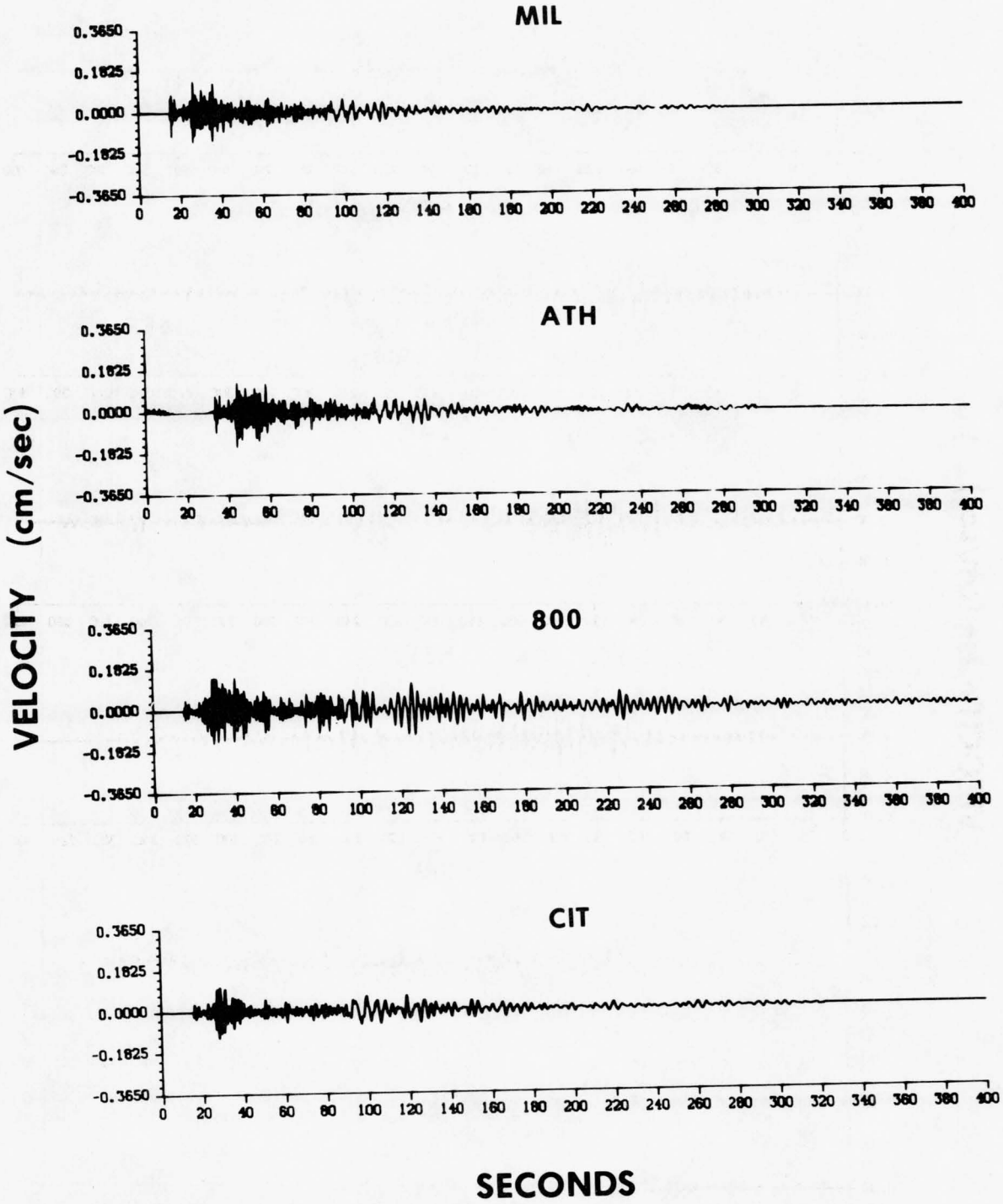

TRANSVERSE COMPONENT
EVENT COLBY

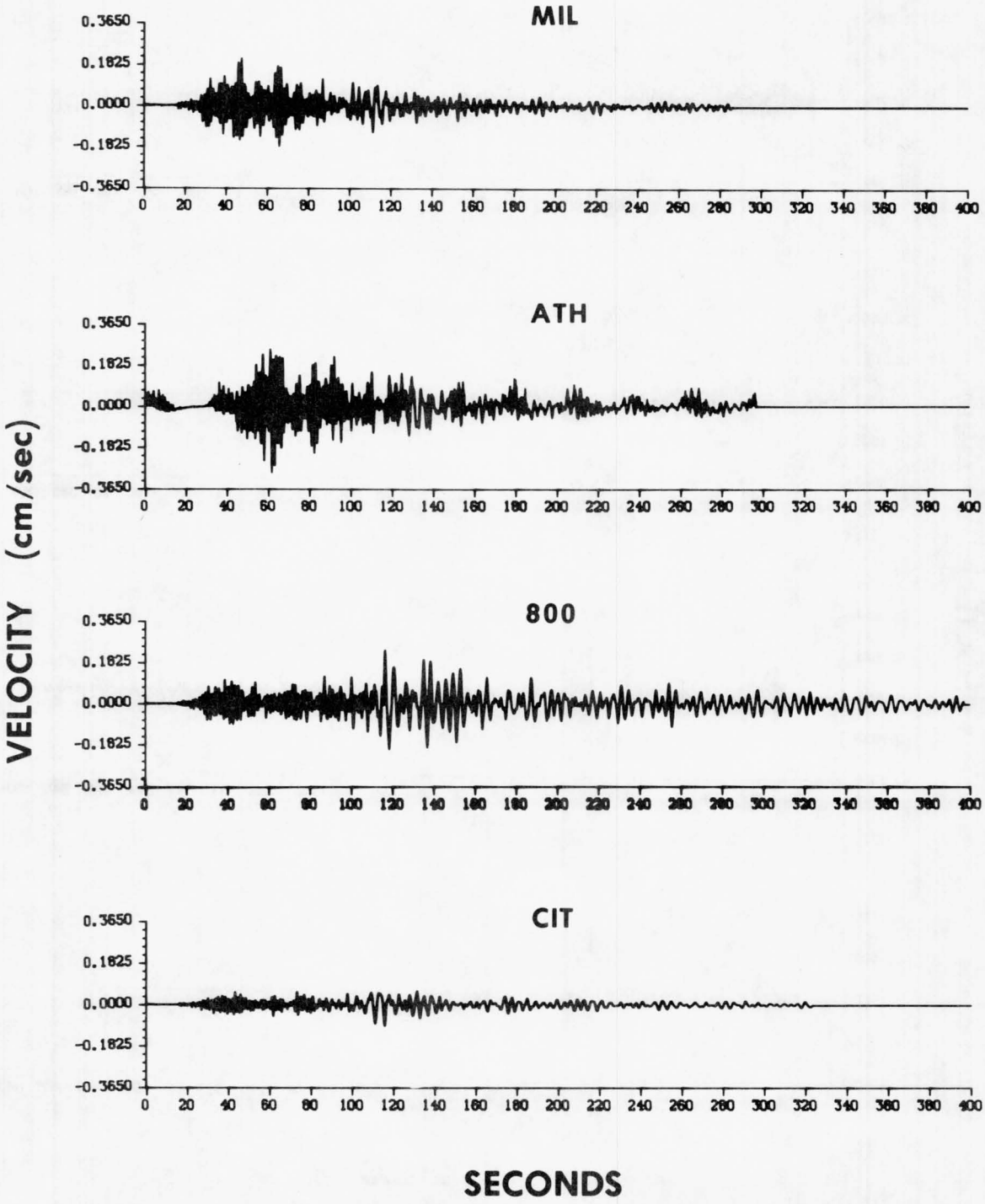

RADIAL COMPONENT
EVENT COLBY

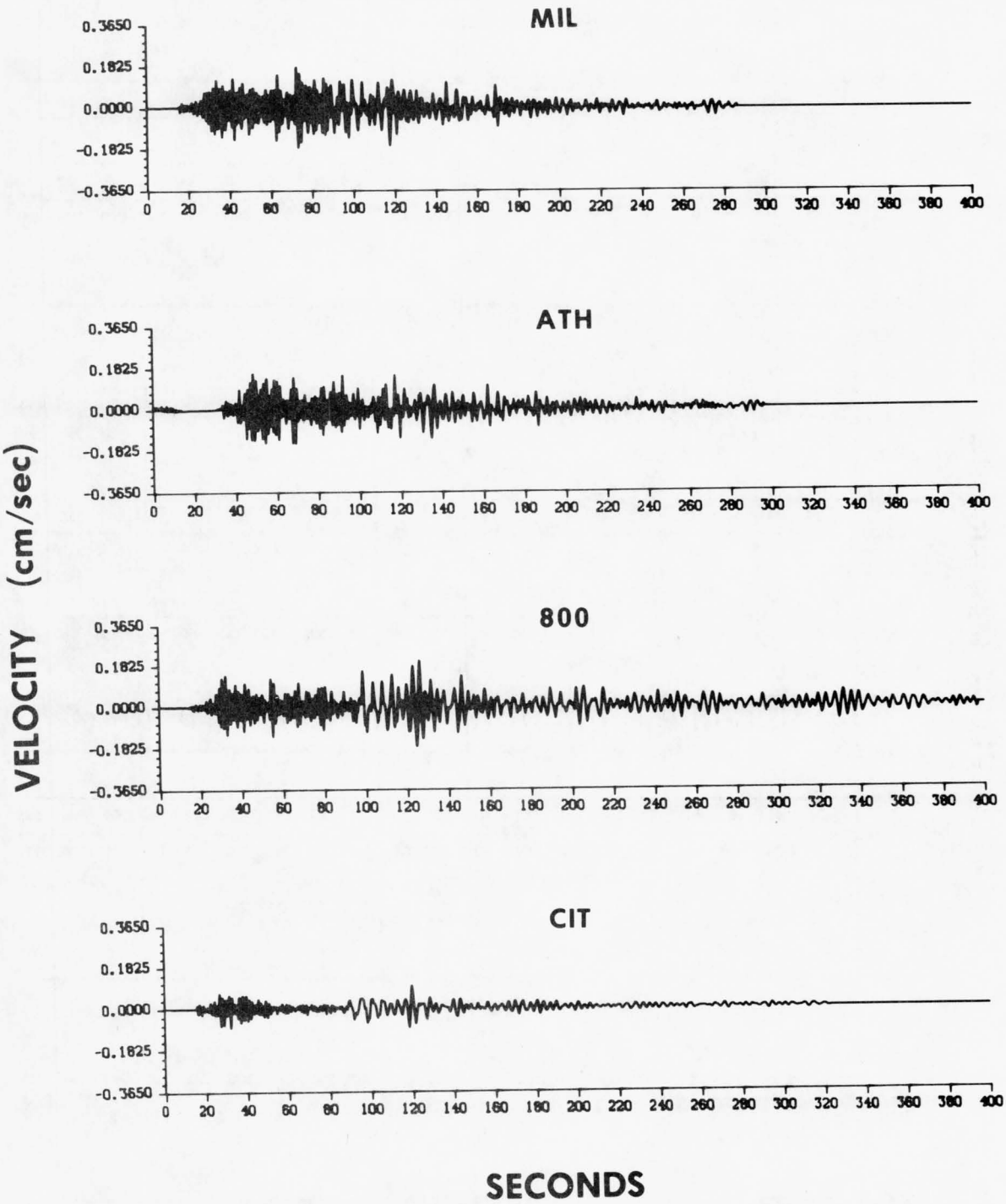

VERTICAL COMPONENT
EVENT CREWLINE

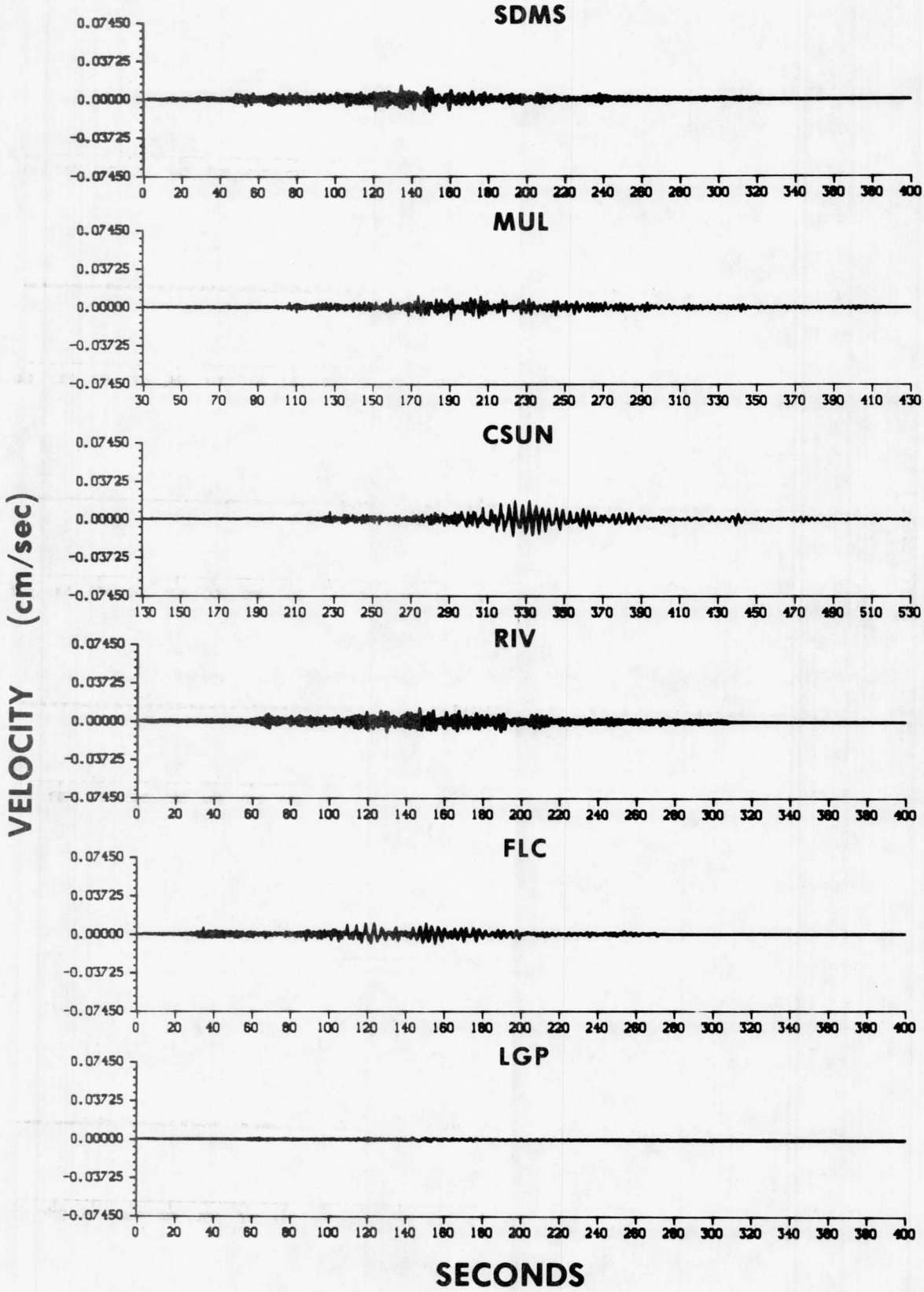

VERTICAL COMPONENT
EVENT CREWLINE

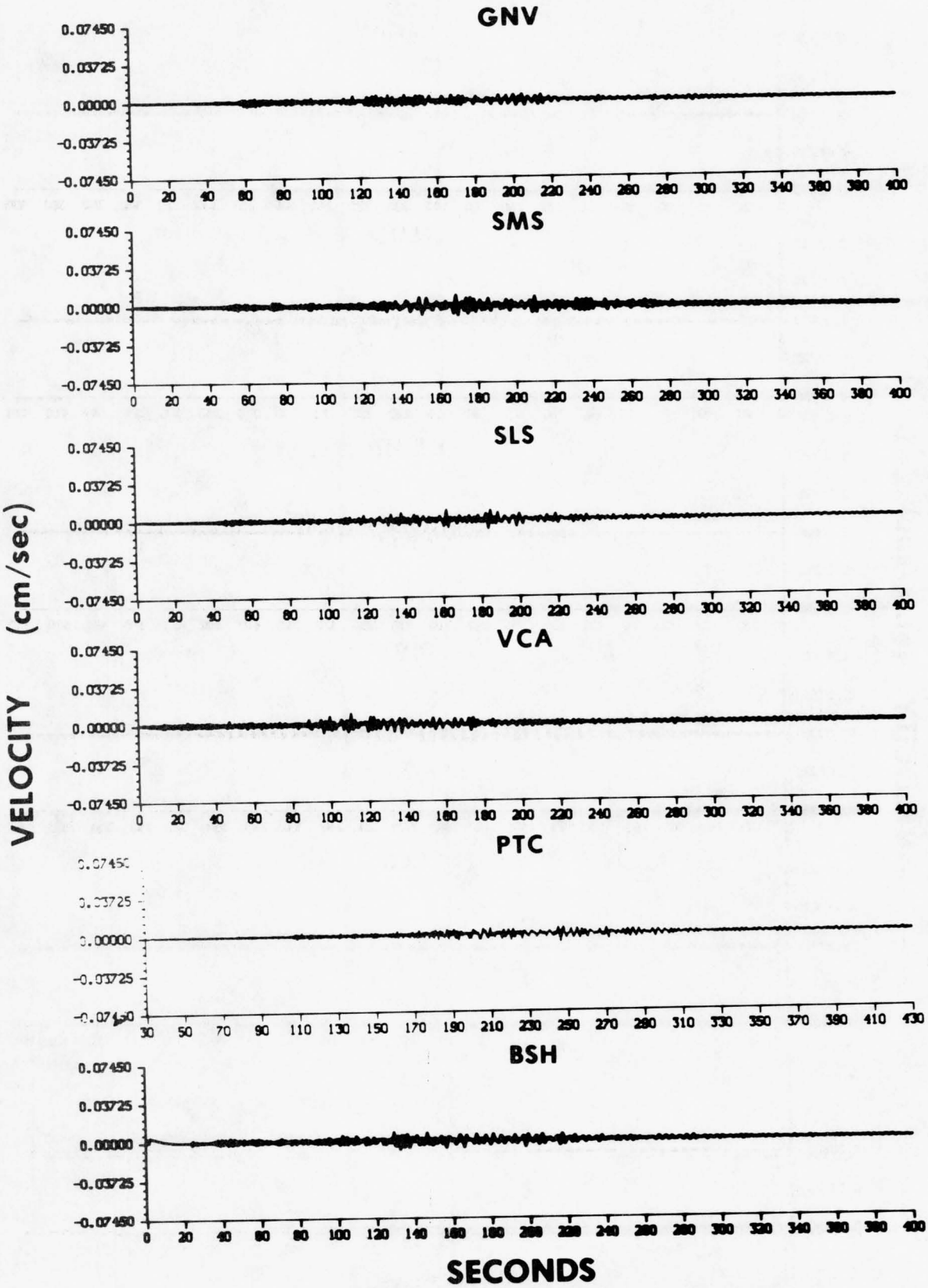

VERTICAL COMPONENT
EVENT CREWLINE

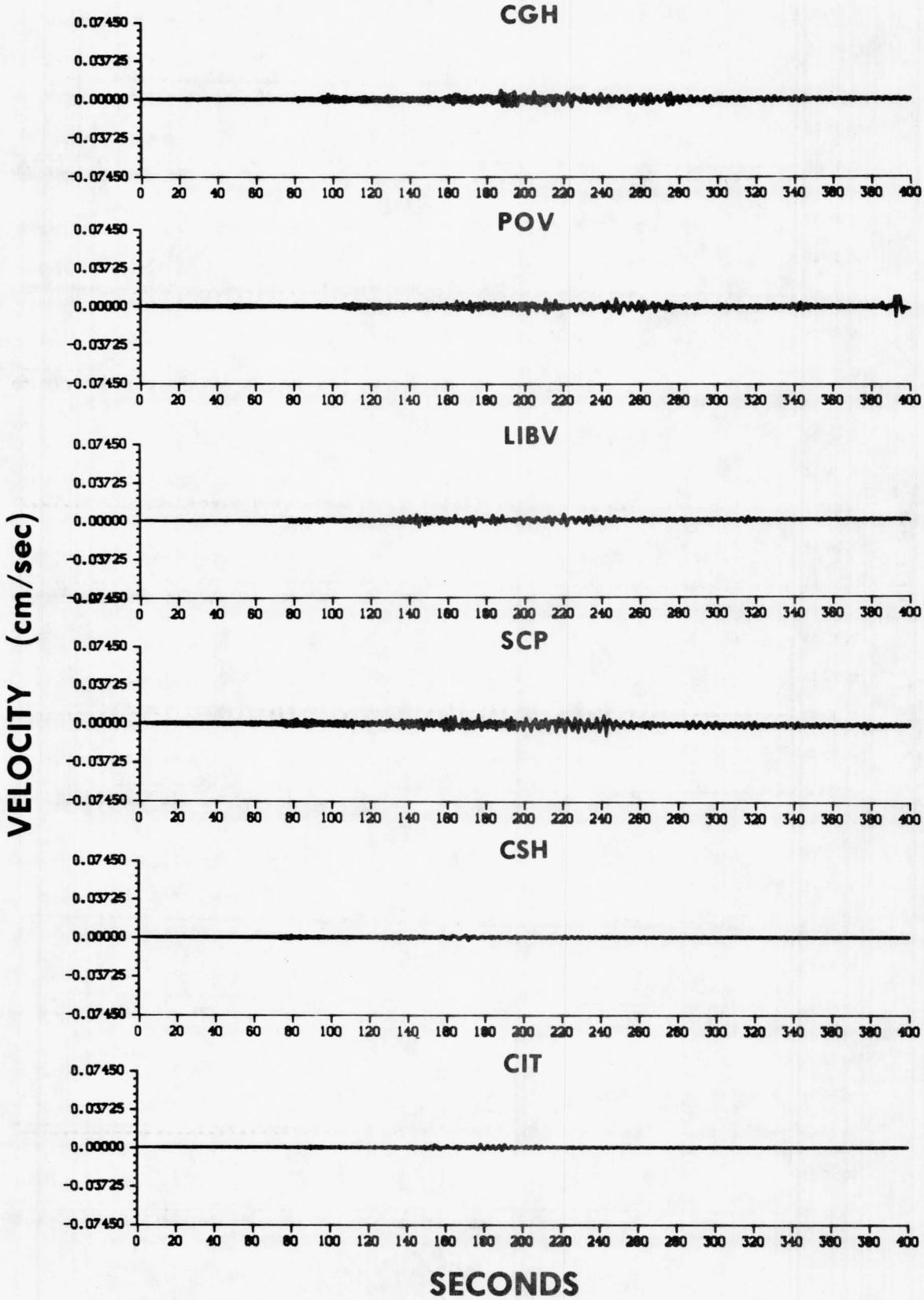

TRANSVERSE COMPONENT
EVENT CREWLINE

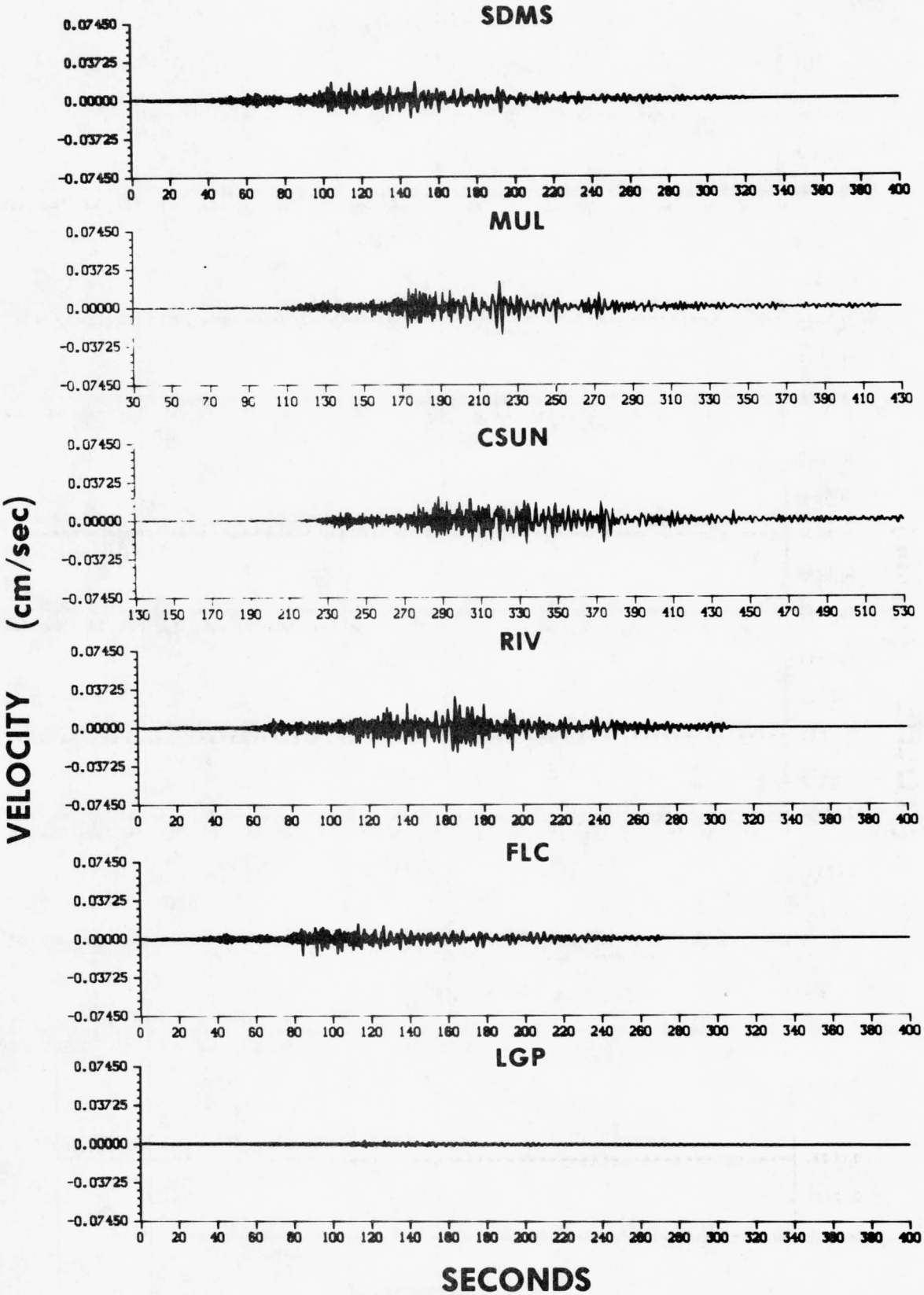

TRANSVERSE COMPONENT
EVENT CREWLINE

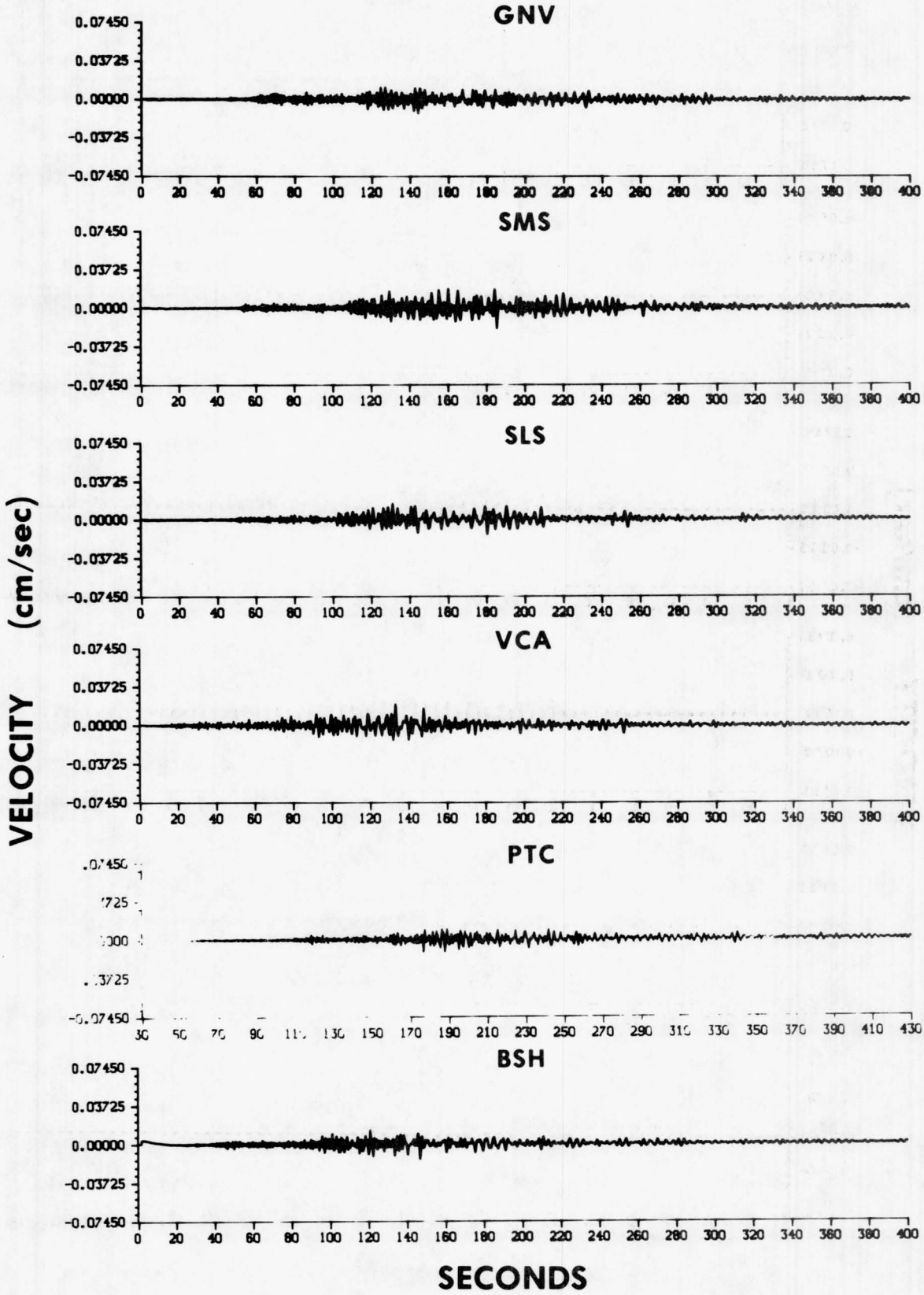

TRANSVERSE COMPONENT
EVENT CREWLINE

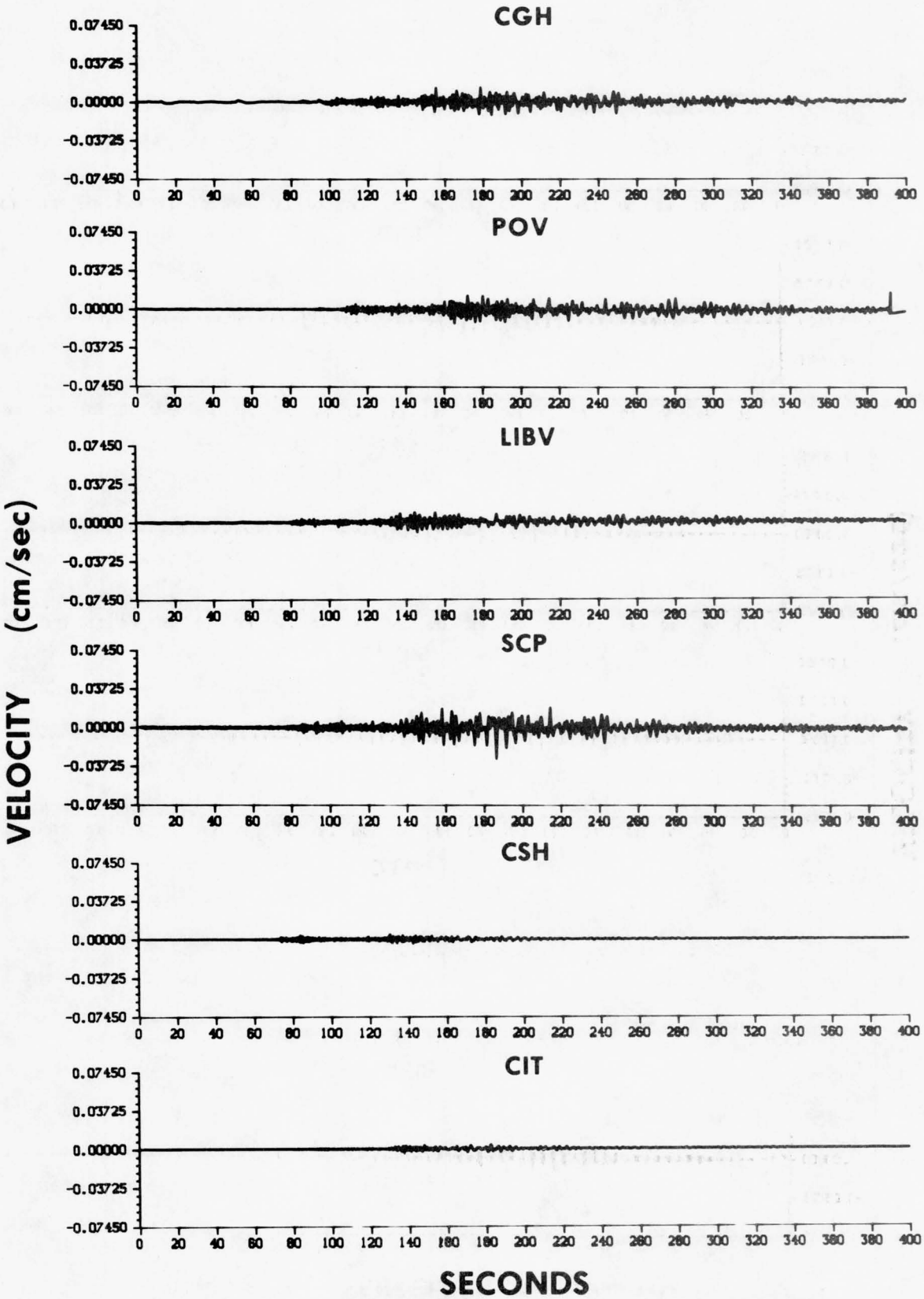

RADIAL COMPONENT
EVENT CREWLINE

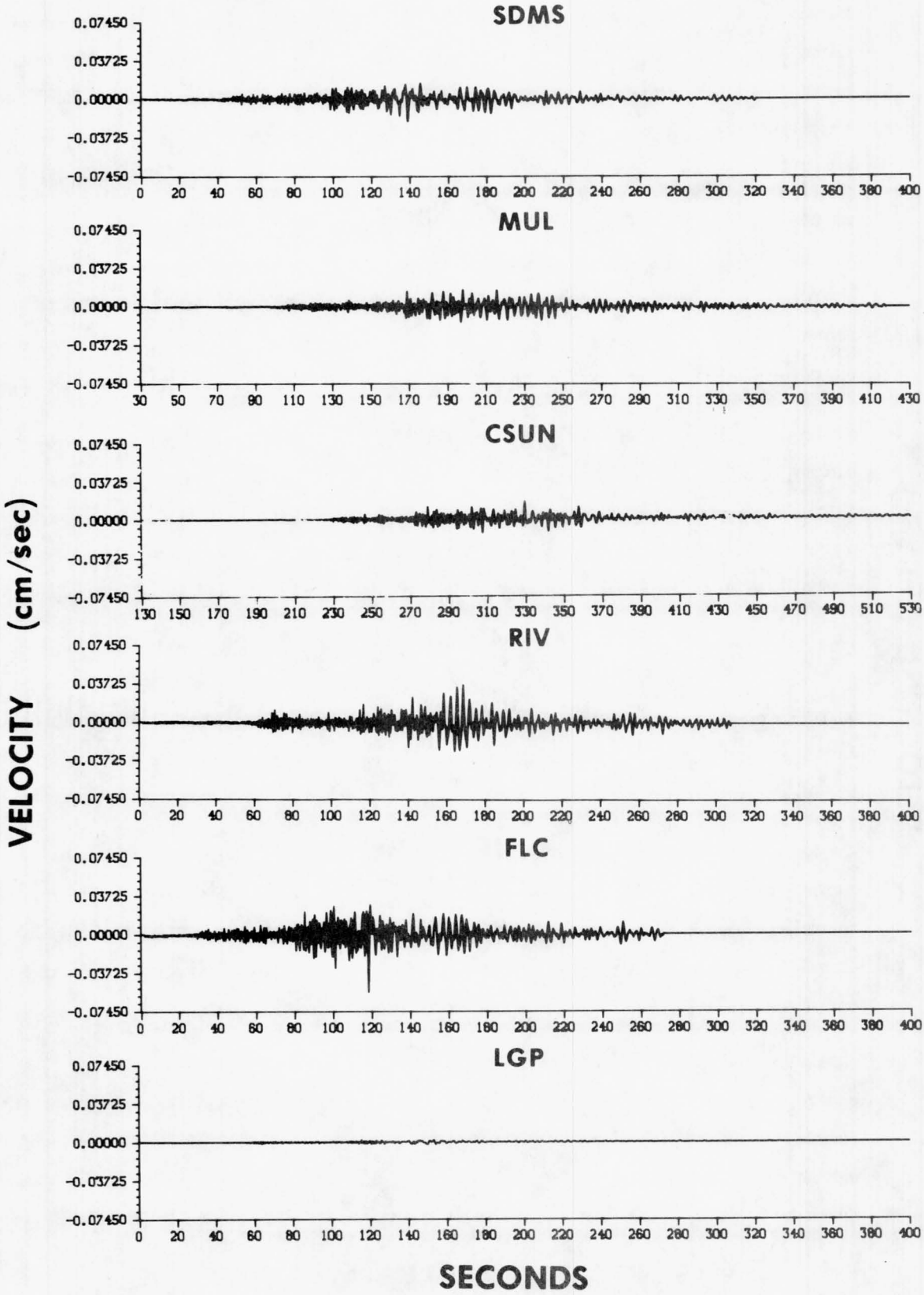

RADIAL COMPONENT
EVENT CREWLINE

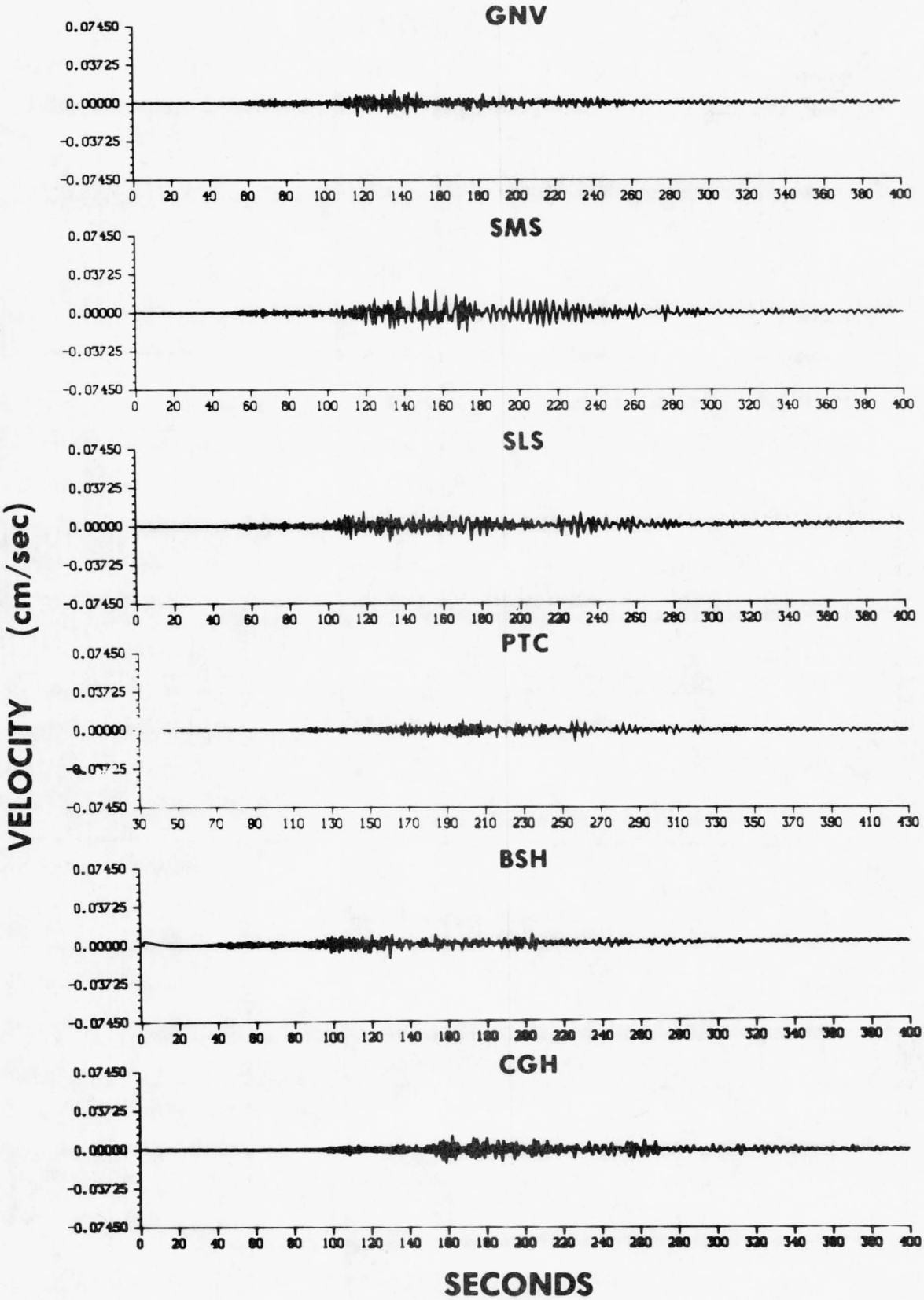

RADIAL COMPONENT
EVENT CREWLINE

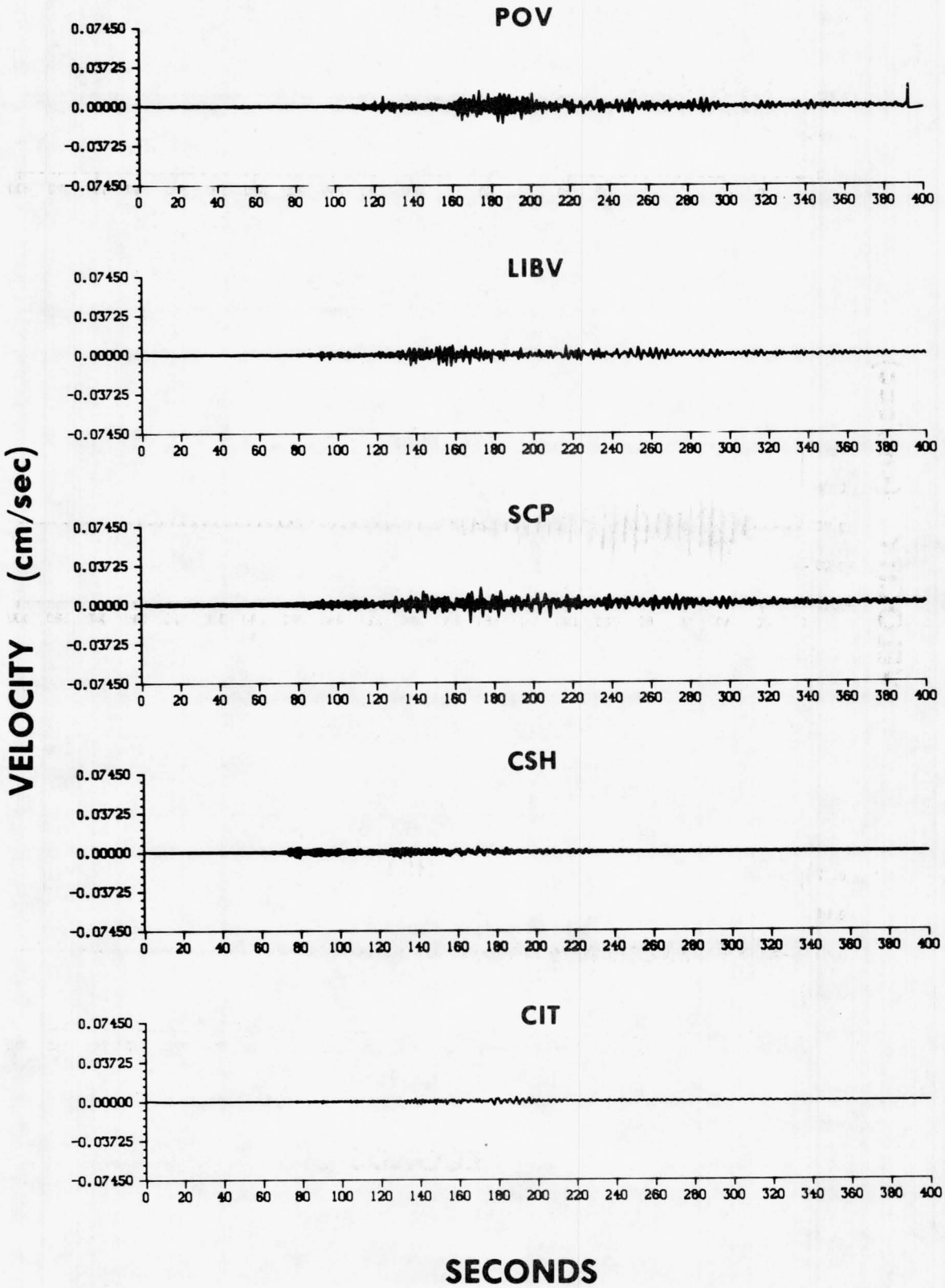

VERTICAL COMPONENT
EVENT ESTUARY

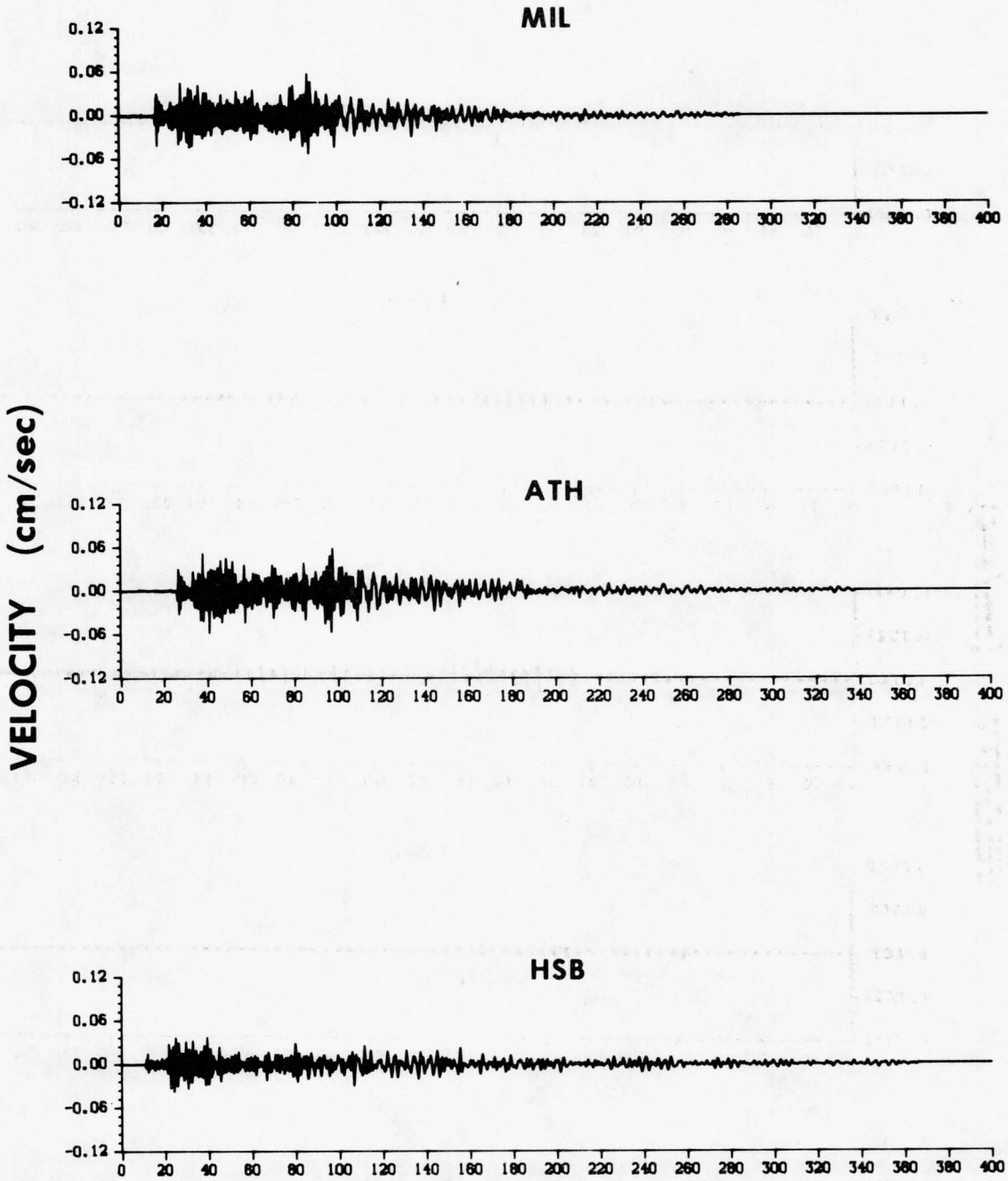

TRANSVERSE COMPONENT
EVENT ESTUARY

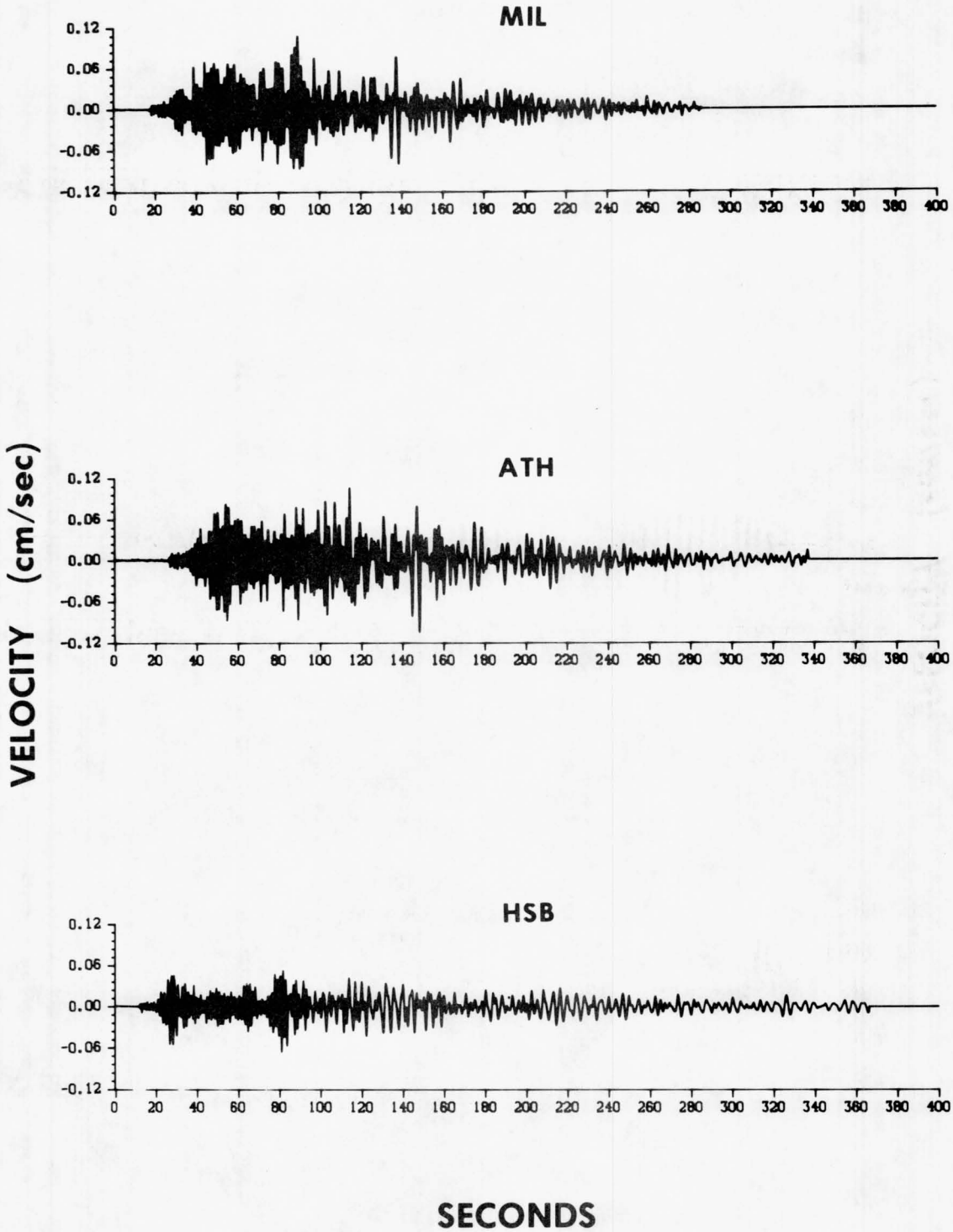

RADIAL COMPONENT
EVENT ESTUARY

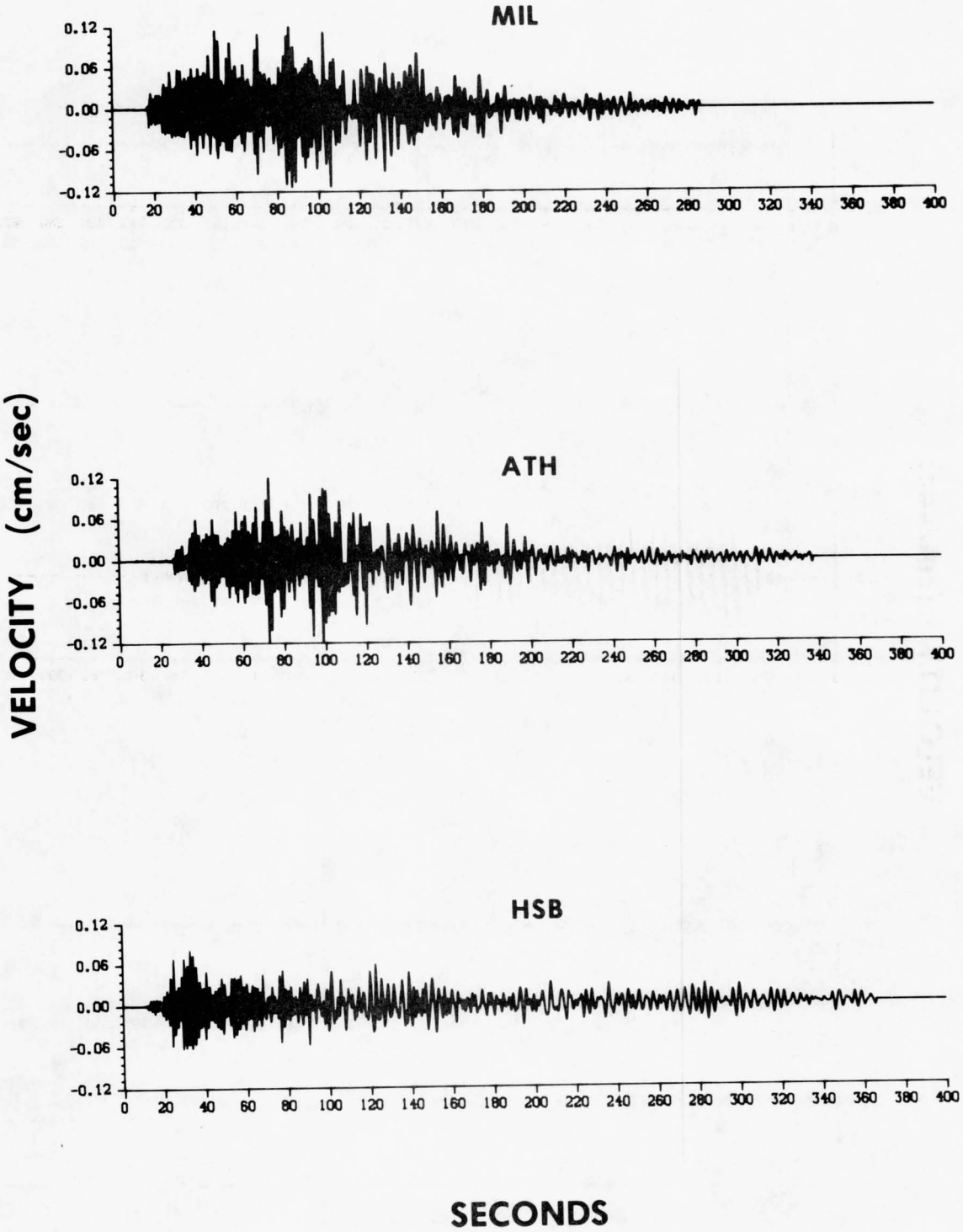

VERTICAL COMPONENT
EVENT FAJY

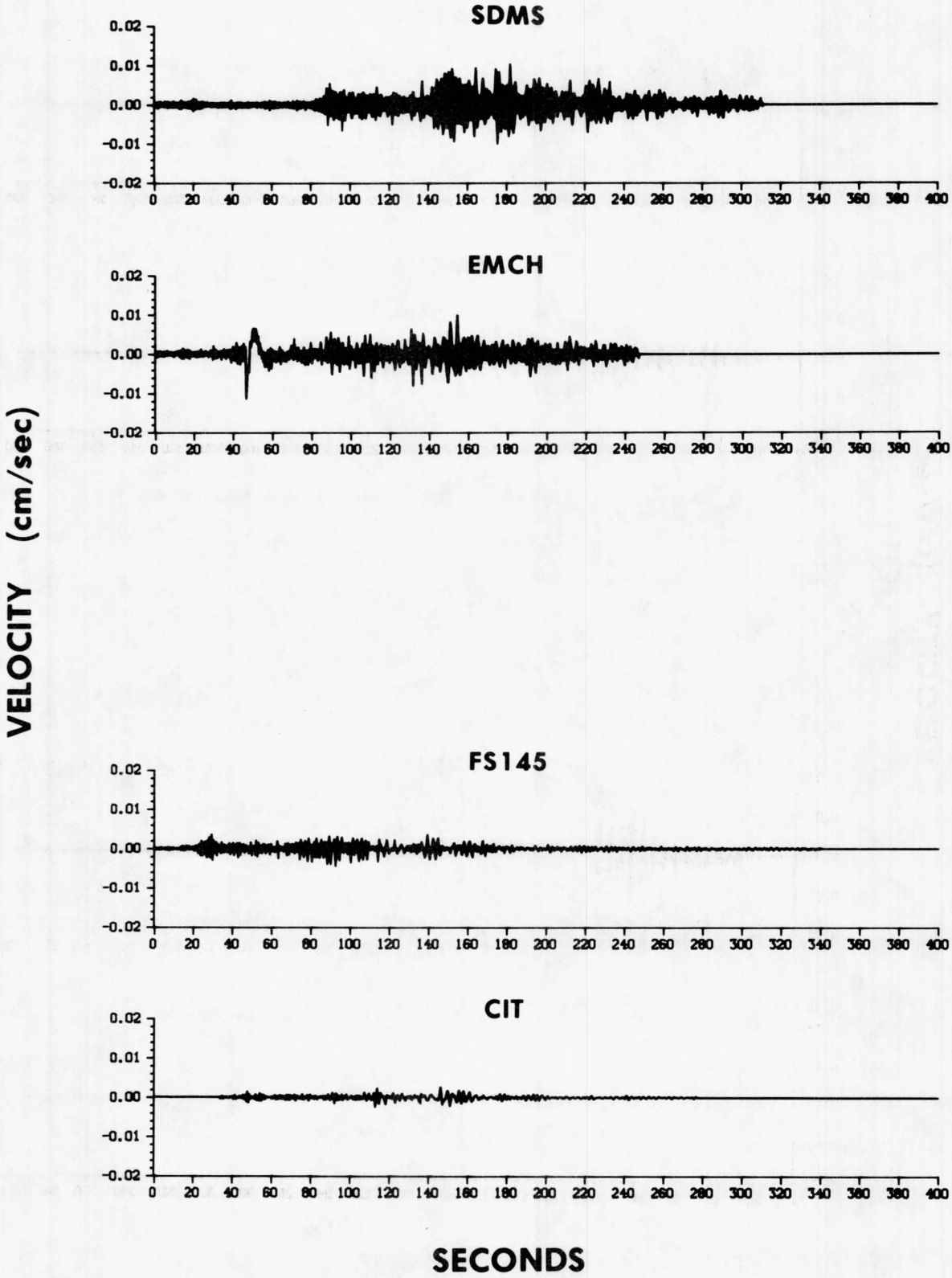

TRANSVERSE COMPONENT
EVENT FAJY

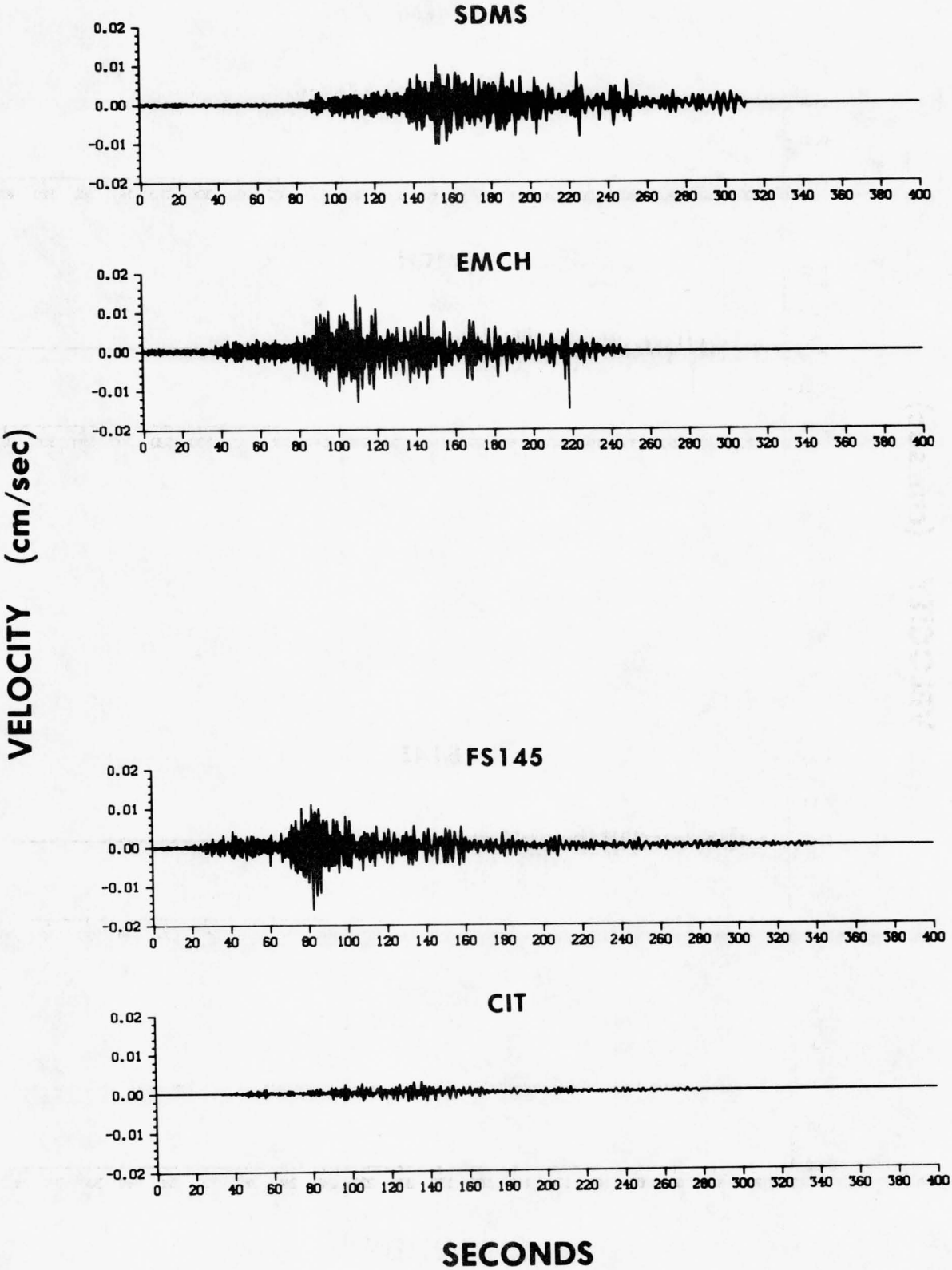

RADIAL COMPONENT
EVENT FAJY

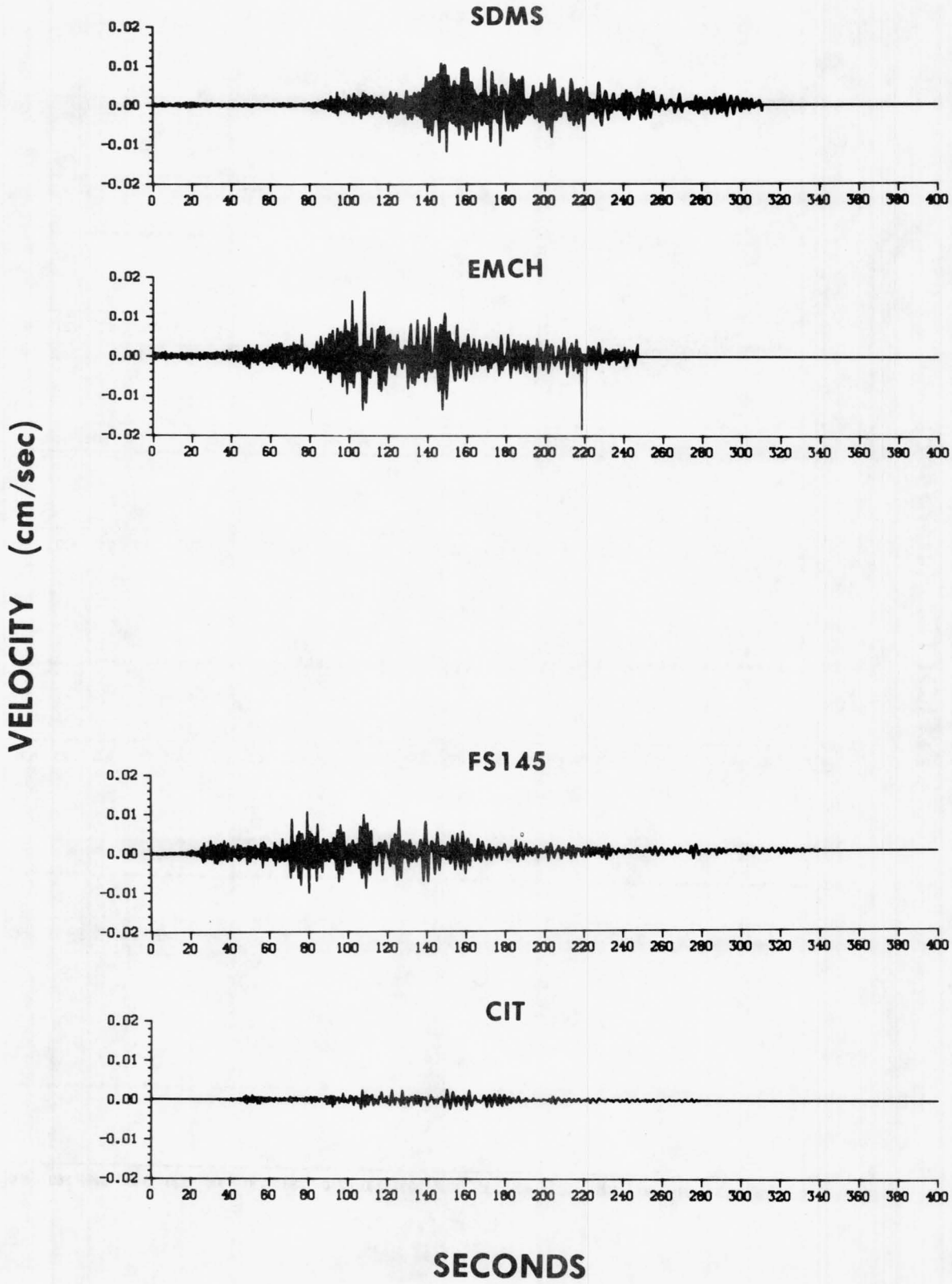

VERTICAL COMPONENT
EVENT FONDUTTA

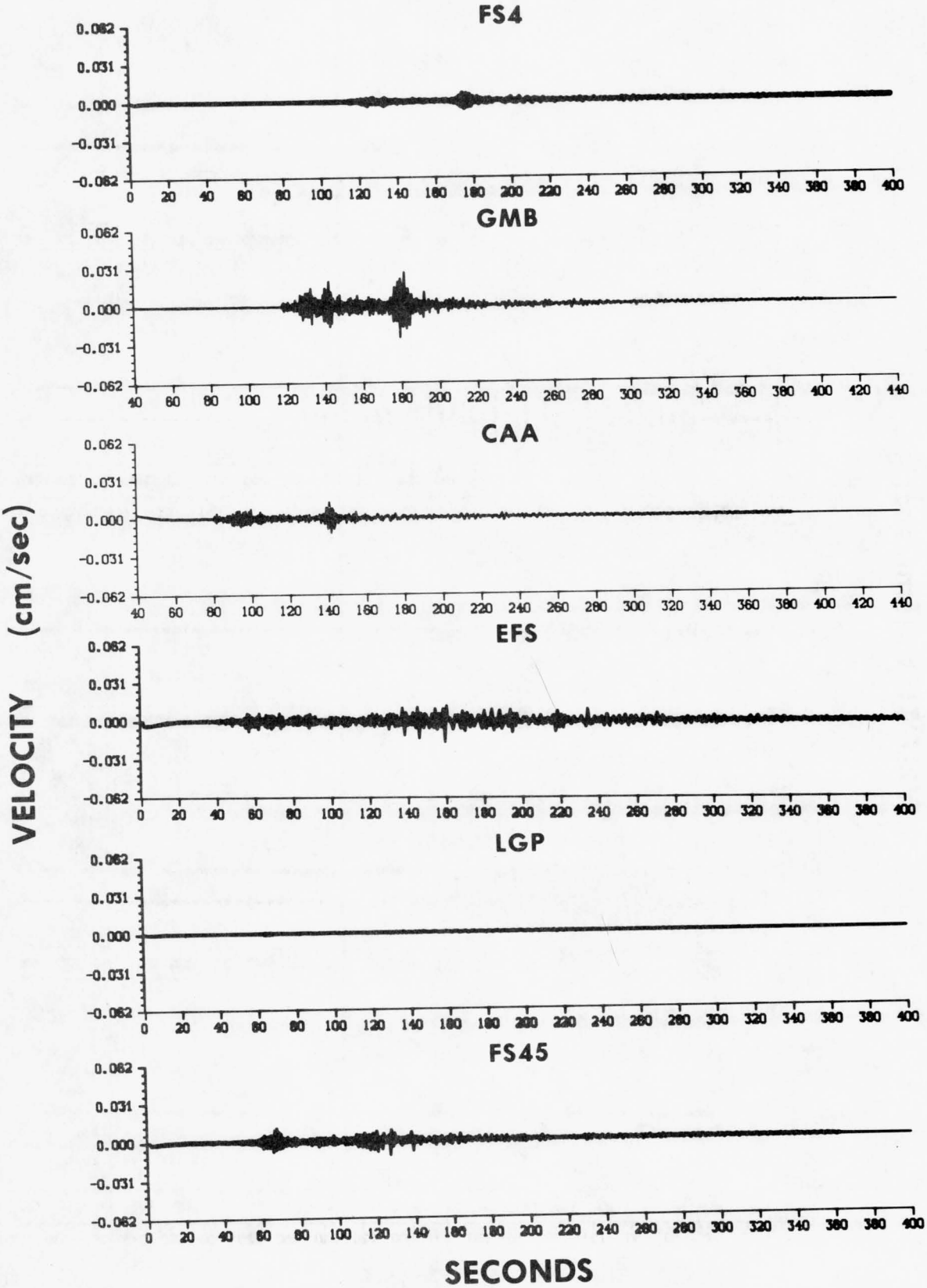

VERTICAL COMPONENT
EVENT FONDUTTA

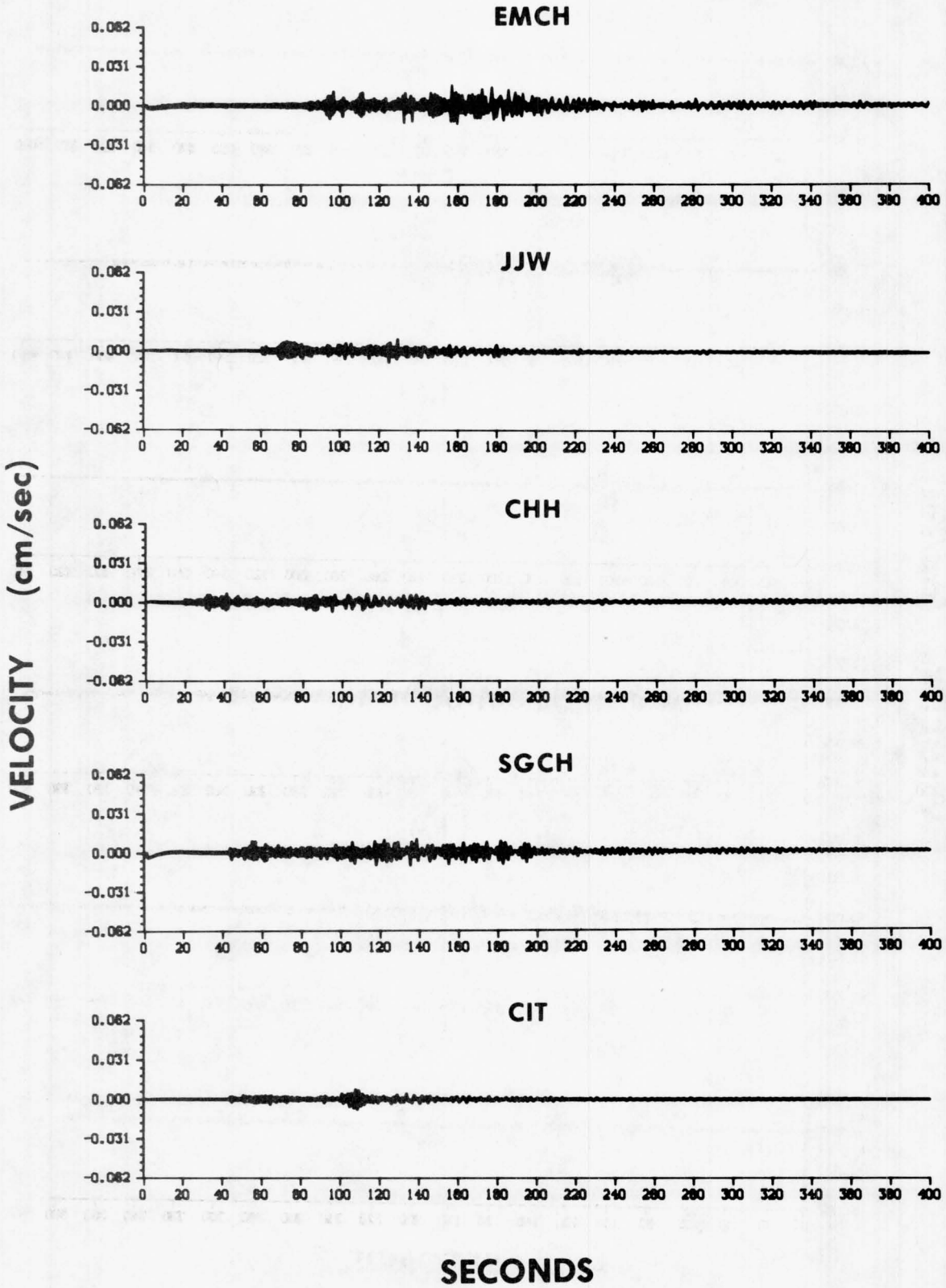

TRANSVERSE COMPONENT
EVENT FONDUTTA

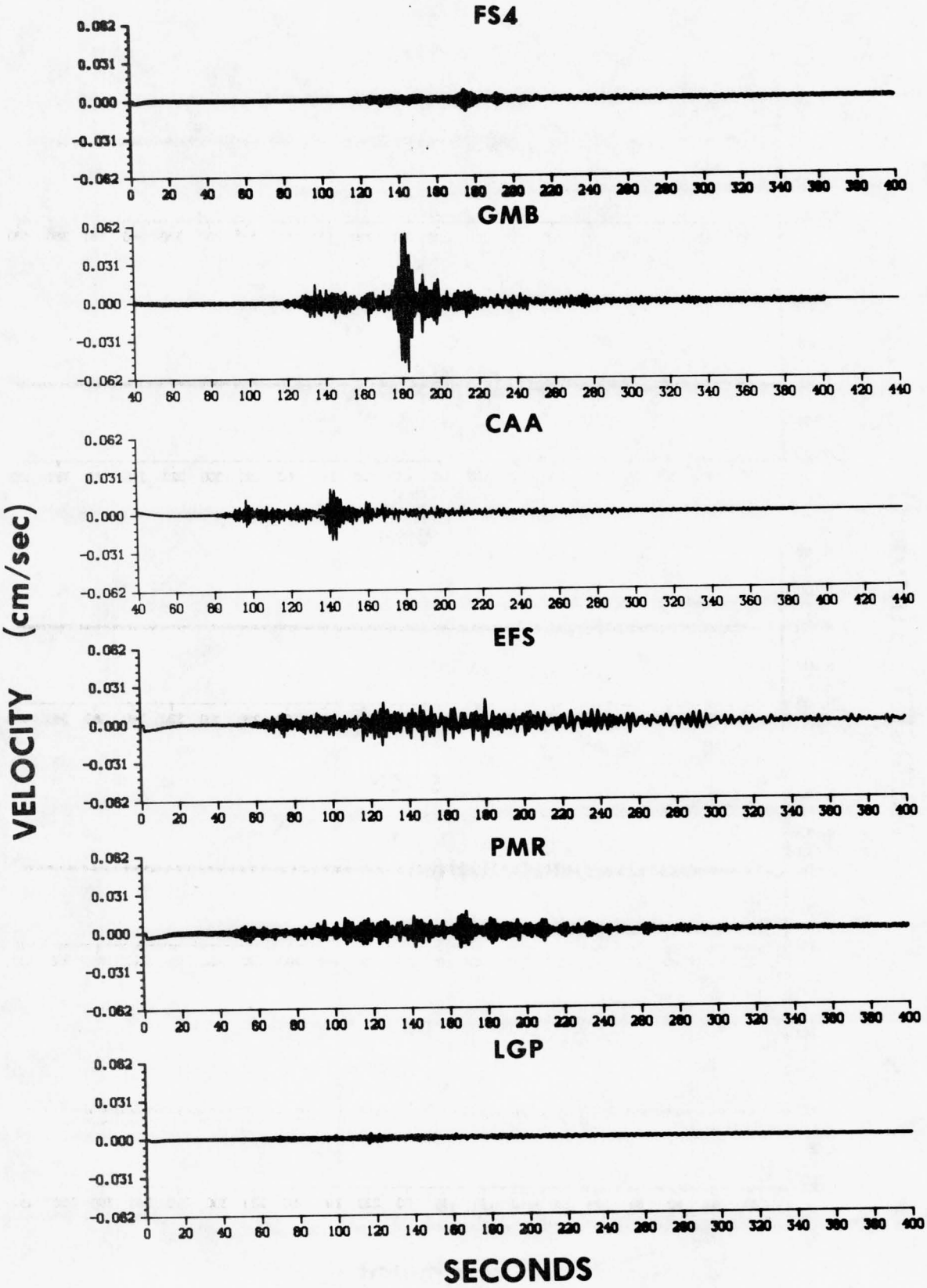

TRANSVERSE COMPONENT
EVENT FONDUTTA

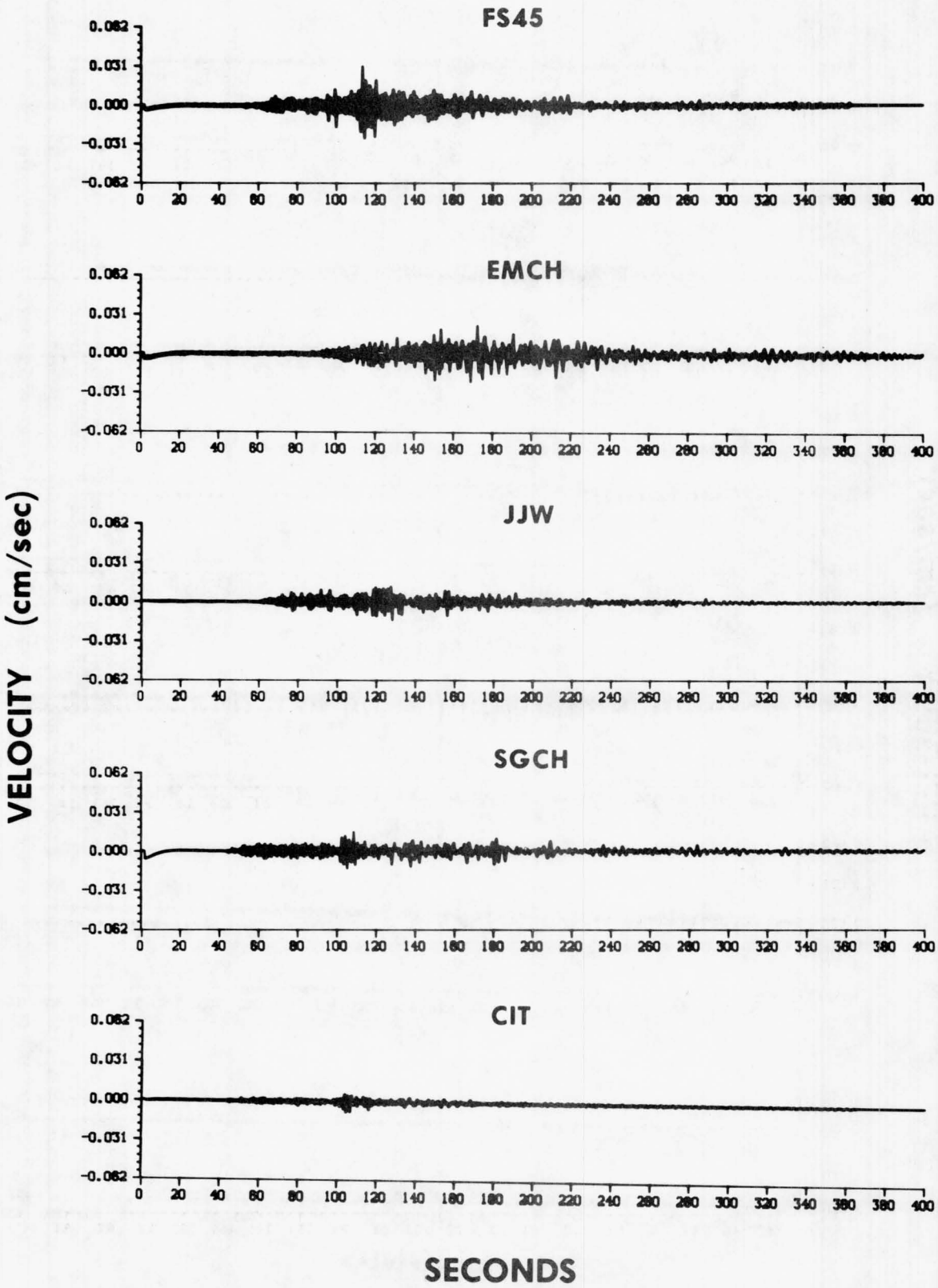

RADIAL COMPONENT
EVENT FONDUTTA

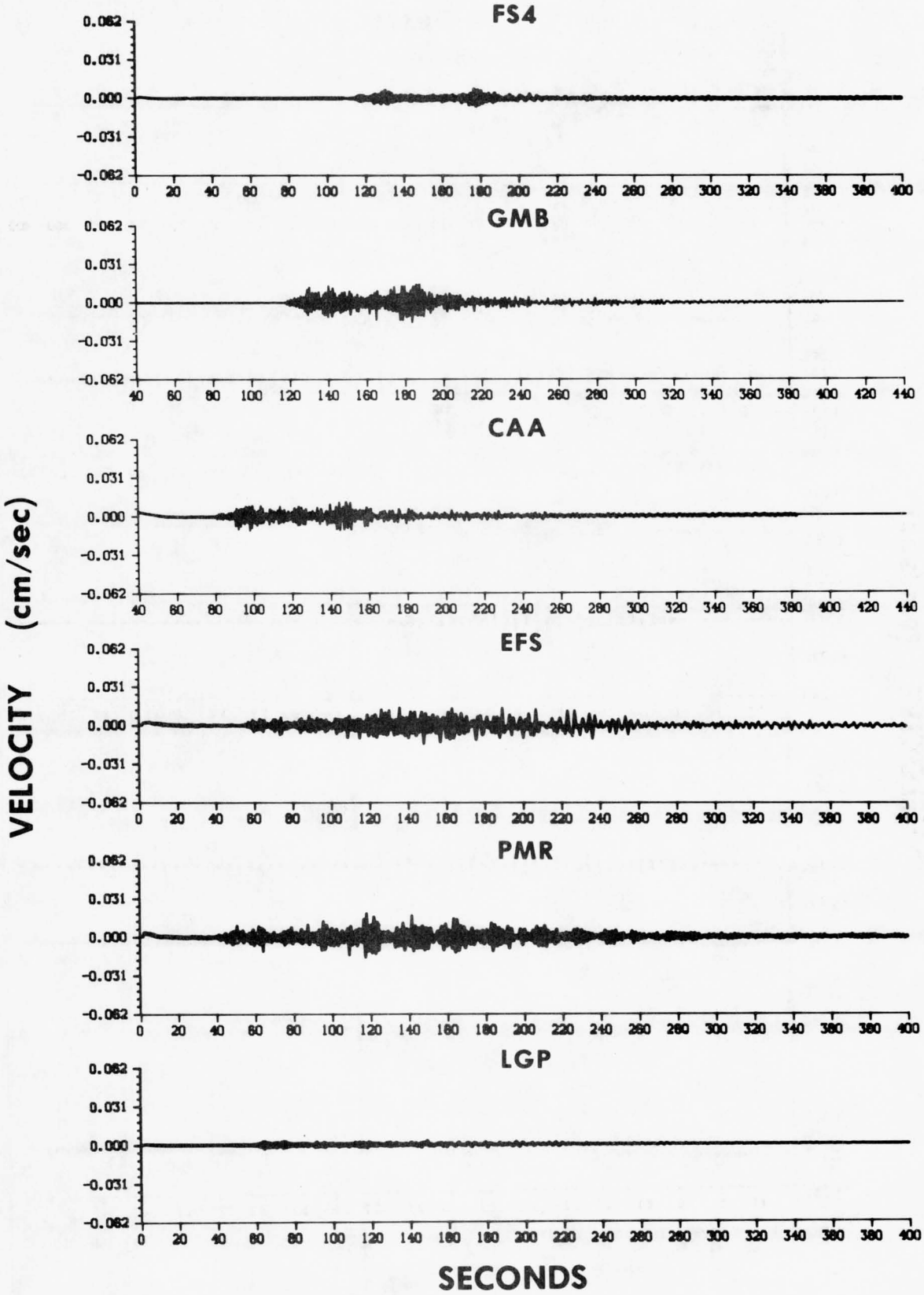

RADIAL COMPONENT
EVENT FONDUTTA

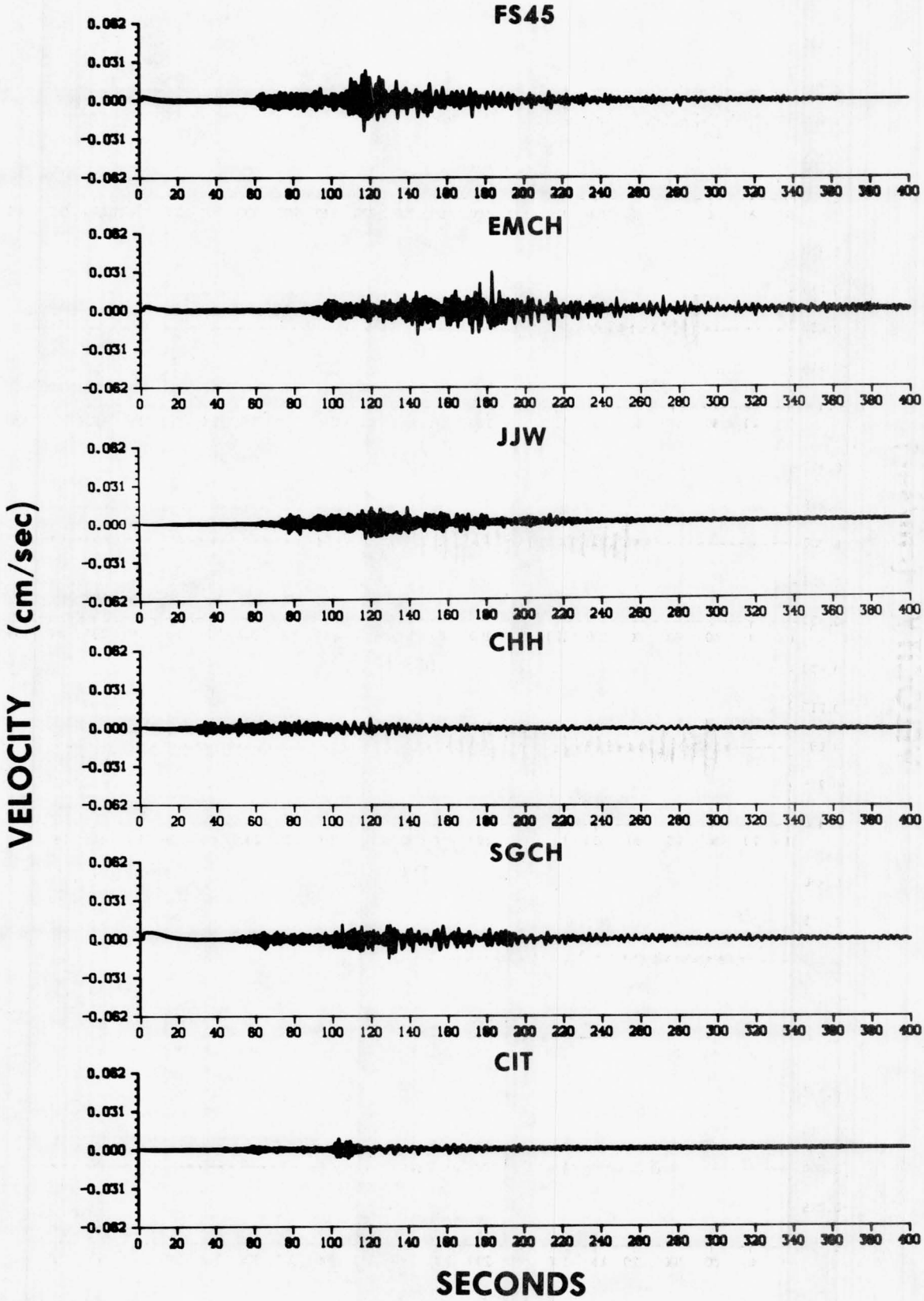

VERTICAL COMPONENT
EVENT FONTINA

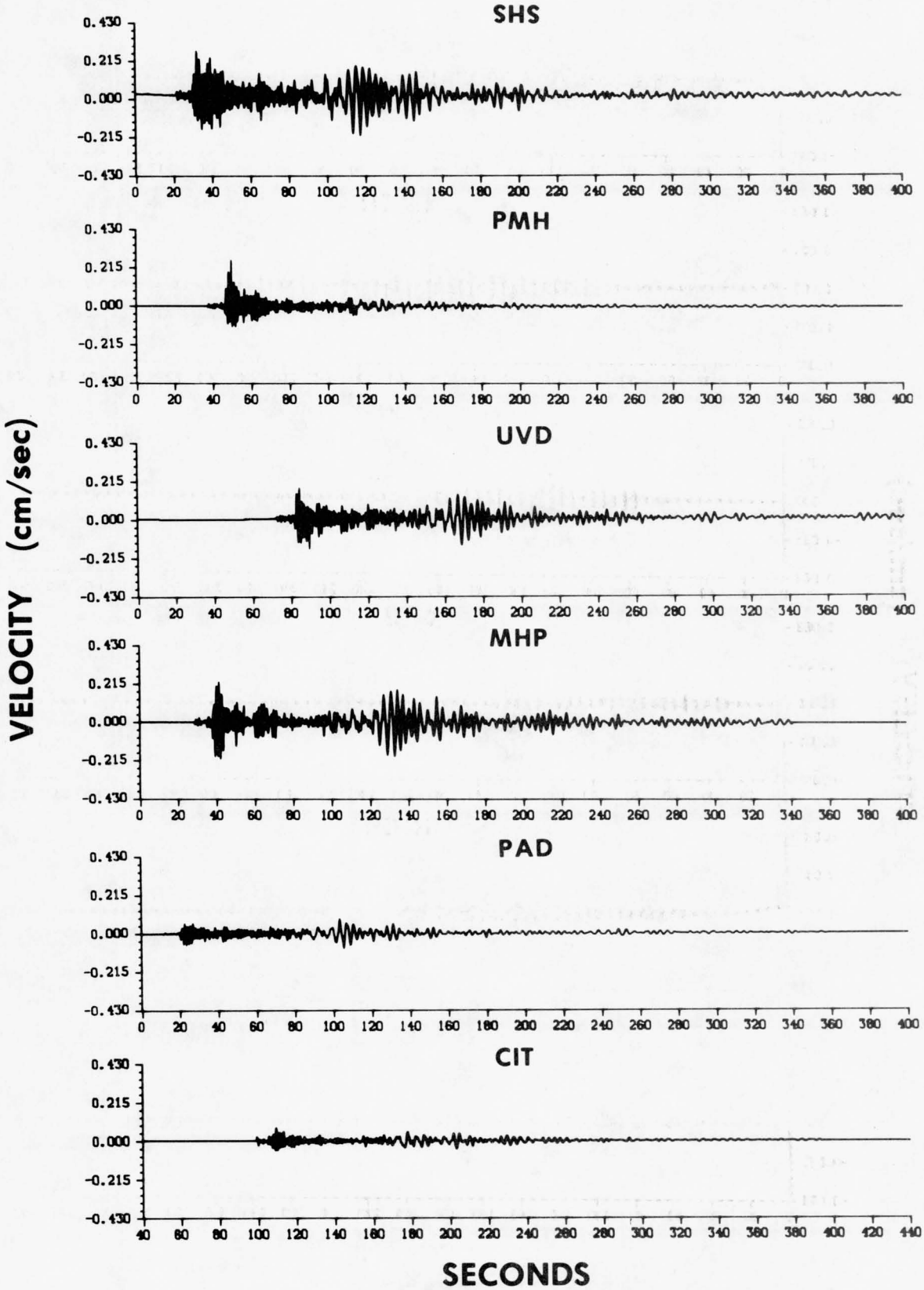

TRANSVERSE COMPONENT
EVENT FONTINA

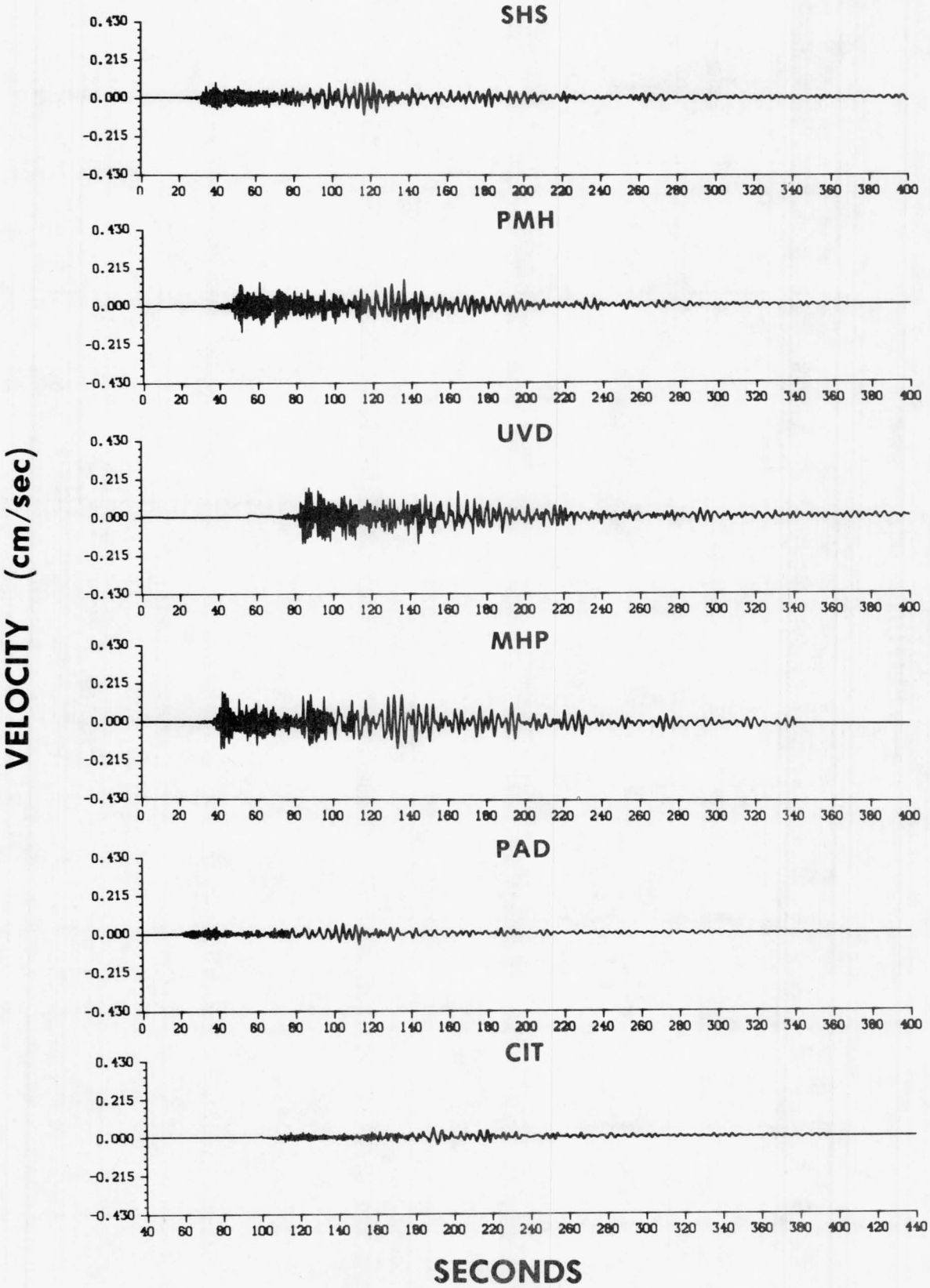

RADIAL COMPONENT
EVENT FONTINA

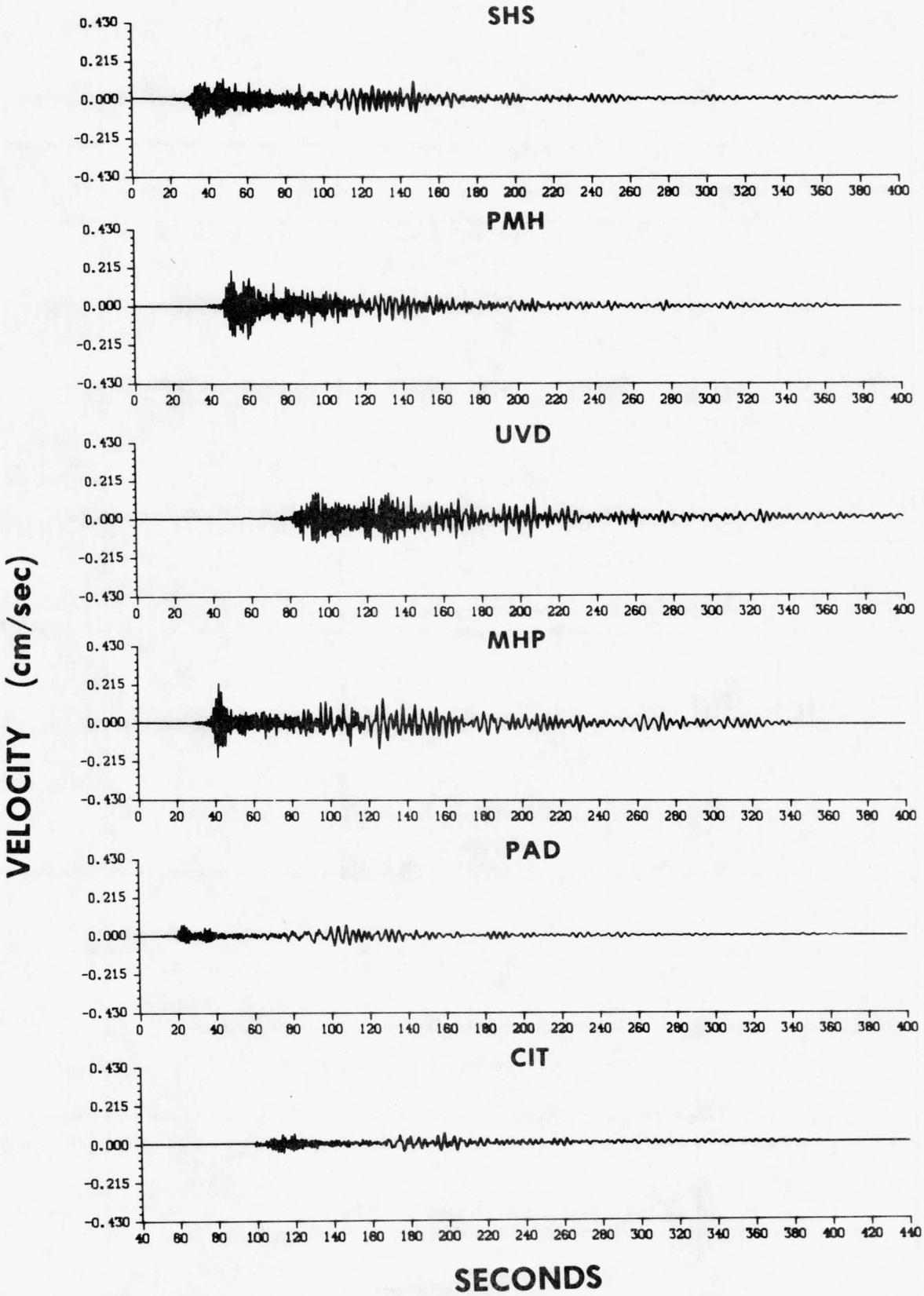

VERTICAL COMPONENT
EVENT ICEBERG

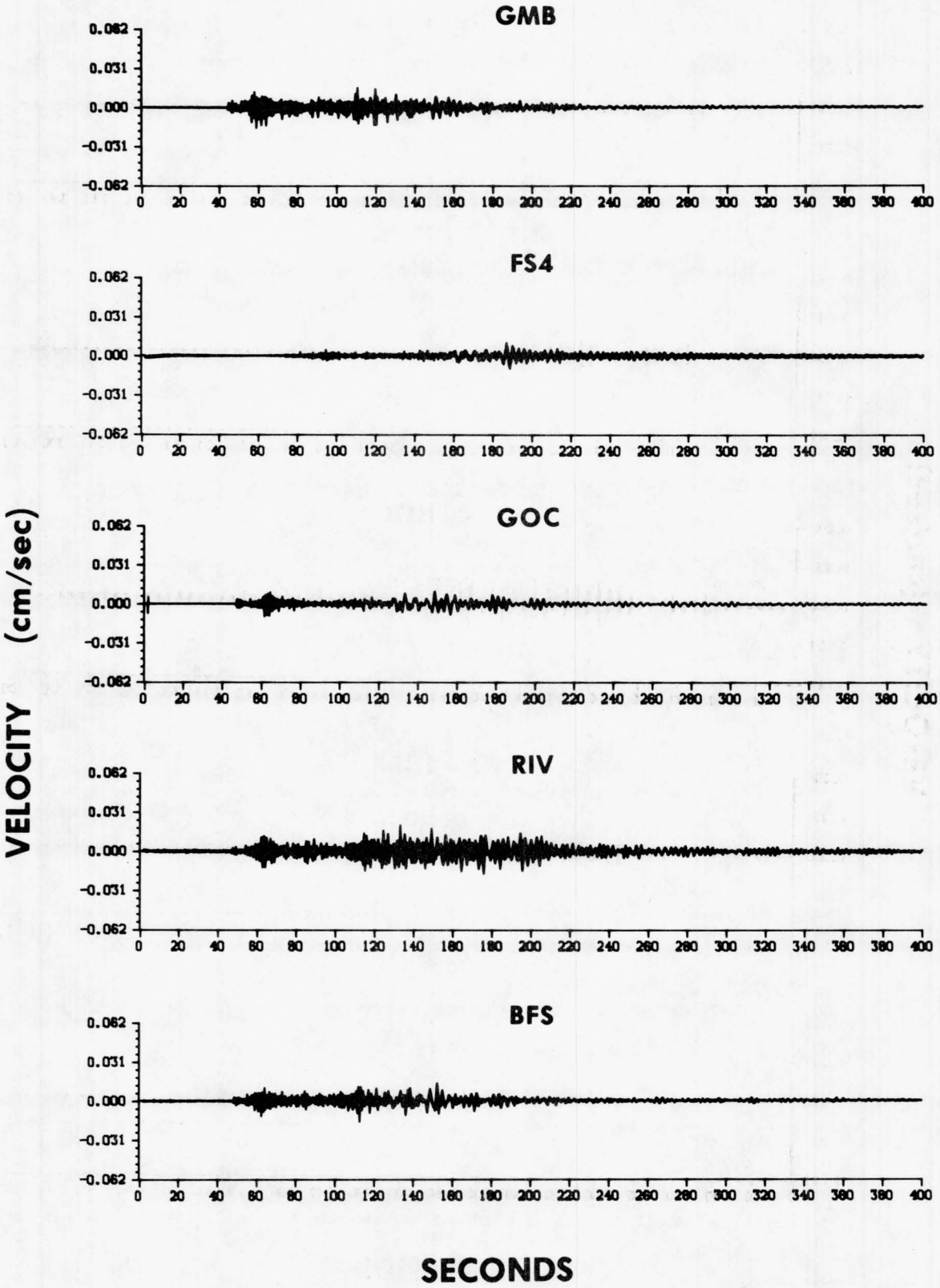

VERTICAL COMPONENT
EVENT ICEBERG

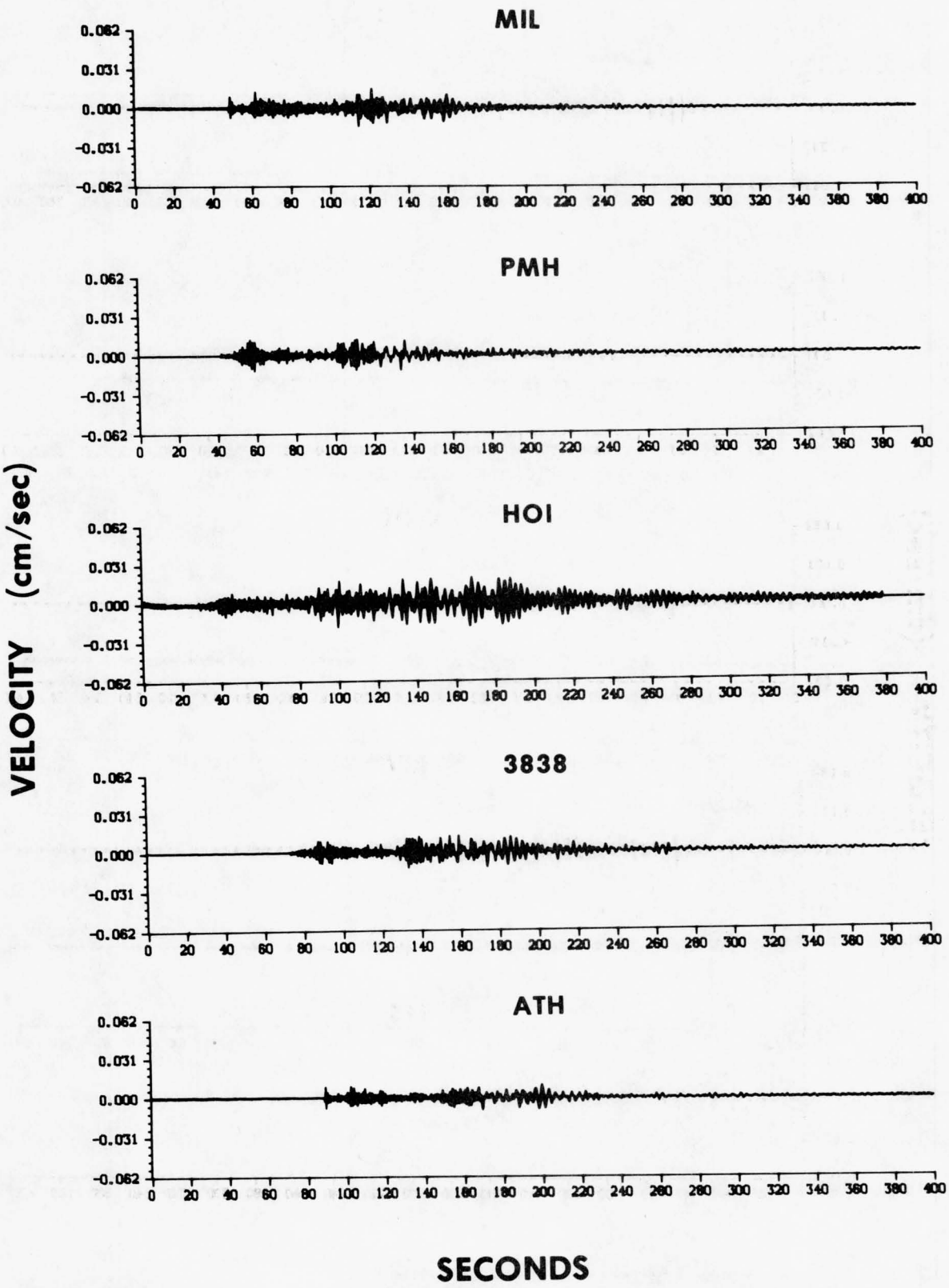

VERTICAL COMPONENT
EVENT ICEBERG

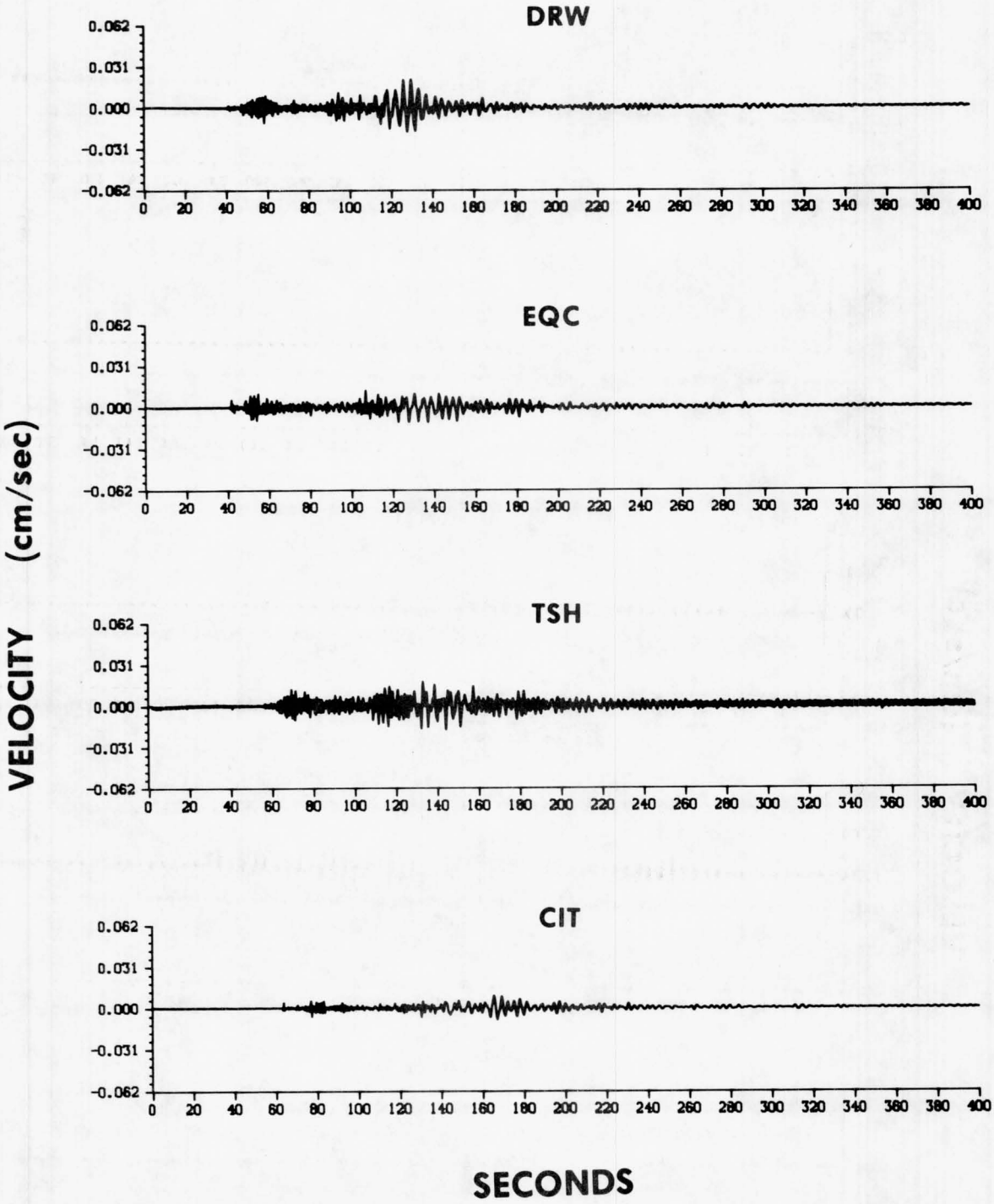

TRANSVERSE COMPONENT
EVENT ICEBERG

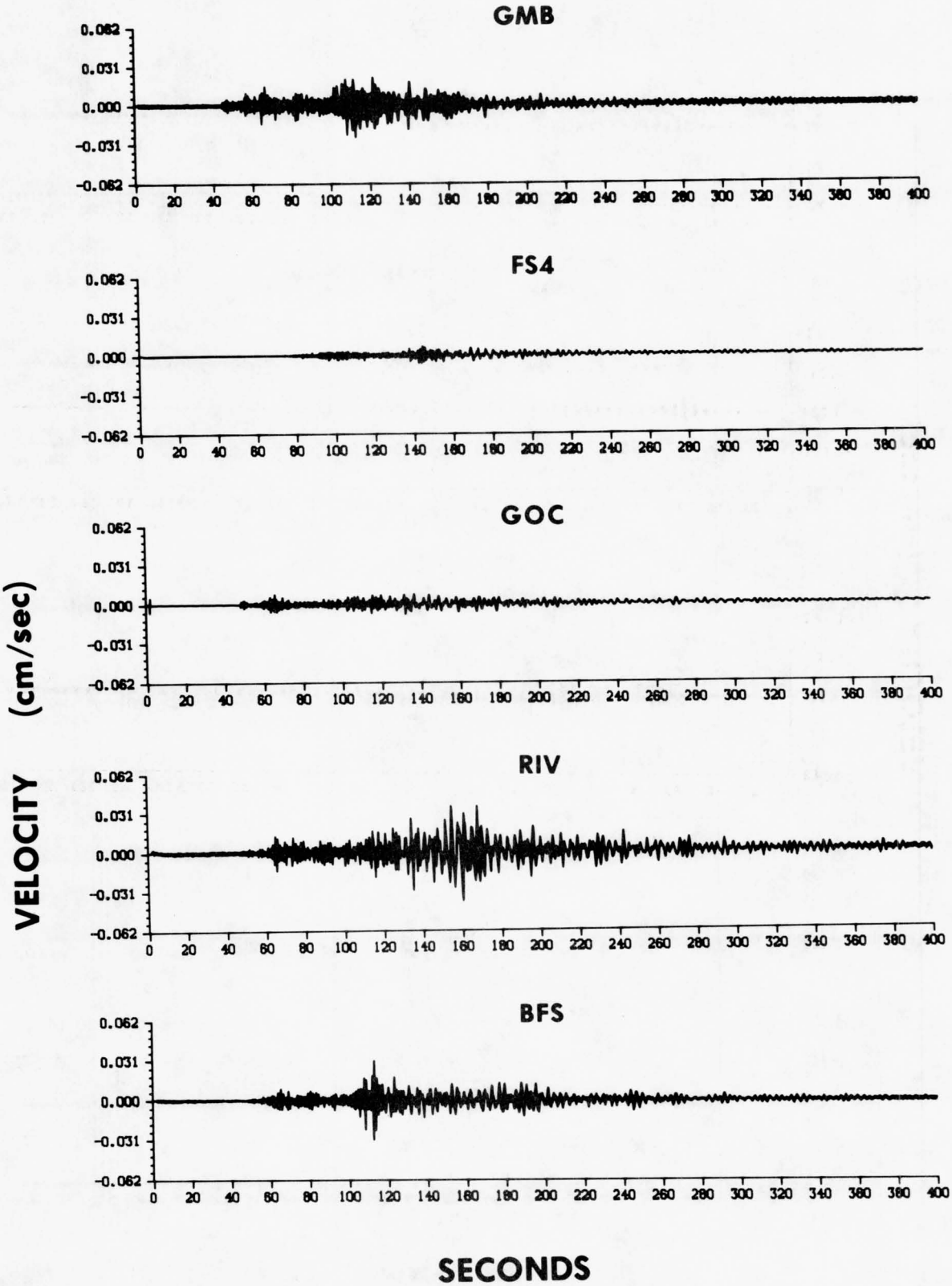

TRANSVERSE COMPONENT
EVENT ICEBERG

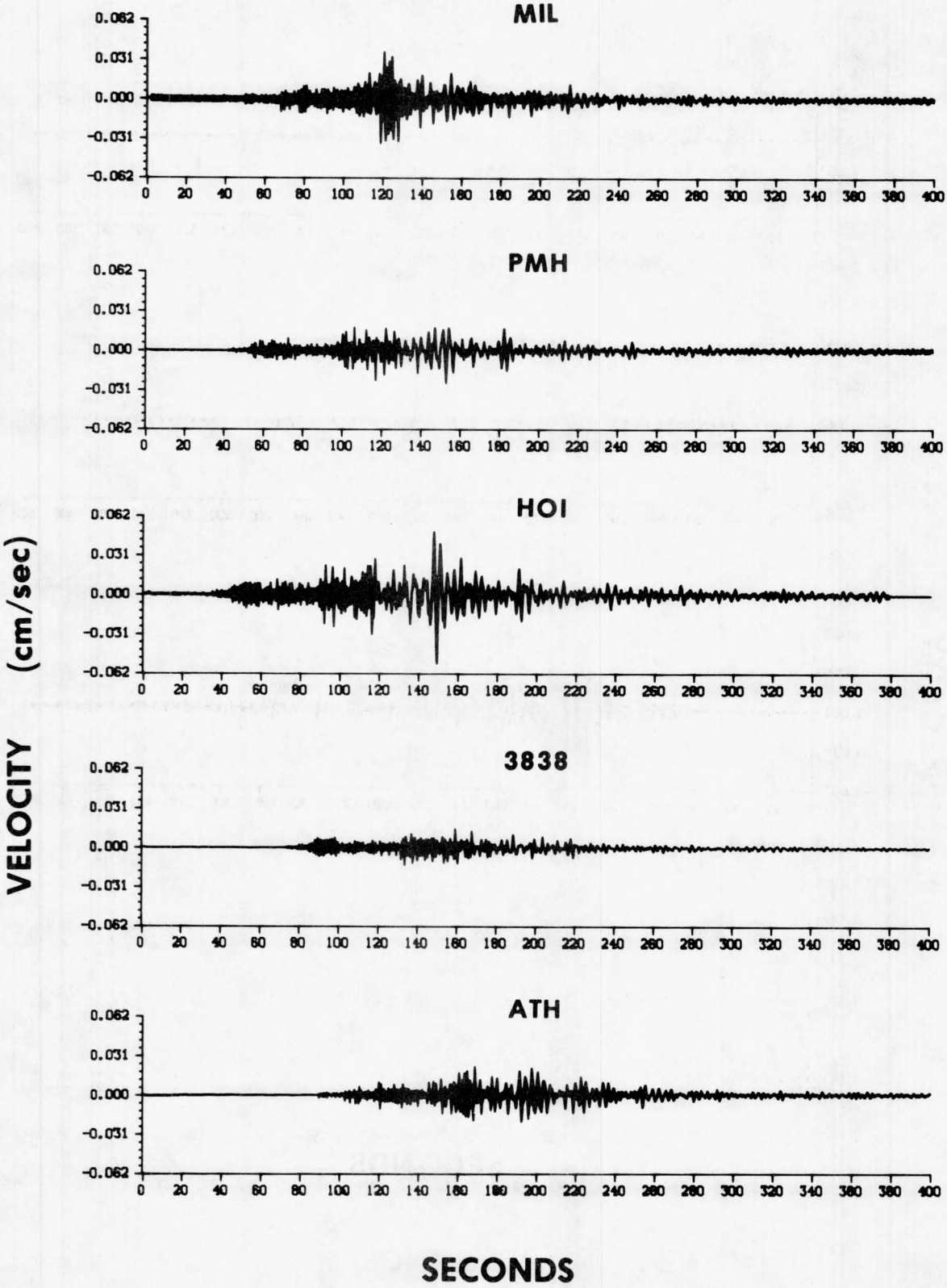

TRANSVERSE COMPONENT
EVENT ICEBERG

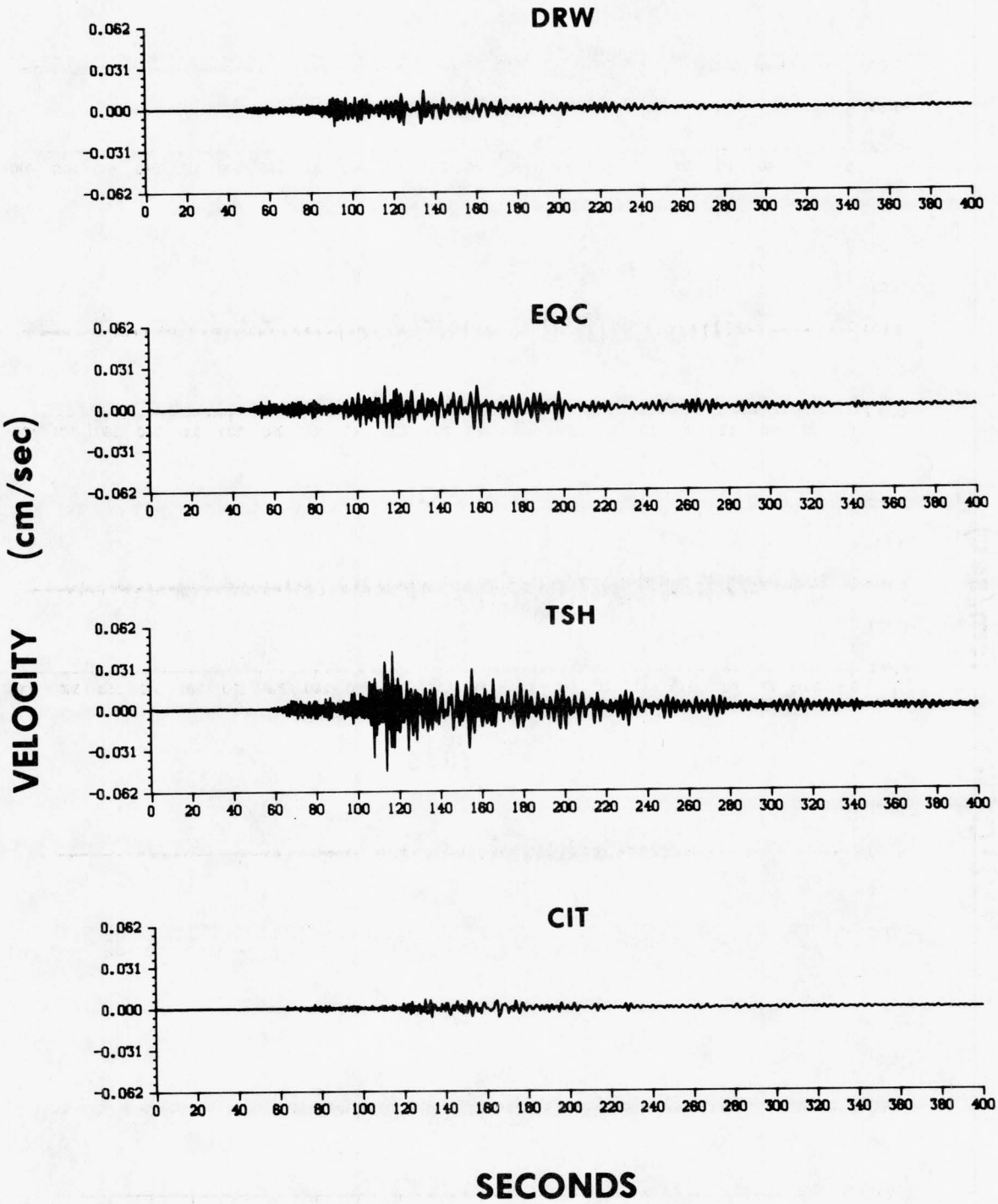

RADIAL COMPONENT
EVENT ICEBERG

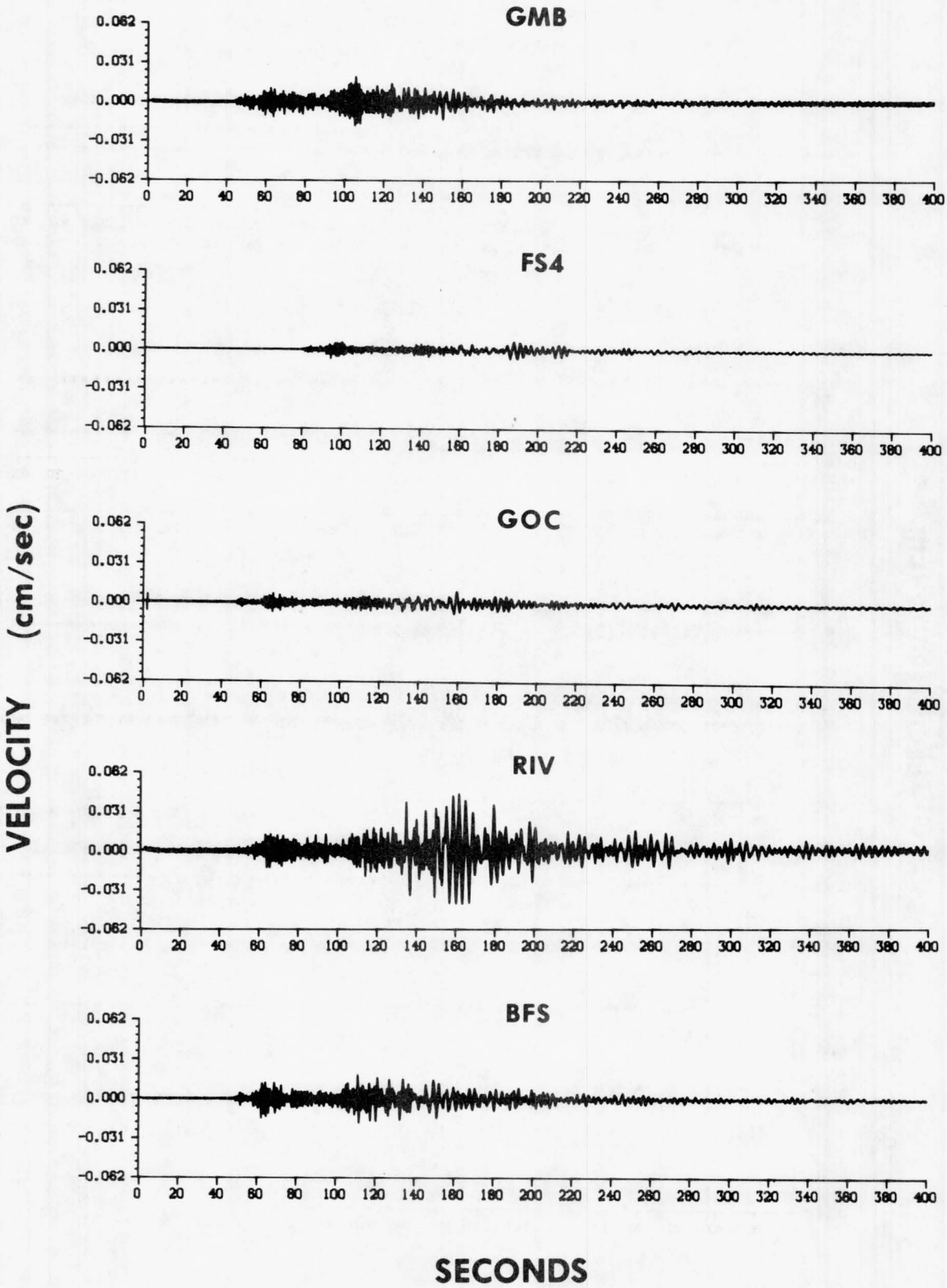

RADIAL COMPONENT
EVENT ICEBERG

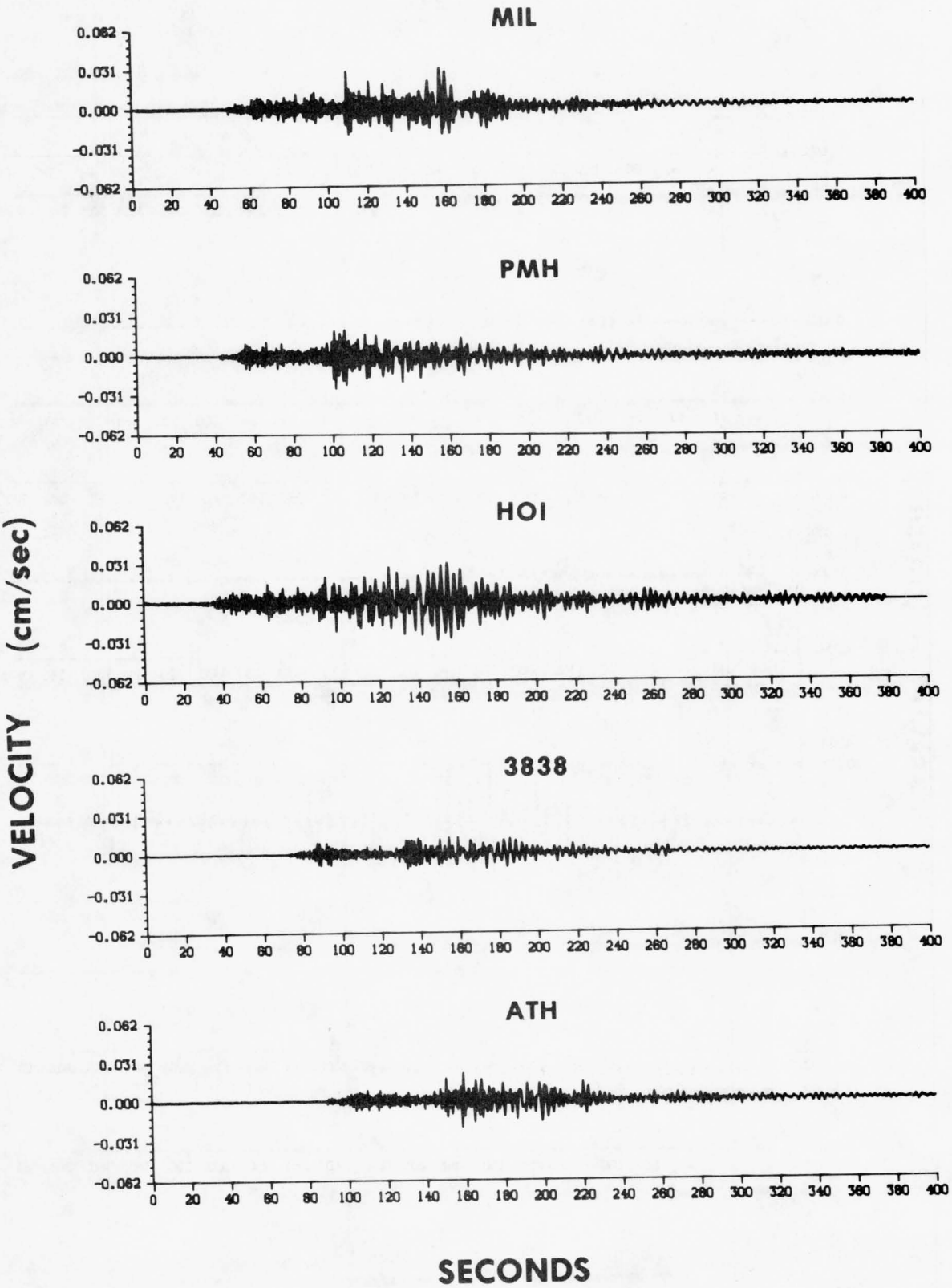

RADIAL COMPONENT
EVENT ICEBERG

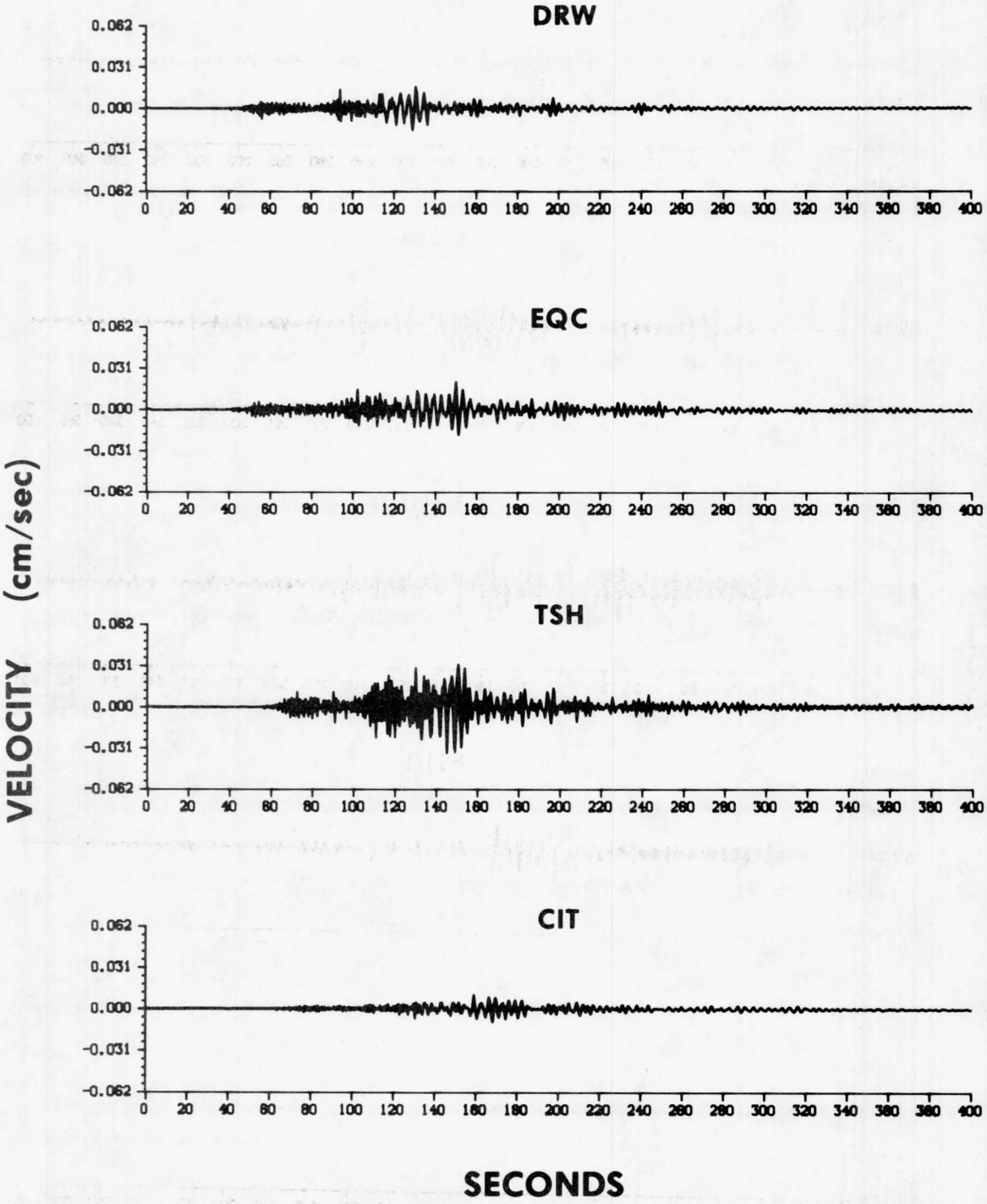

VERTICAL COMPONENT
EVENT MAST

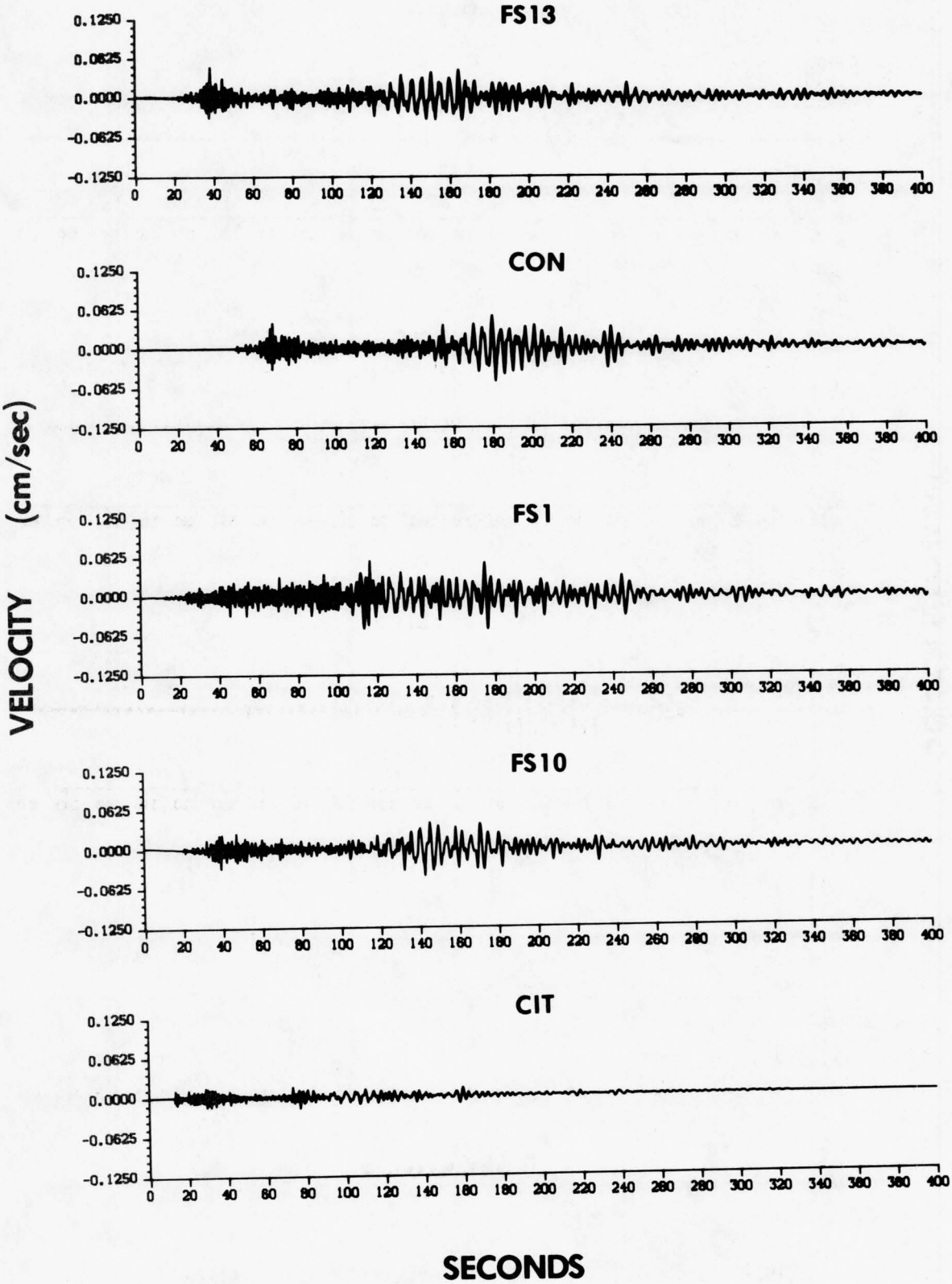

TRANSVERSE COMPONENT
EVENT MAST

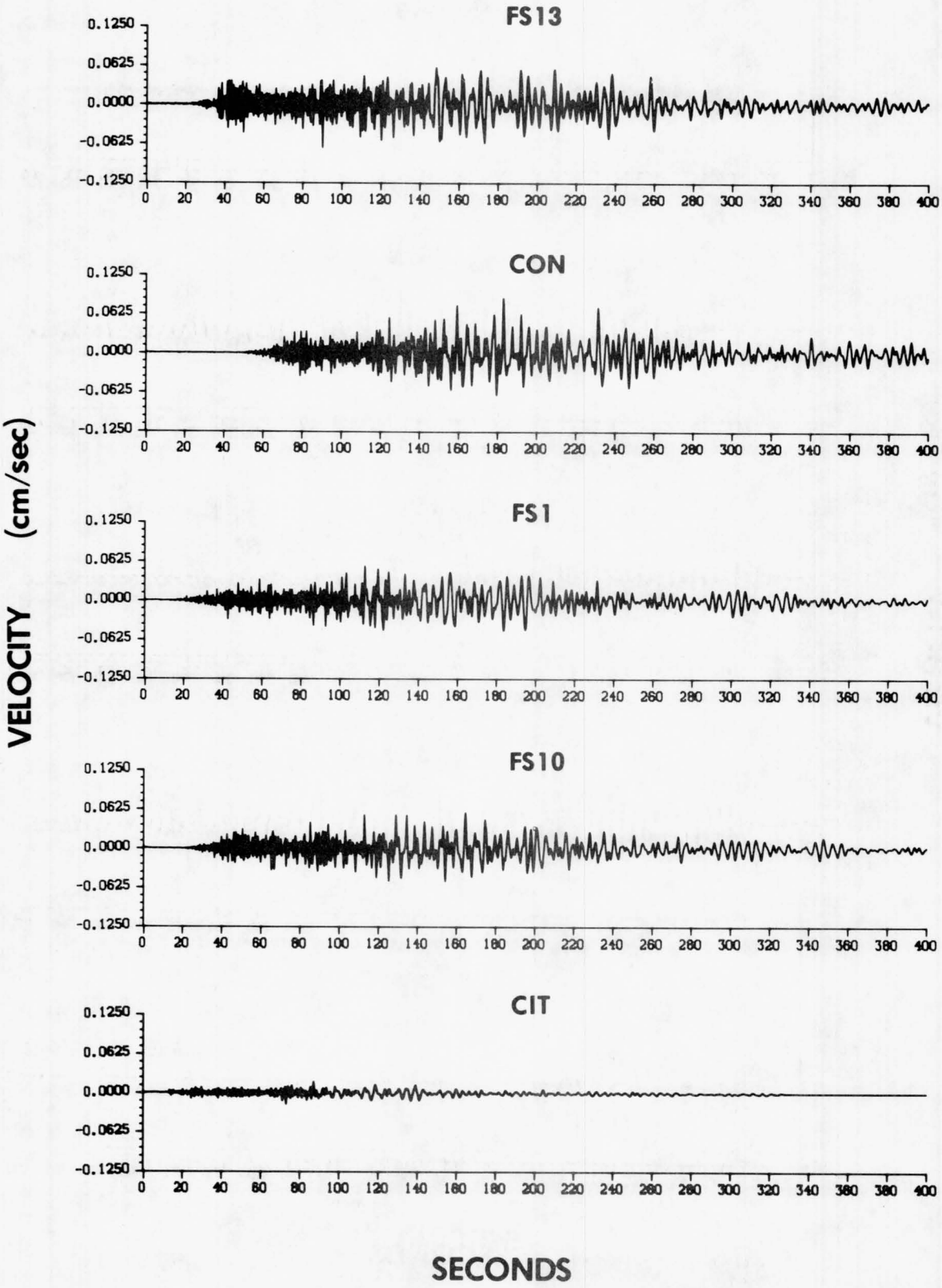

RADIAL COMPONENT
EVENT MAST

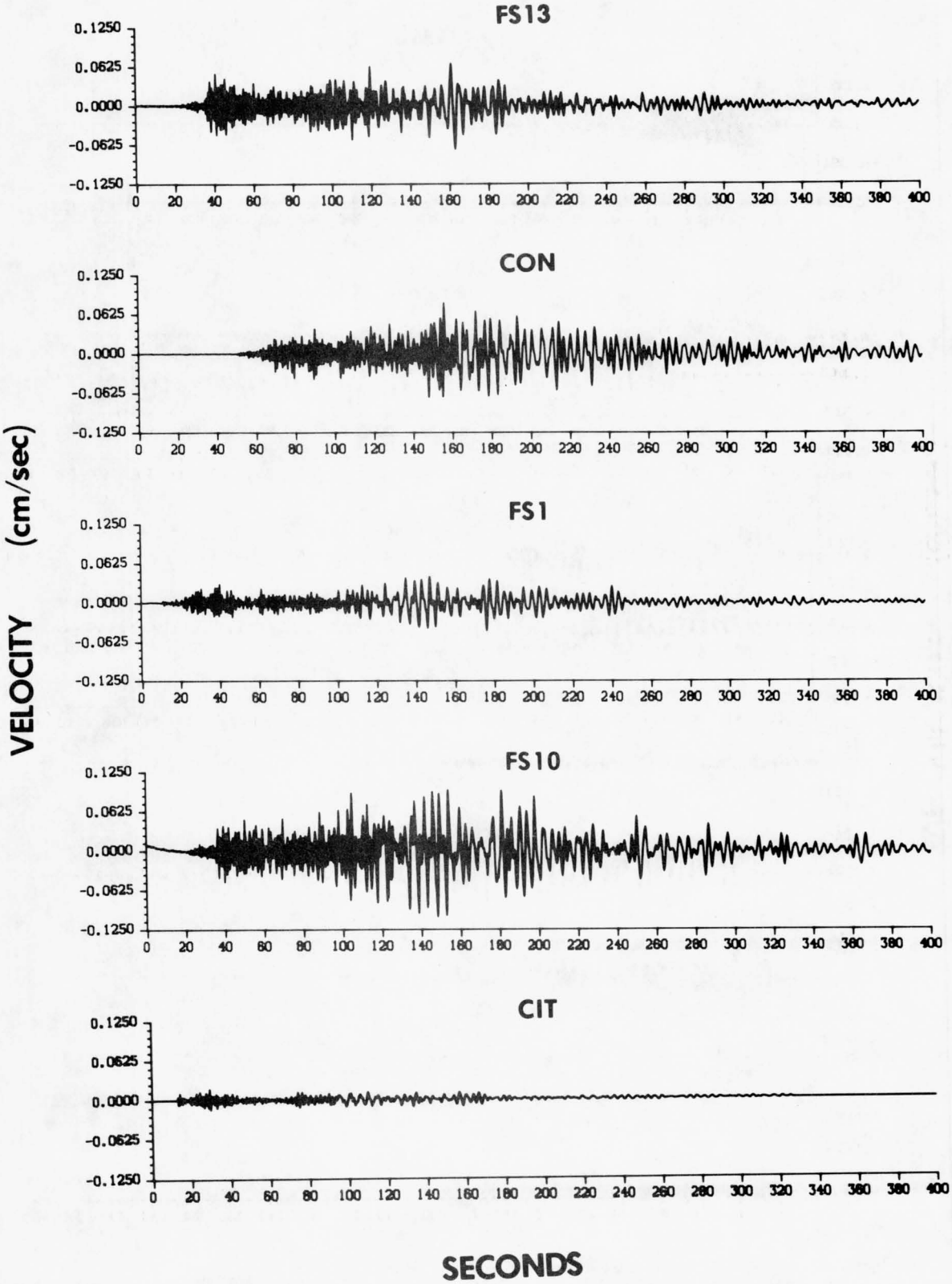

VERTICAL COMPONENT
EVENT MUENSTER

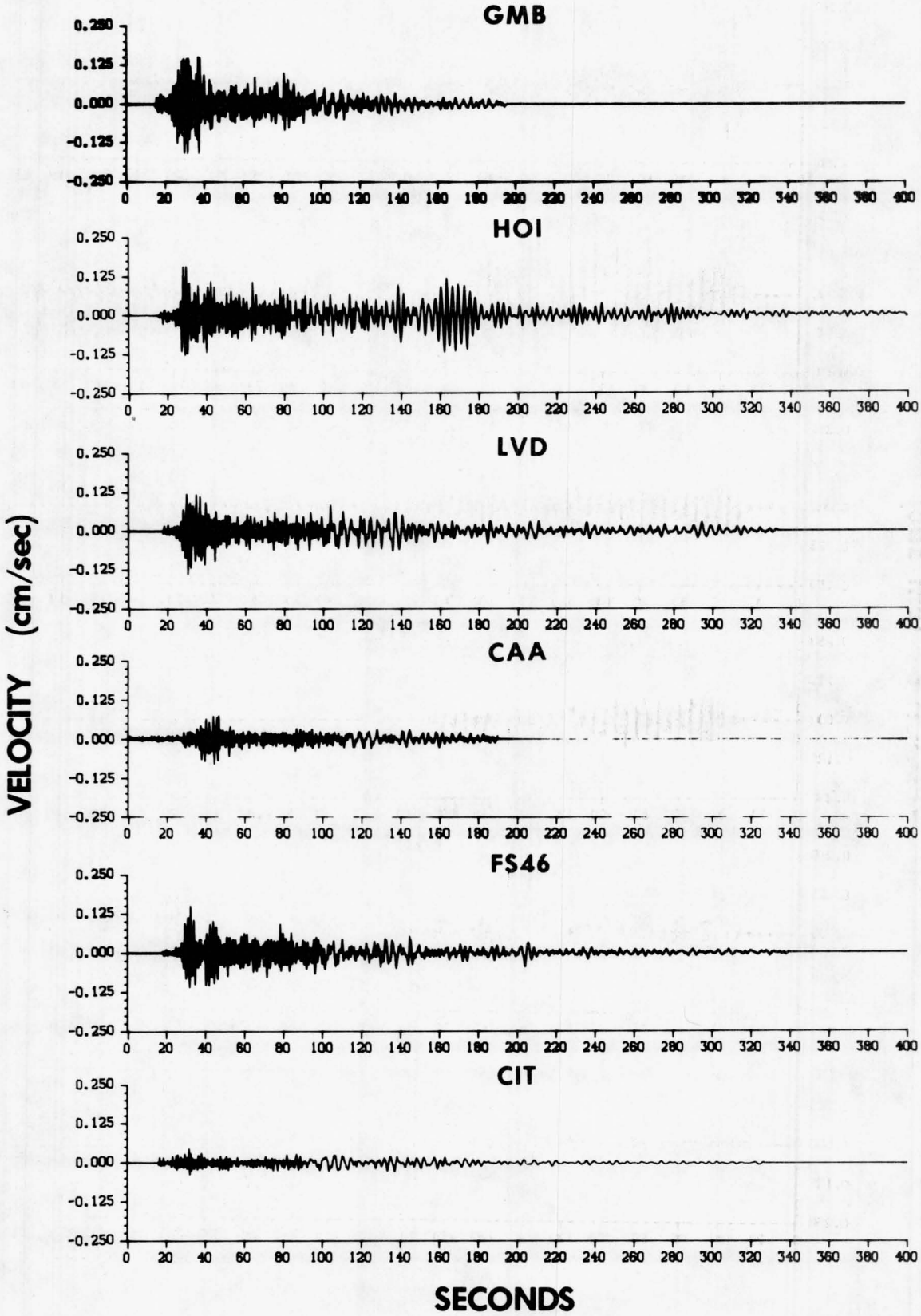

TRANSVERSE COMPONENT
EVENT MUENSTER

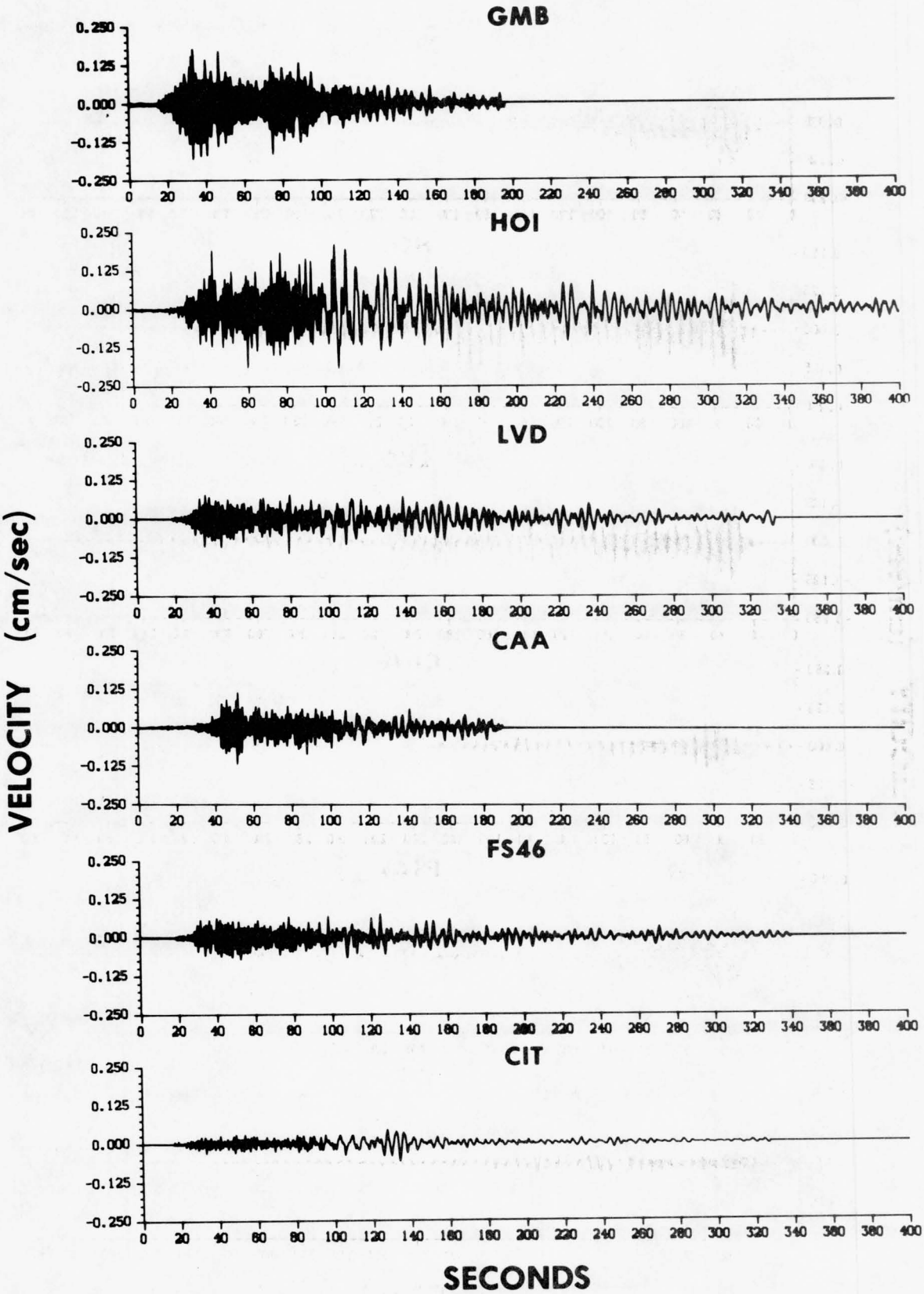

RADIAL COMPONENT
EVENT MUENSTER

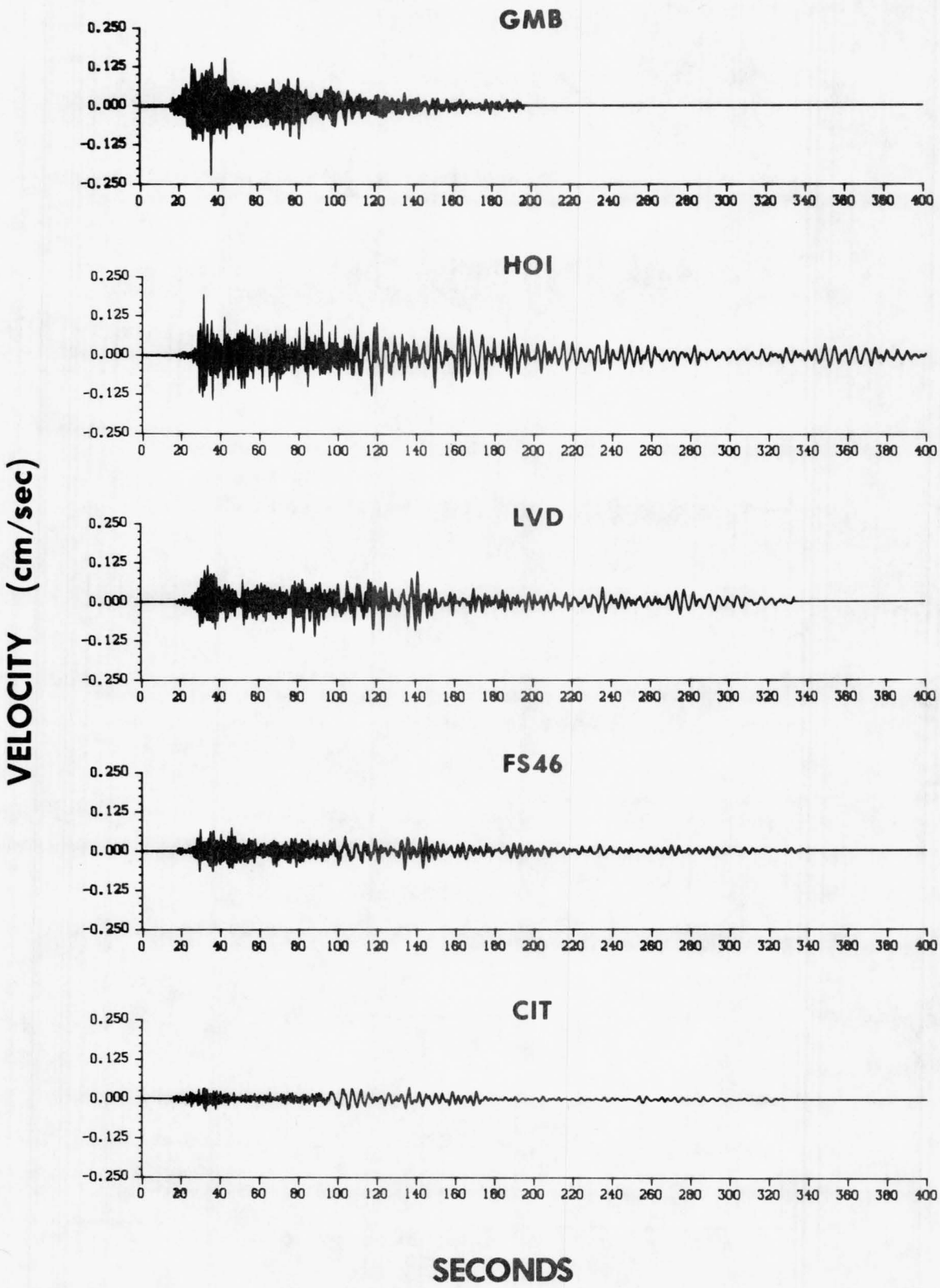

VERTICAL COMPONENT

EVENT PEPATO

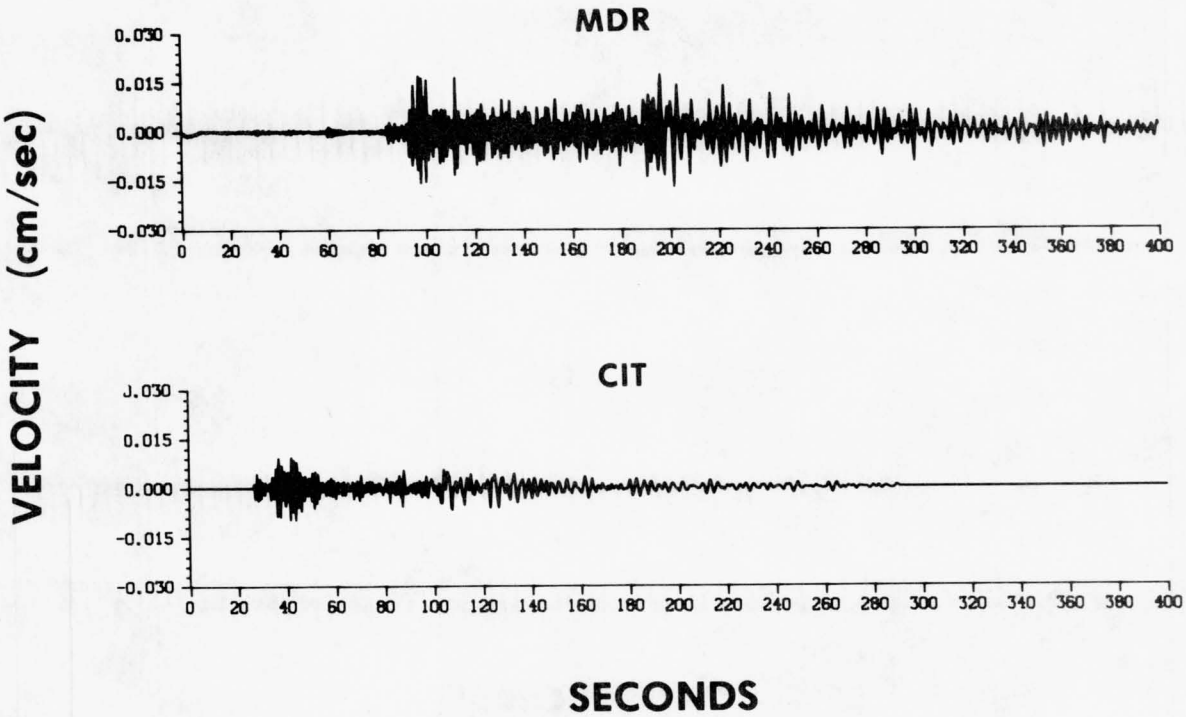

TRANSVERSE COMPONENT

EVENT PEPATO

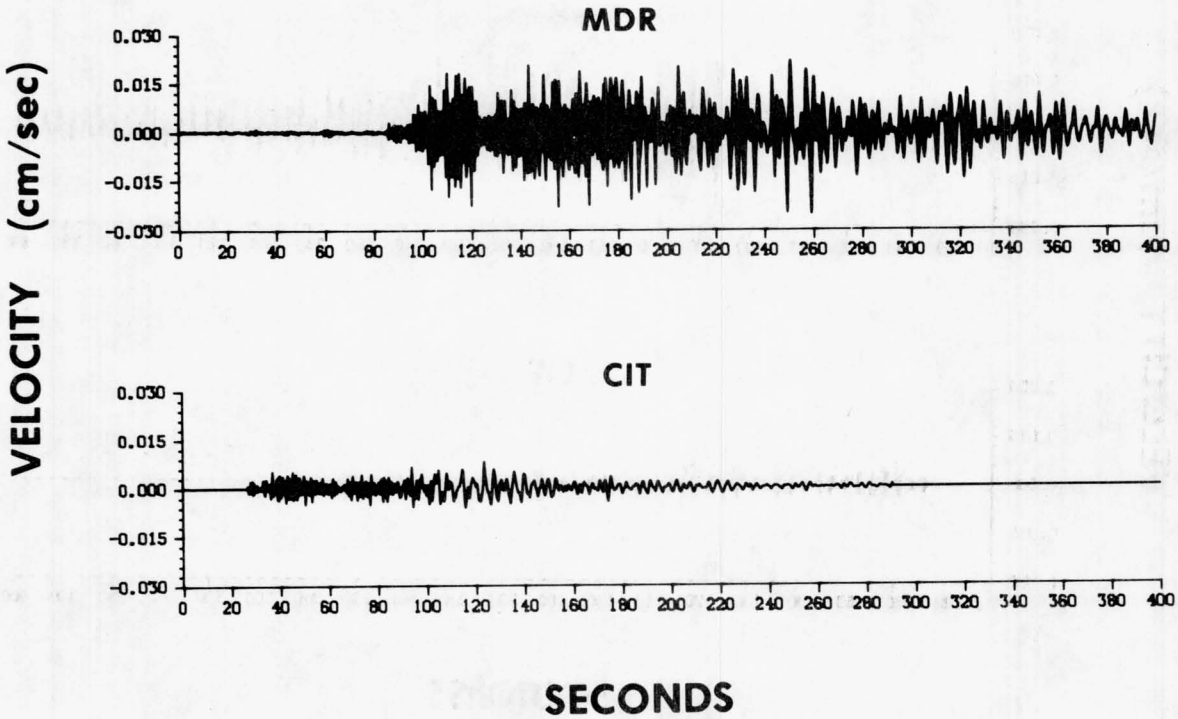

RADIAL COMPONENT

EVENT PEPATO

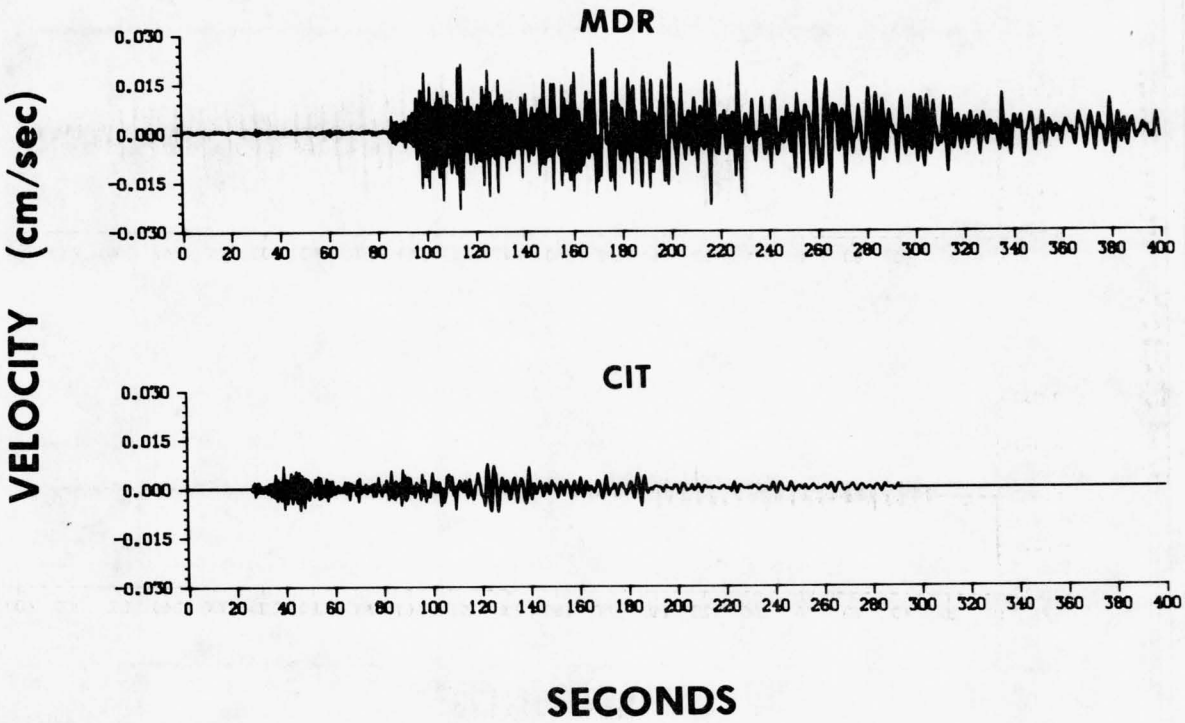

VERTICAL COMPONENT
EVENT POOL

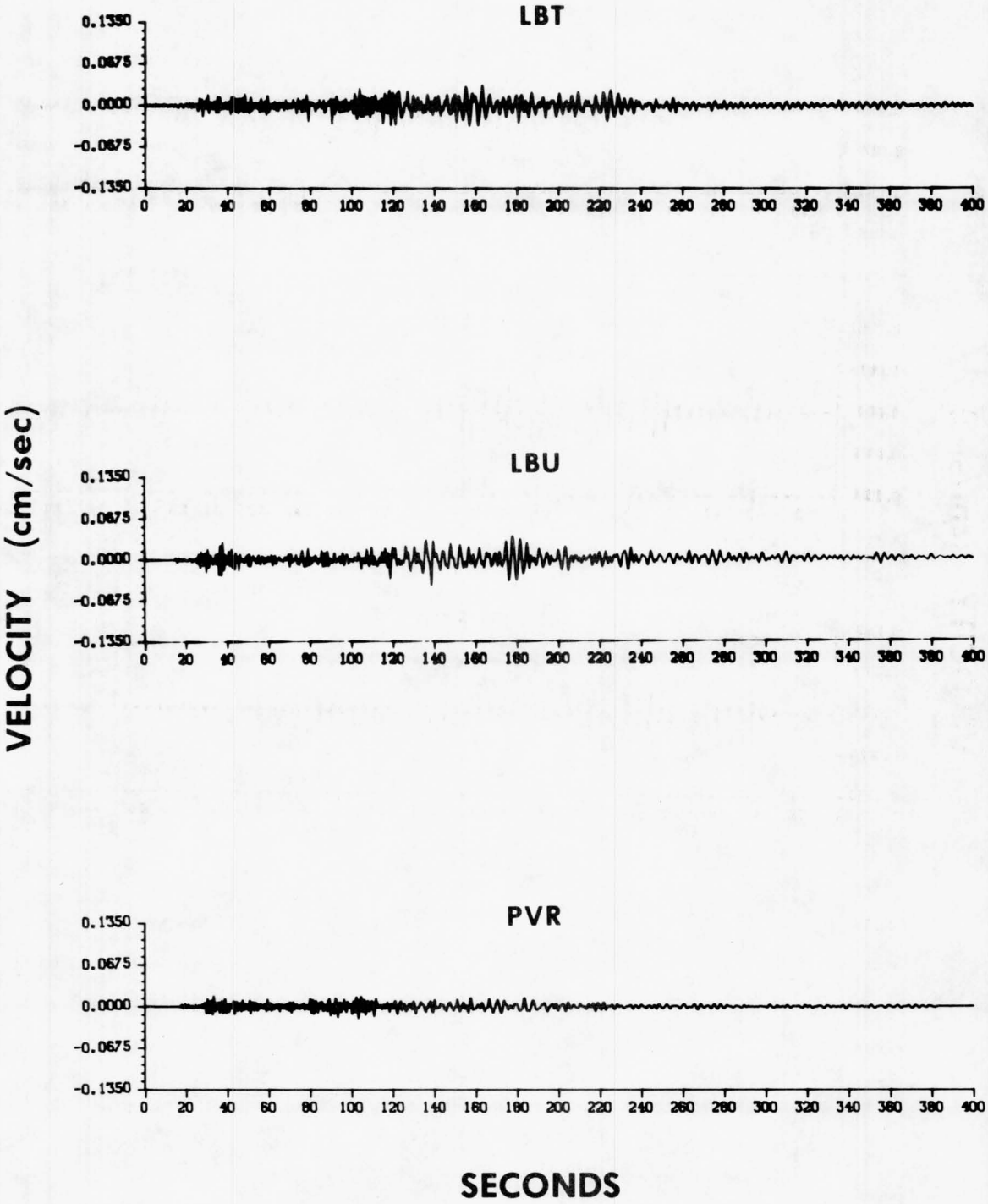

TRANSVERSE COMPONENT
EVENT POOL

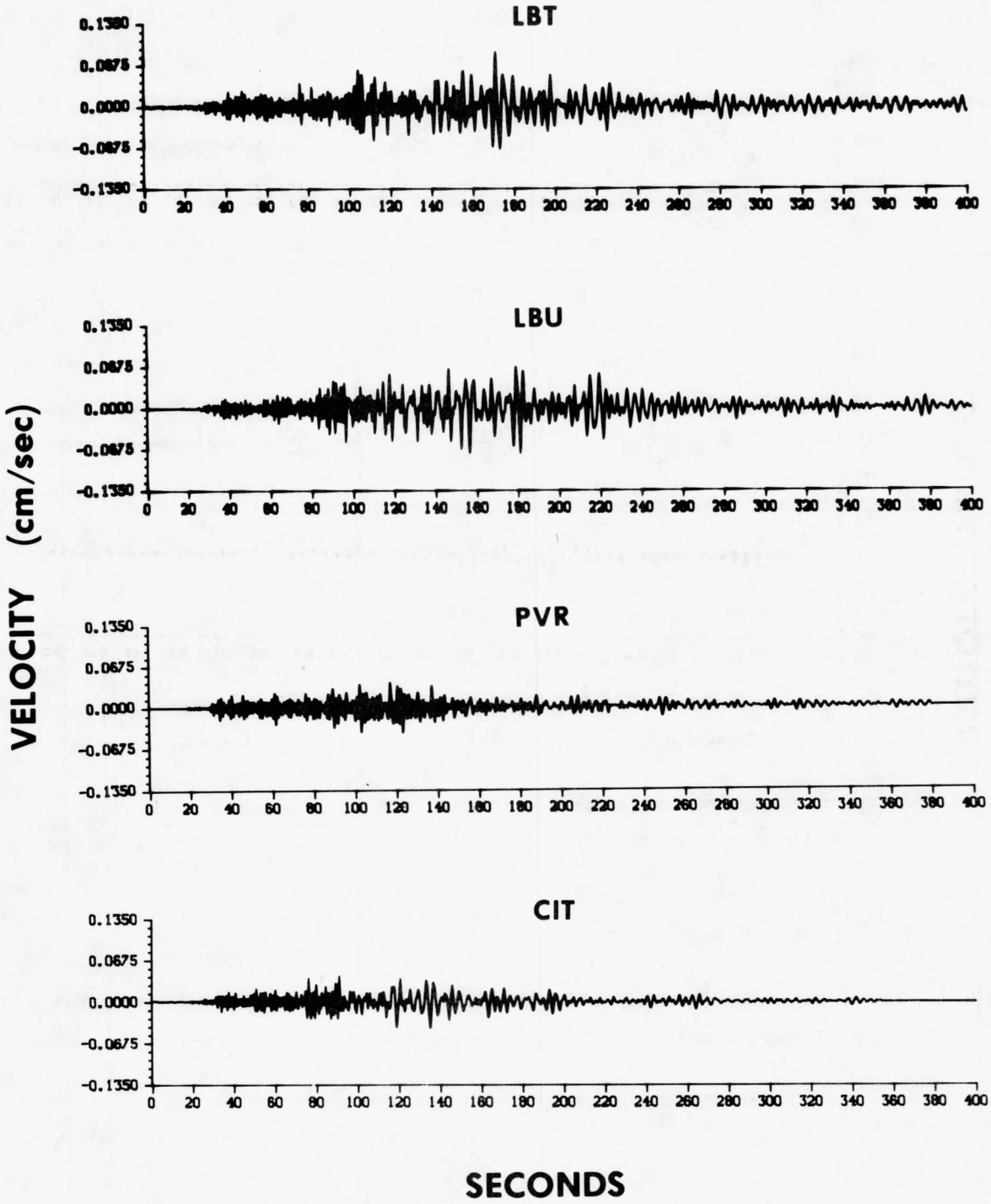

RADIAL COMPONENT
EVENT POOL

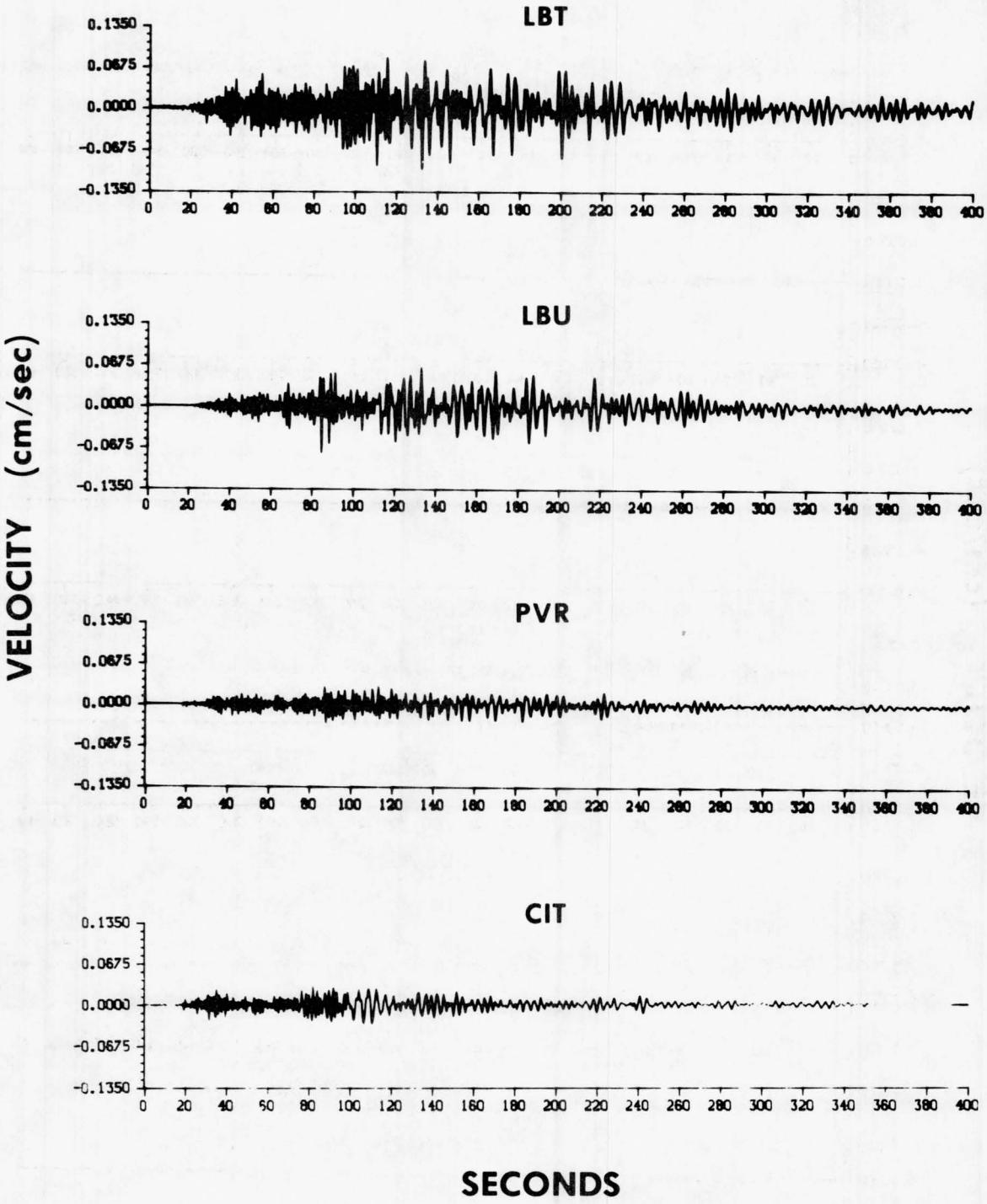

VERTICAL COMPONENT
EVENT RUDDER

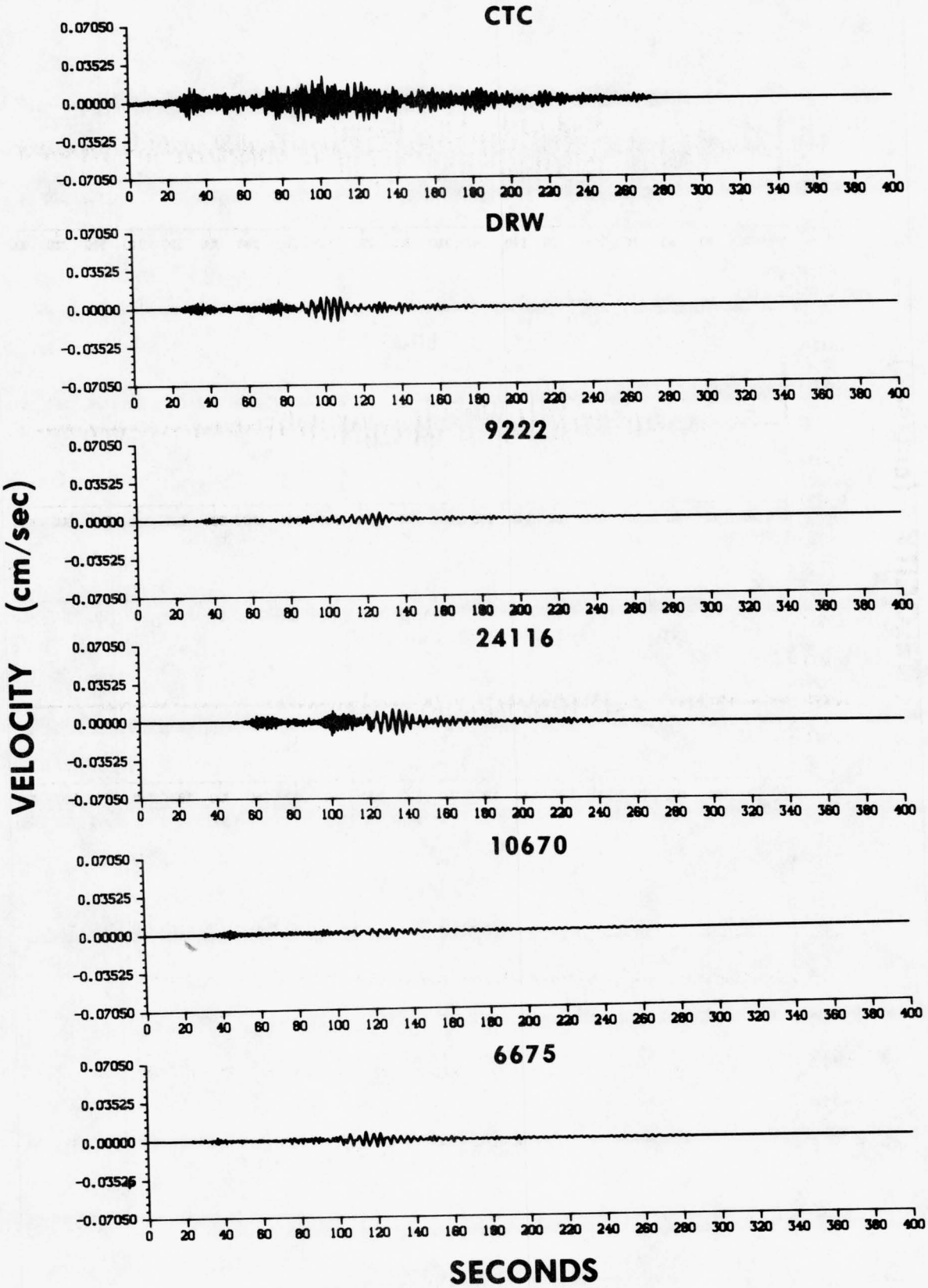

VERTICAL COMPONENT
EVENT RUDDER

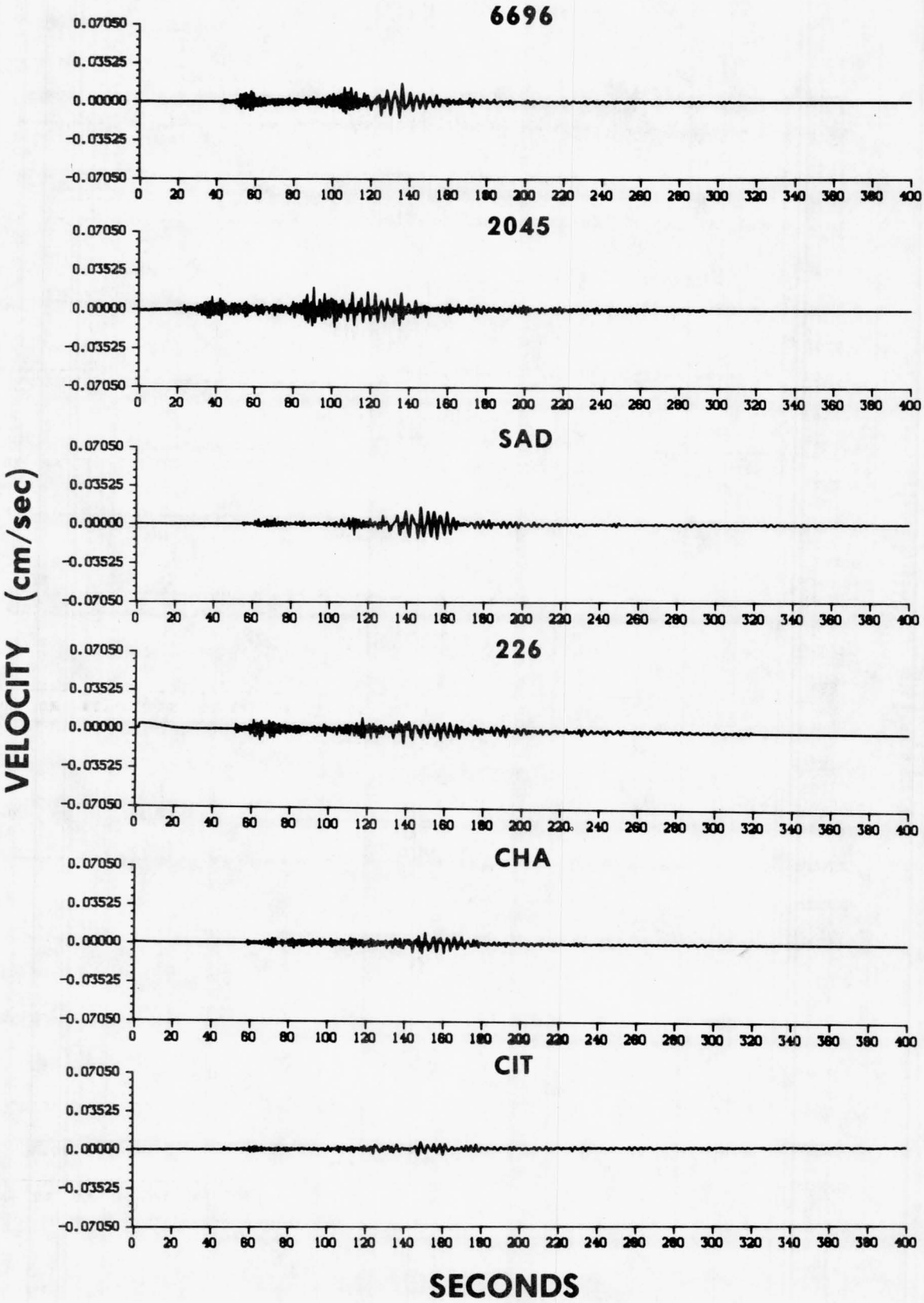

TRANSVERSE COMPONENT
EVENT RUDDER

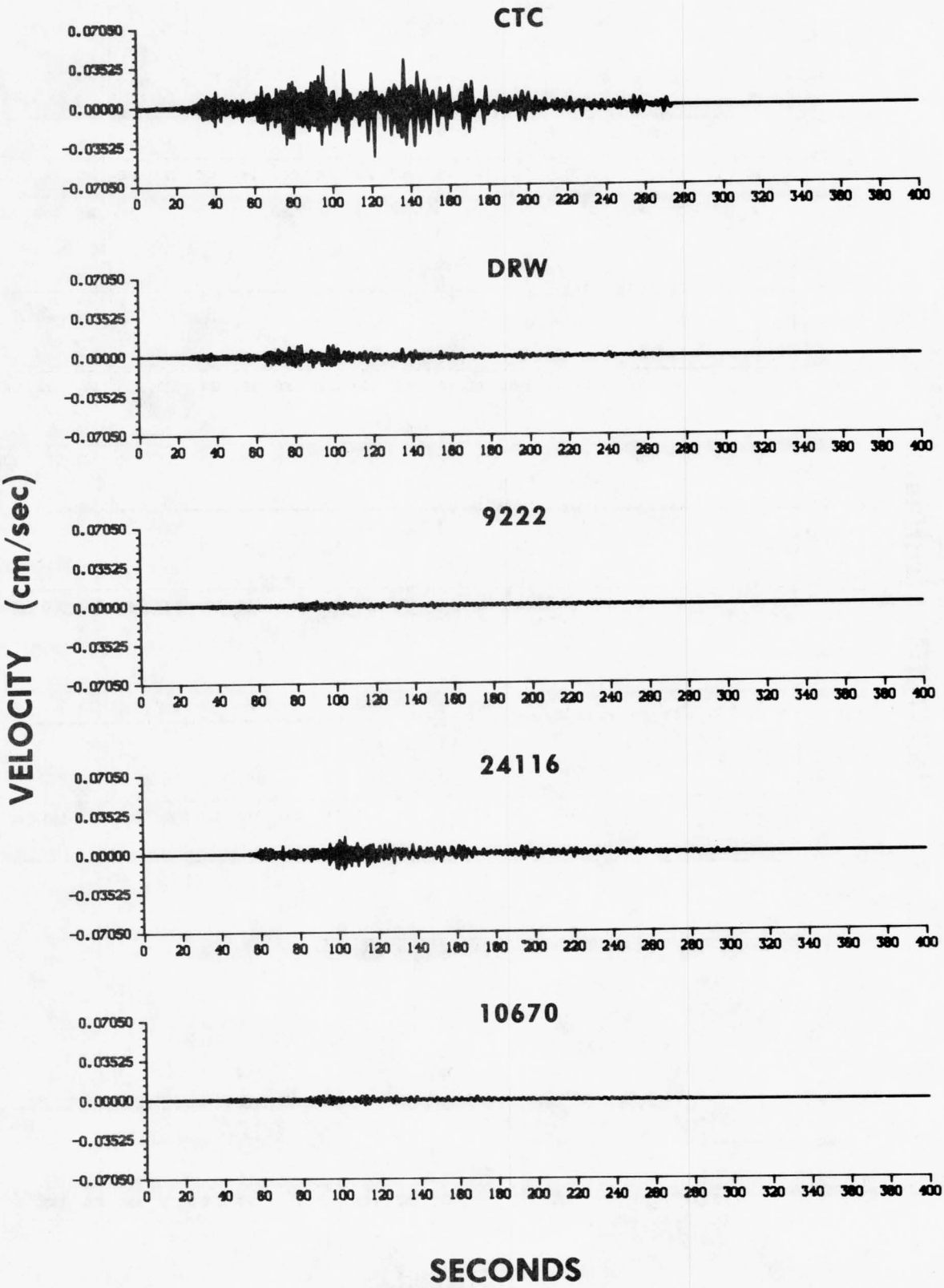

TRANSVERSE COMPONENT
EVENT RUDDER

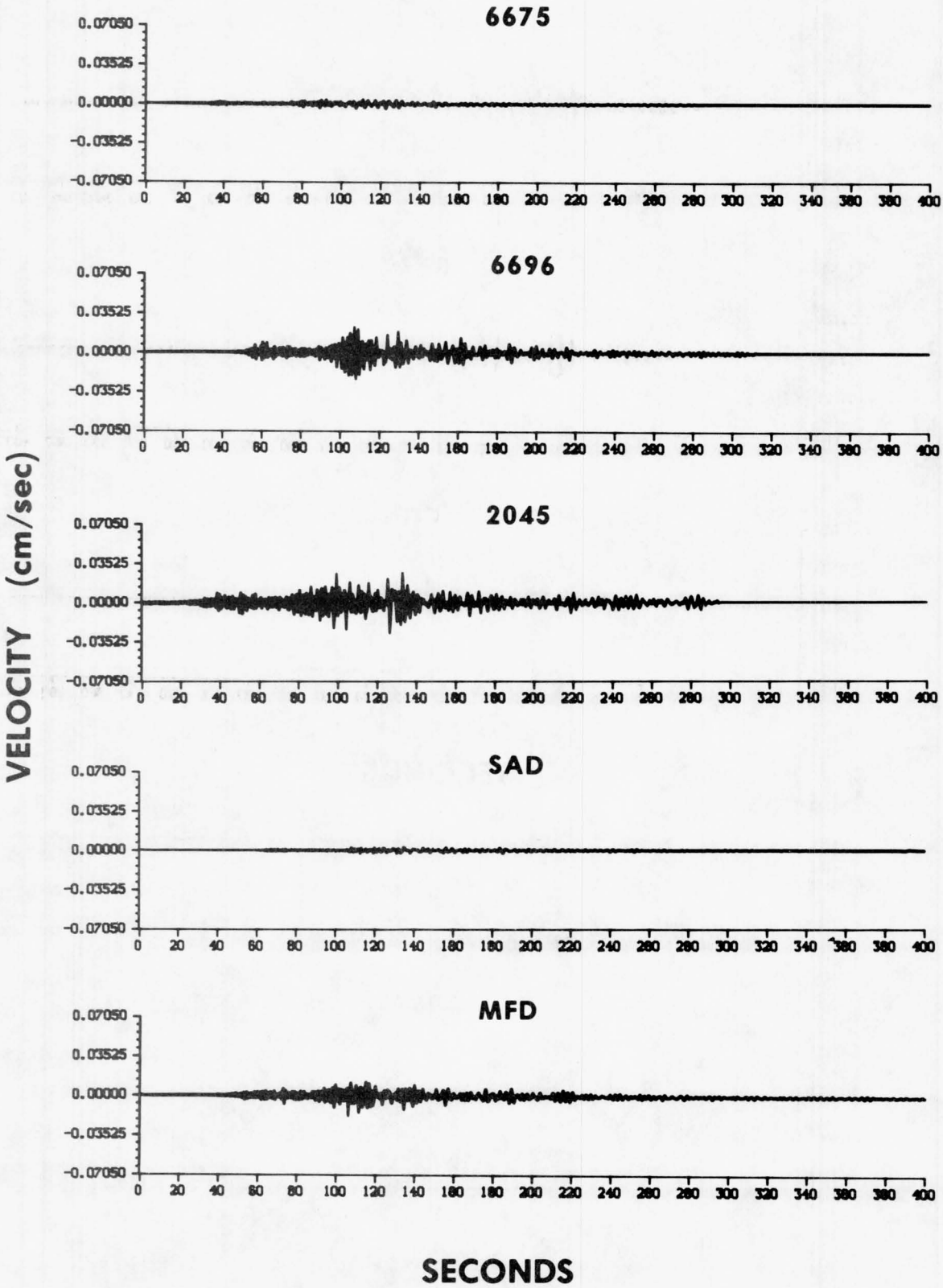

TRANSVERSE COMPONENT
EVENT RUDDER

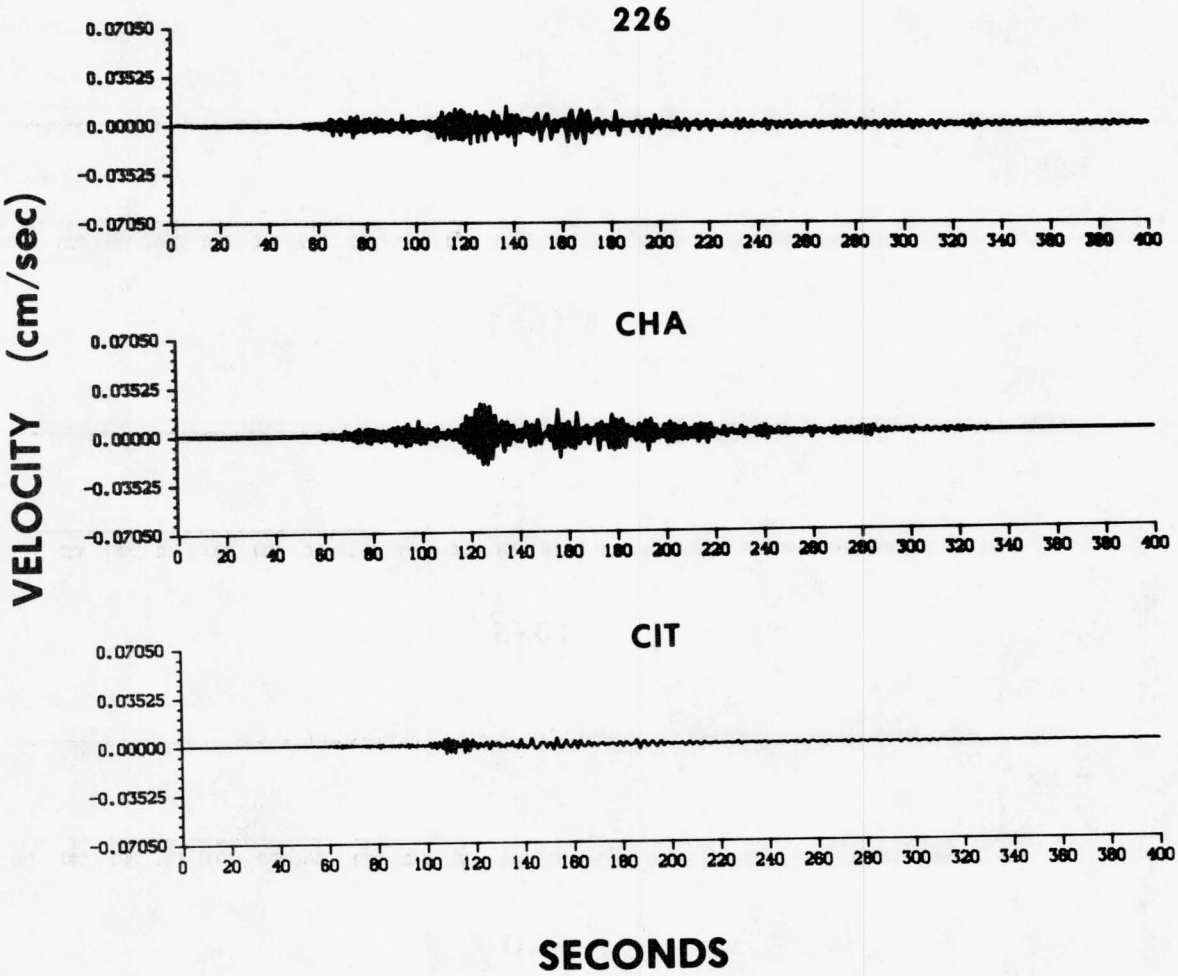

RADIAL COMPONENT
EVENT RUDDER

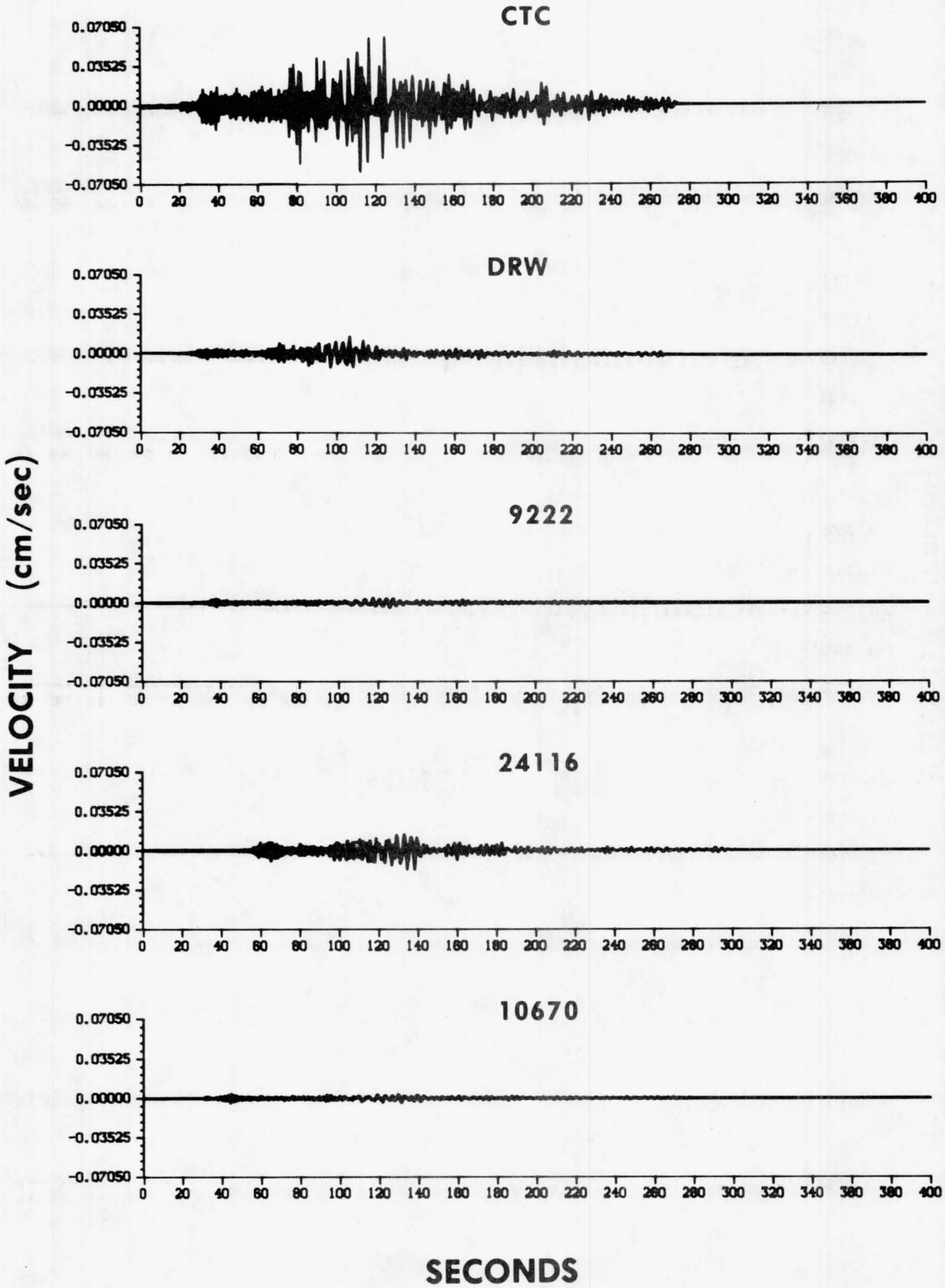

RADIAL COMPONENT
EVENT RUDDER

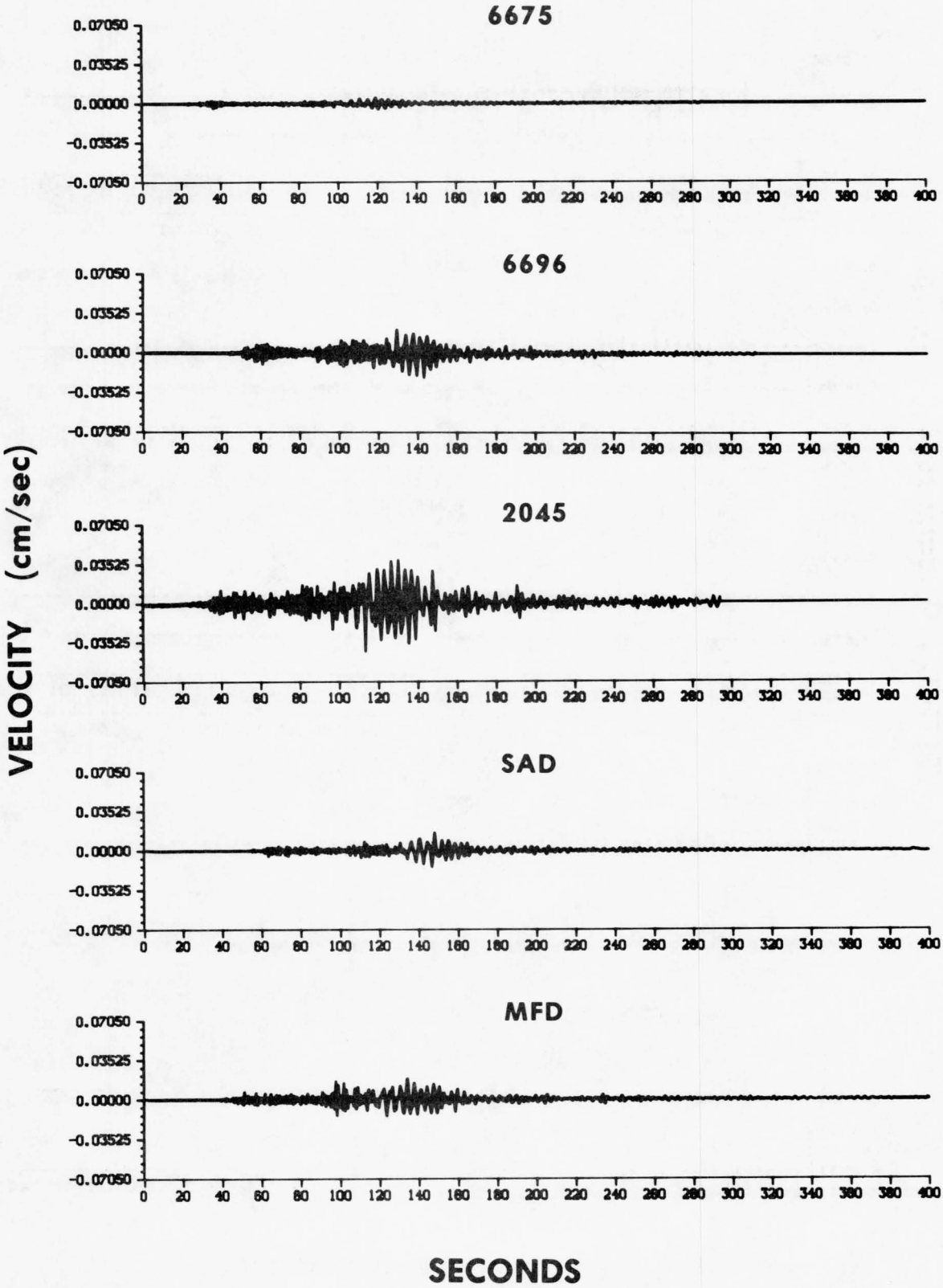

RADIAL COMPONENT
EVENT RUDDER

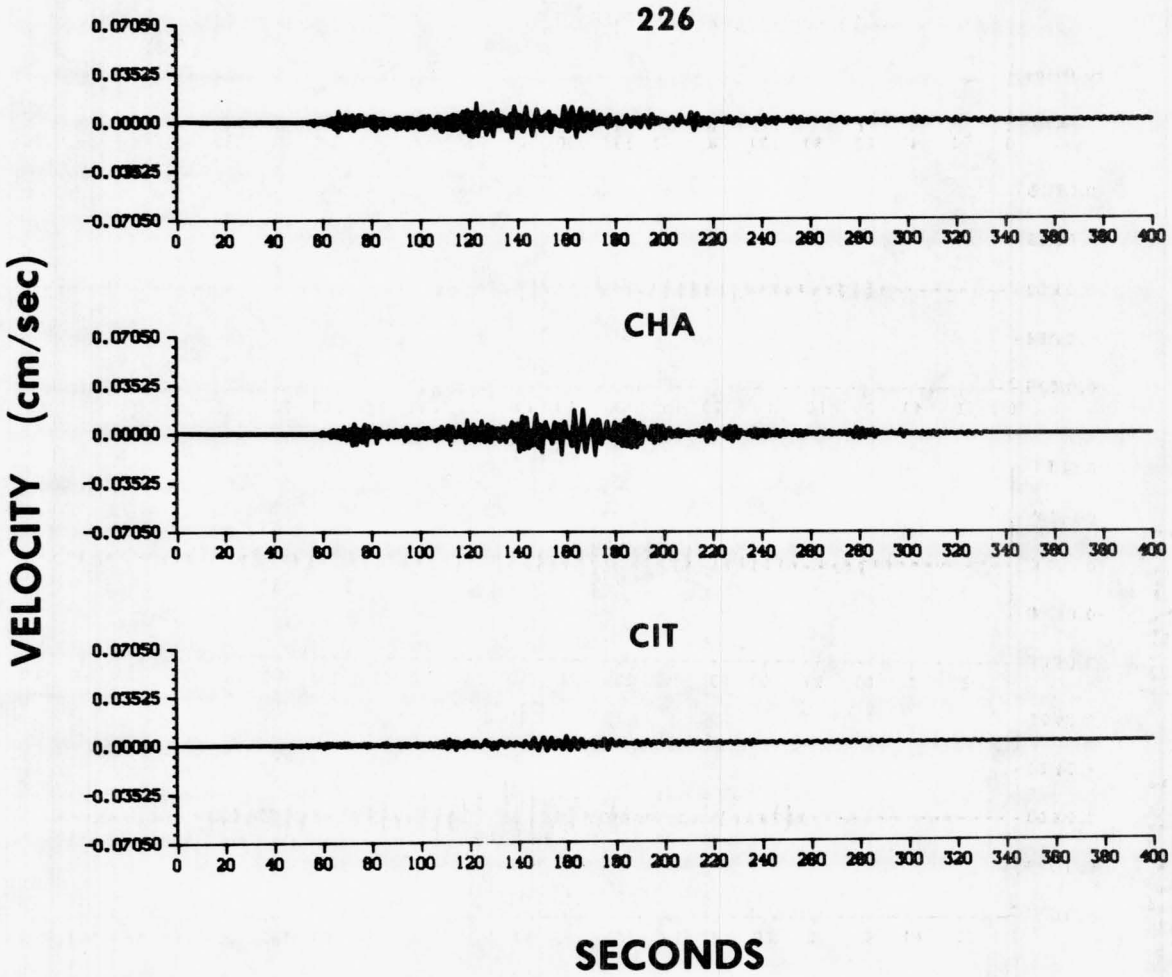

VERTICAL COMPONENT
EVENT SCANTLING

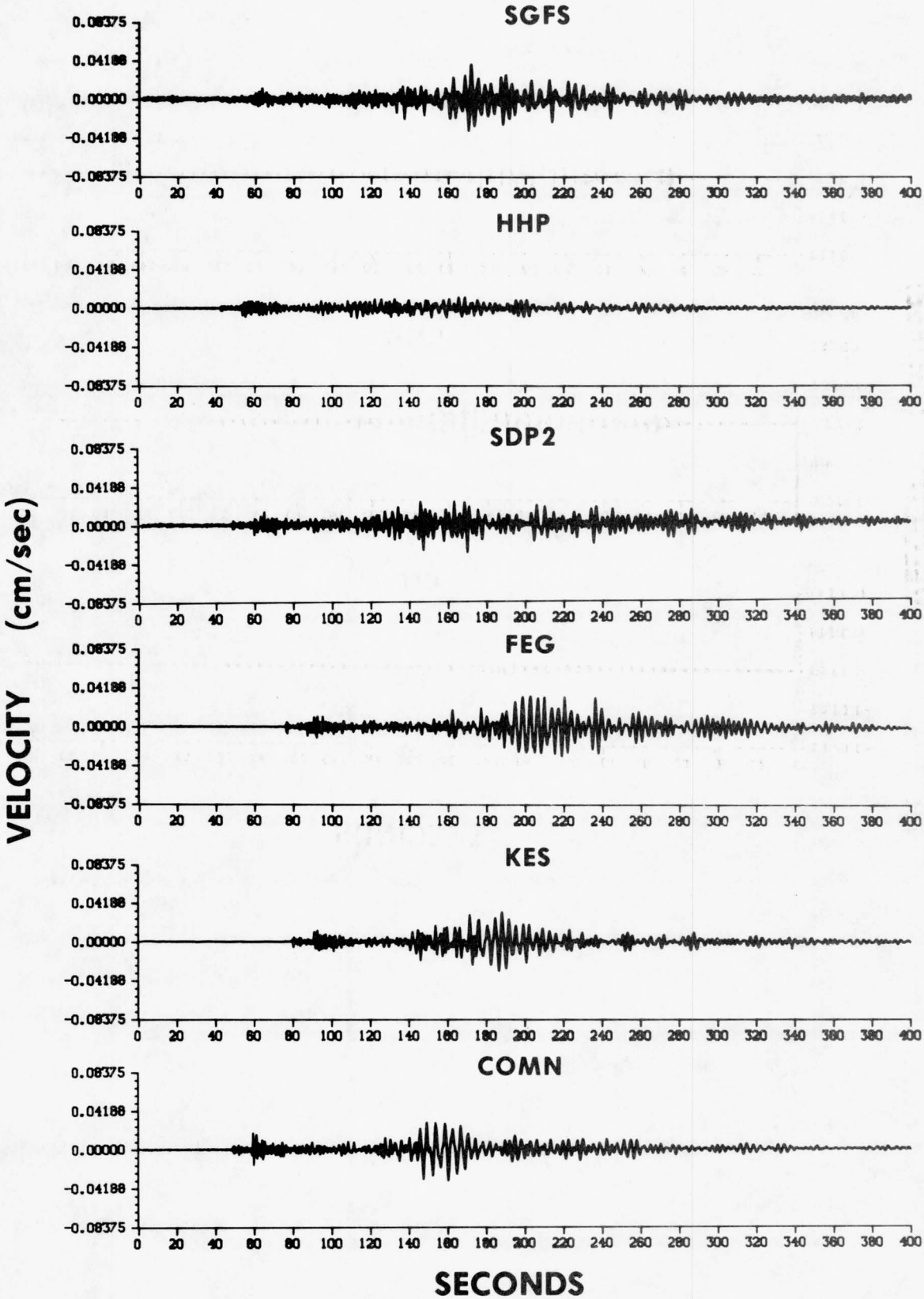

VERTICAL COMPONENT
EVENT SCANTLING

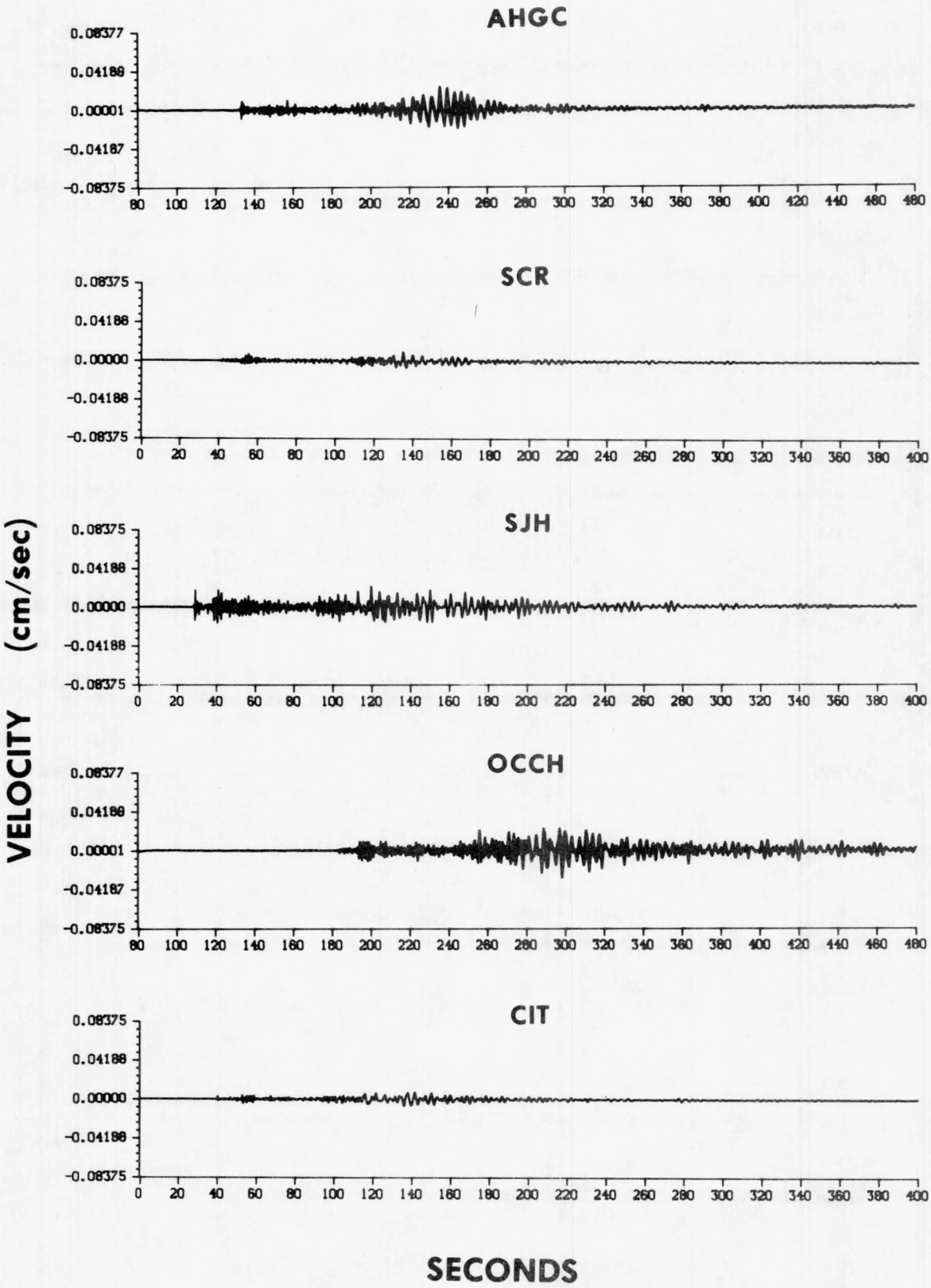

TRANSVERSE COMPONENT
EVENT SCANTLING

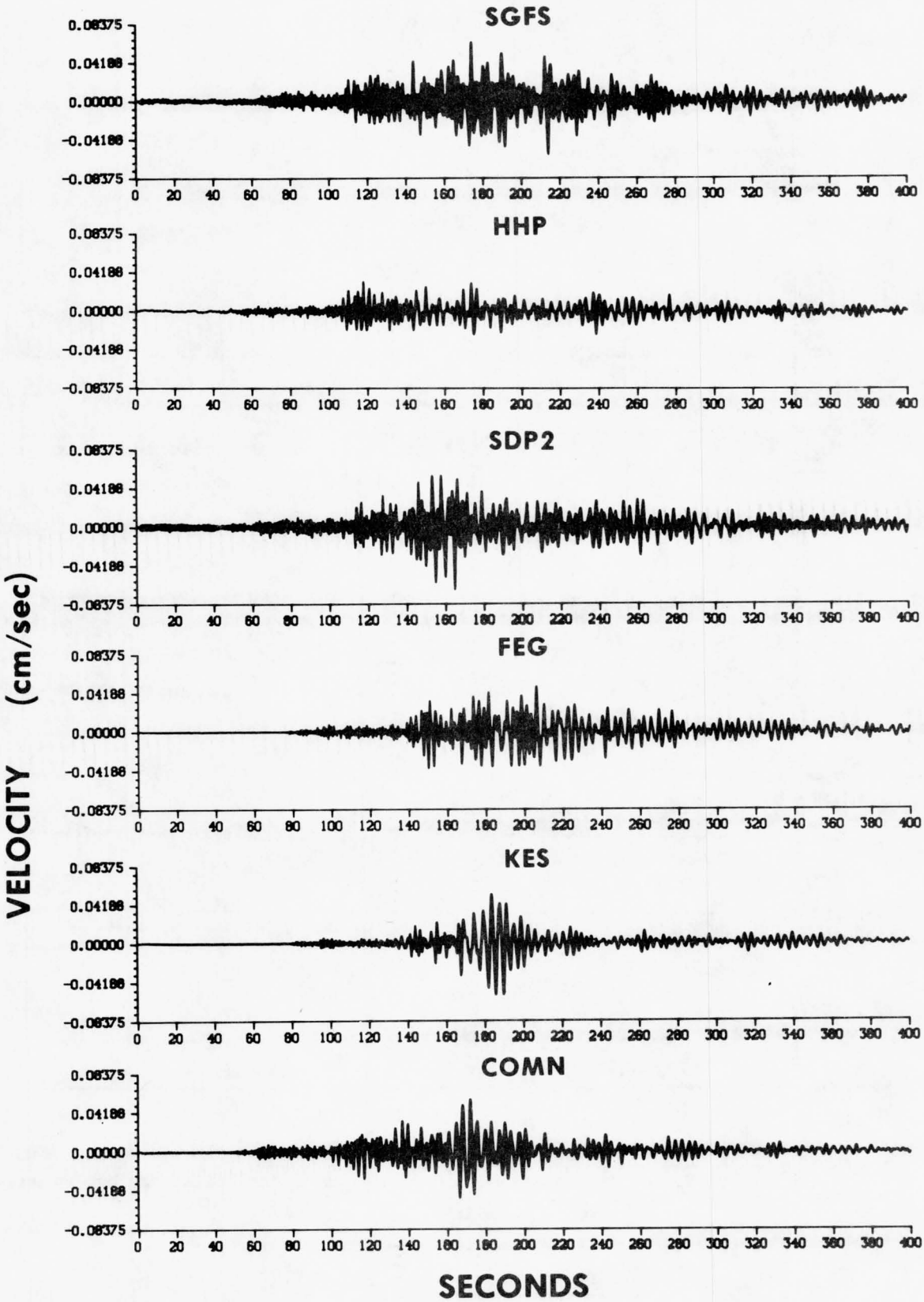

TRANSVERSE COMPONENT
EVENT SCANTLING

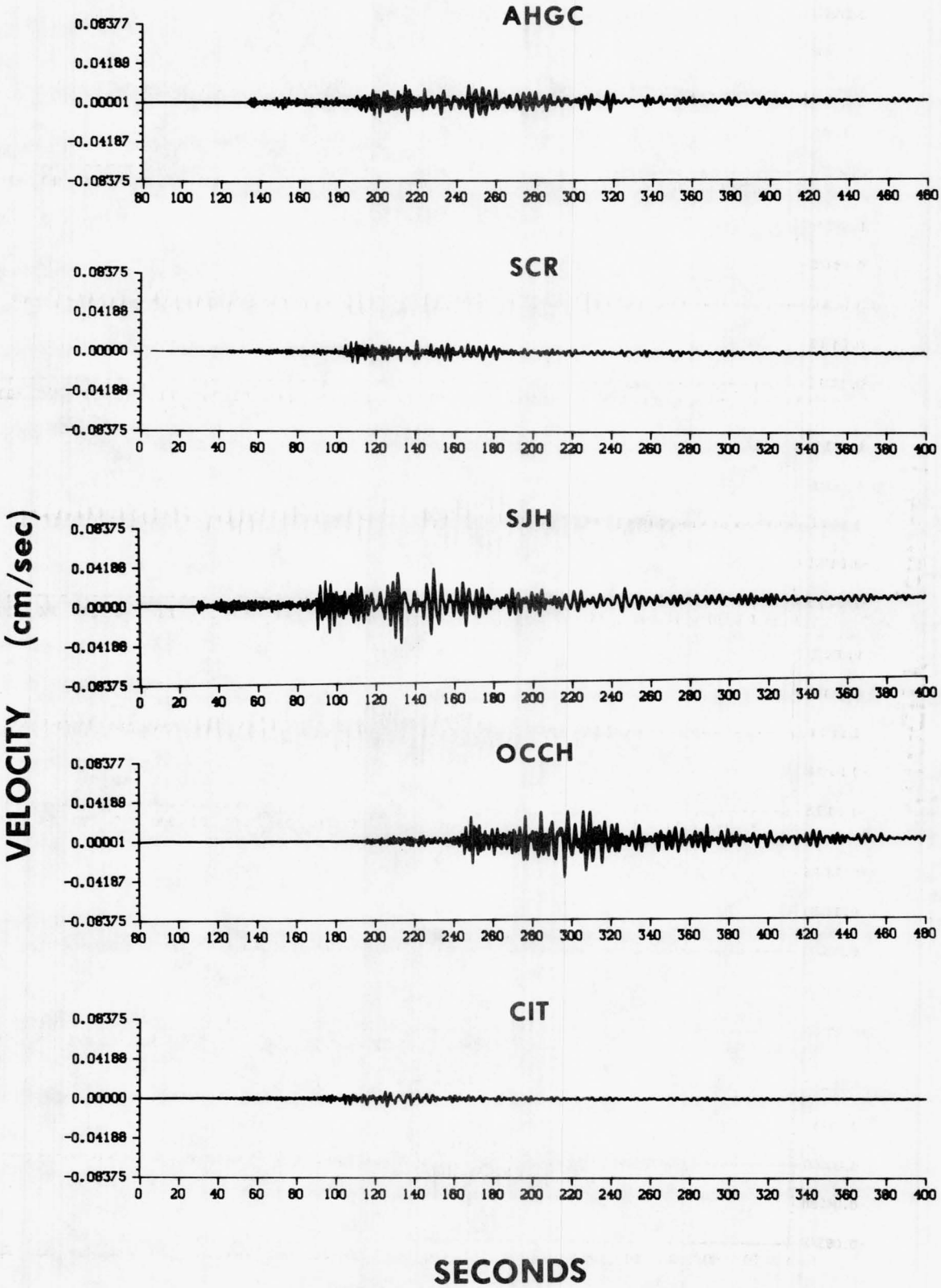

RADIAL COMPONENT
EVENT SCANTLING

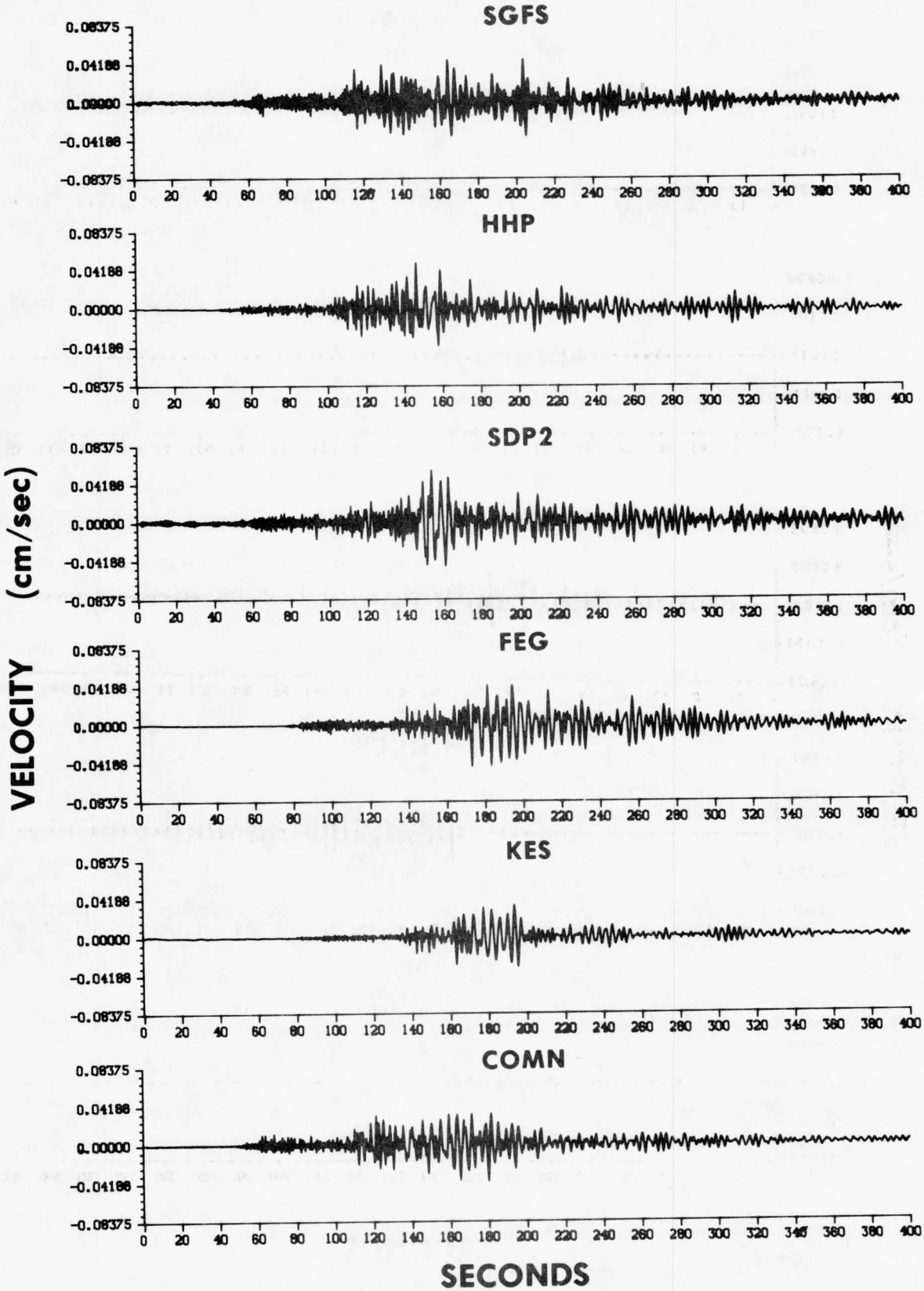

RADIAL COMPONENT
EVENT SCANTLING

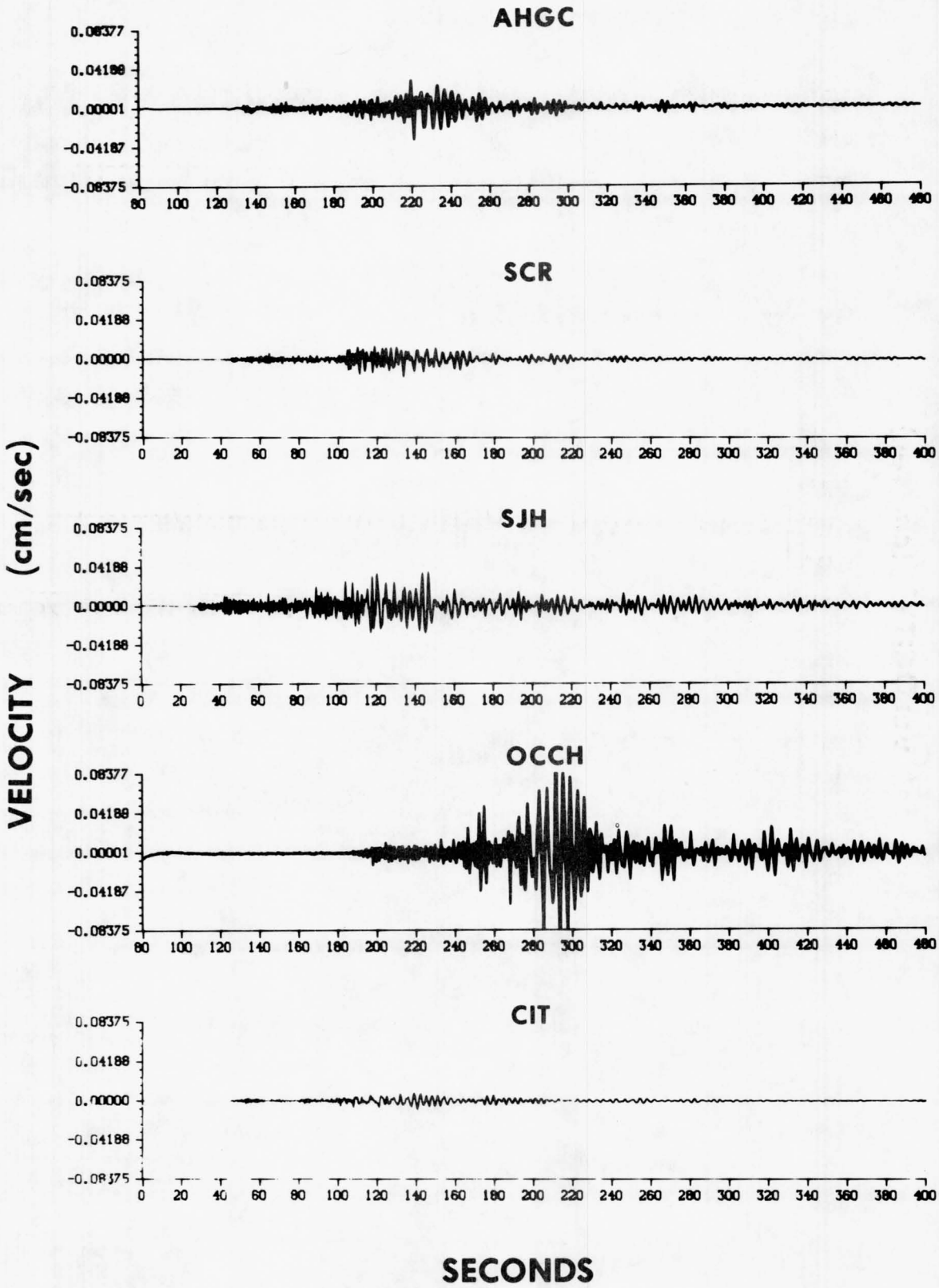

VERTICAL COMPONENT
EVENT STRAIT

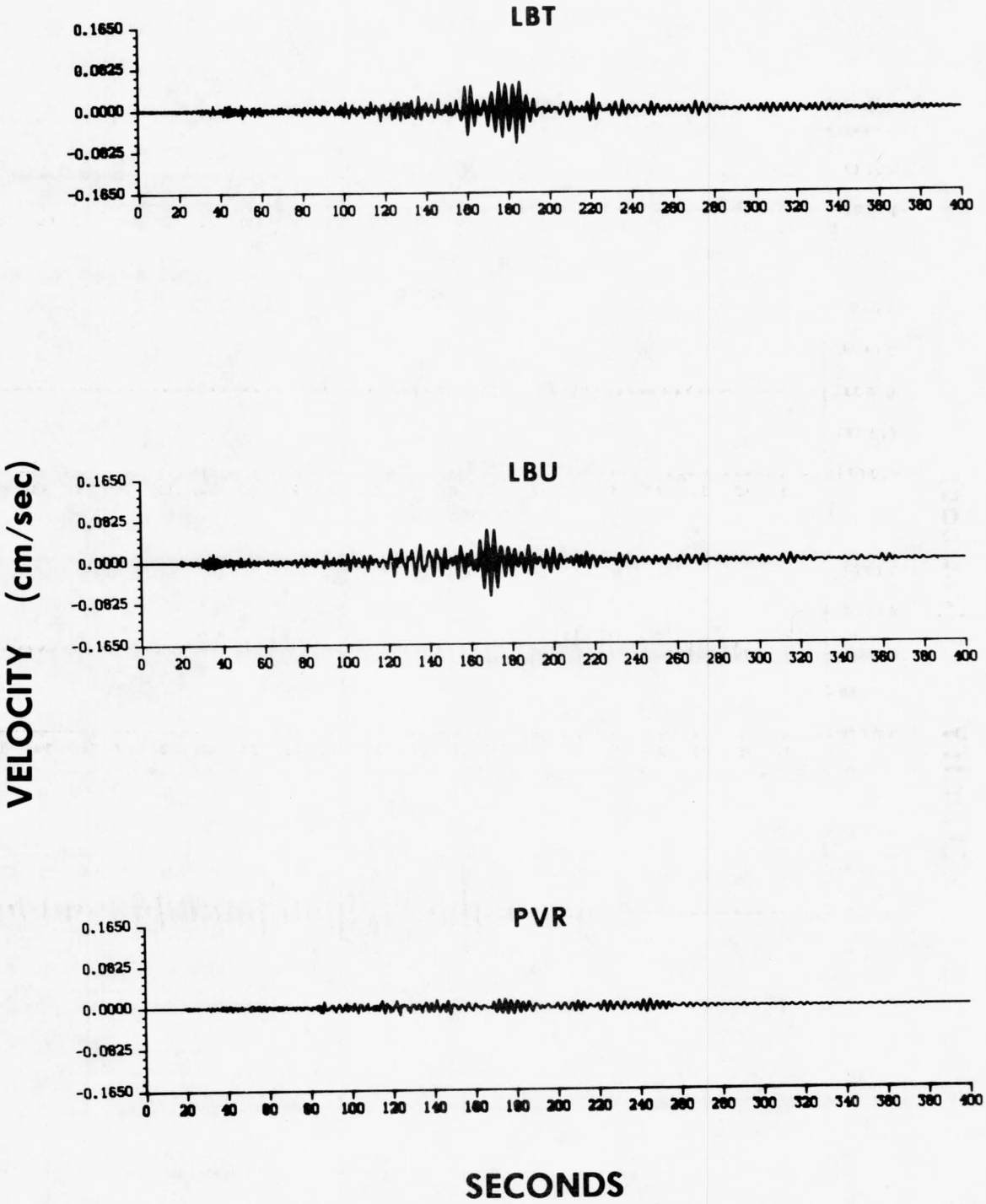

TRANSVERSE COMPONENT
EVENT STRAIT

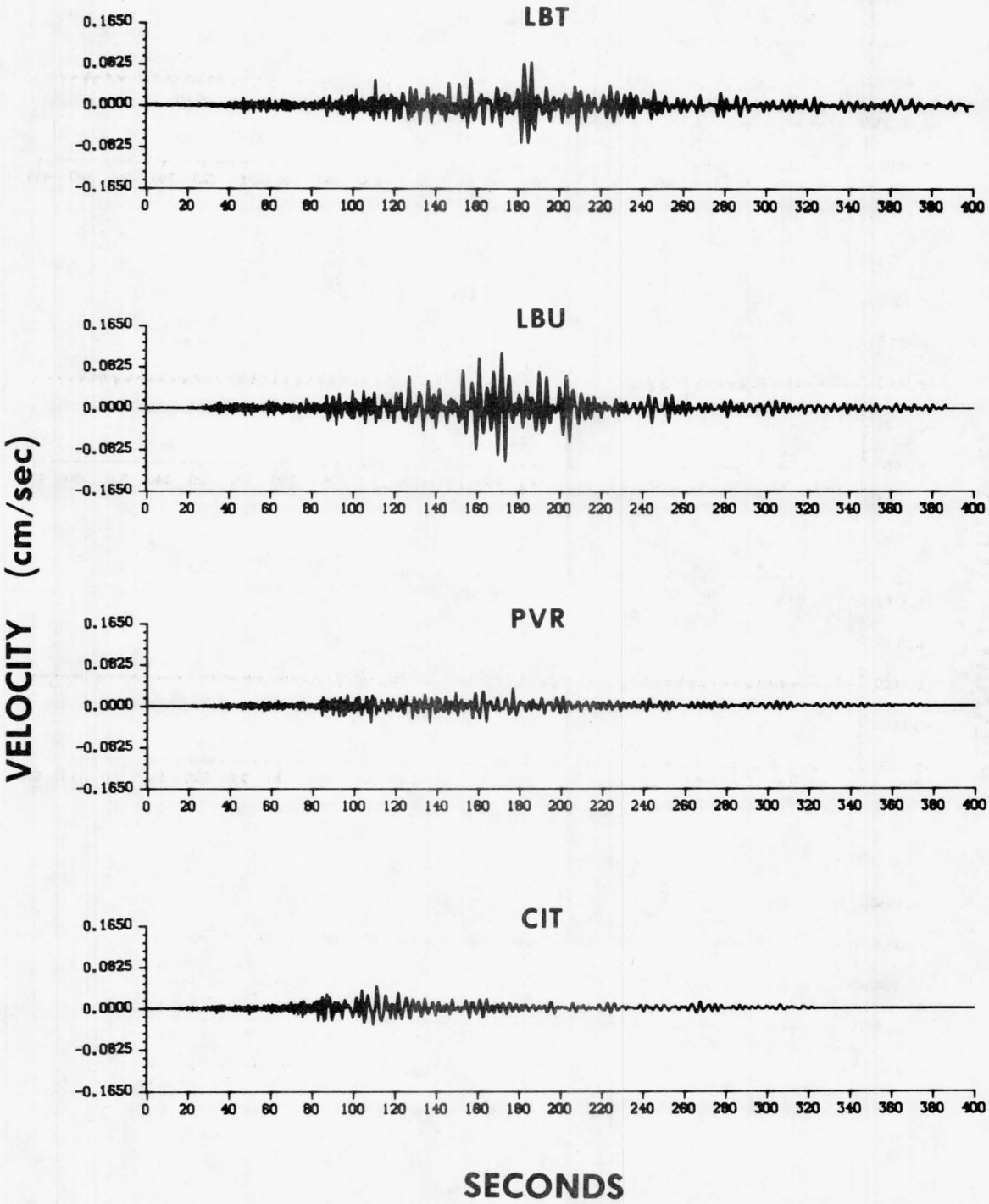

RADIAL COMPONENT
EVENT STRAIT

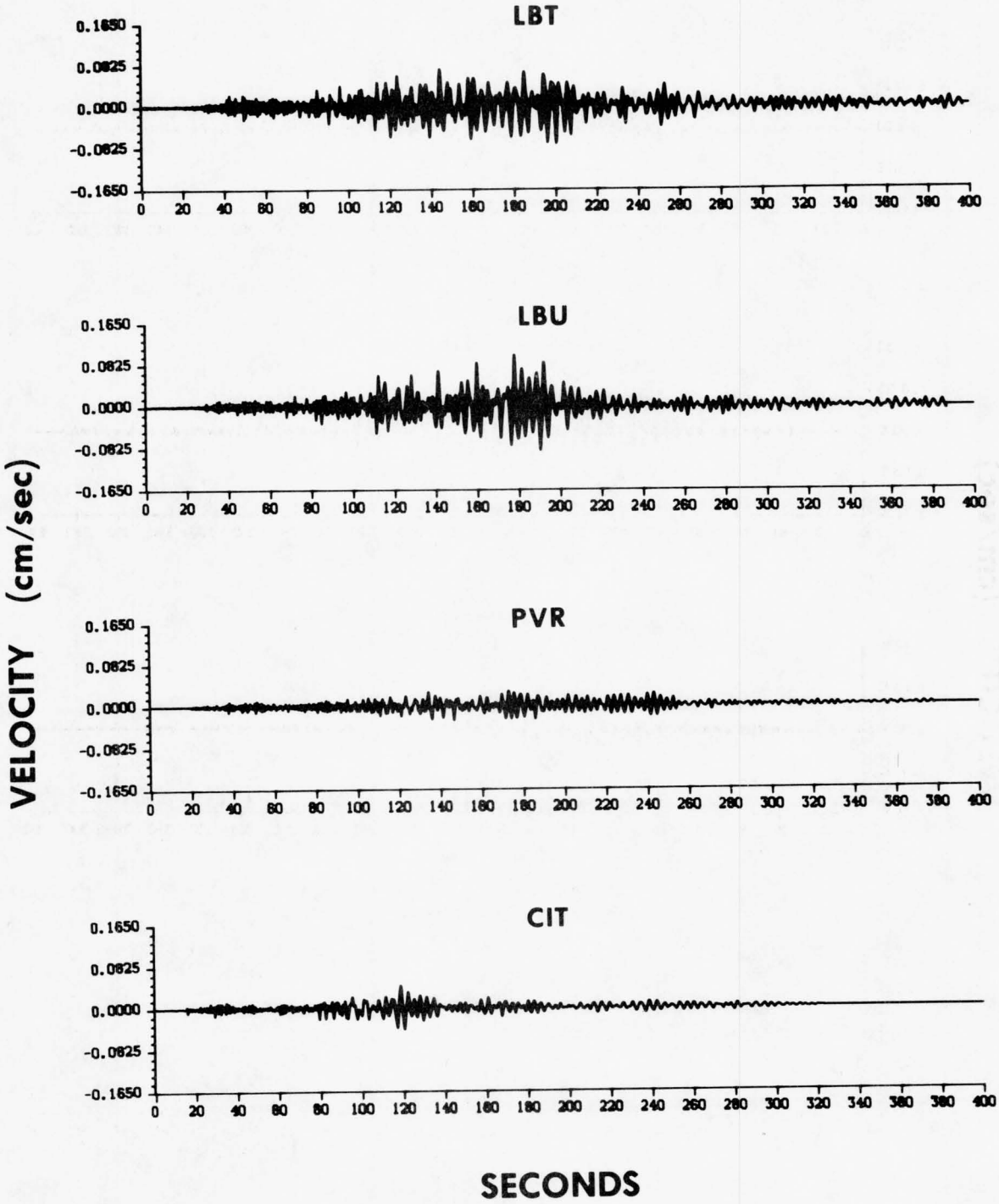

APPENDIX C

Site transfer functions arranged according to nuclear events.

EVENT BACKBEACH

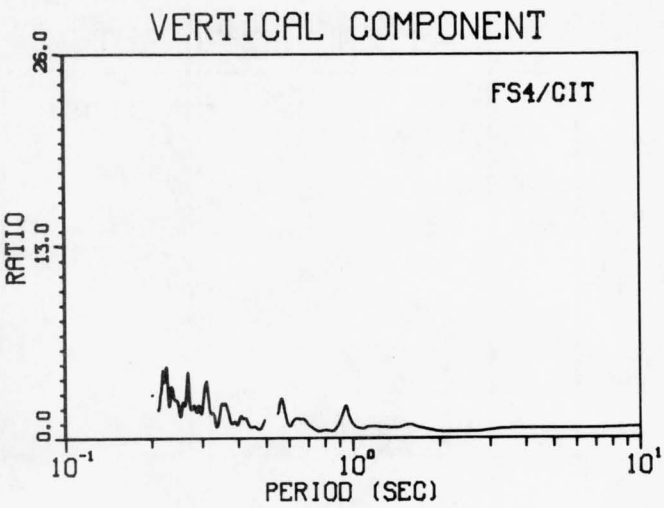

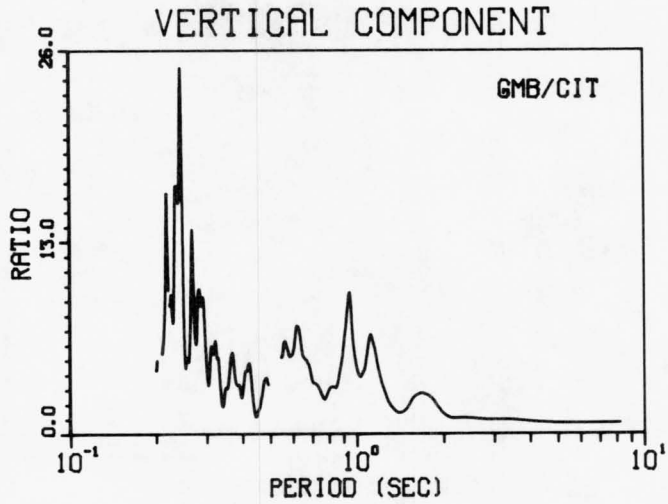

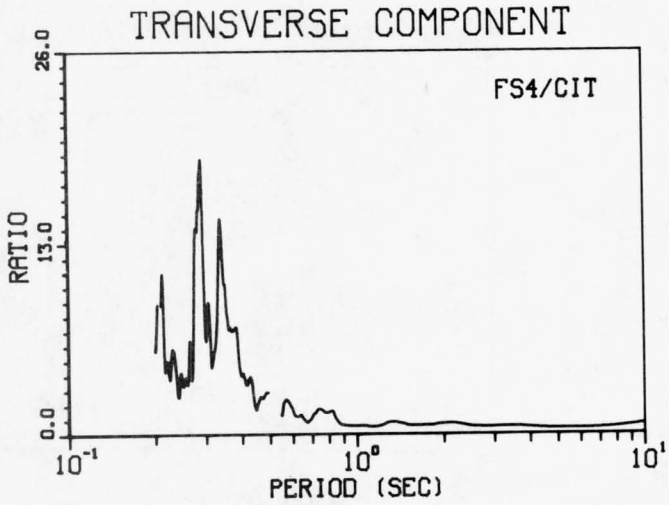

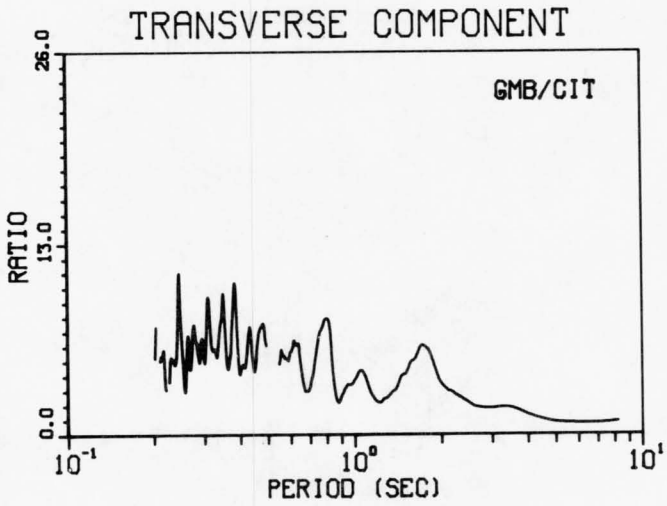

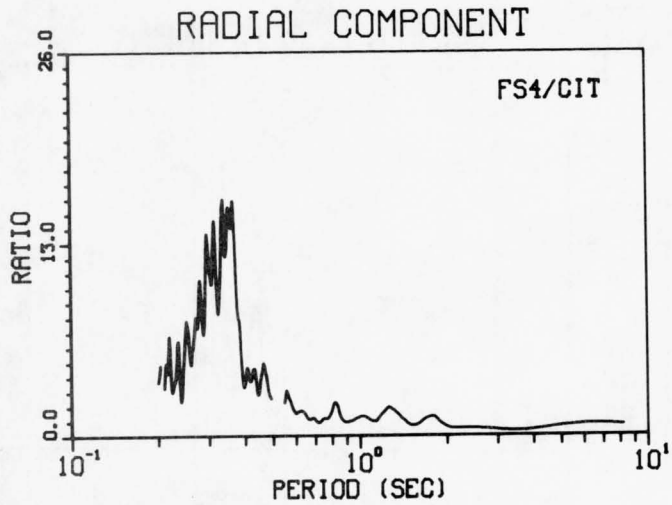

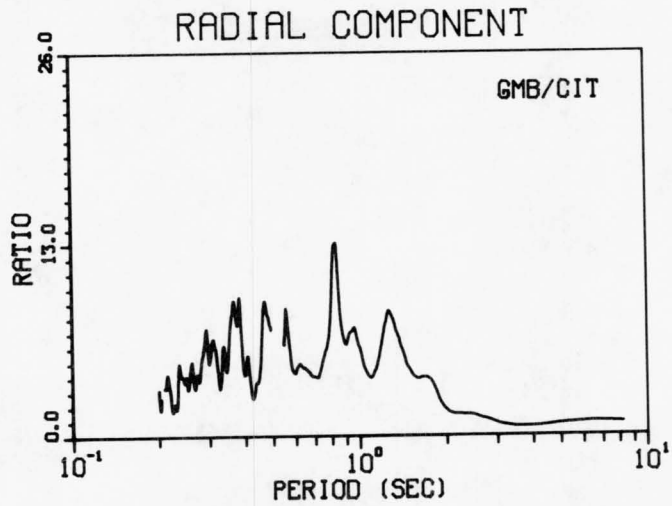

EVENT BACKBEACH

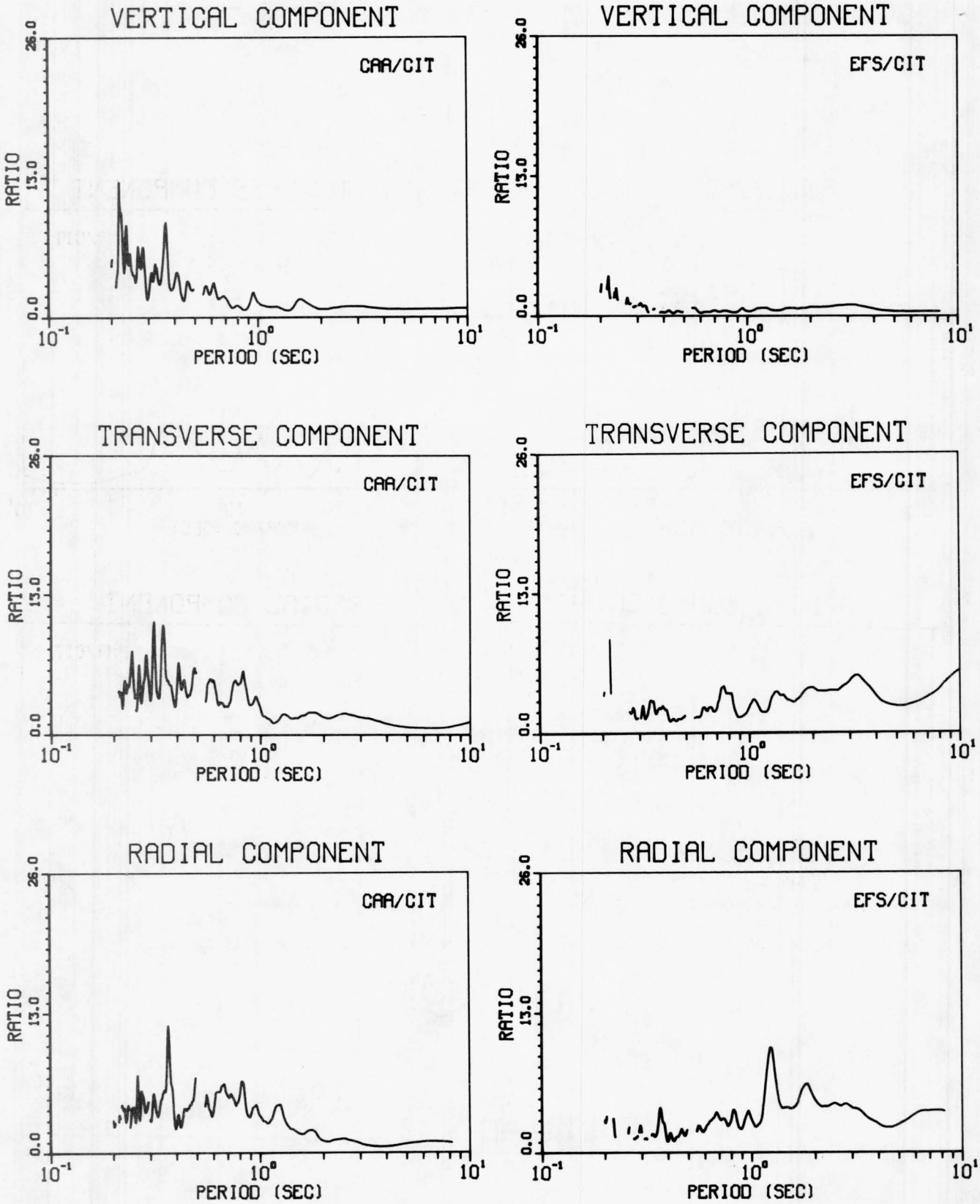

EVENT BACKBEACH

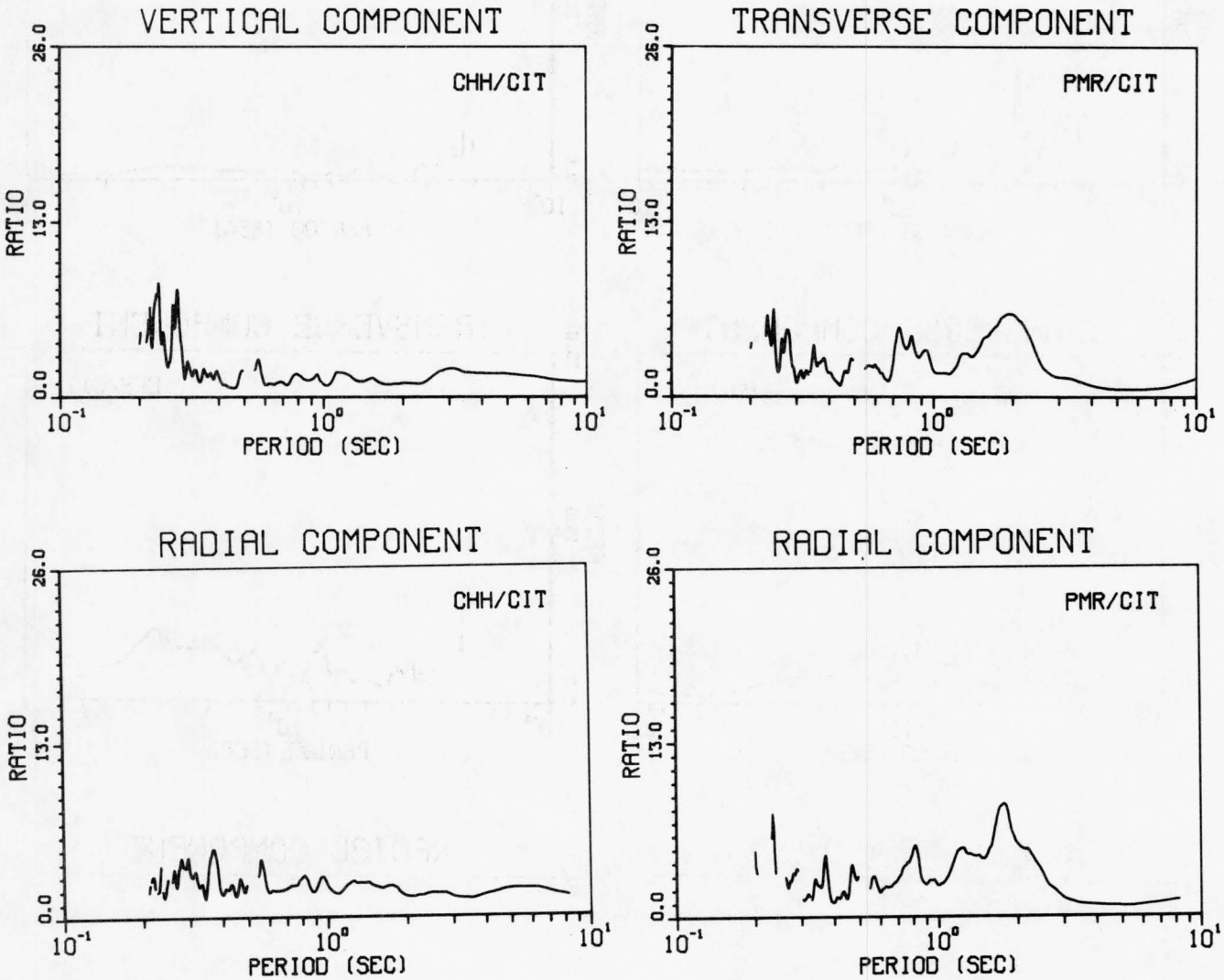

EVENT BACKBEACH

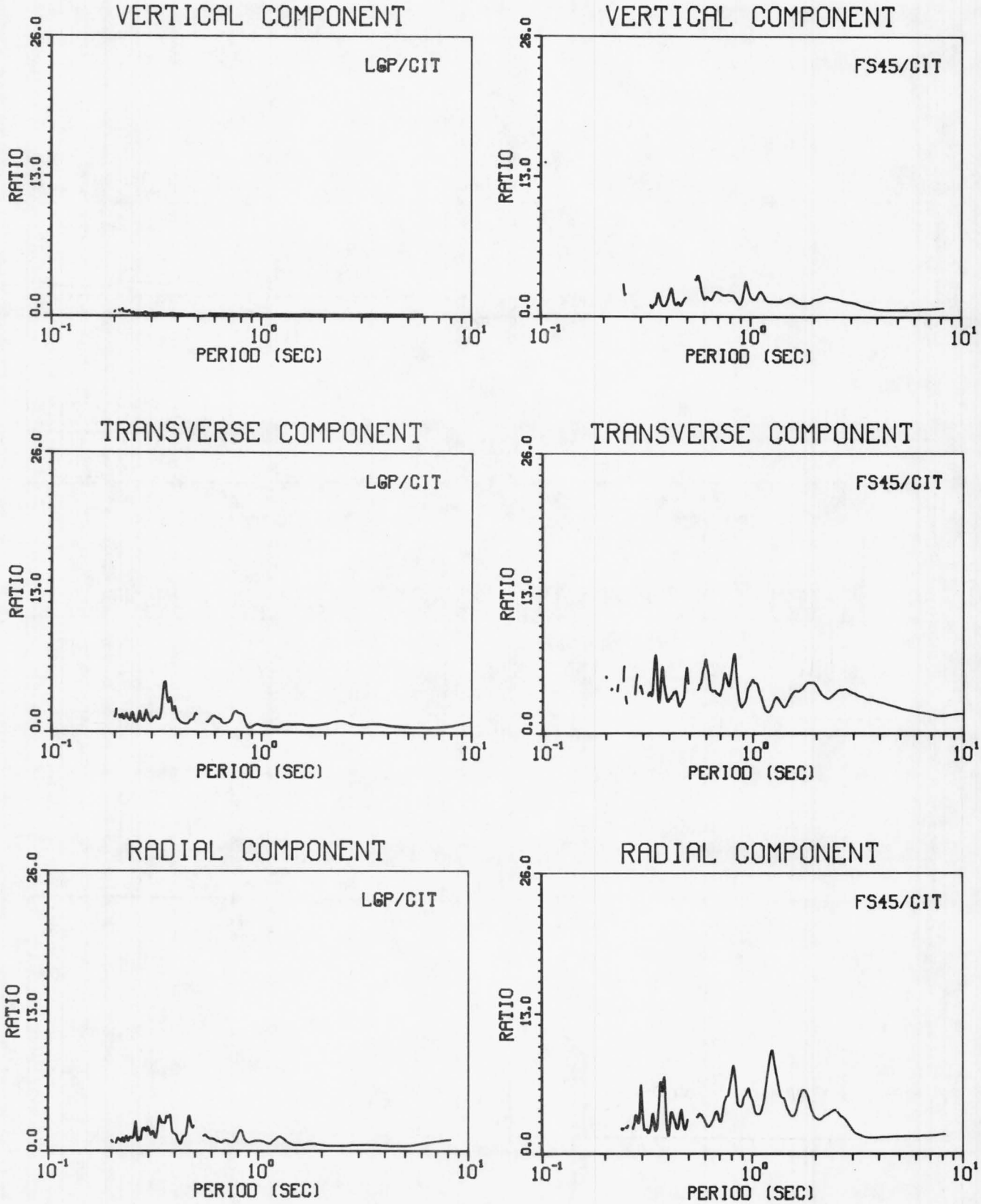

EVENT BACKBEACH

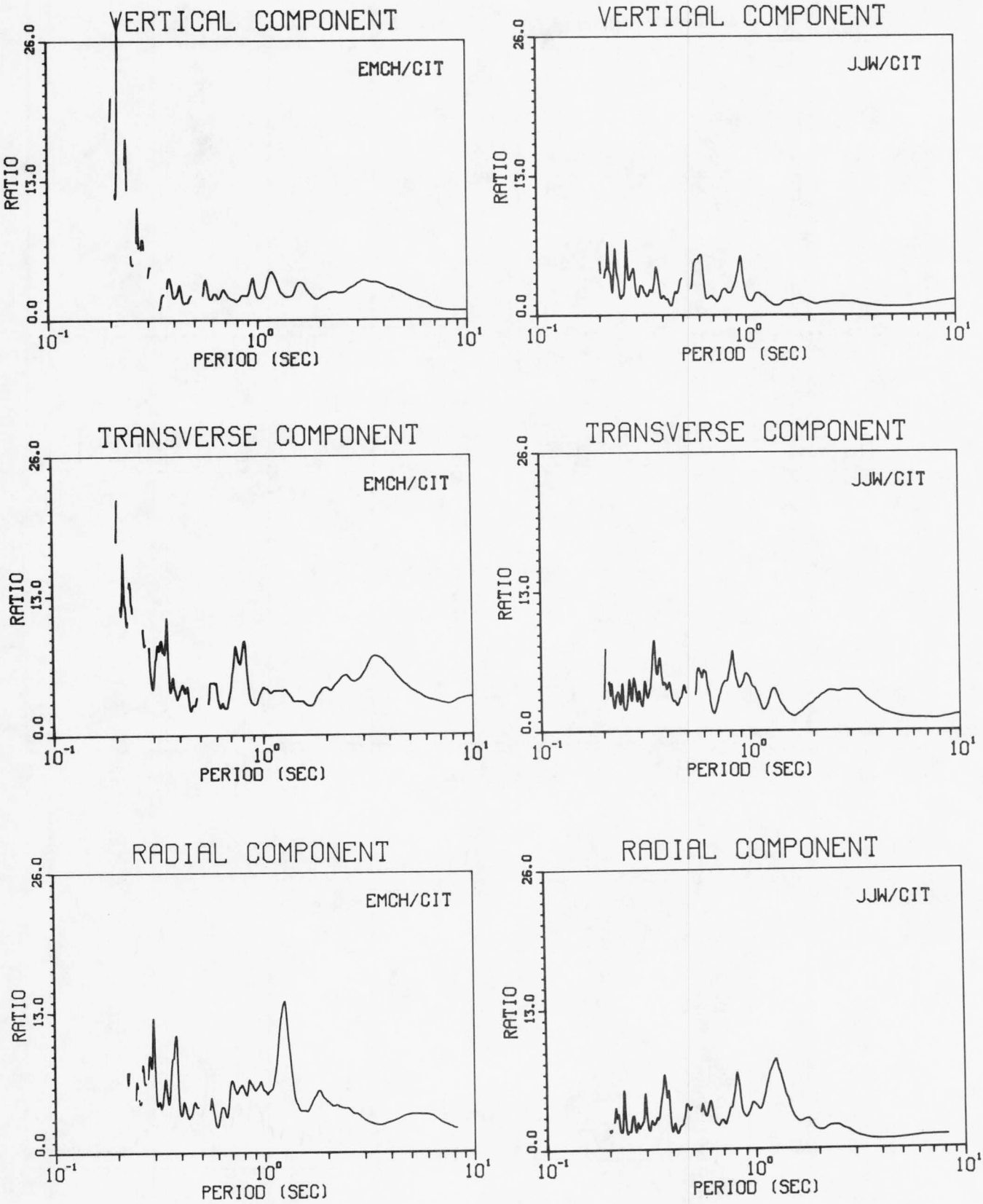

EVENT BACKBEACH

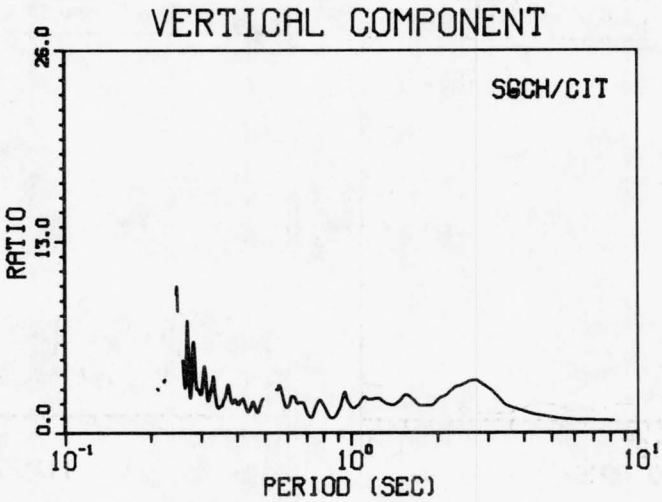

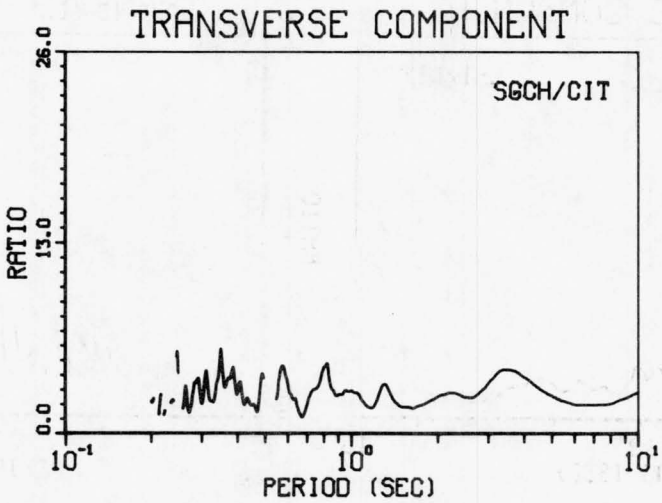

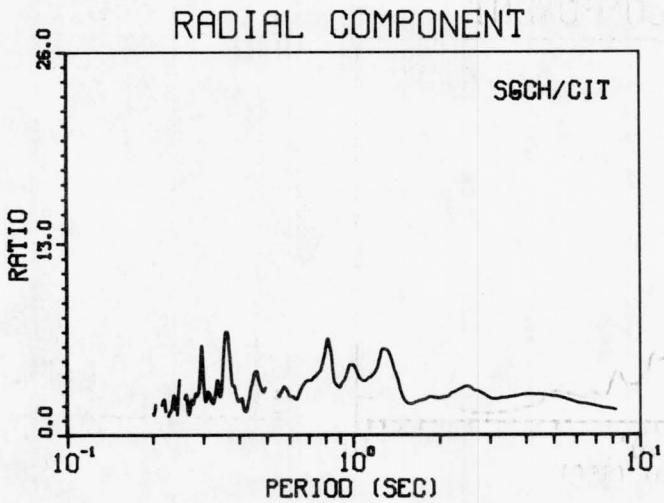

EVENT BILLET

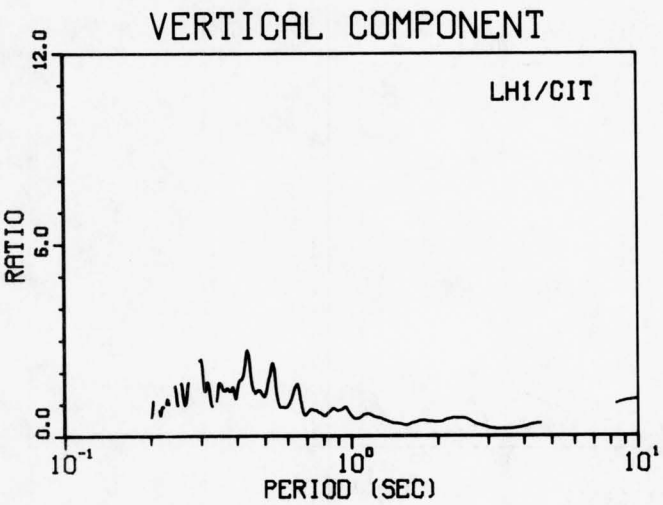

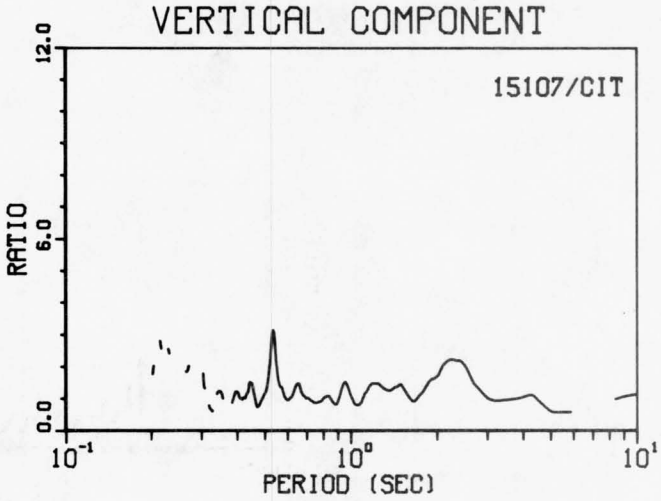

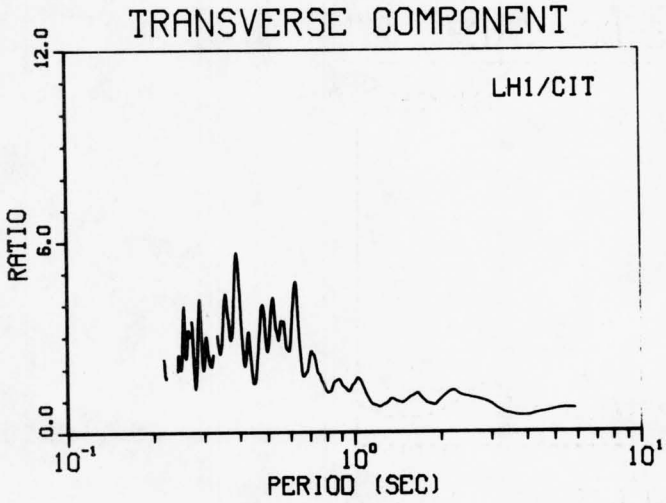

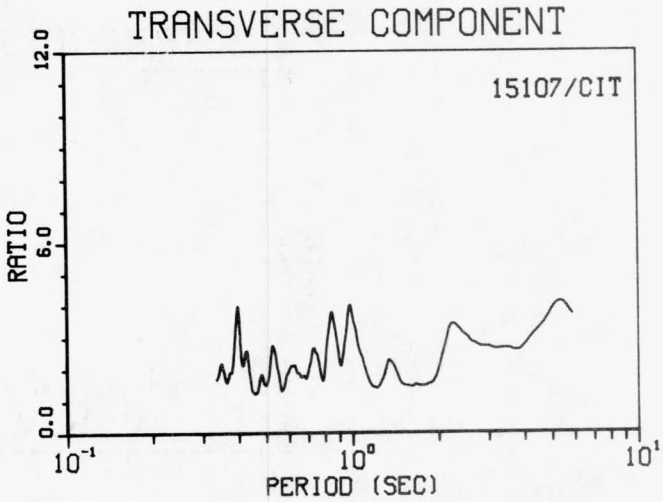

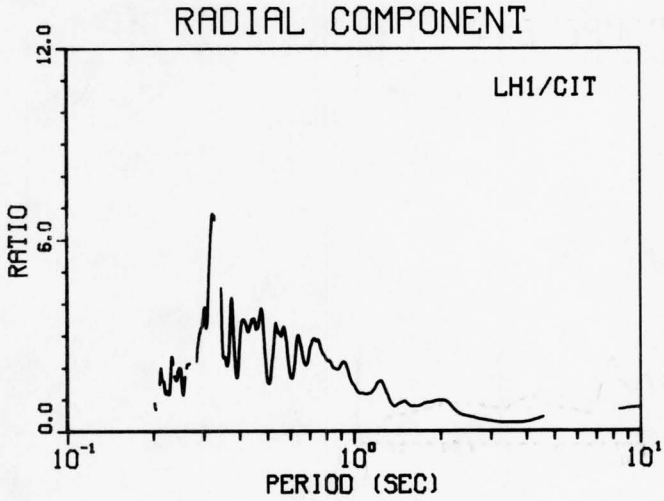

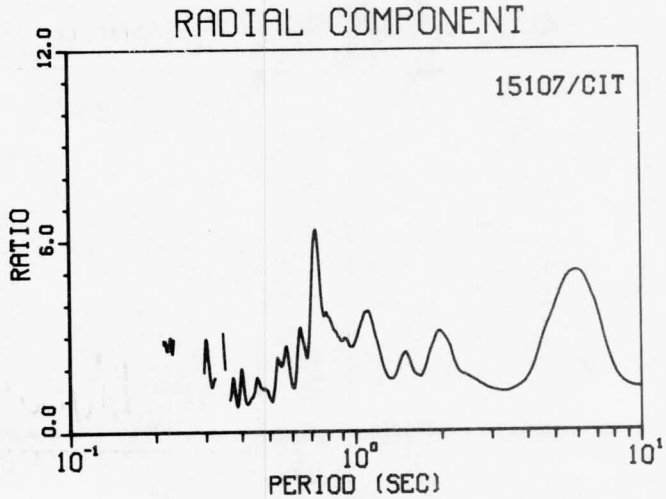

EVENT BILLET

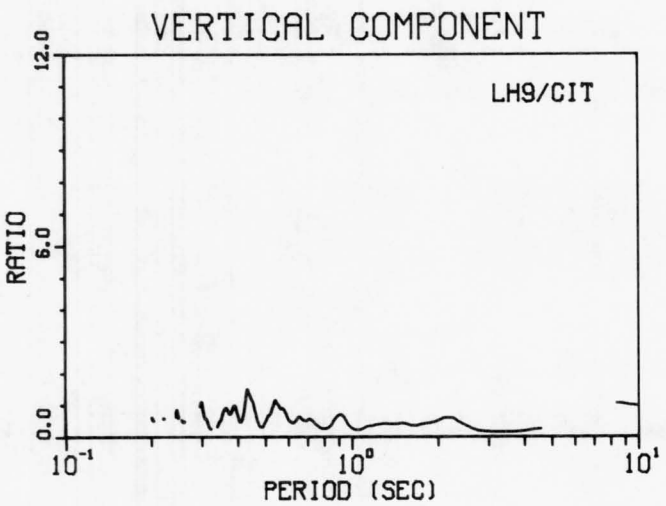

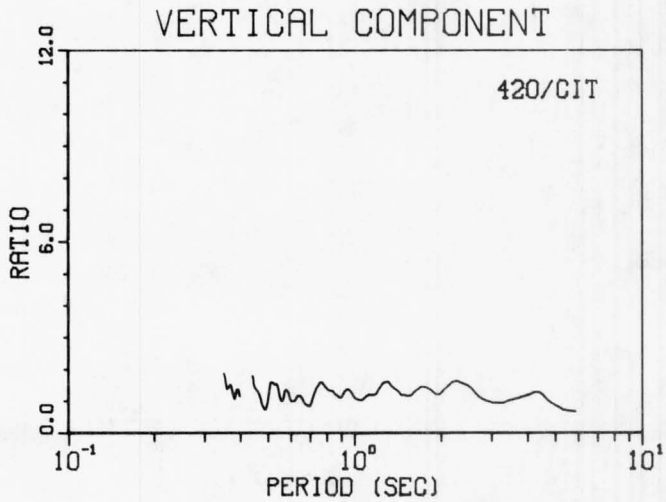

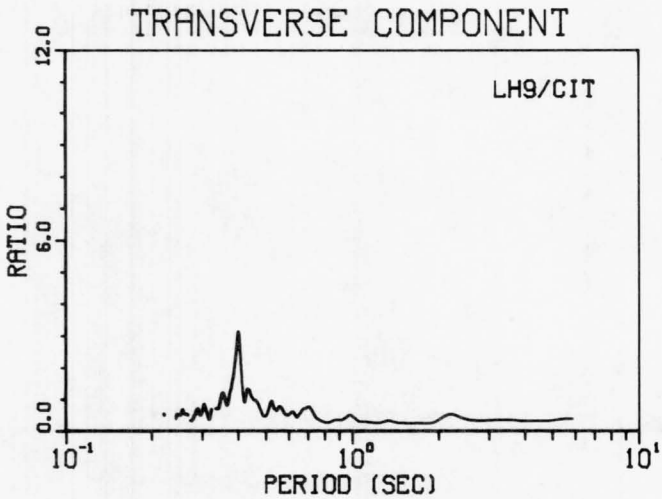

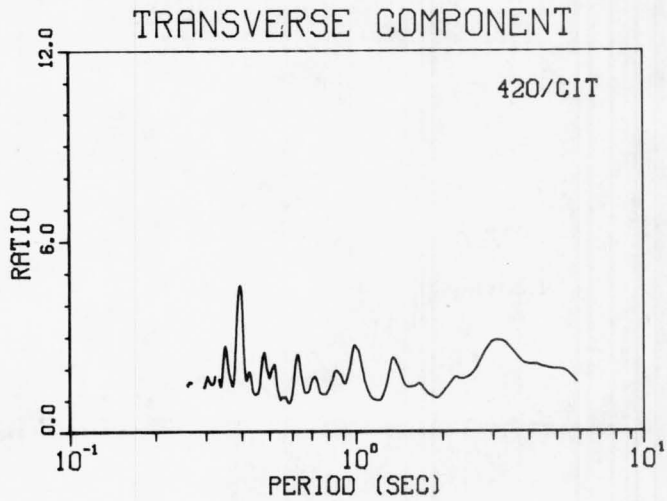

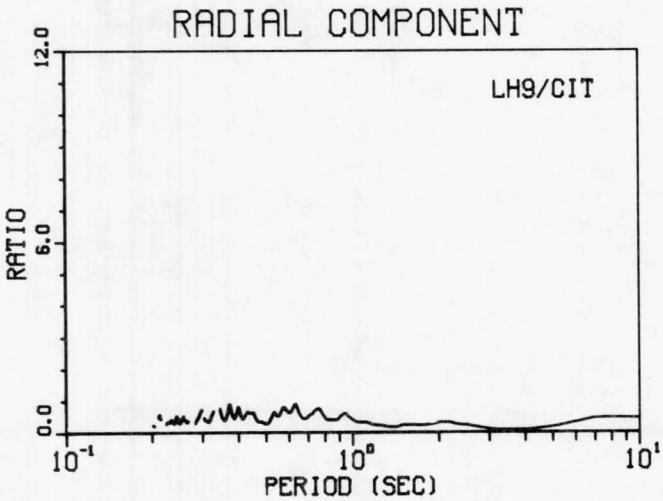

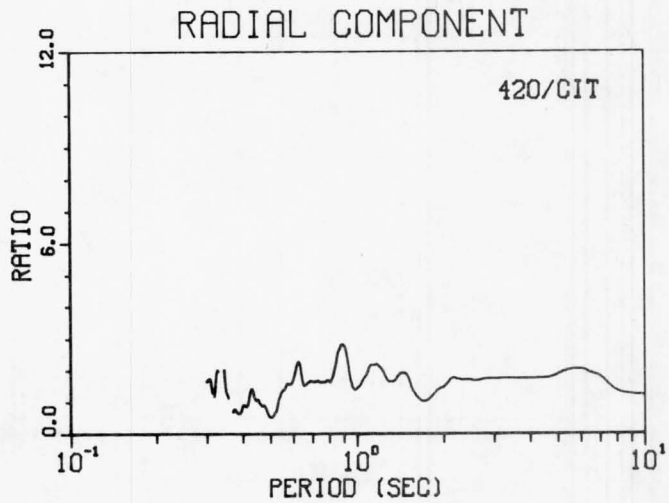

EVENT BILLET

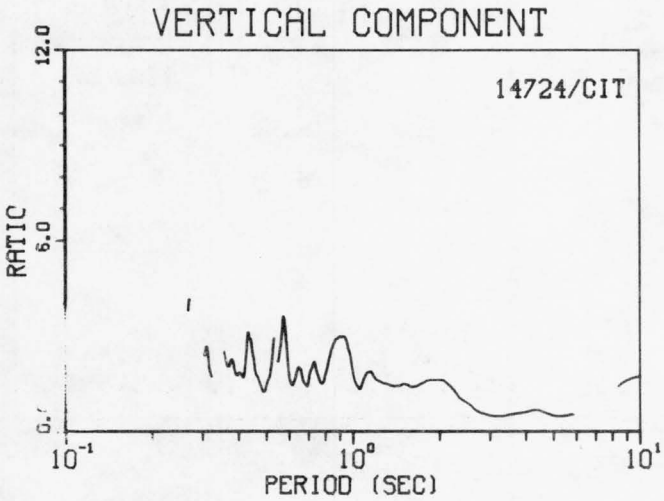

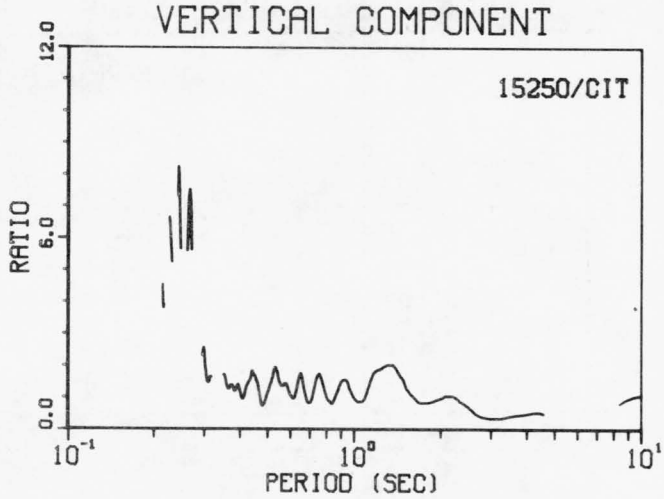

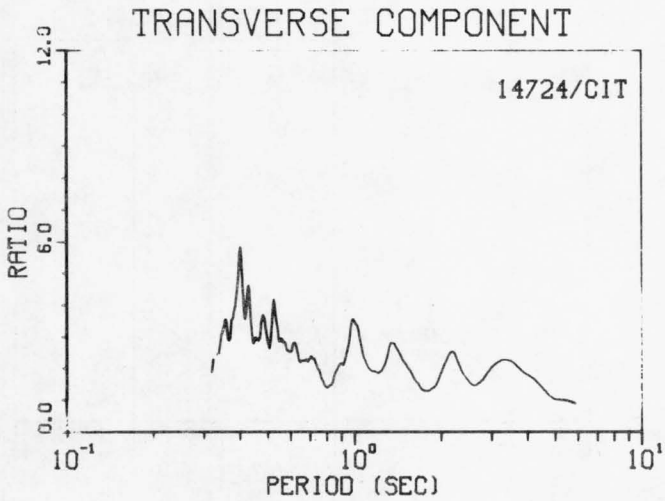

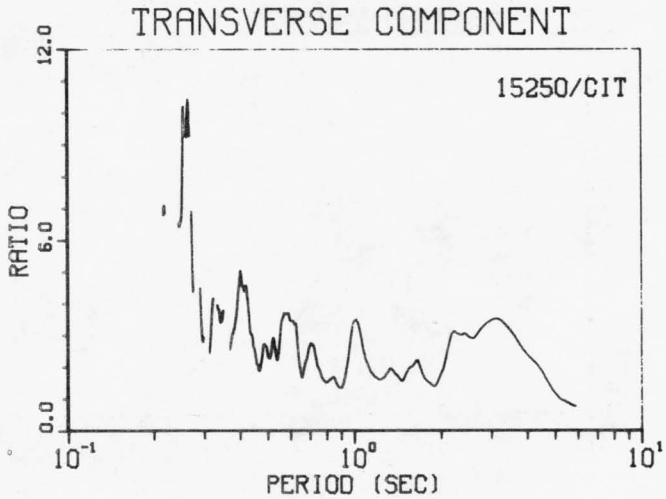

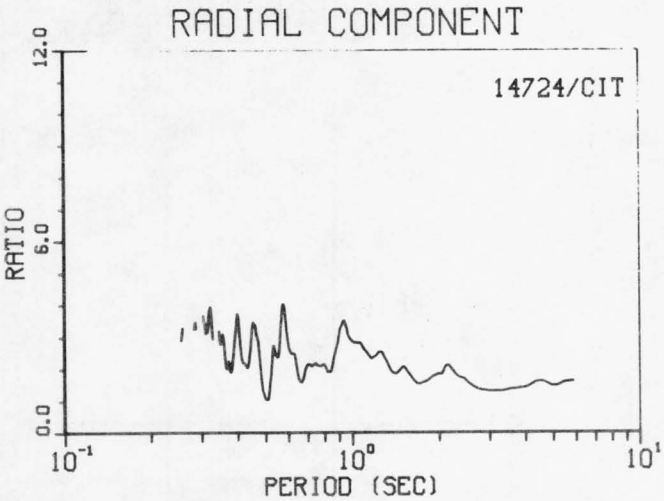

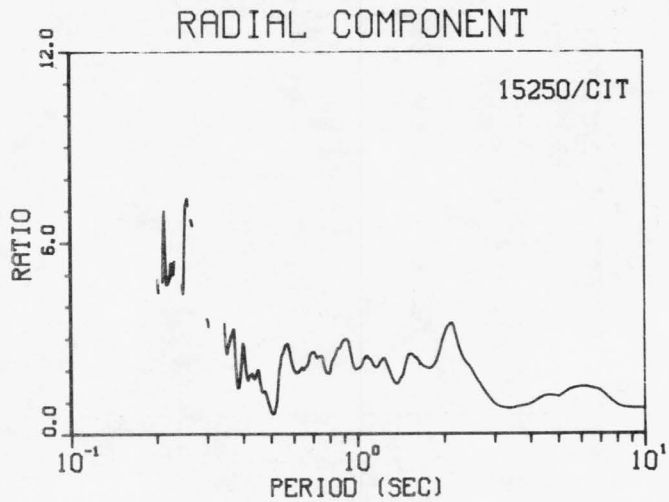

EVENT BILLET

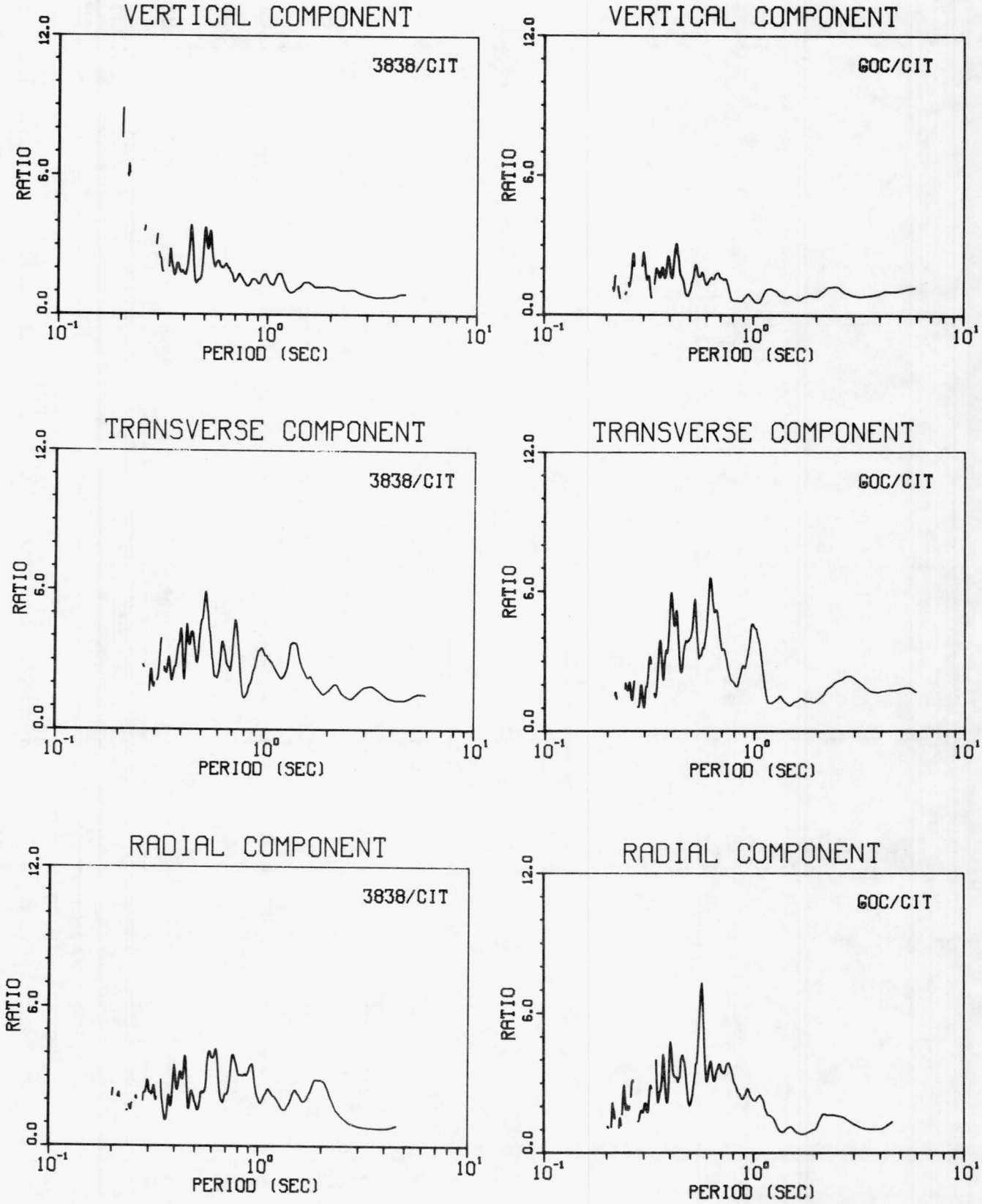

EVENT BILLET

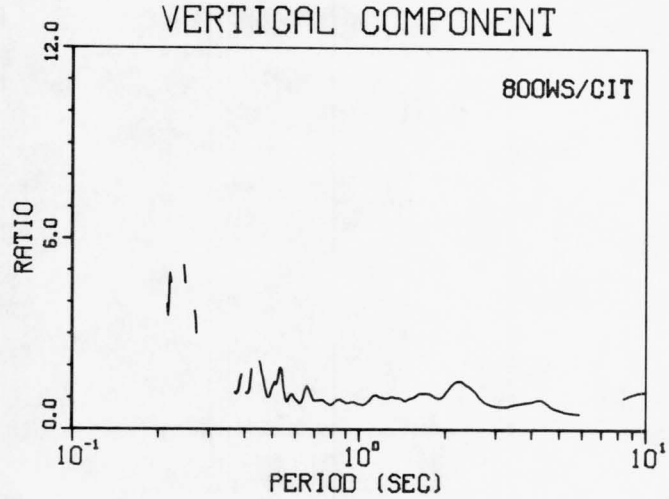

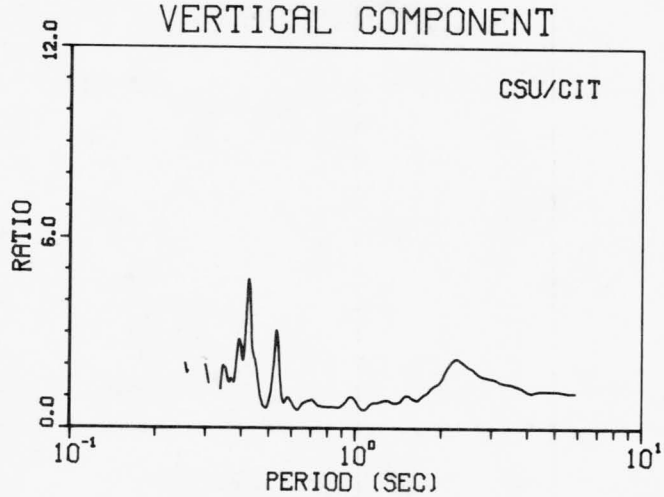

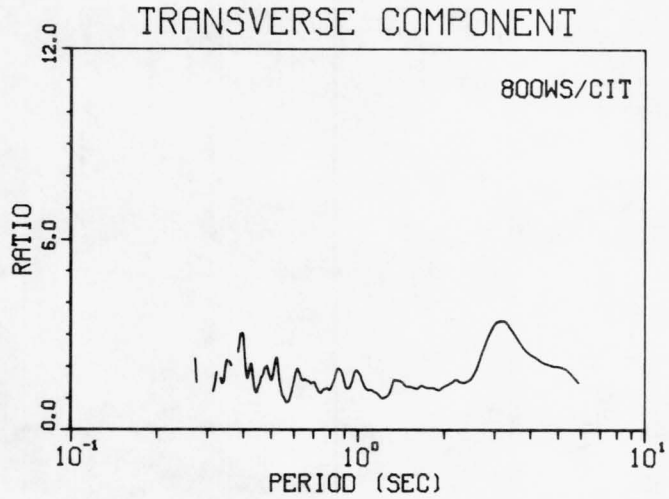

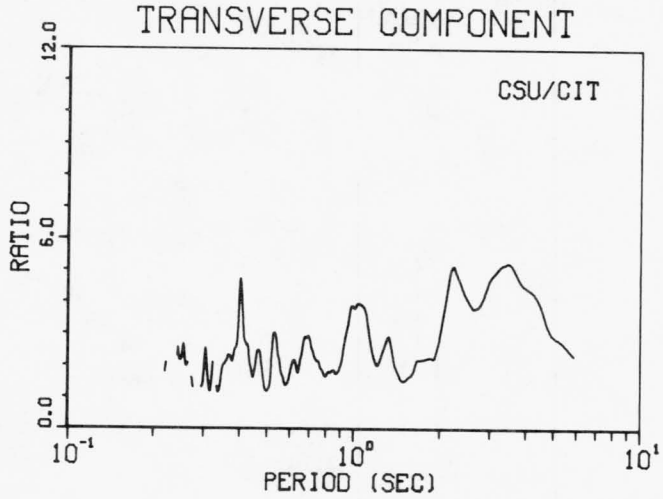

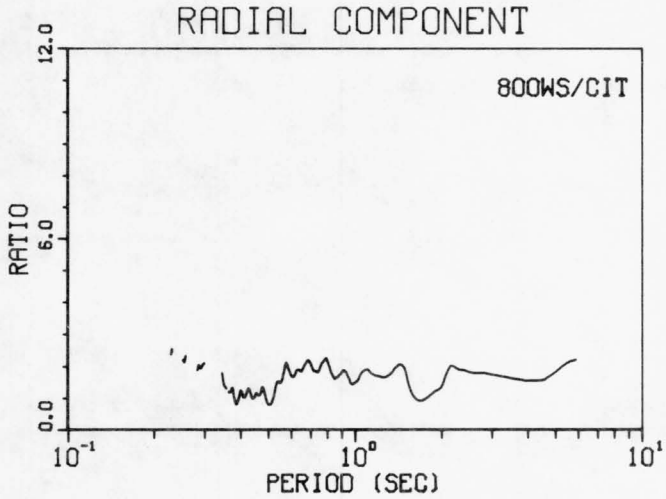

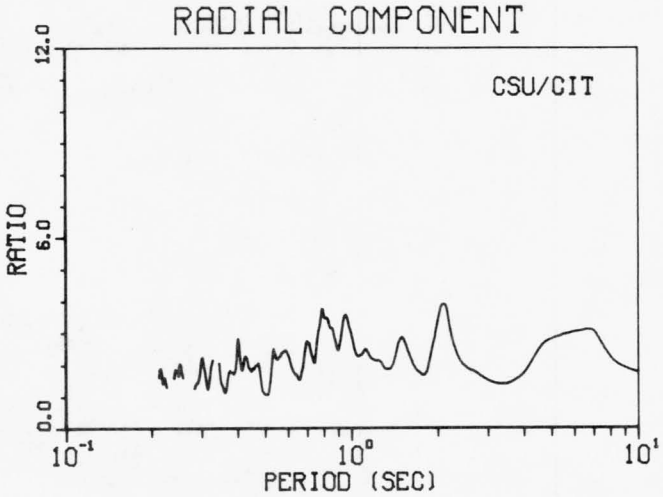

EVENT BILLET

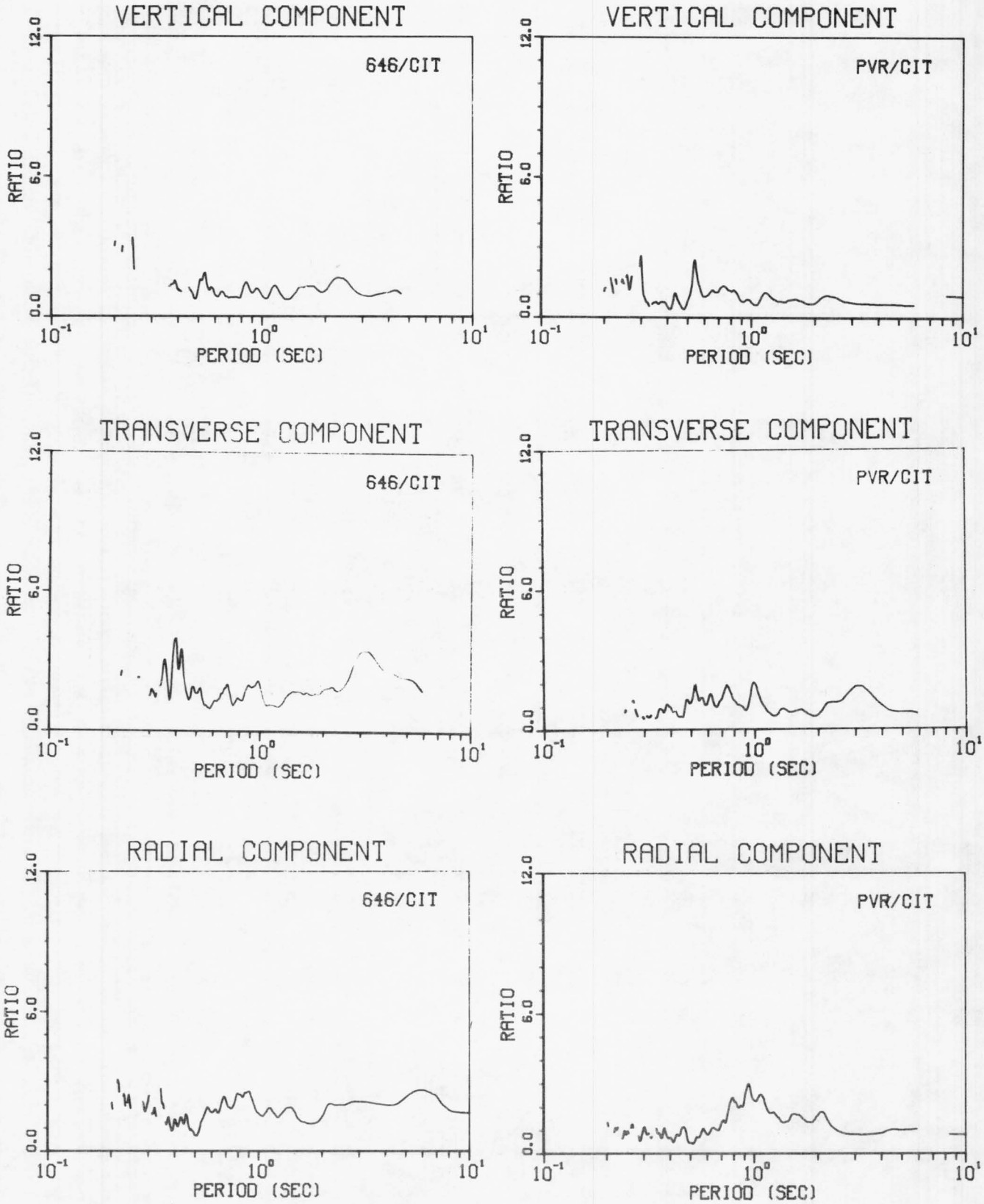

EVENT BILLET

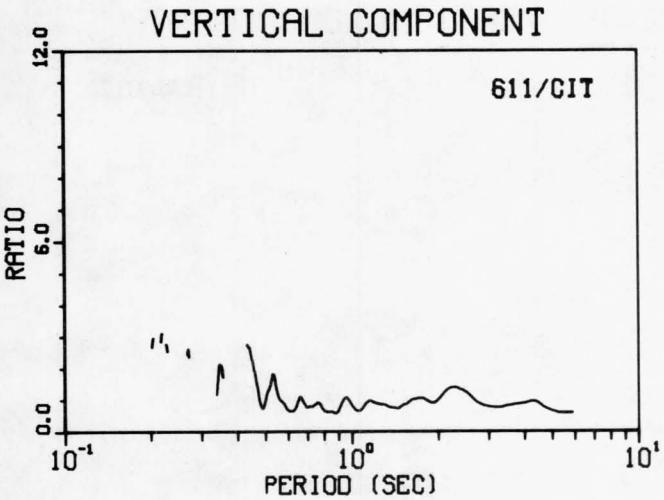

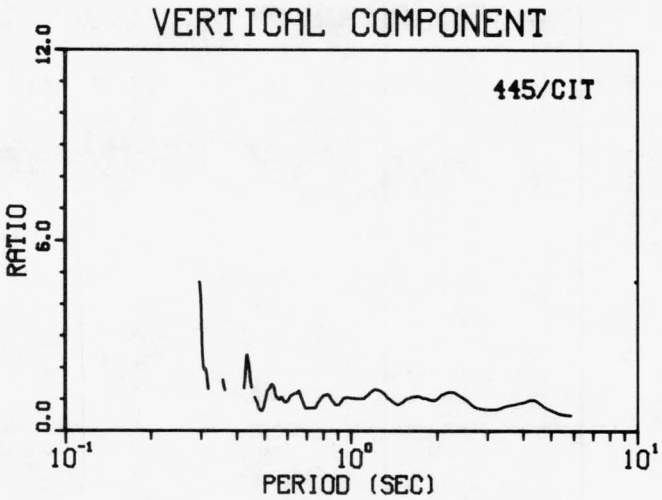

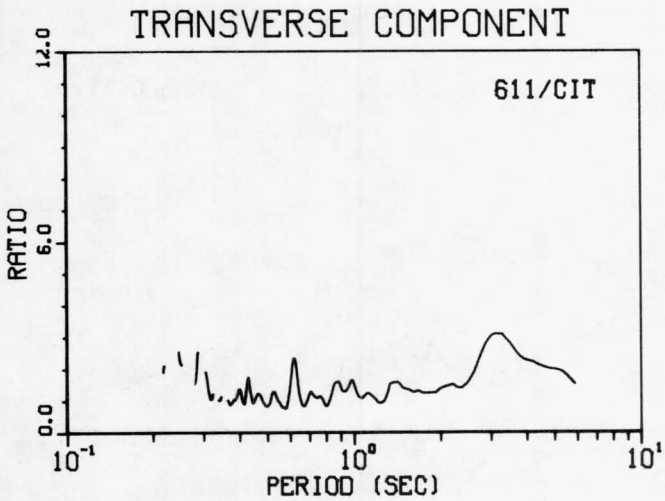

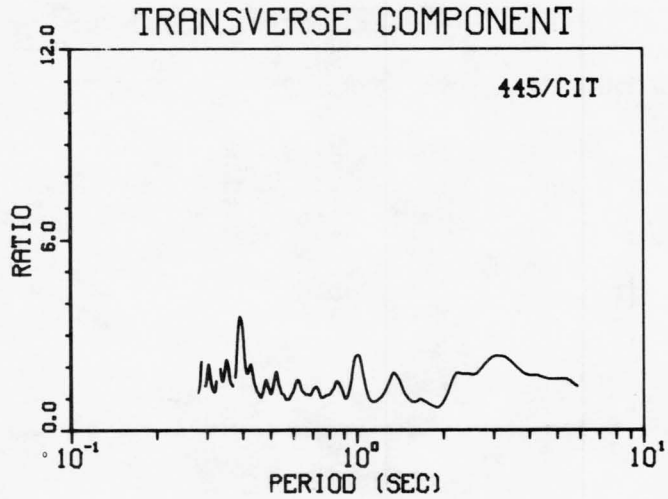

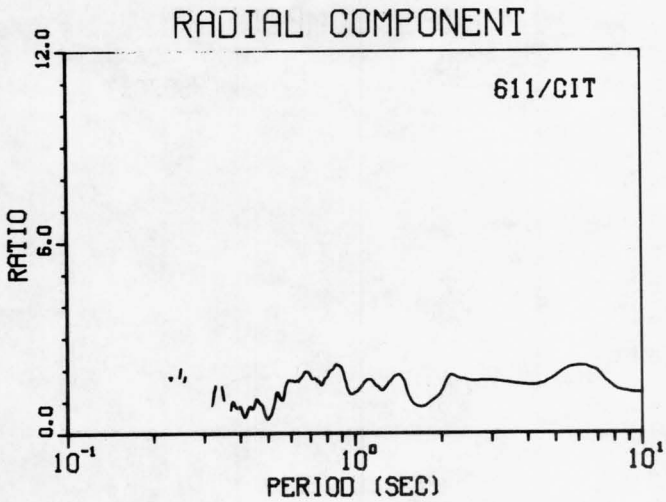

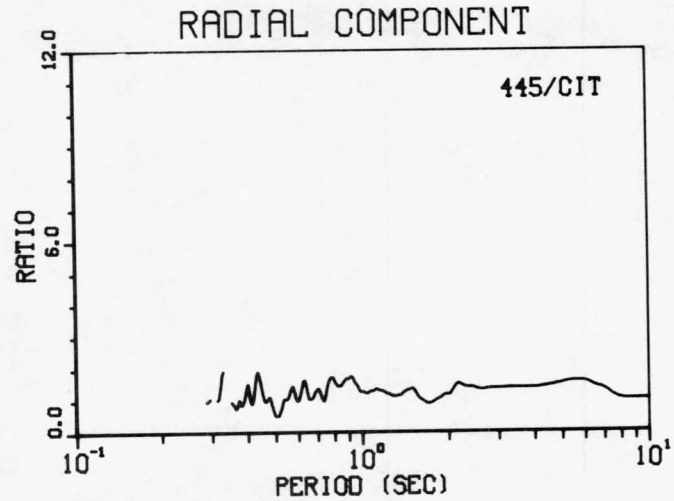

EVENT BILLET

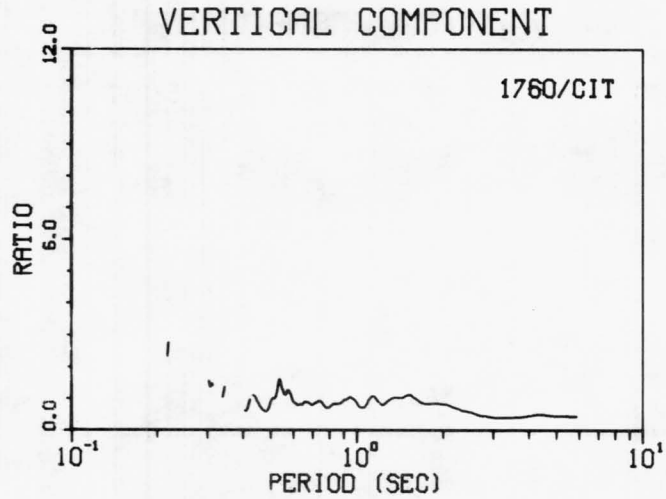

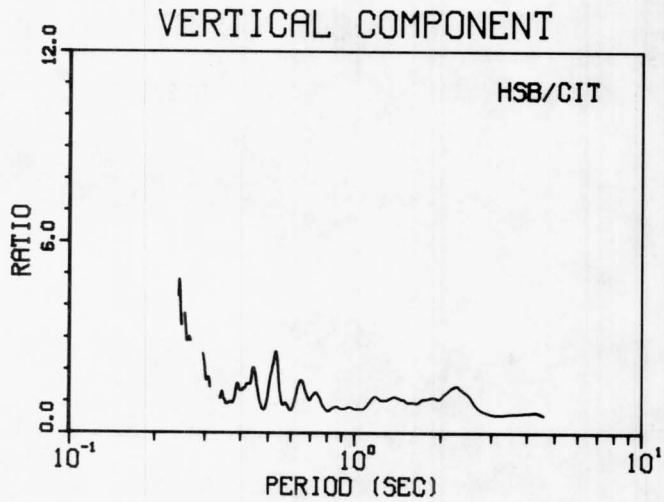

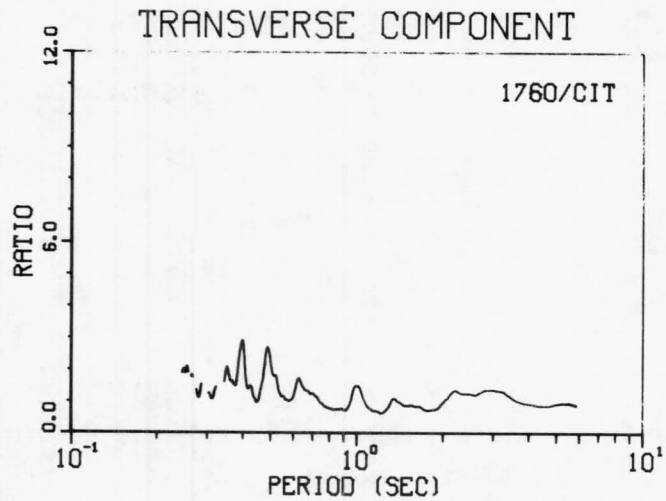

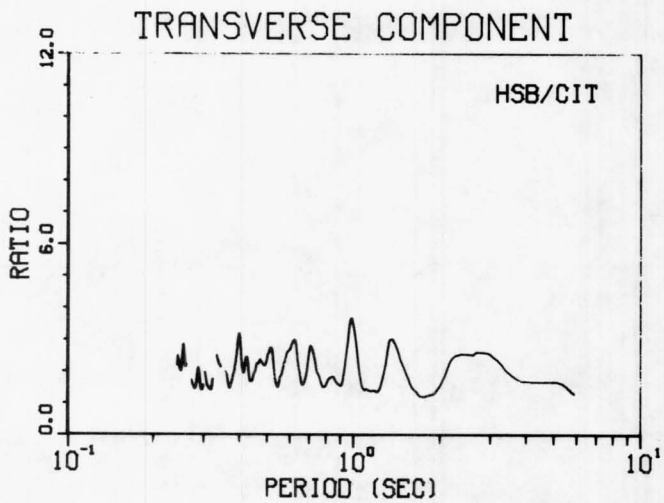

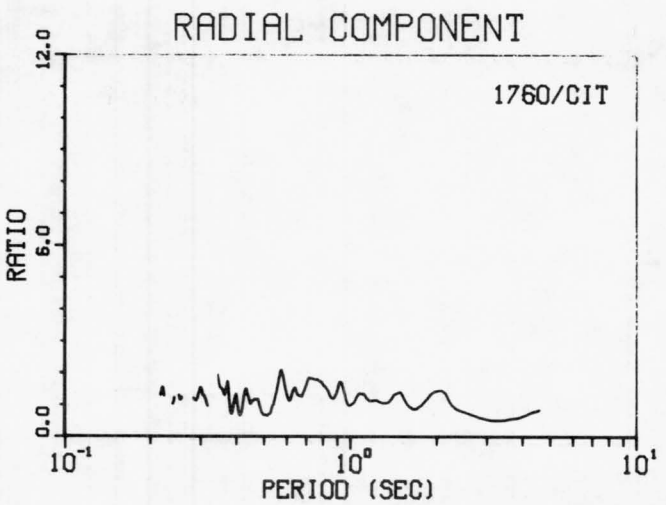

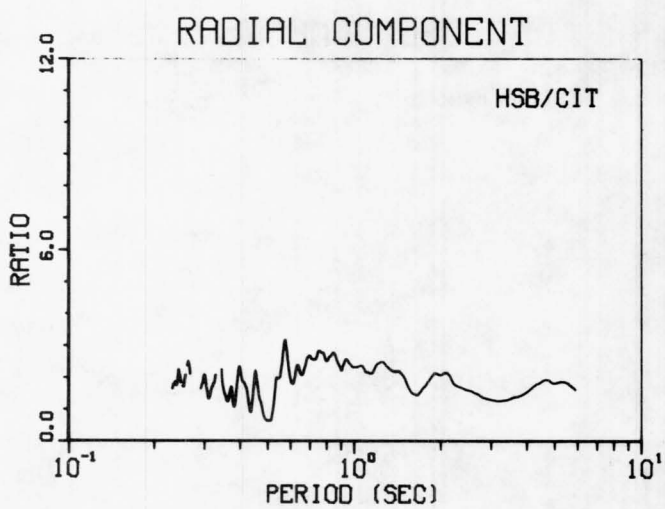

EVENT BILLET

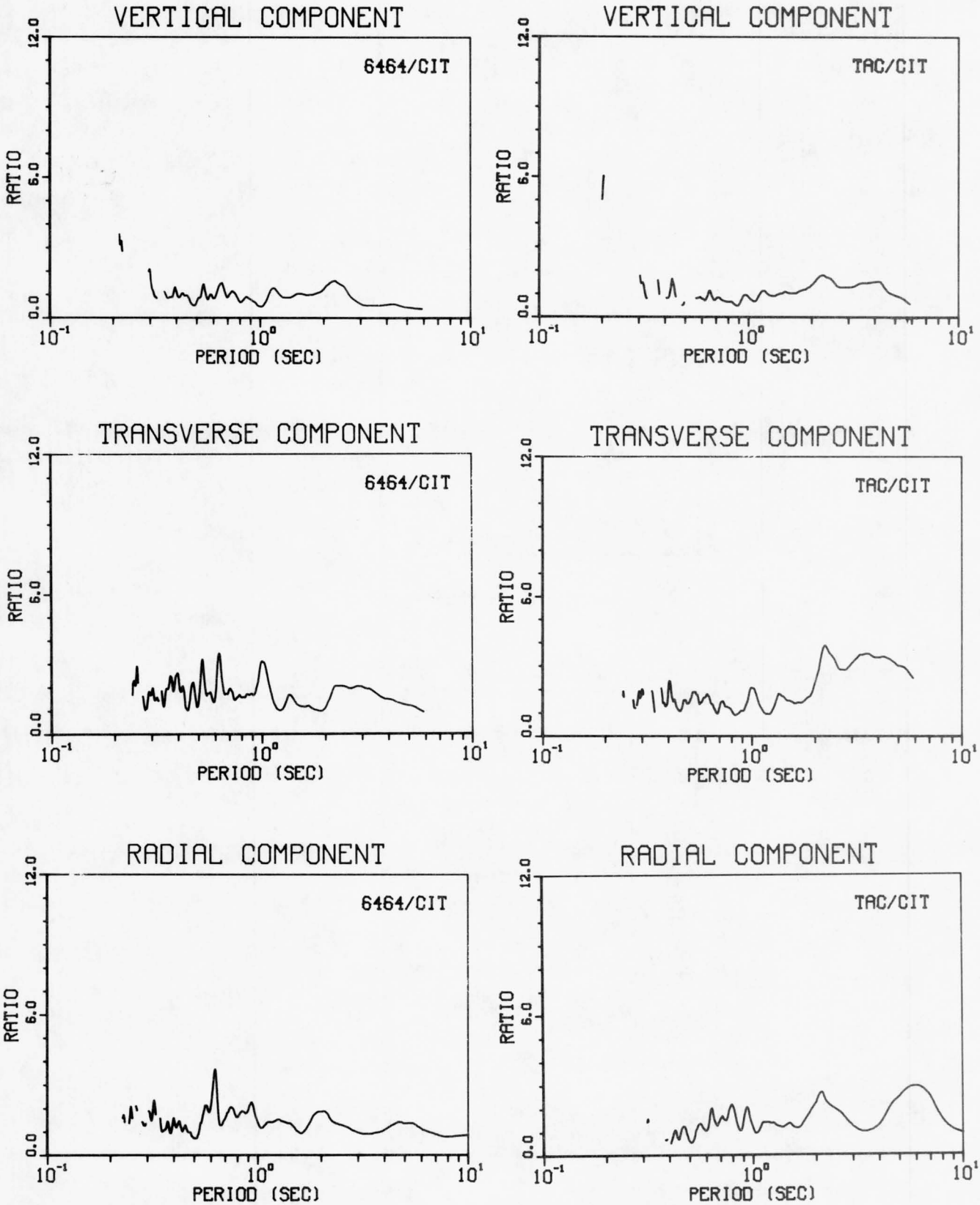

EVENT BILLET

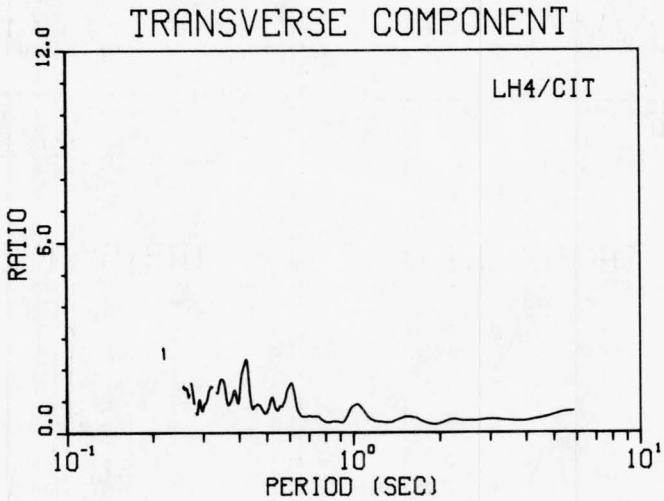

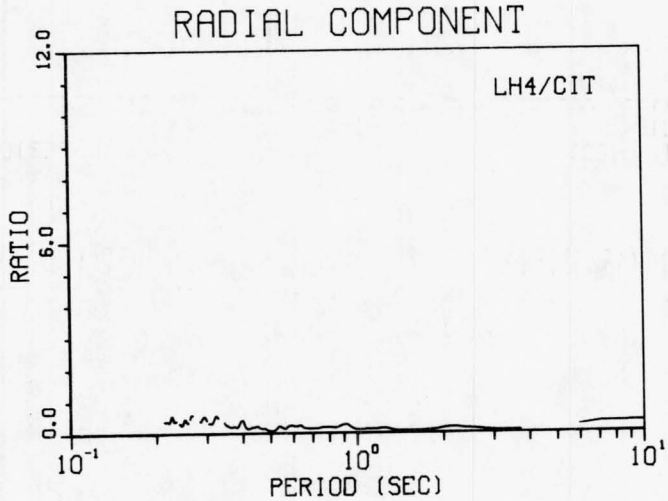

EVENT CAMEMBERT

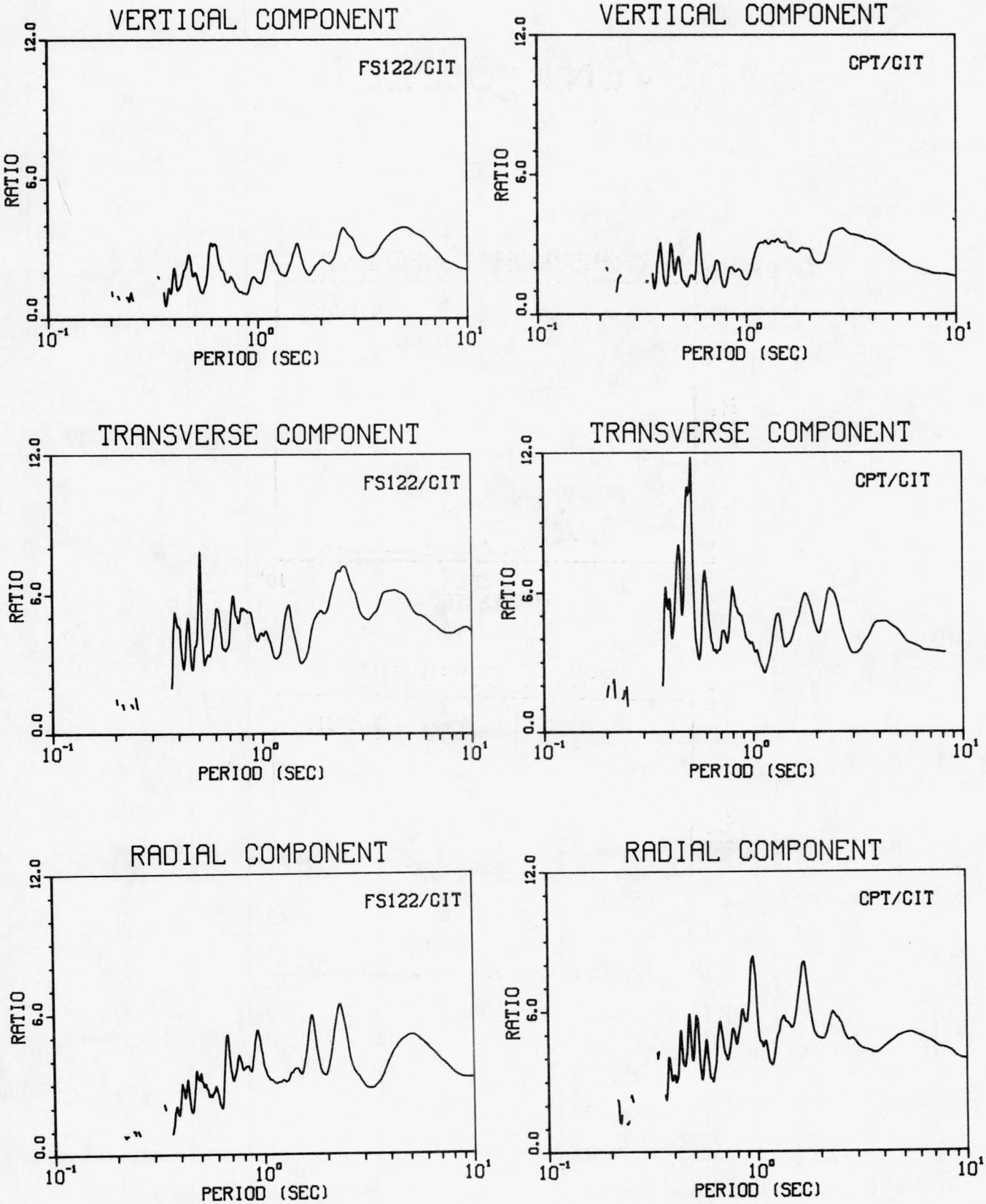

EVENT CAMEMBERT

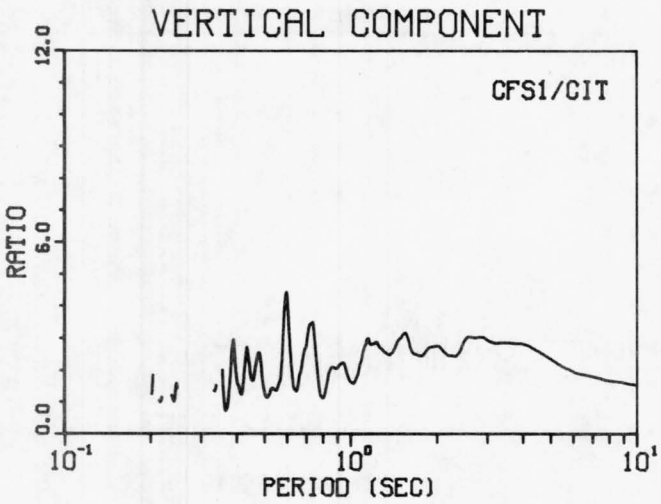

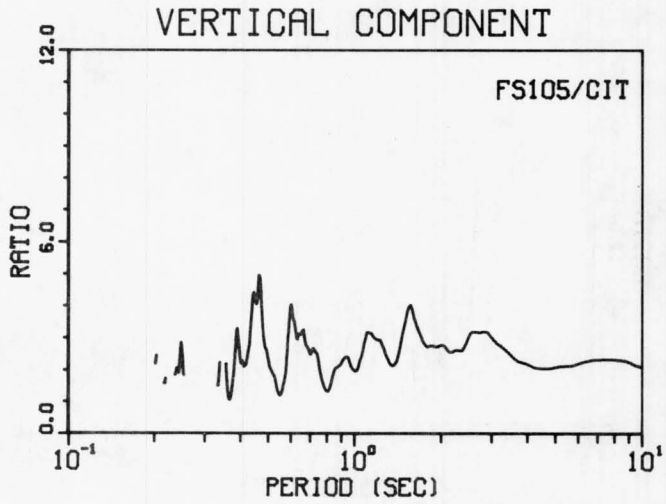

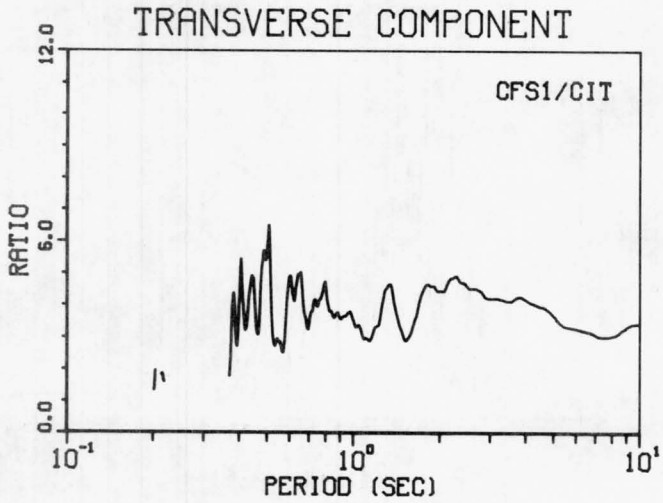

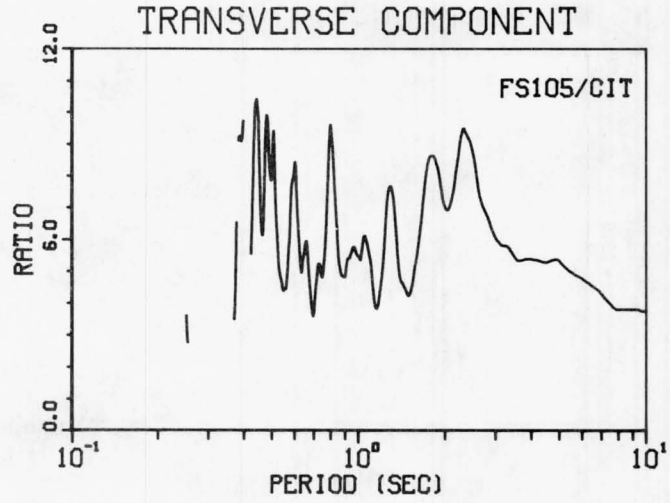

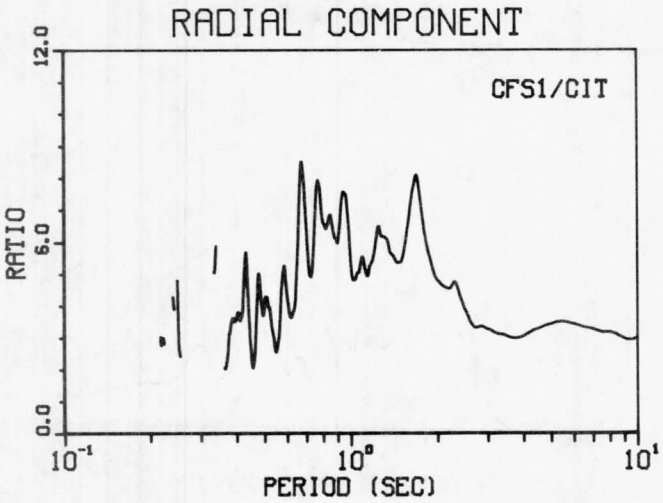

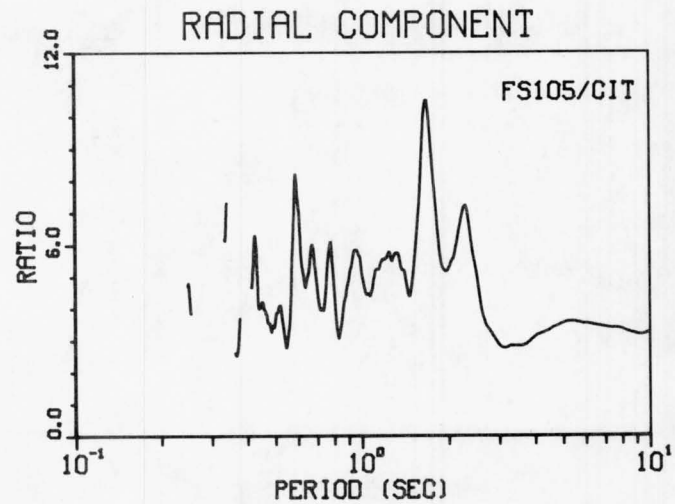

EVENT CHESHIRE

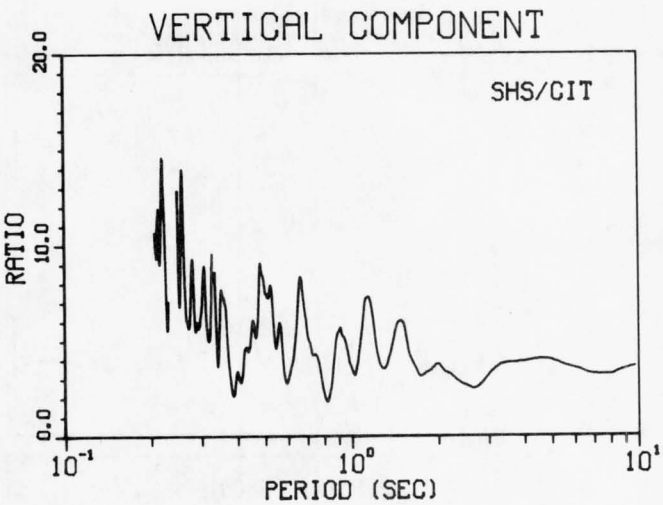

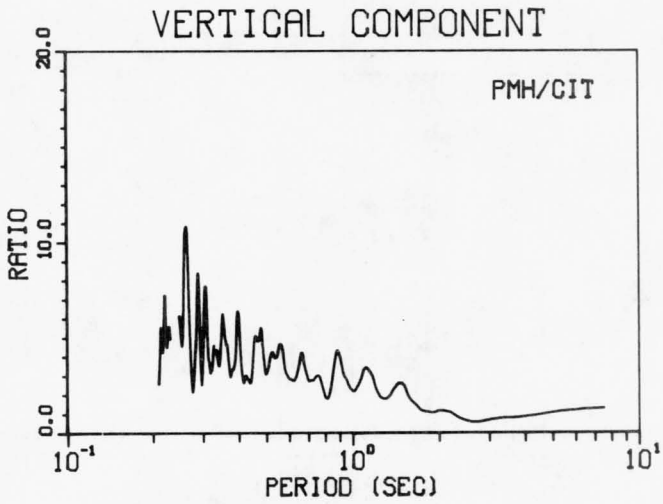

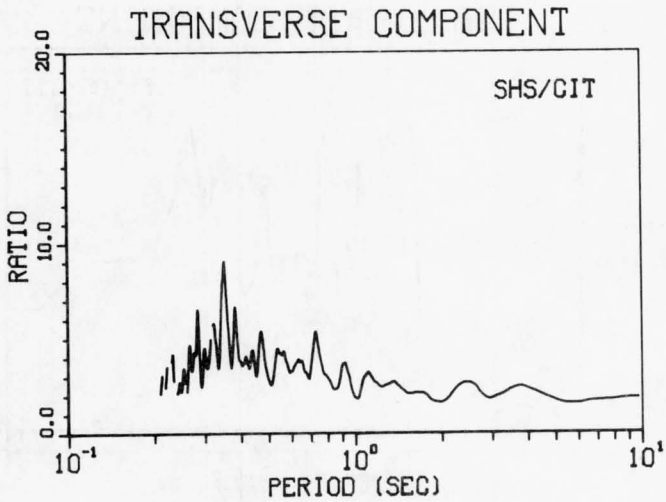

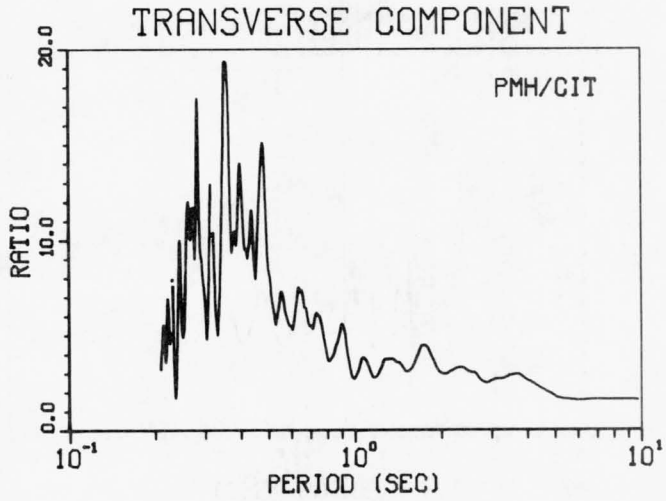

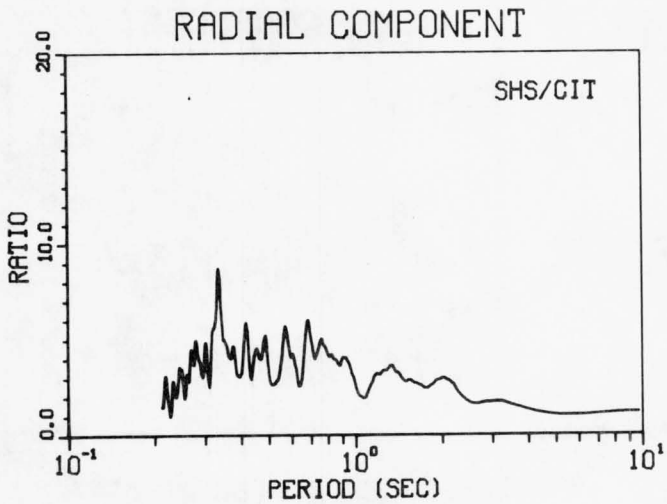

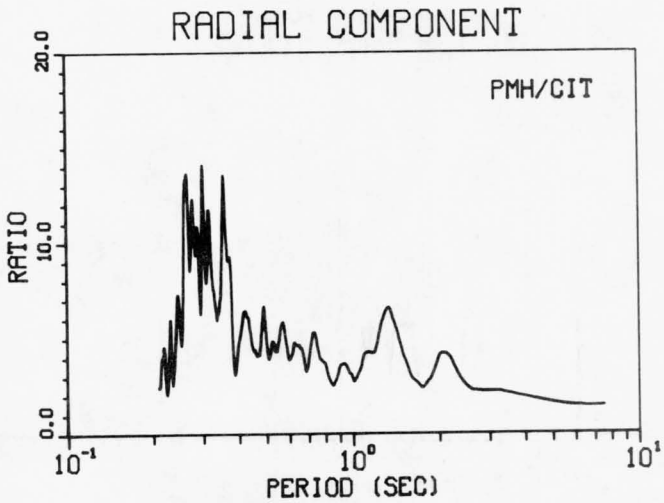

EVENT CHESHIRE

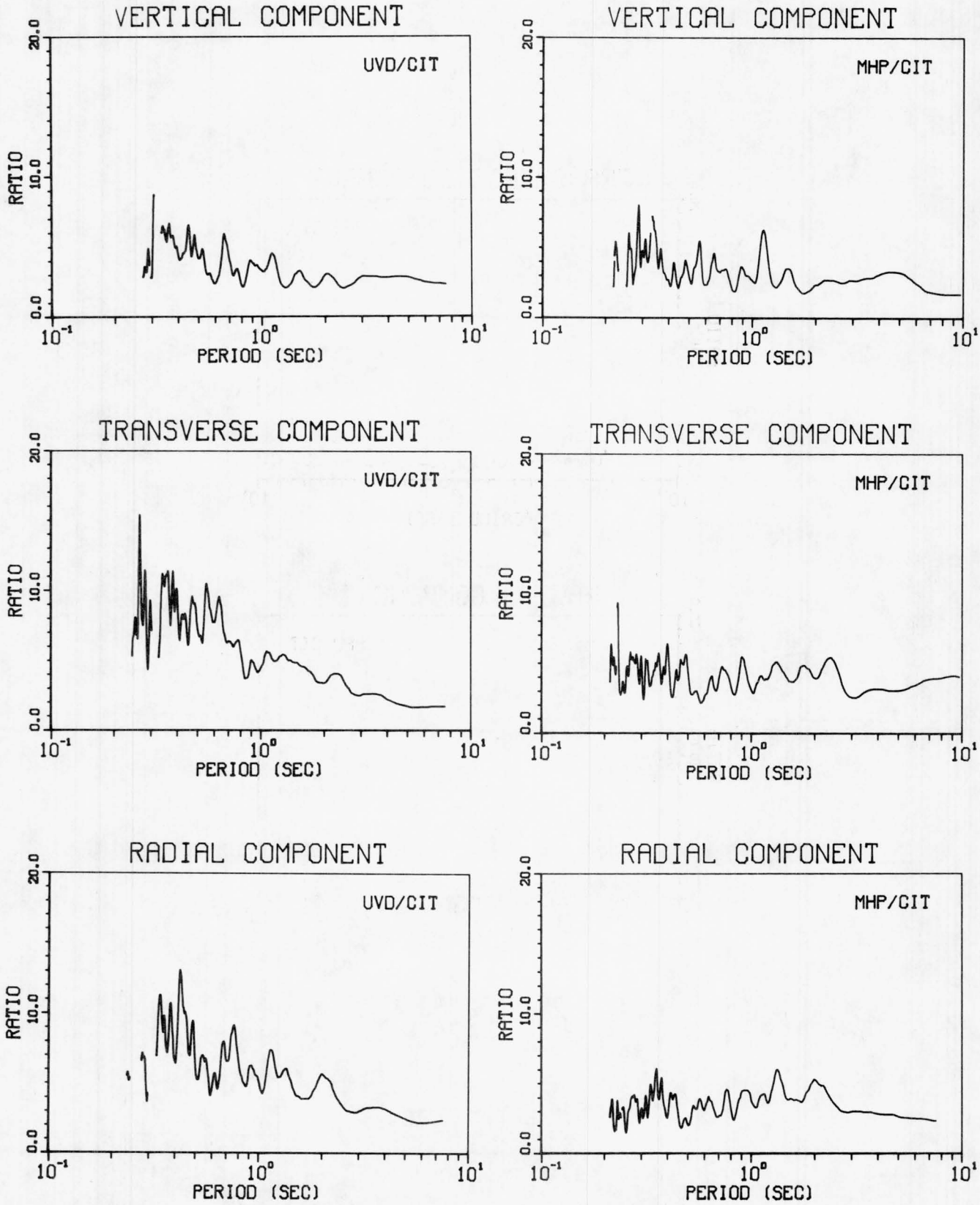

EVENT CHESHIRE

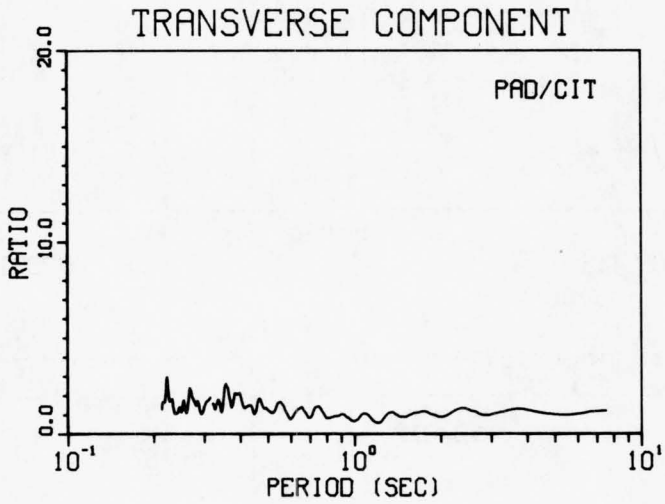

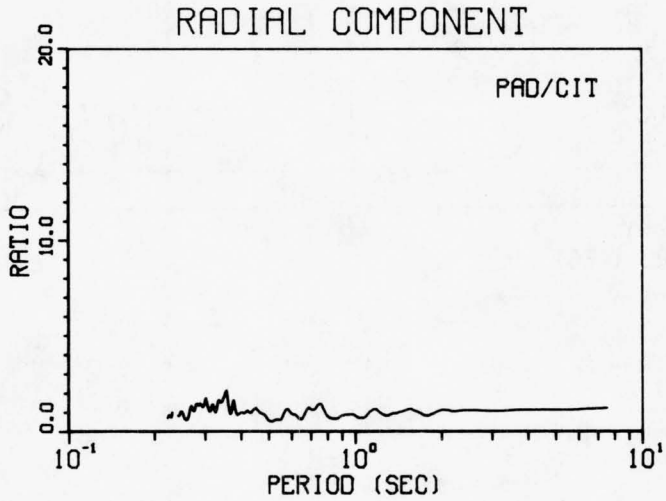

EVENT CHIBERTA

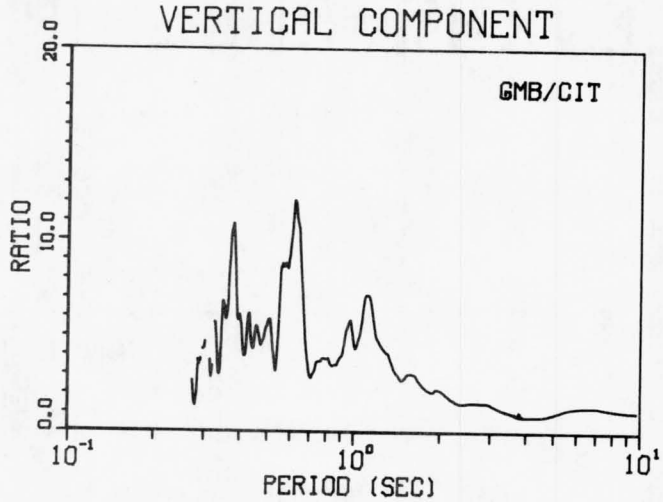

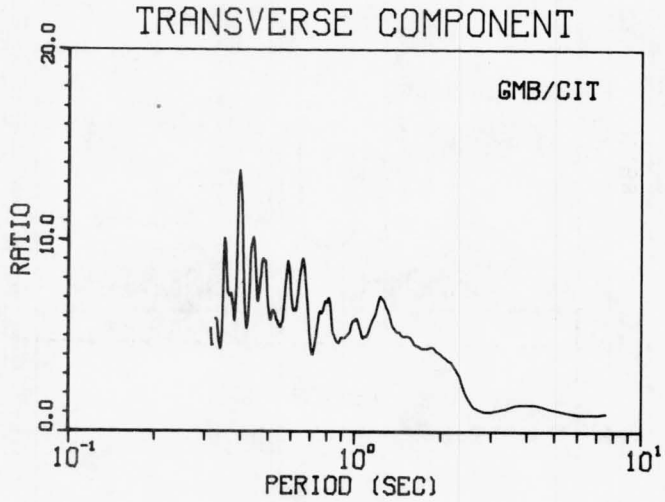

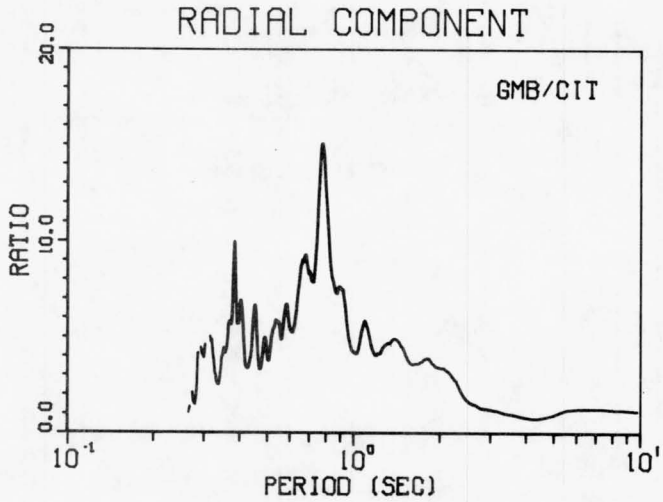

EVENT CHIBERTA

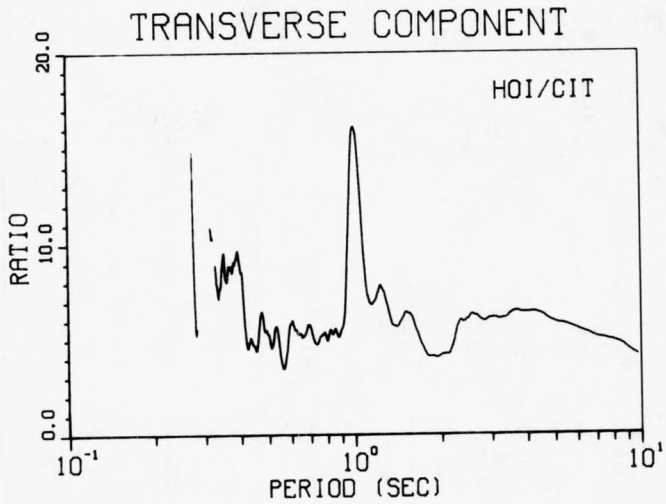

EVENT CHIBERTA

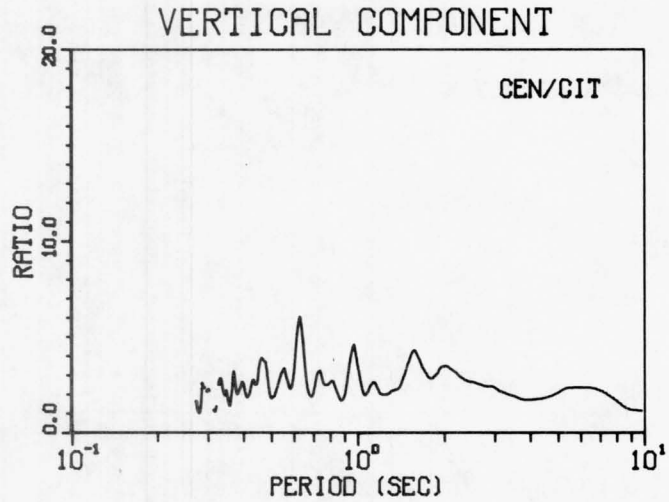

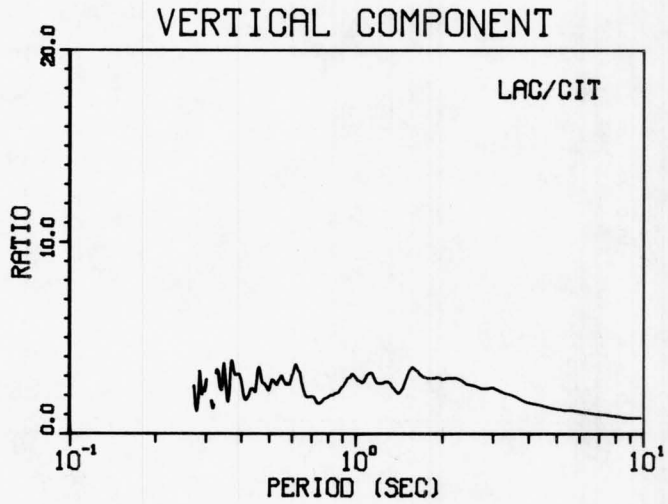

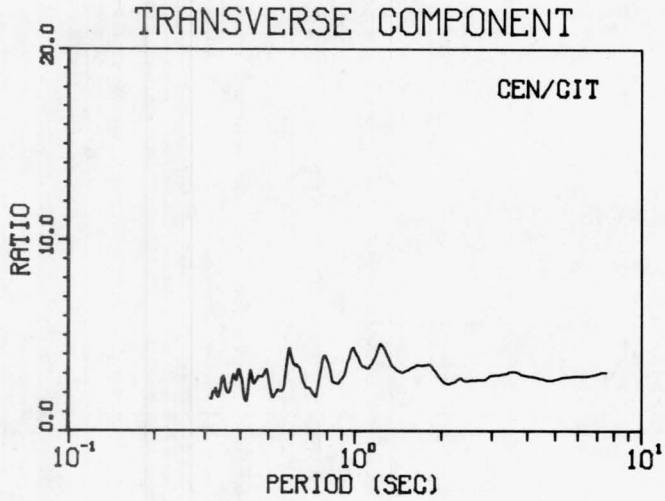

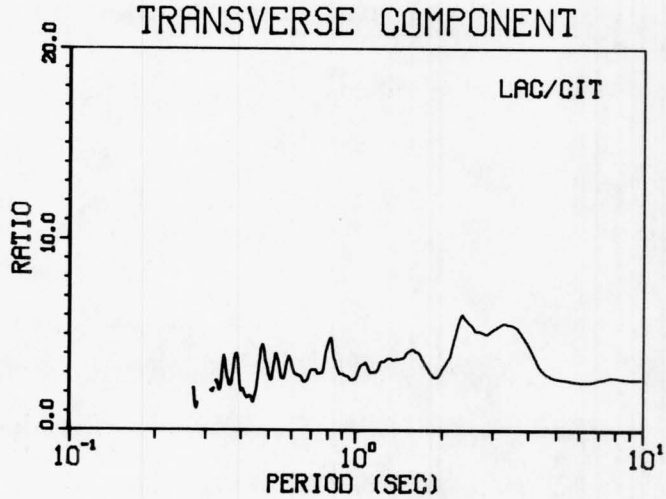

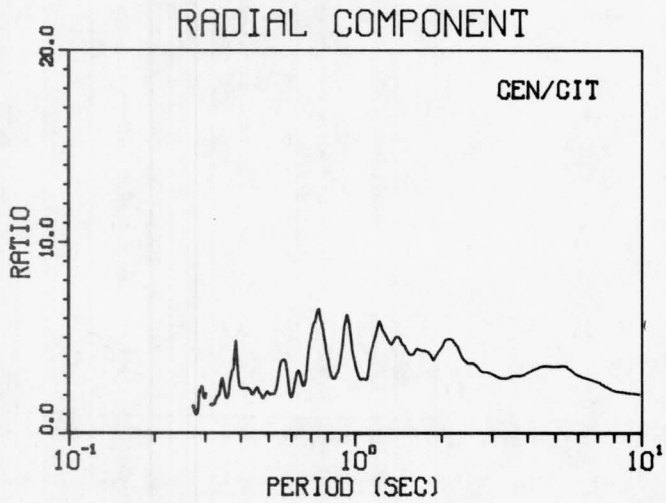

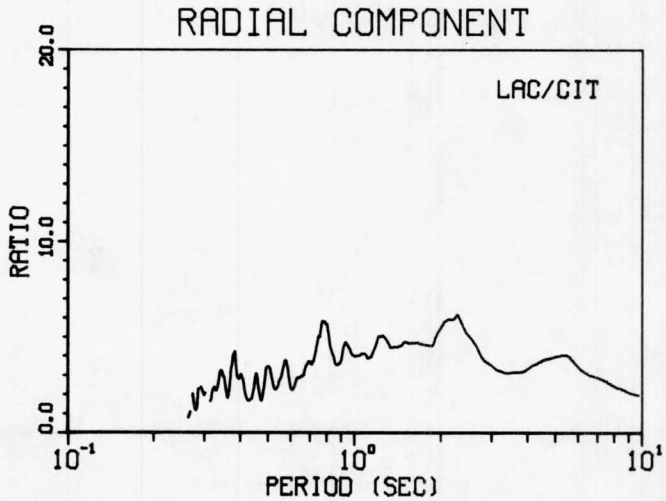

EVENT CHIBERTA

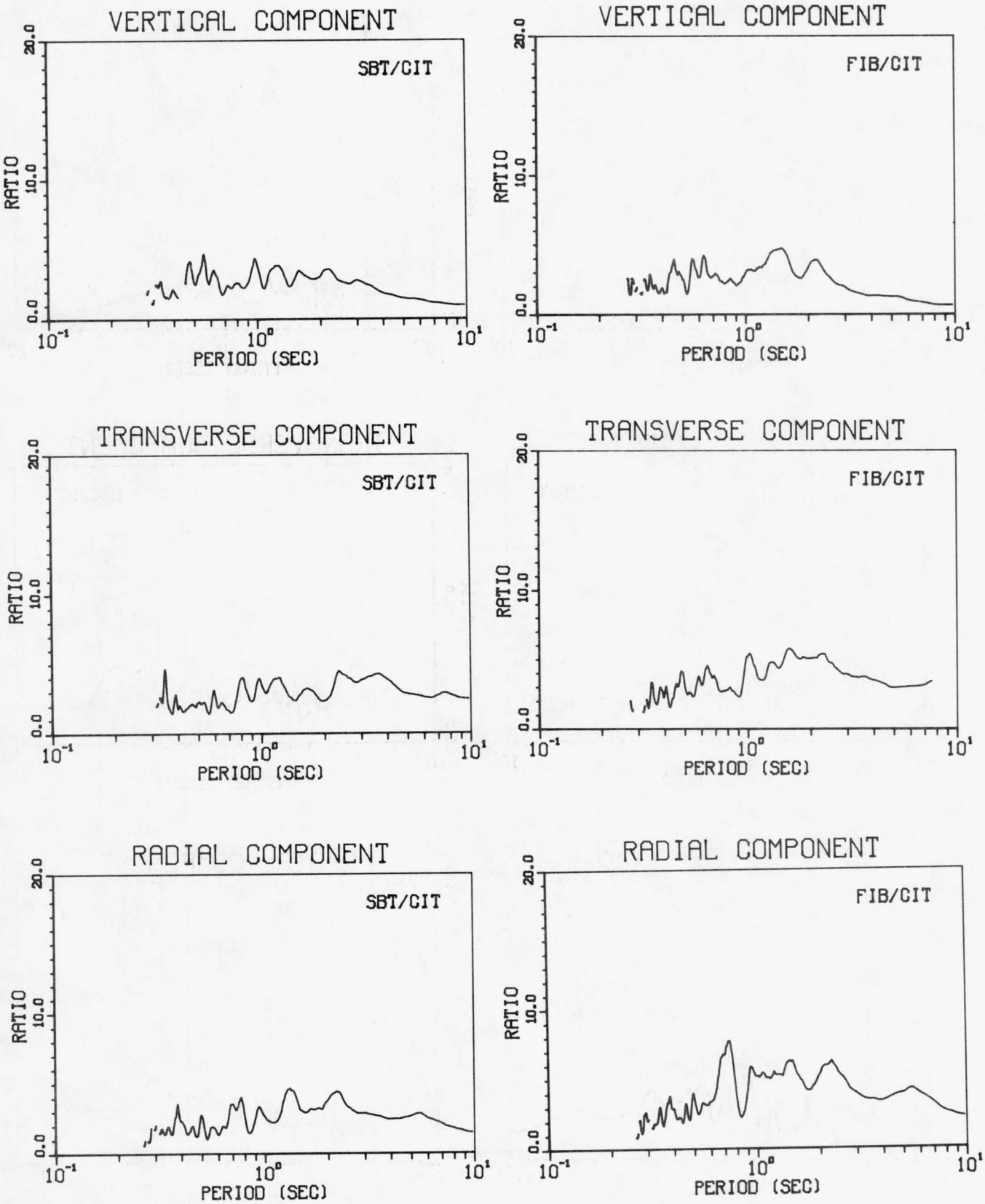

EVENT COLBY

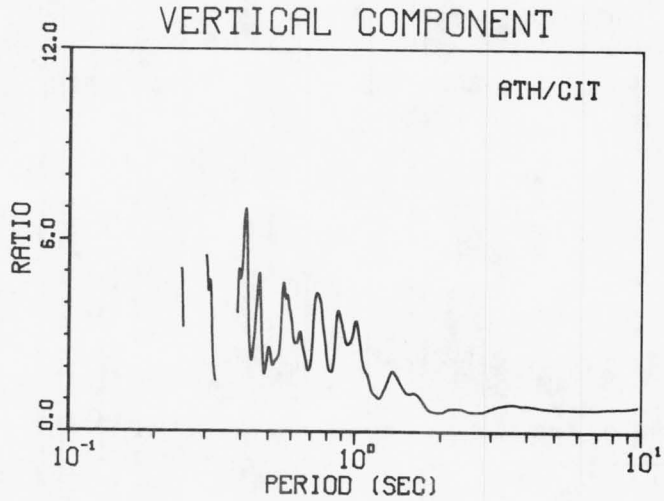
VERTICAL COMPONENT
ATH/CIT
RATIO
12.0
6.0
0.0
10^{-1}
10^{0}
10^{1}
PERIOD (SEC)

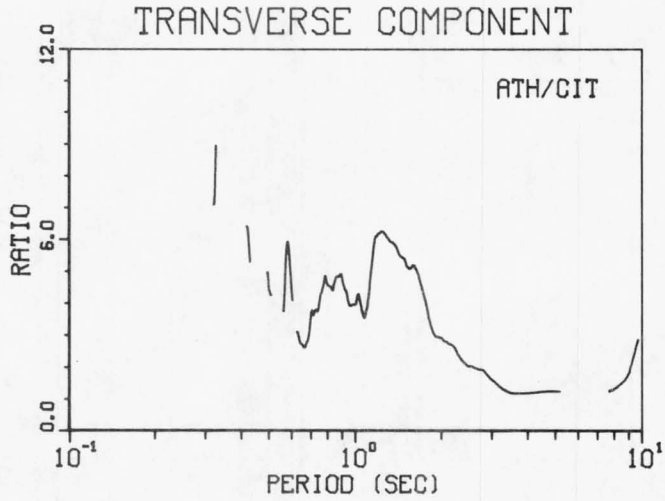
TRANSVERSE COMPONENT
ATH/CIT
RATIO
12.0
6.0
0.0
10^{-1}
10^{0}
10^{1}
PERIOD (SEC)

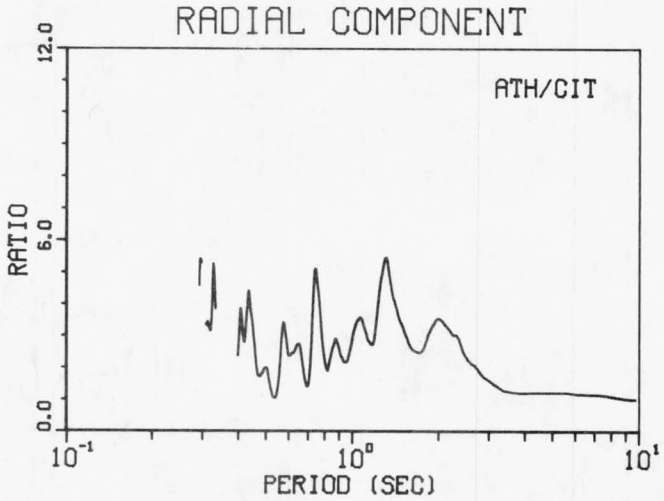
RADIAL COMPONENT
ATH/CIT
RATIO
12.0
6.0
0.0
10^{-1}
10^{0}
10^{1}
PERIOD (SEC)

EVENT COLBY

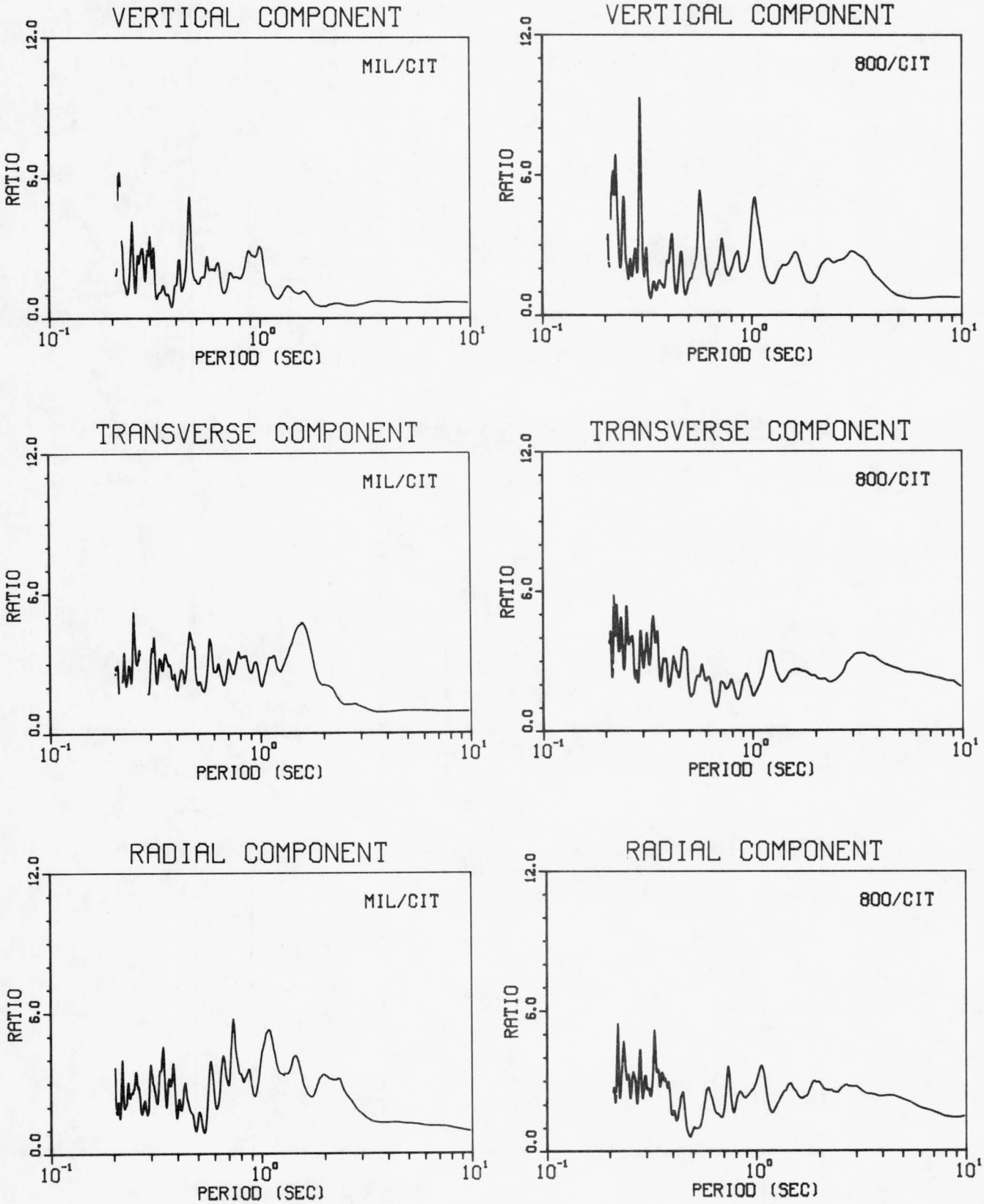
VERTICAL COMPONENT
MIL/CIT
VERTICAL COMPONENT
800/CIT
TRANSVERSE COMPONENT
MIL/CIT
TRANSVERSE COMPONENT
800/CIT
RADIAL COMPONENT
MIL/CIT
RADIAL COMPONENT
800/CIT
RATIO
12.0
6.0
0.0
10^{-1}
10^{0}
10^{1}
PERIOD (SEC)

EVENT CREWLINE

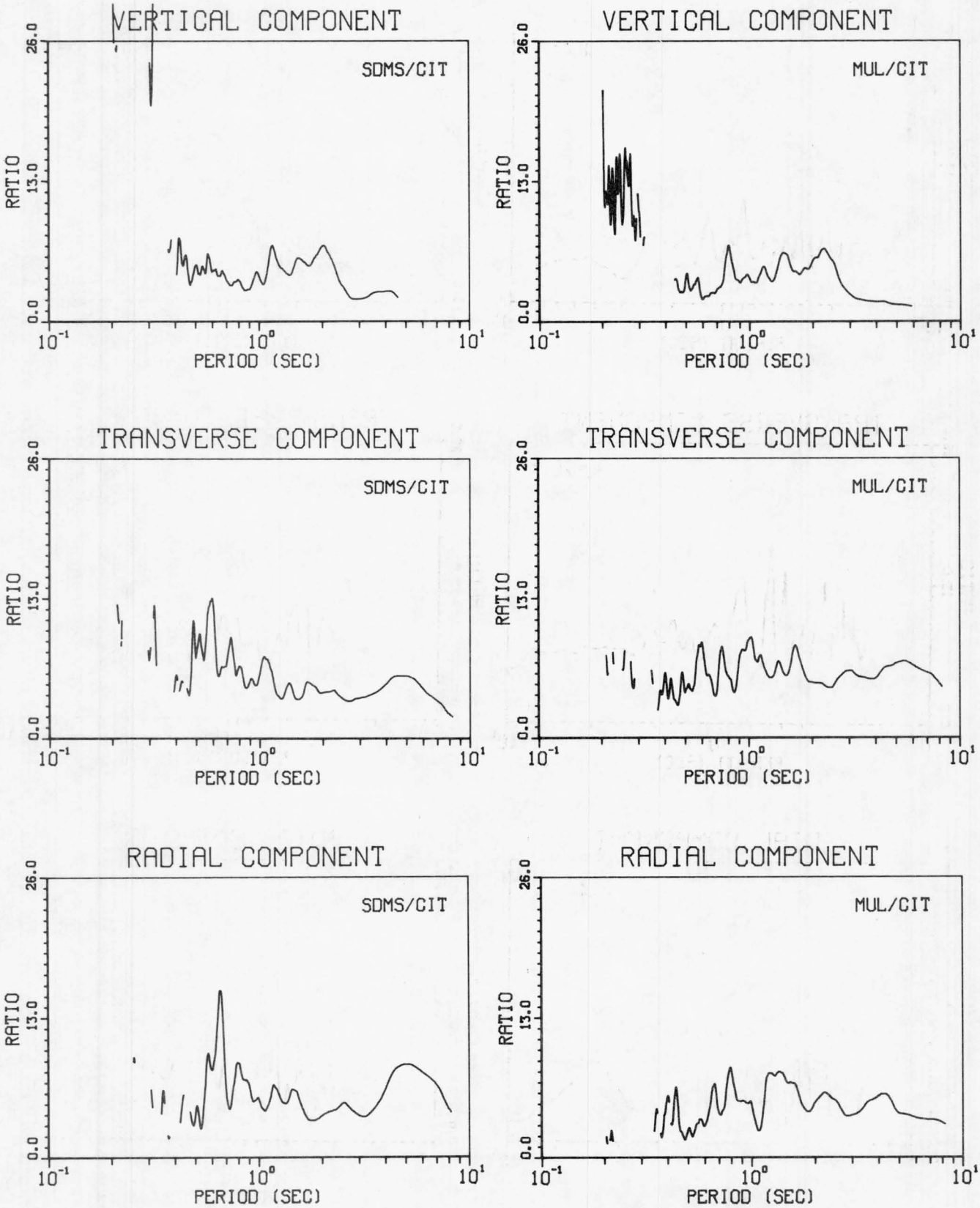

EVENT CREWLINE

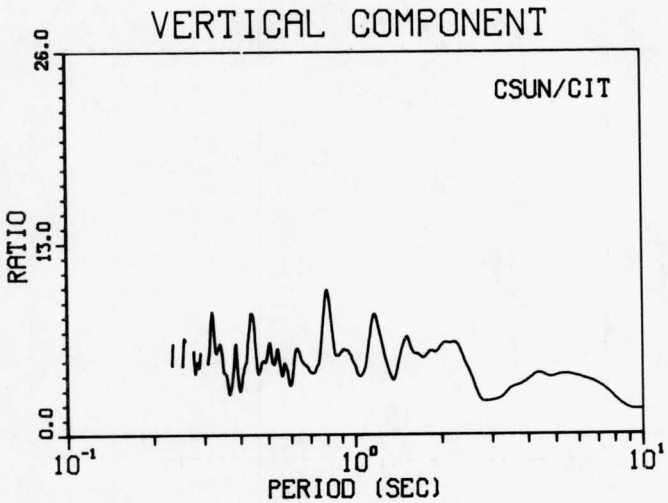

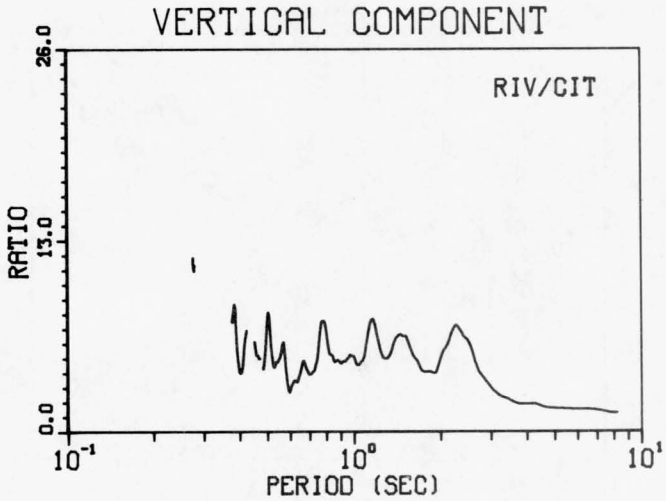

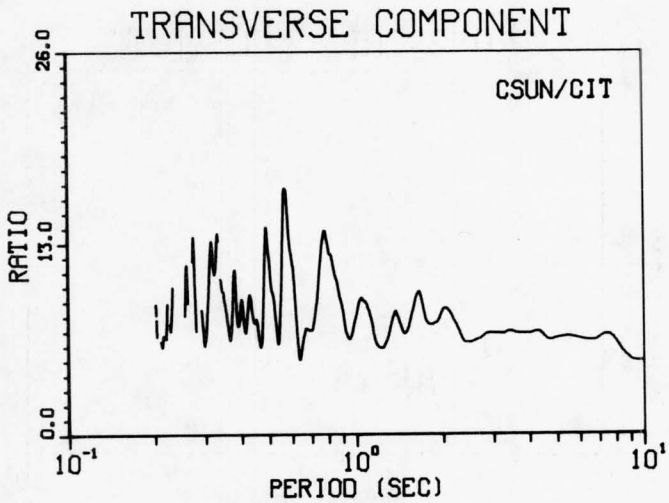

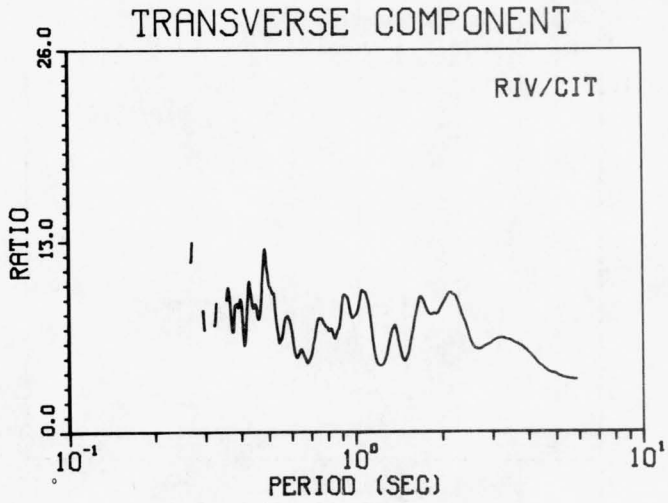

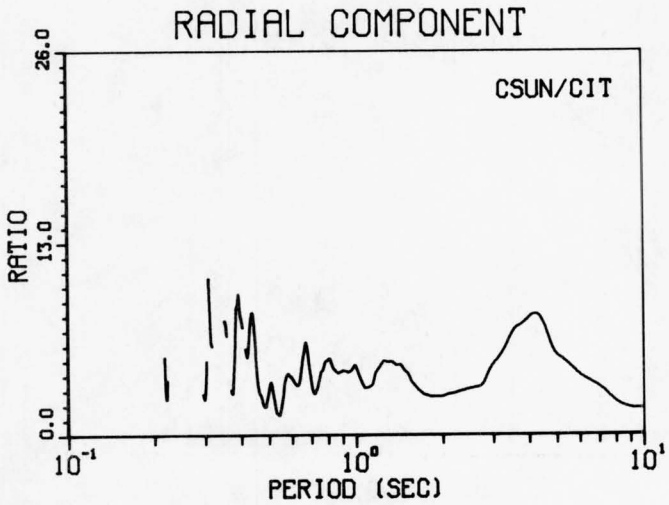

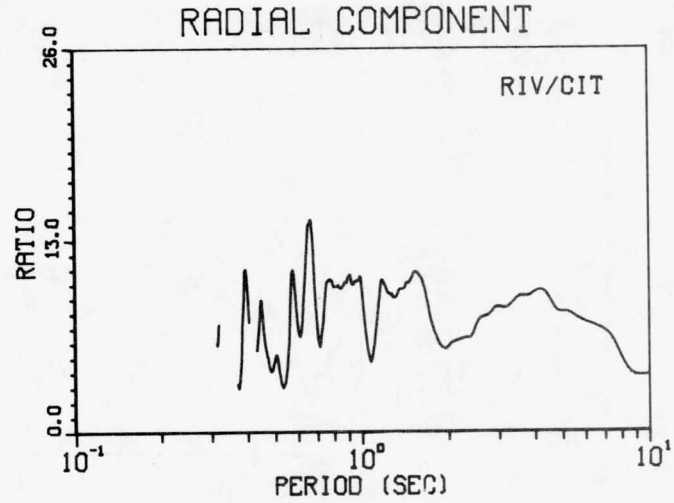

EVENT CREWLINE

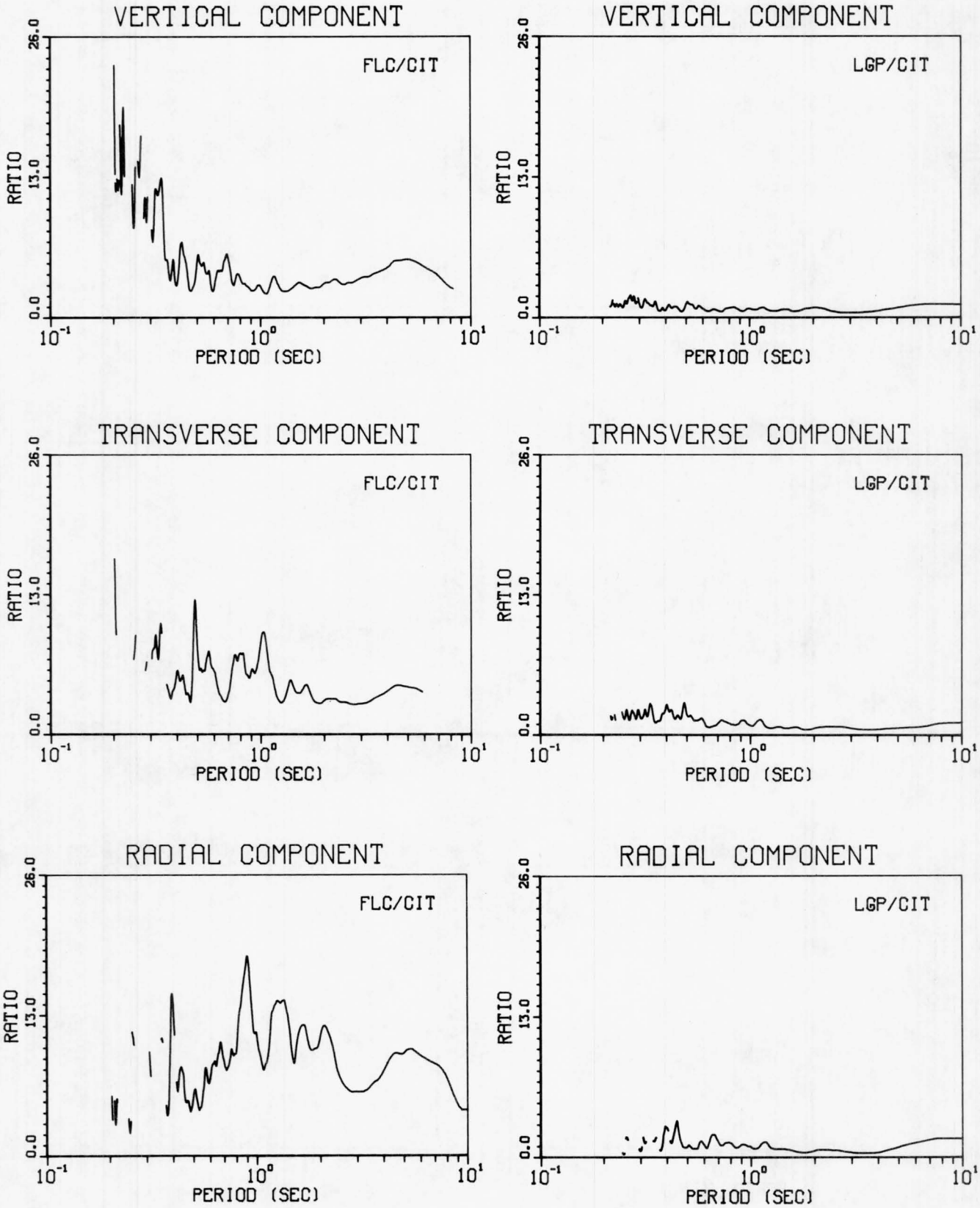

EVENT CREWLINE

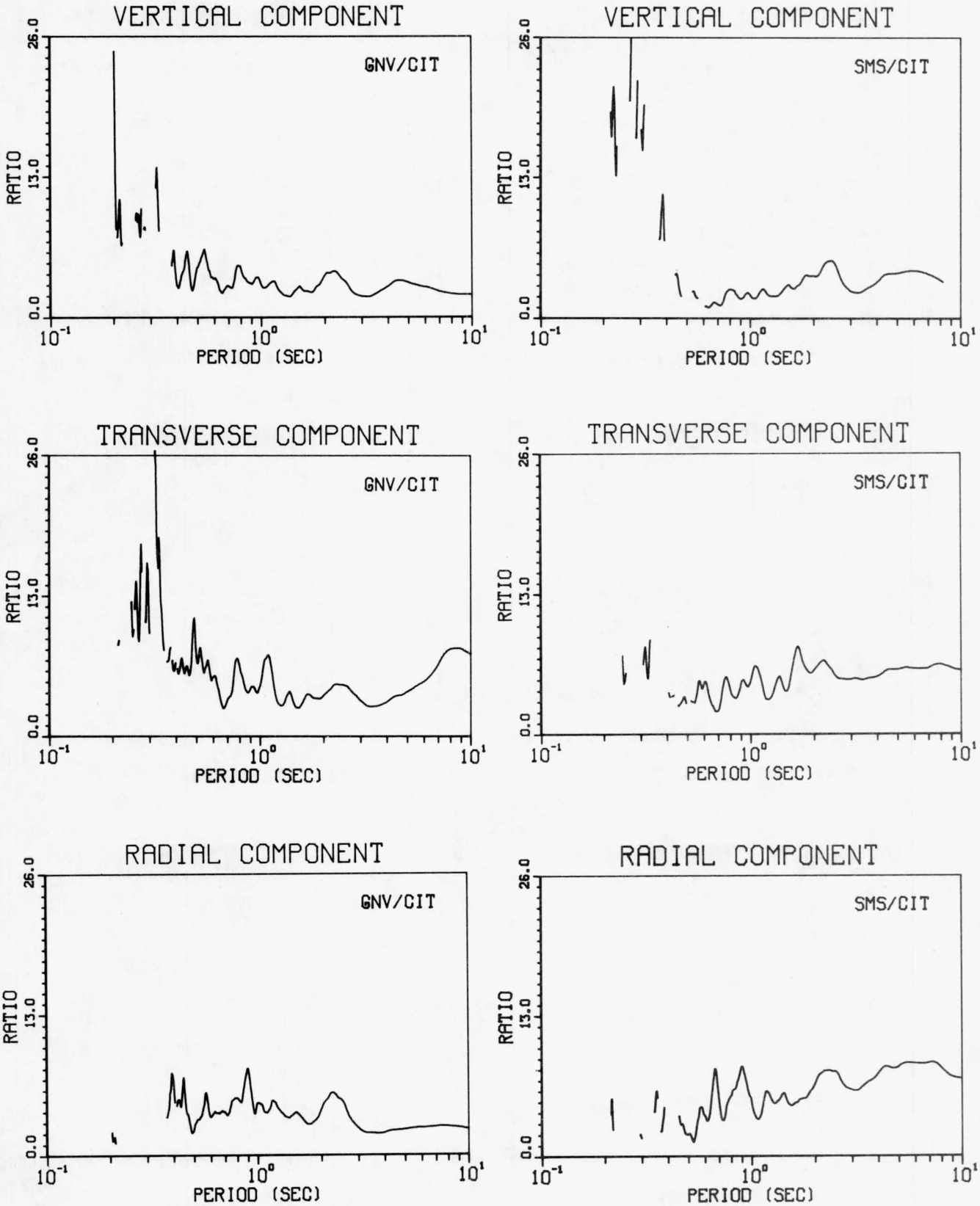

EVENT CREWLINE

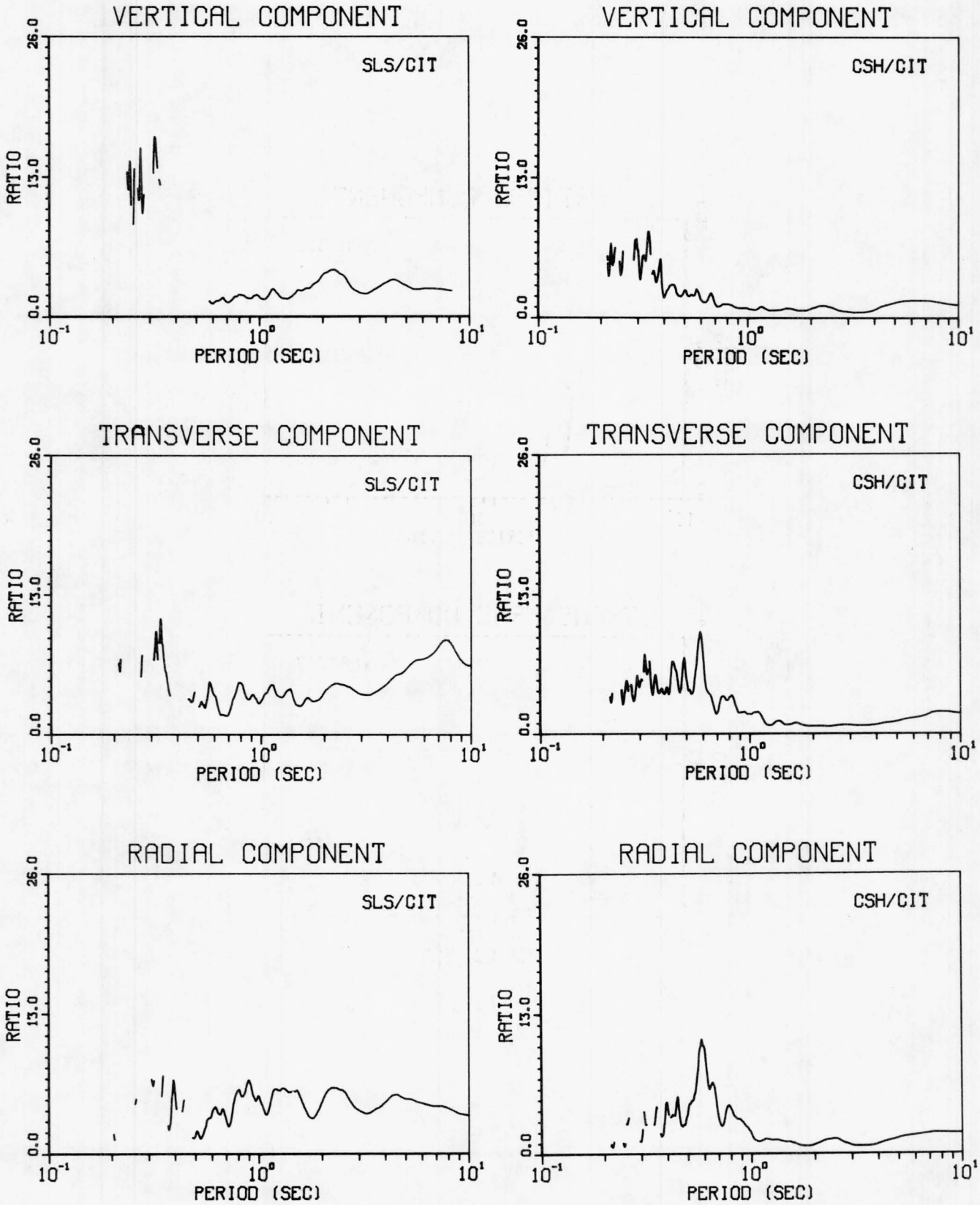

EVENT CREWLINE

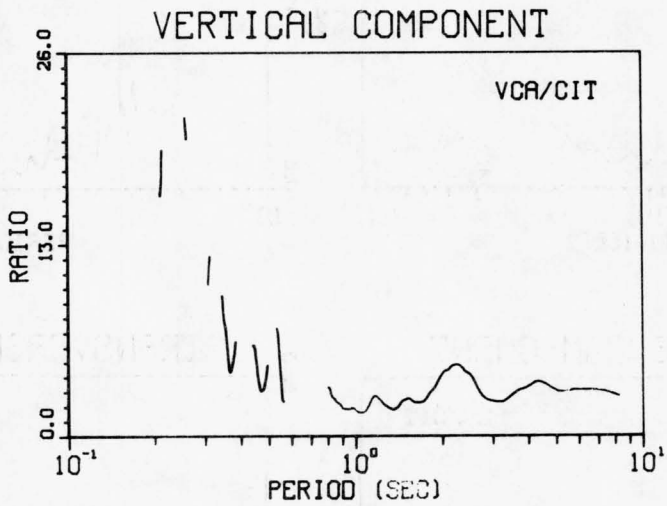

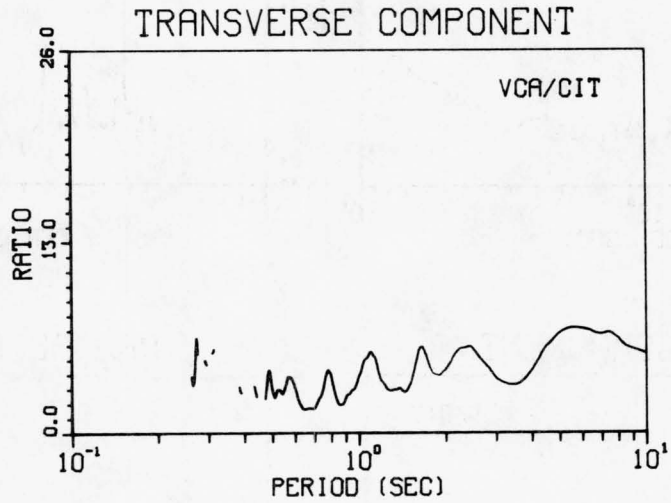

EVENT CREWLINE

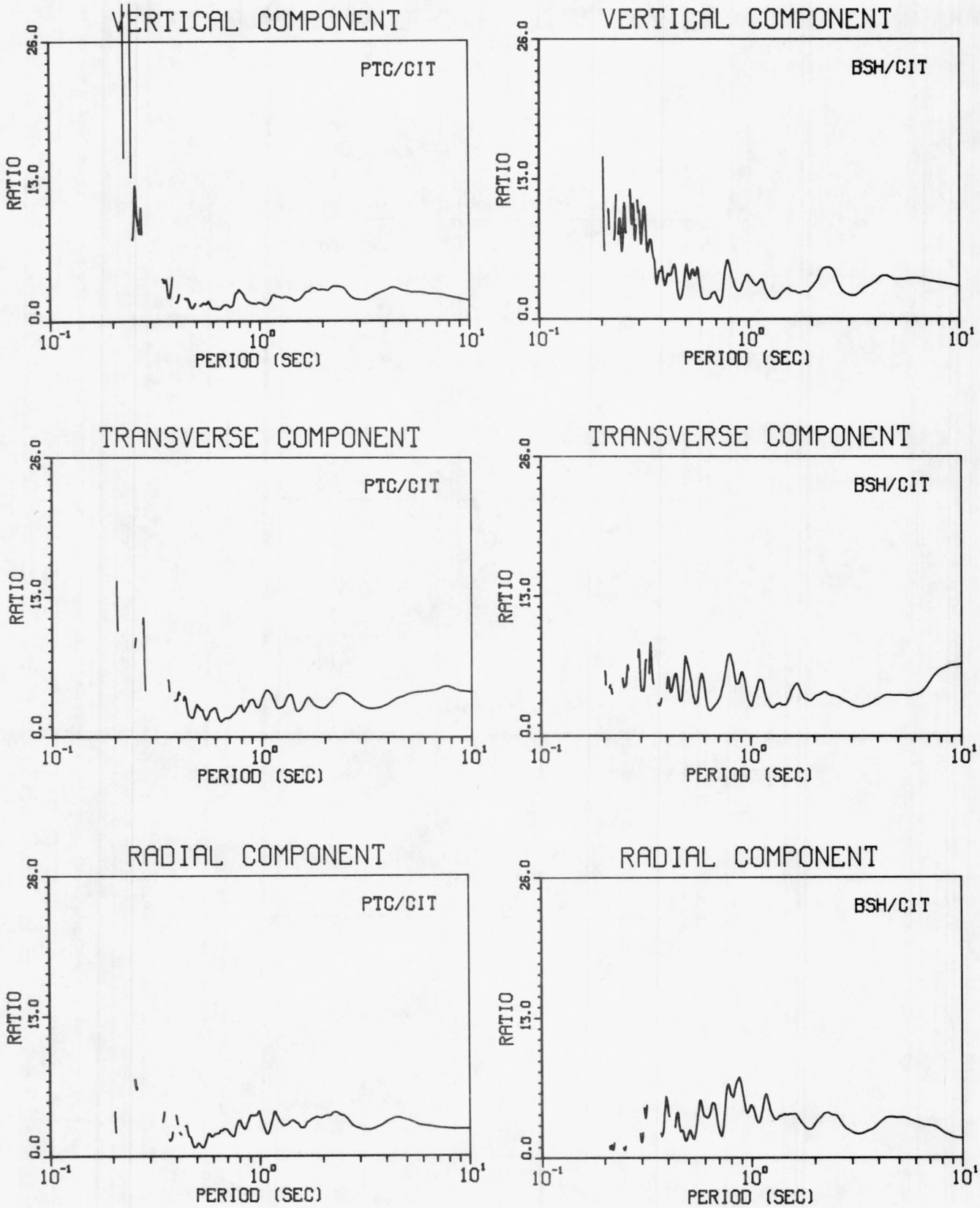

EVENT CREWLINE

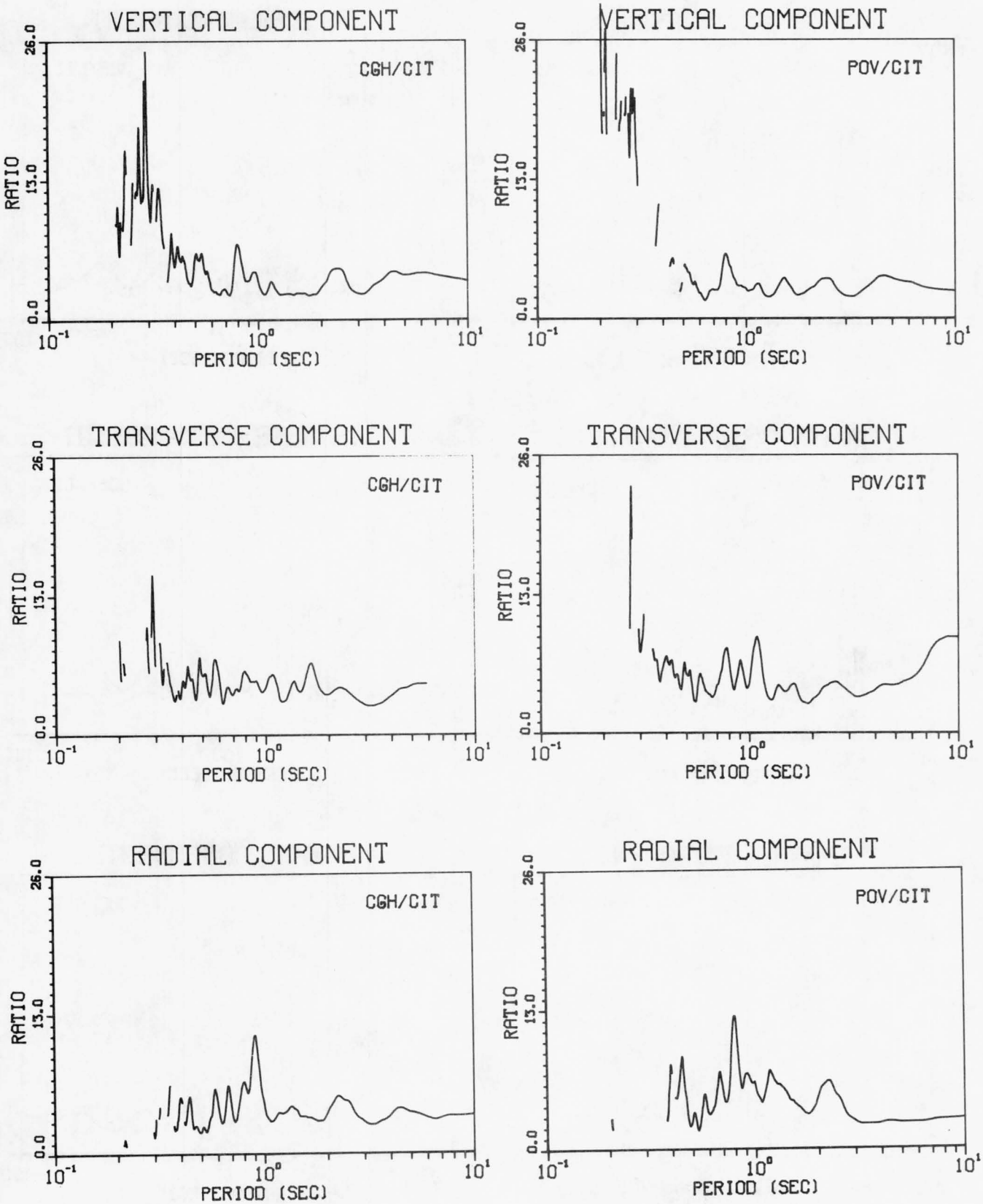

EVENT CREWLINE

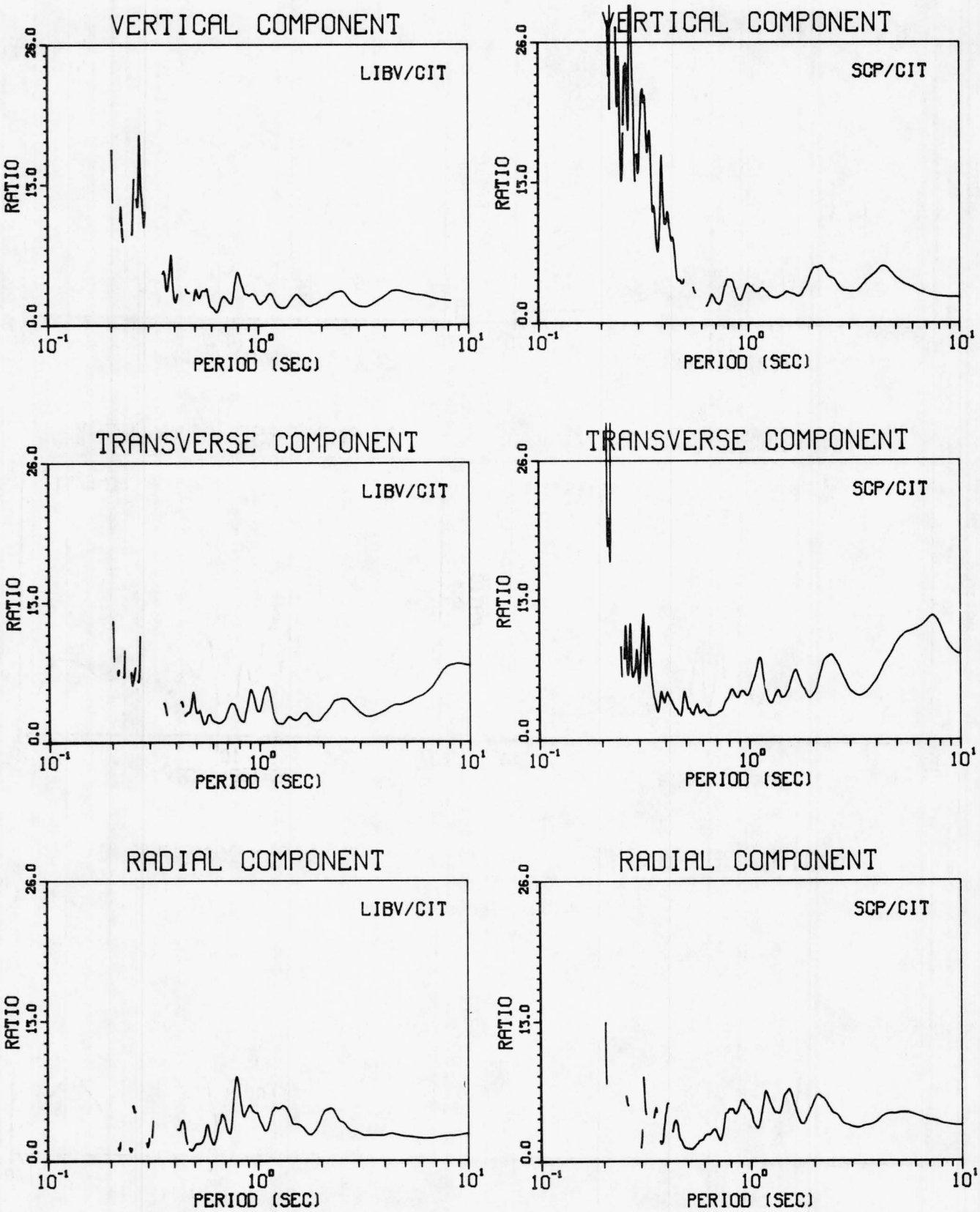

EVENT FAJY

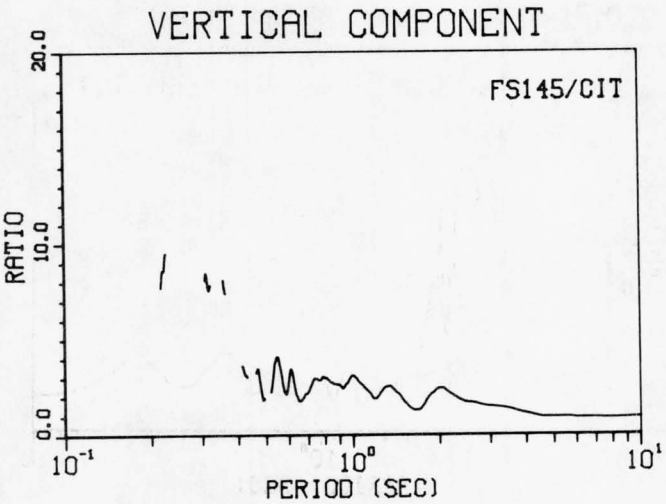
VERTICAL COMPONENT
FS145/CIT
RATIO
20.0
10.0
0.0
10^{-1}
10^{0}
10^{1}
PERIOD (SEC)

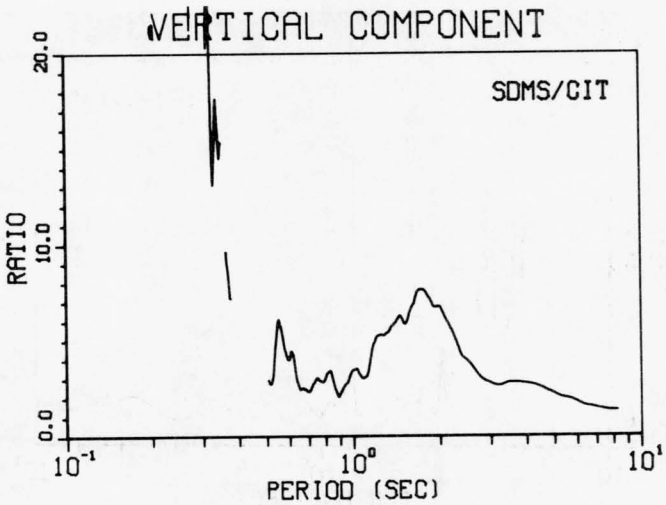
VERTICAL COMPONENT
SDMS/CIT
RATIO
20.0
10.0
0.0
10^{-1}
10^{0}
10^{1}
PERIOD (SEC)

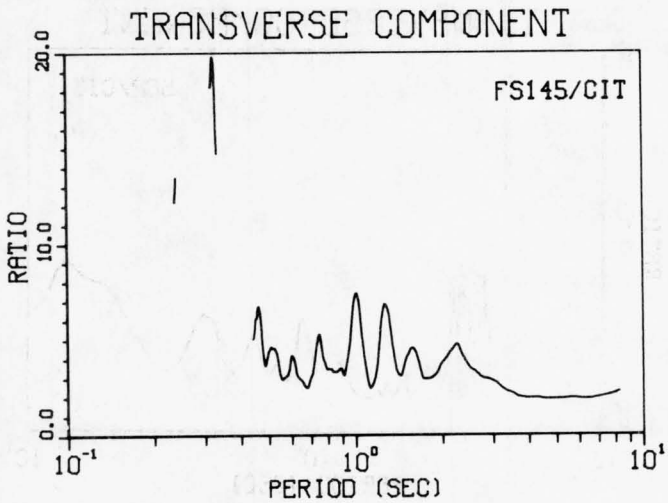
TRANSVERSE COMPONENT
FS145/CIT
RATIO
20.0
10.0
0.0
10^{-1}
10^{0}
10^{1}
PERIOD (SEC)

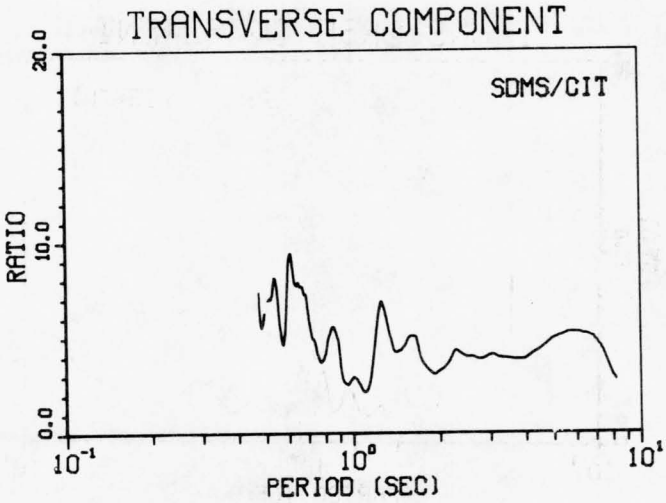
TRANSVERSE COMPONENT
SDMS/CIT
RATIO
20.0
10.0
0.0
10^{-1}
10^{0}
10^{1}
PERIOD (SEC)

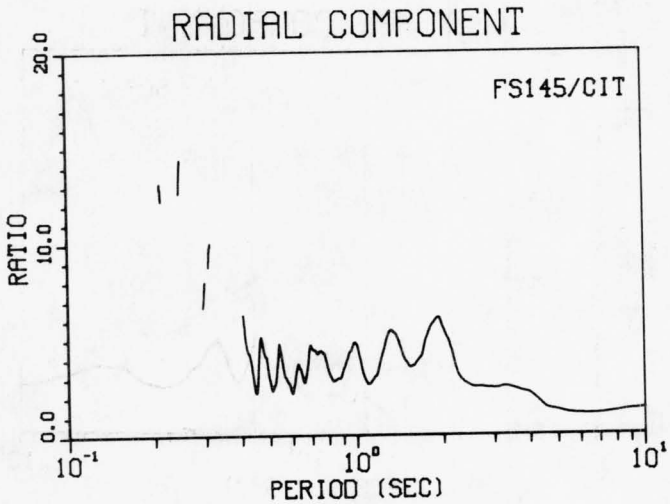
RADIAL COMPONENT
FS145/CIT
RATIO
20.0
10.0
0.0
10^{-1}
10^{0}
10^{1}
PERIOD (SEC)

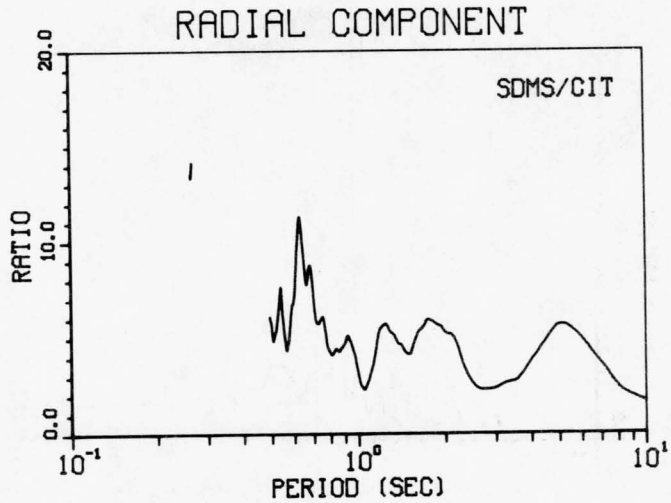
RADIAL COMPONENT
SDMS/CIT
RATIO
20.0
10.0
0.0
10^{-1}
10^{0}
10^{1}
PERIOD (SEC)

EVENT FAJY

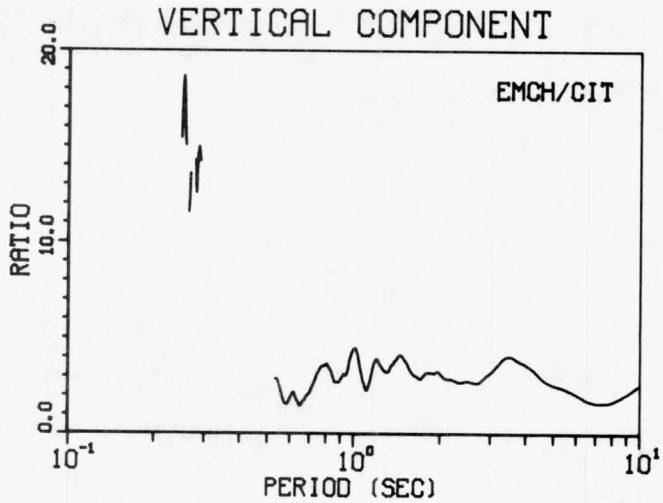
VERTICAL COMPONENT
EMCH/CIT
RATIO
20.0
10.0
0.0
10^{-1}
10^{0}
10^{1}
PERIOD (SEC)

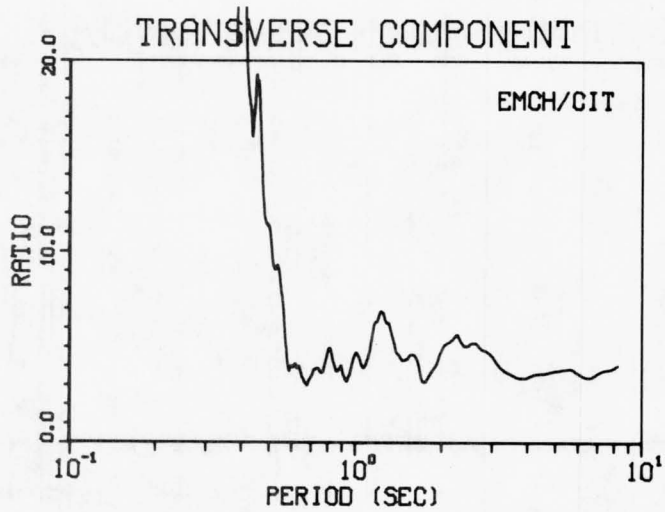
TRANSVERSE COMPONENT
EMCH/CIT
RATIO
20.0
10.0
0.0
10^{-1}
10^{0}
10^{1}
PERIOD (SEC)

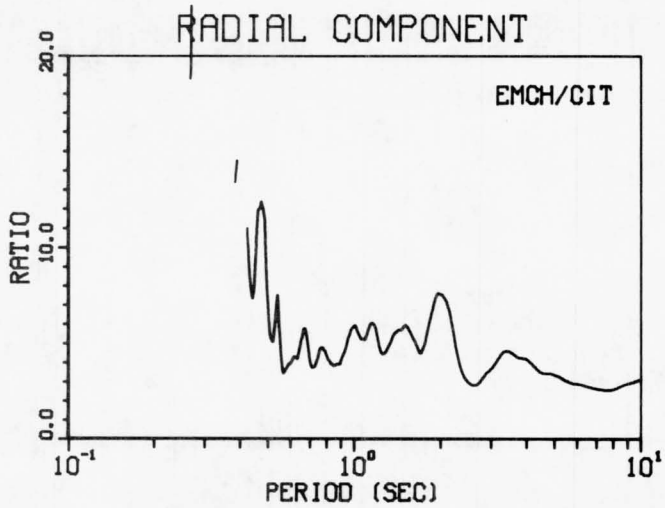
RADIAL COMPONENT
EMCH/CIT
RATIO
20.0
10.0
0.0
10^{-1}
10^{0}
10^{1}
PERIOD (SEC)

EVENT FONDUTTA

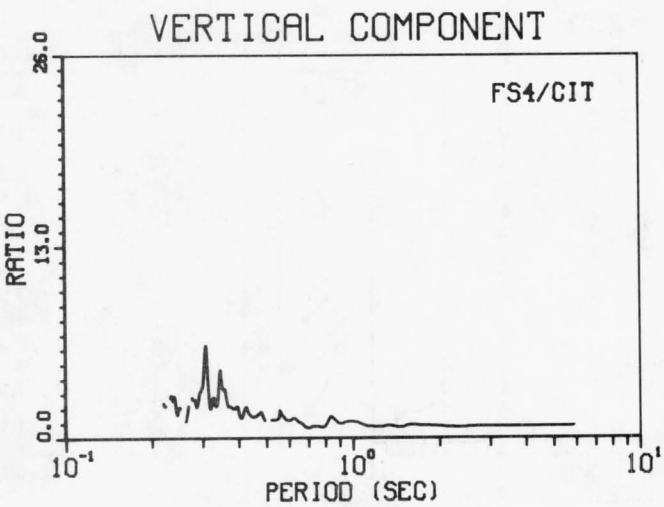

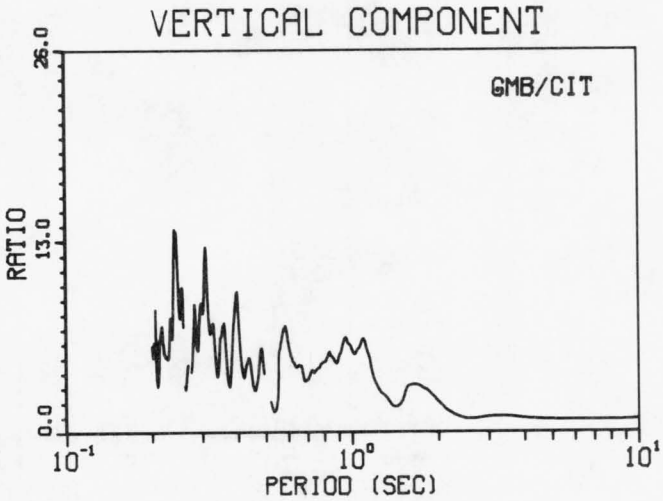

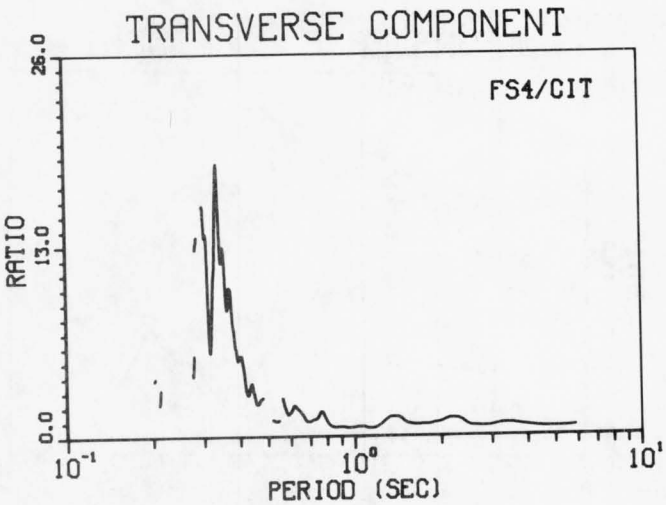

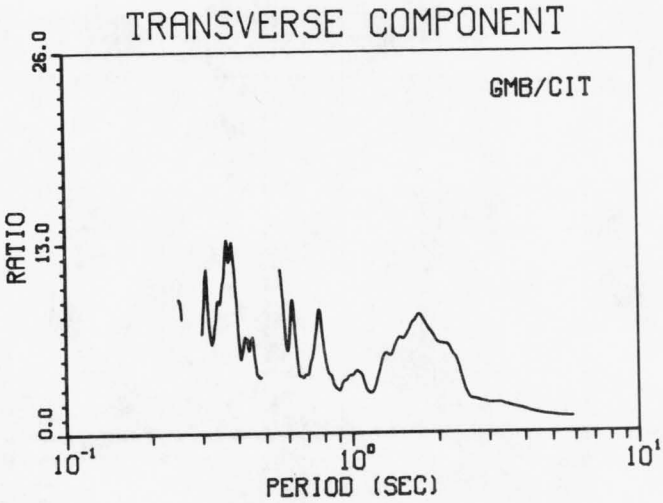

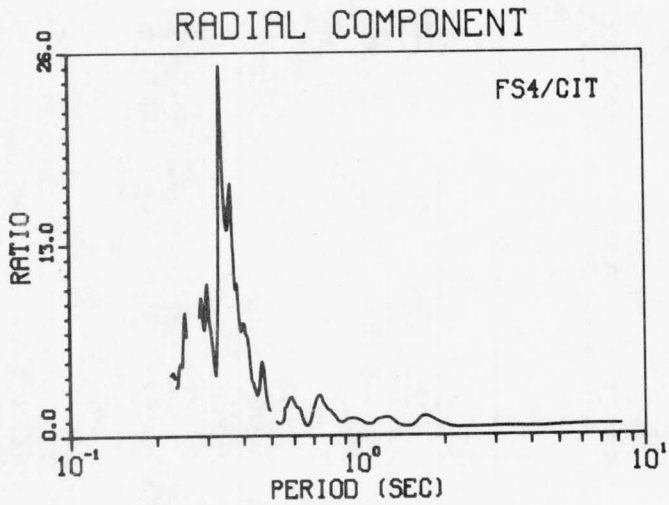

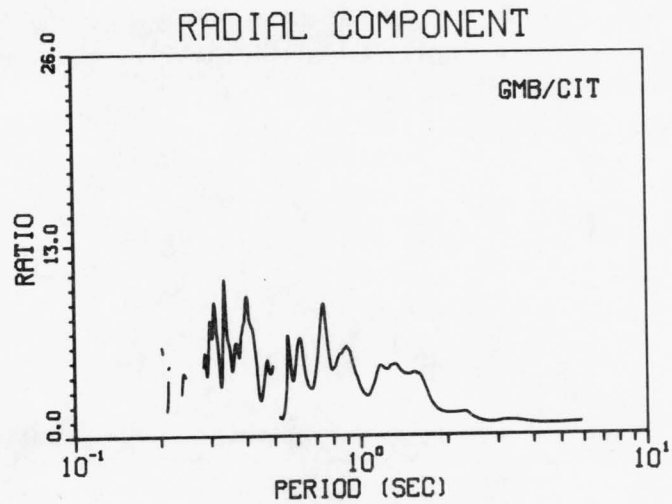

EVENT FONDUTTA

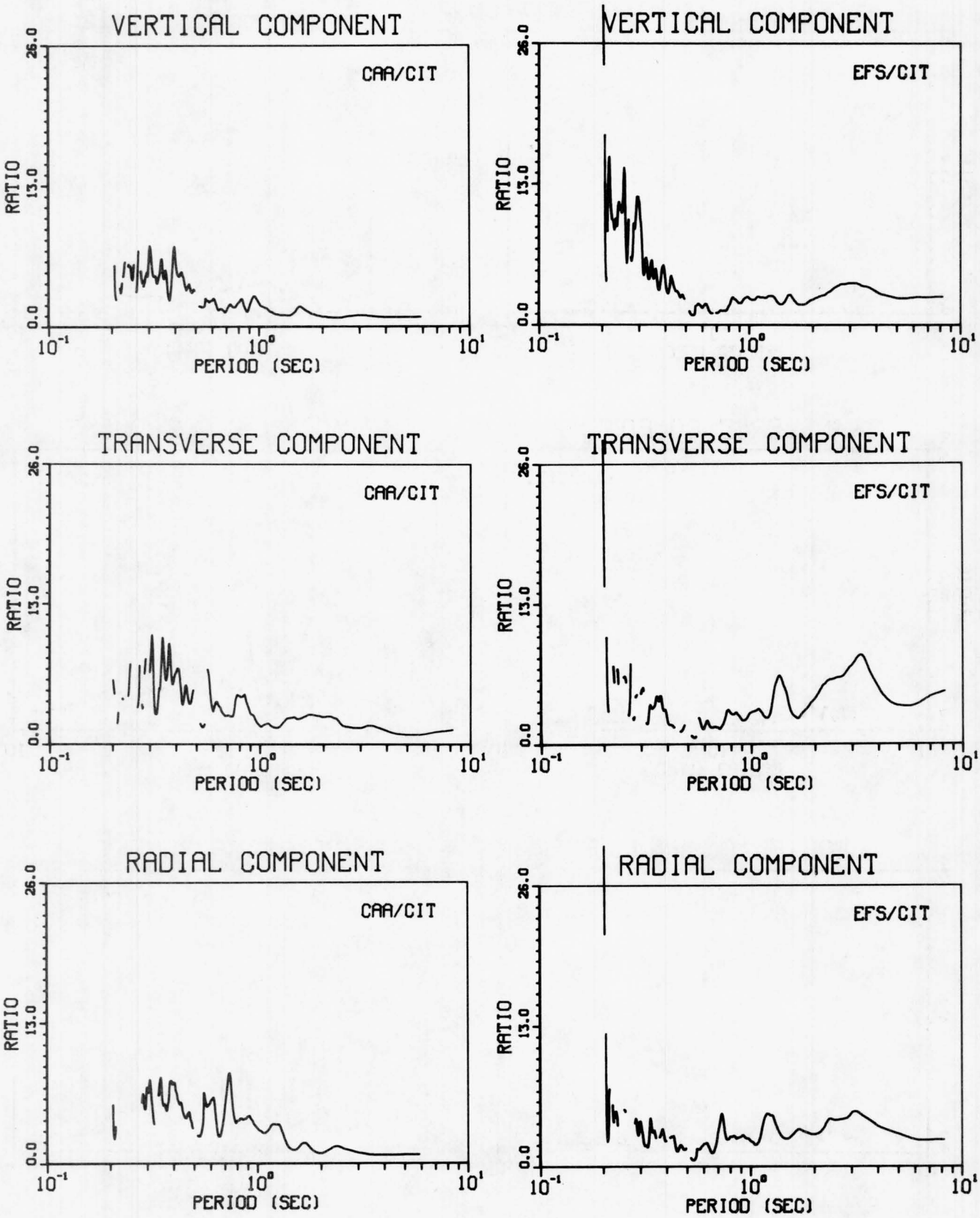

EVENT FONDUTTA

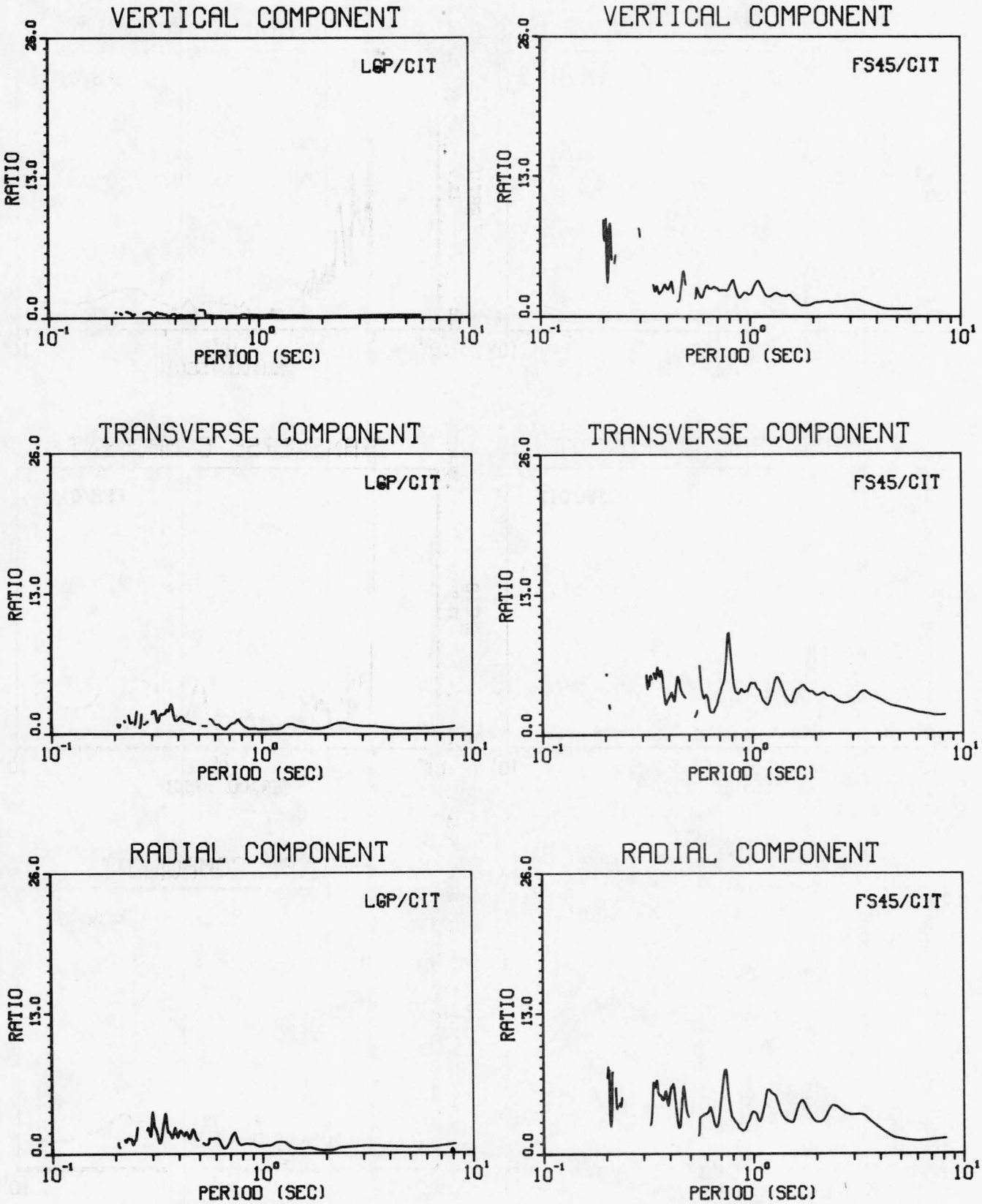

EVENT FONDUTTA

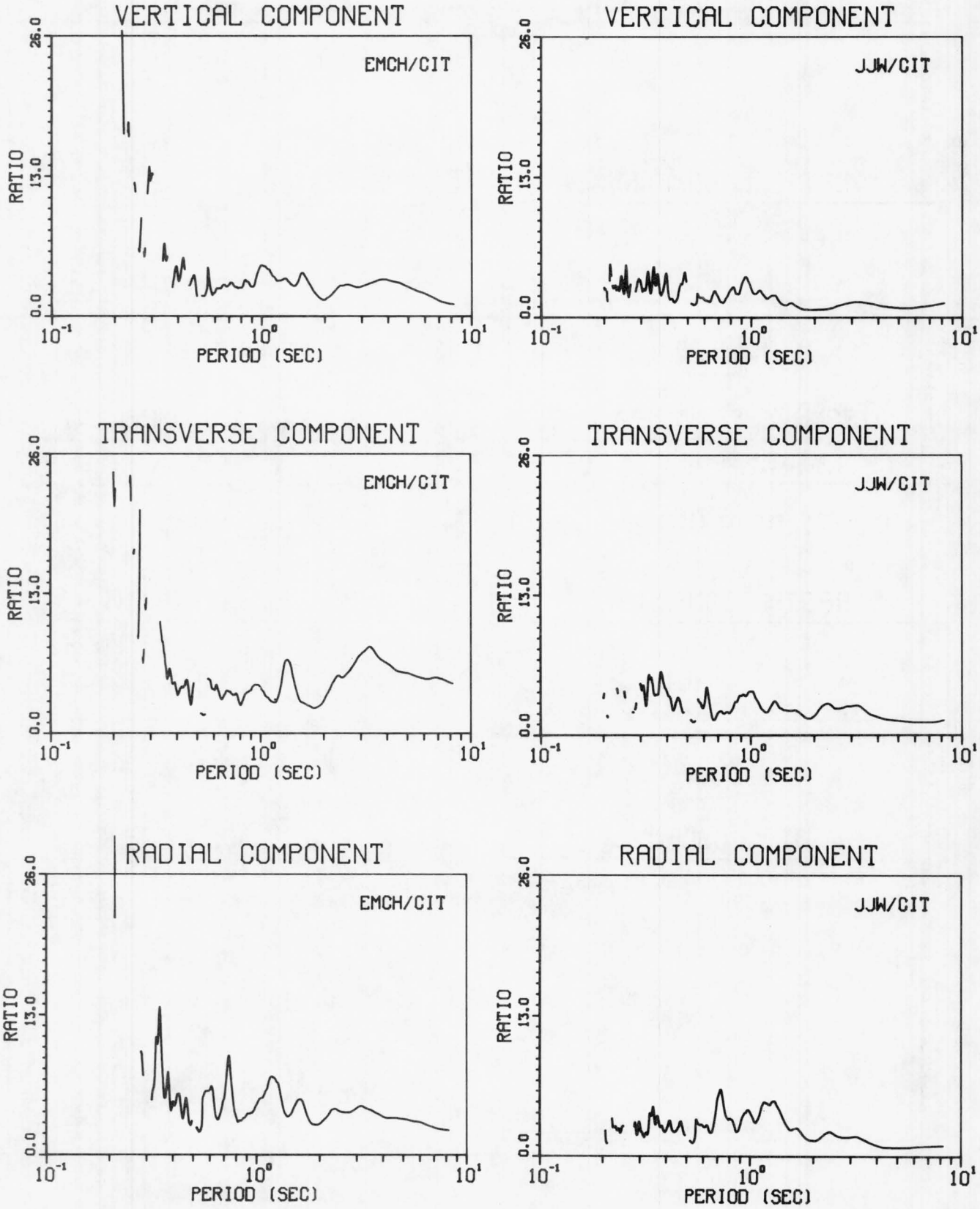

EVENT FONDUTTA

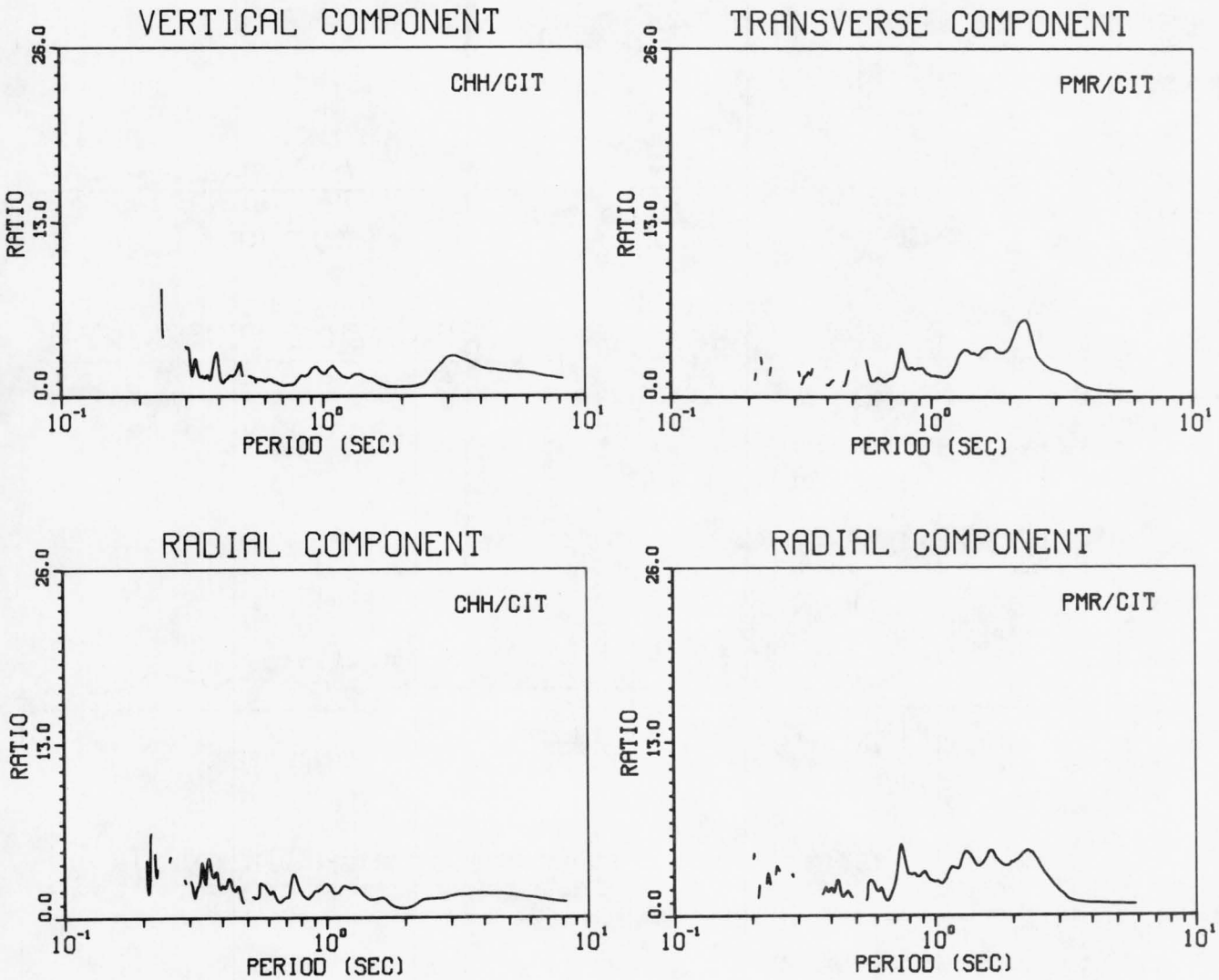

EVENT FONDUTTA

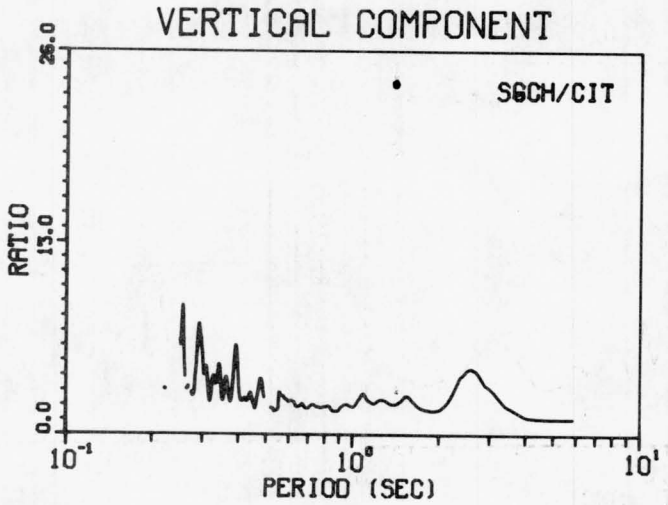

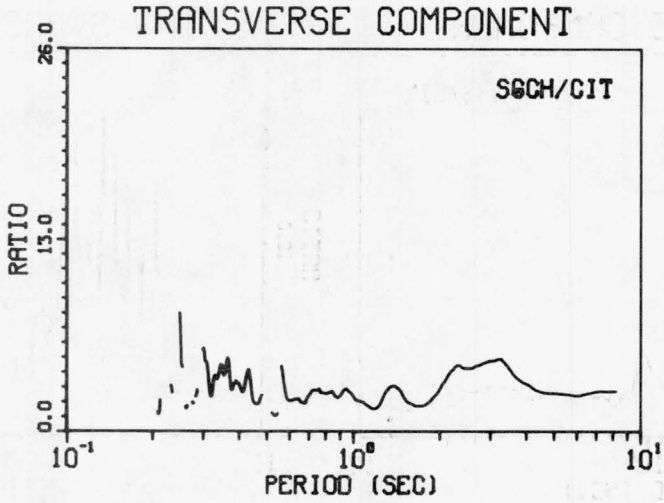

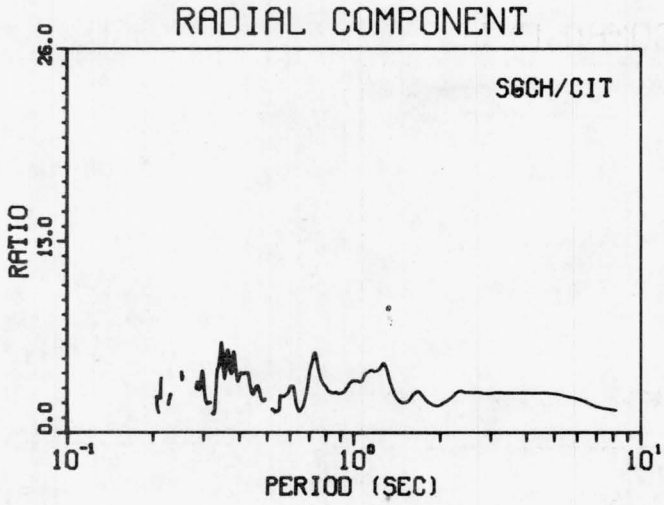

EVENT FONTINA

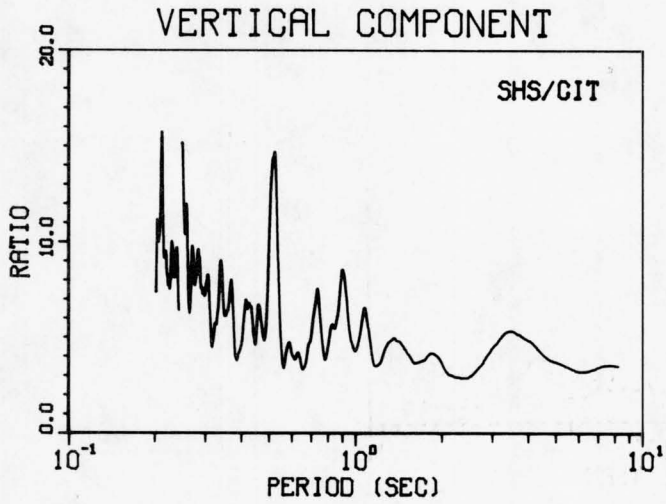

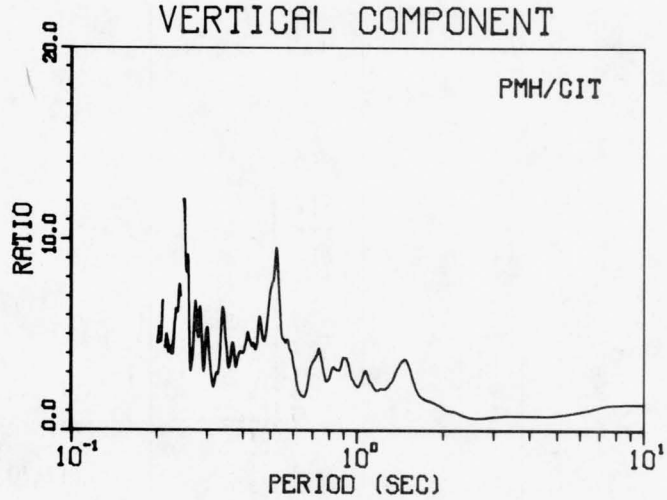

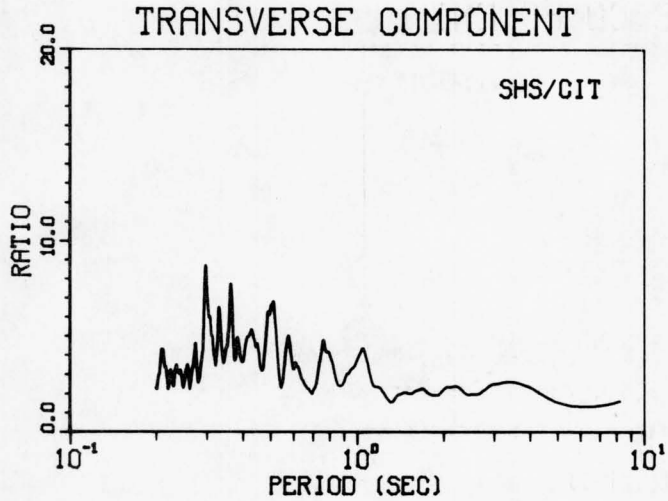

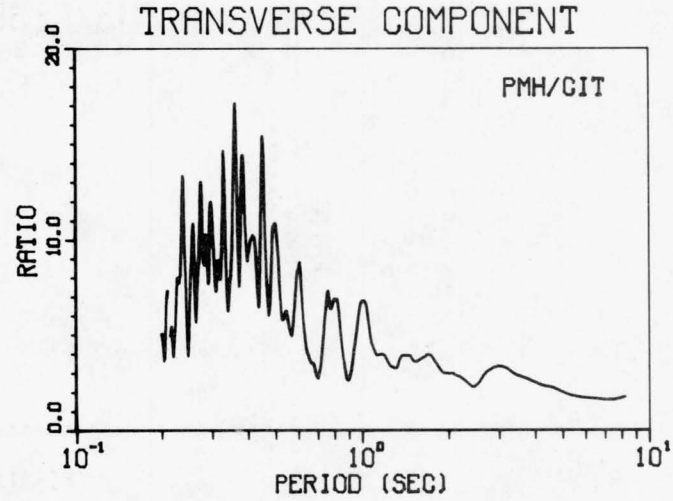

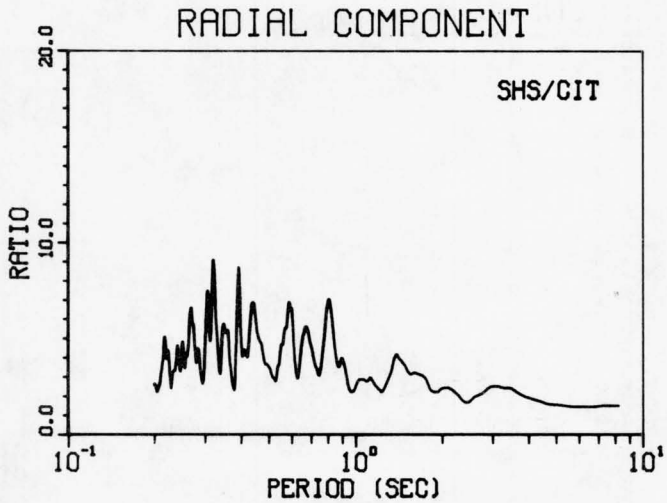

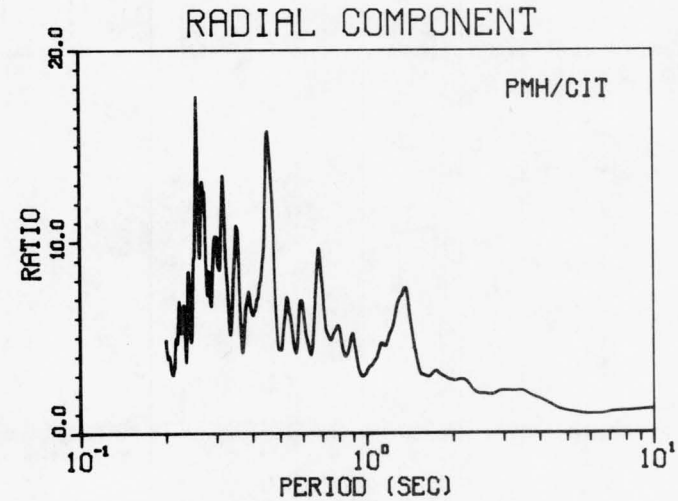

EVENT FONTINA

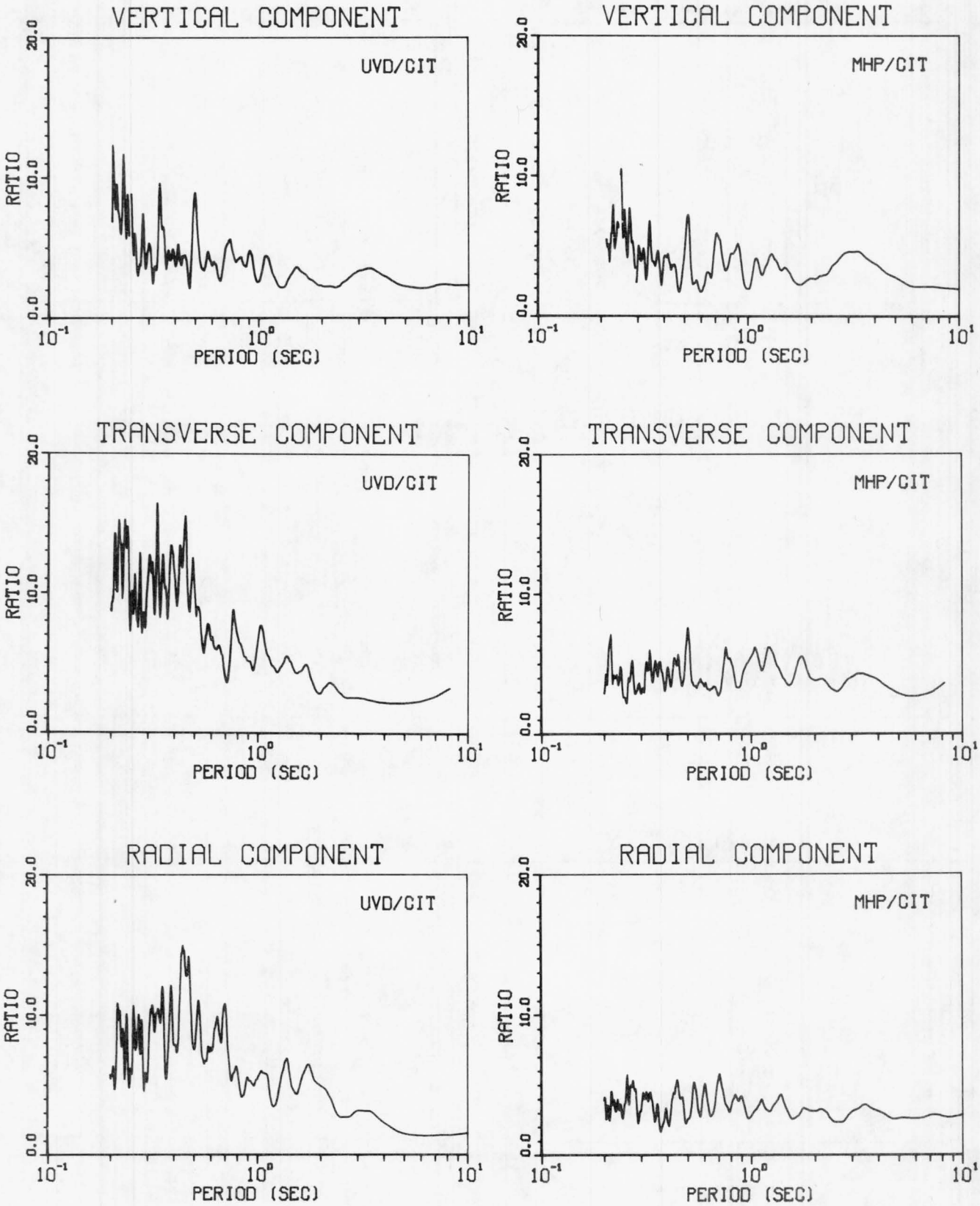

EVENT FONTINA

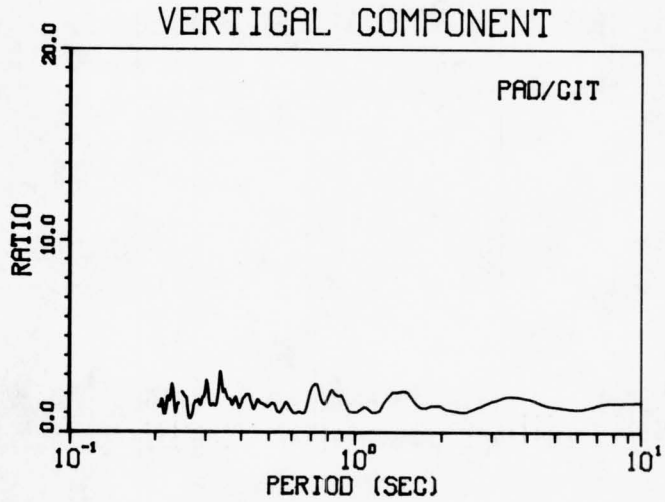

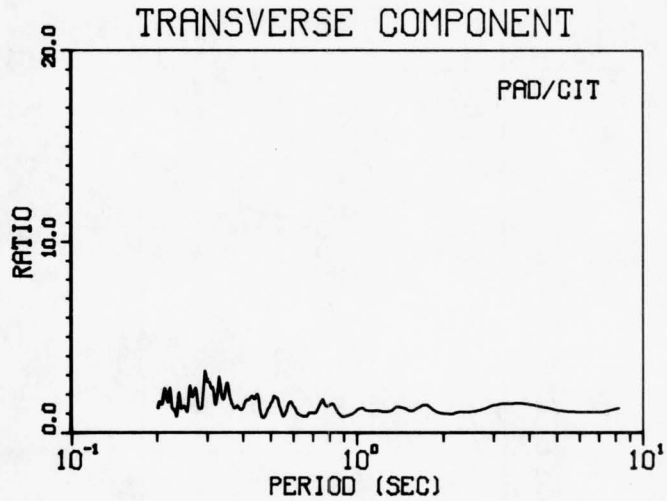

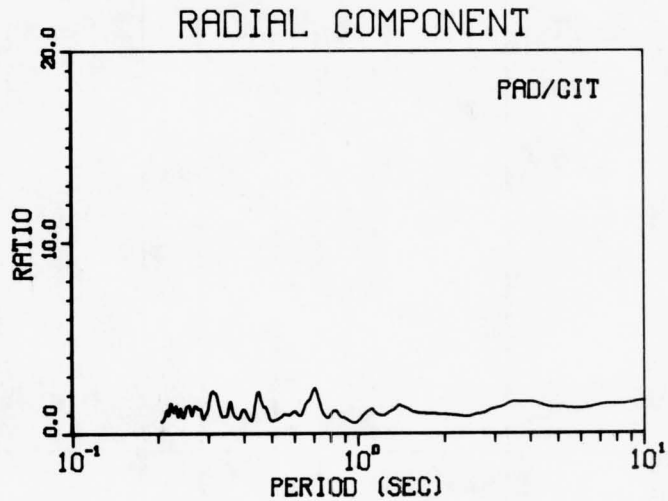

EVENT ICEBERG

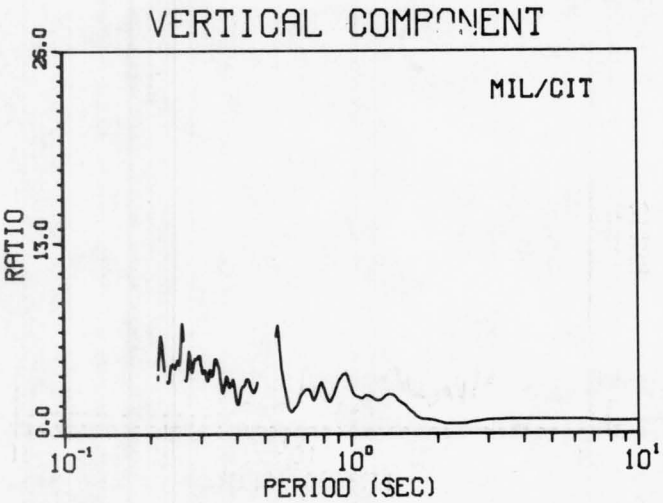

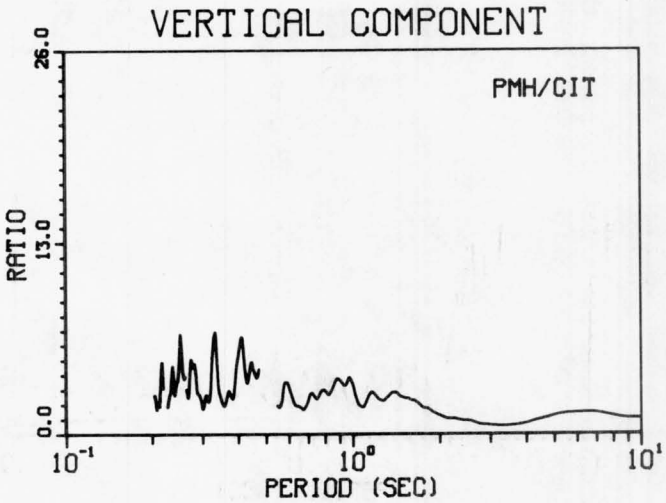

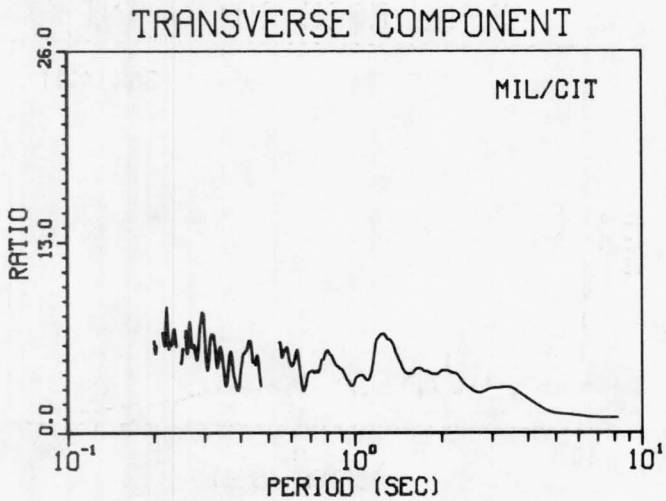

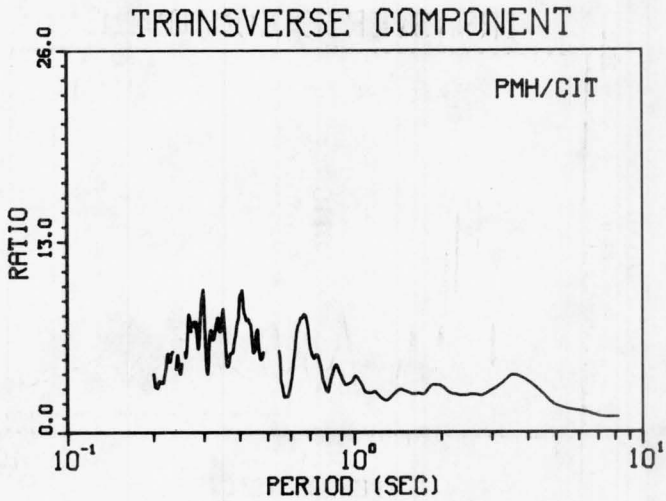

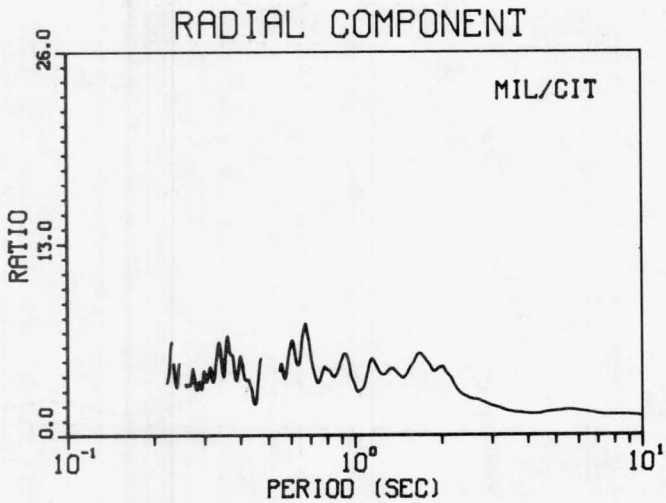

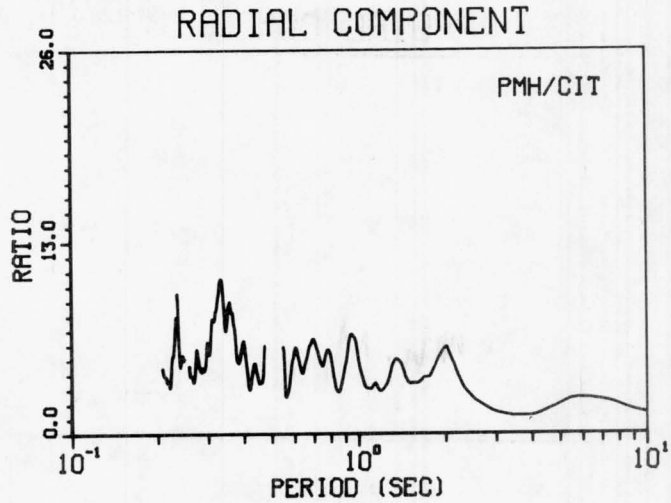

EVENT ICEBERG

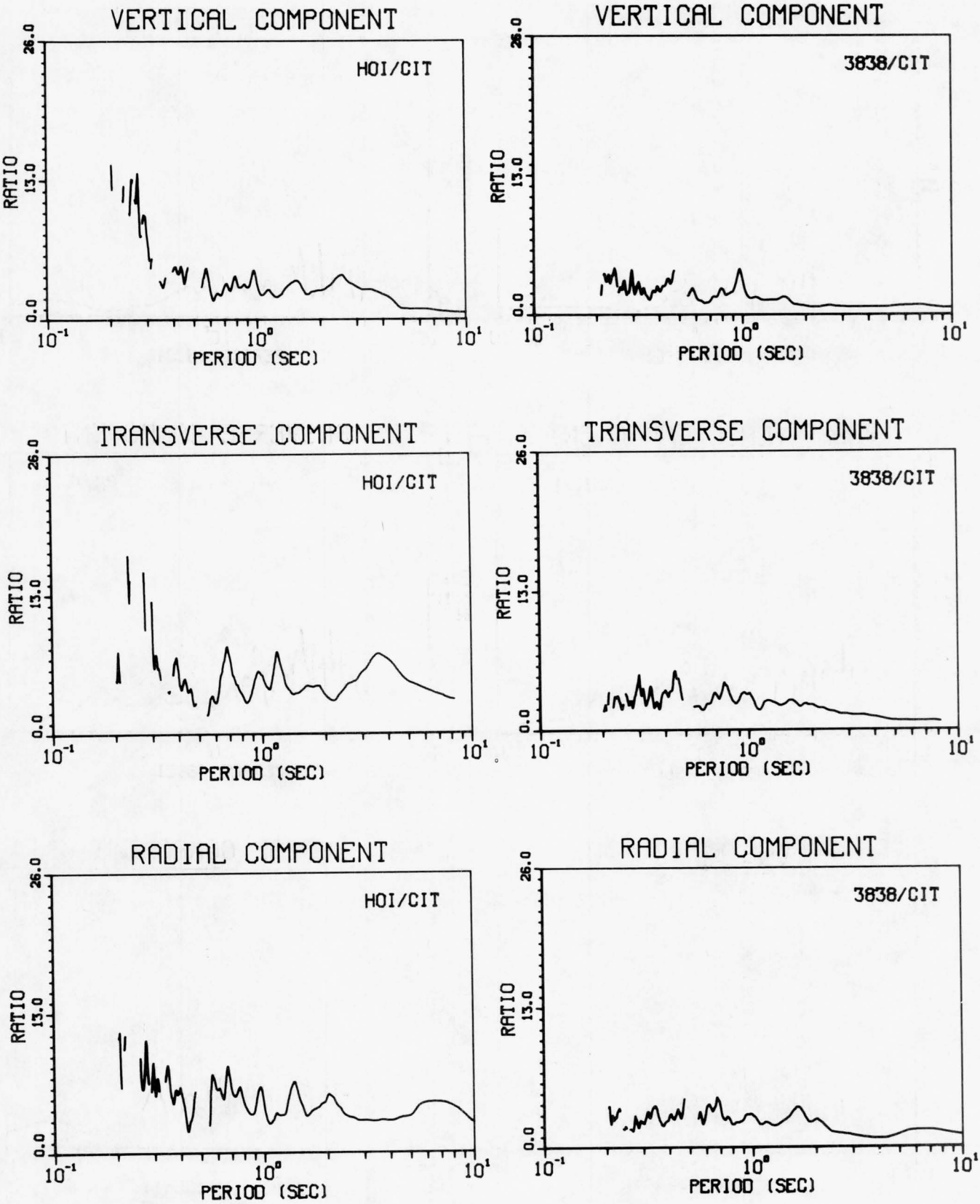

EVENT ICEBERG

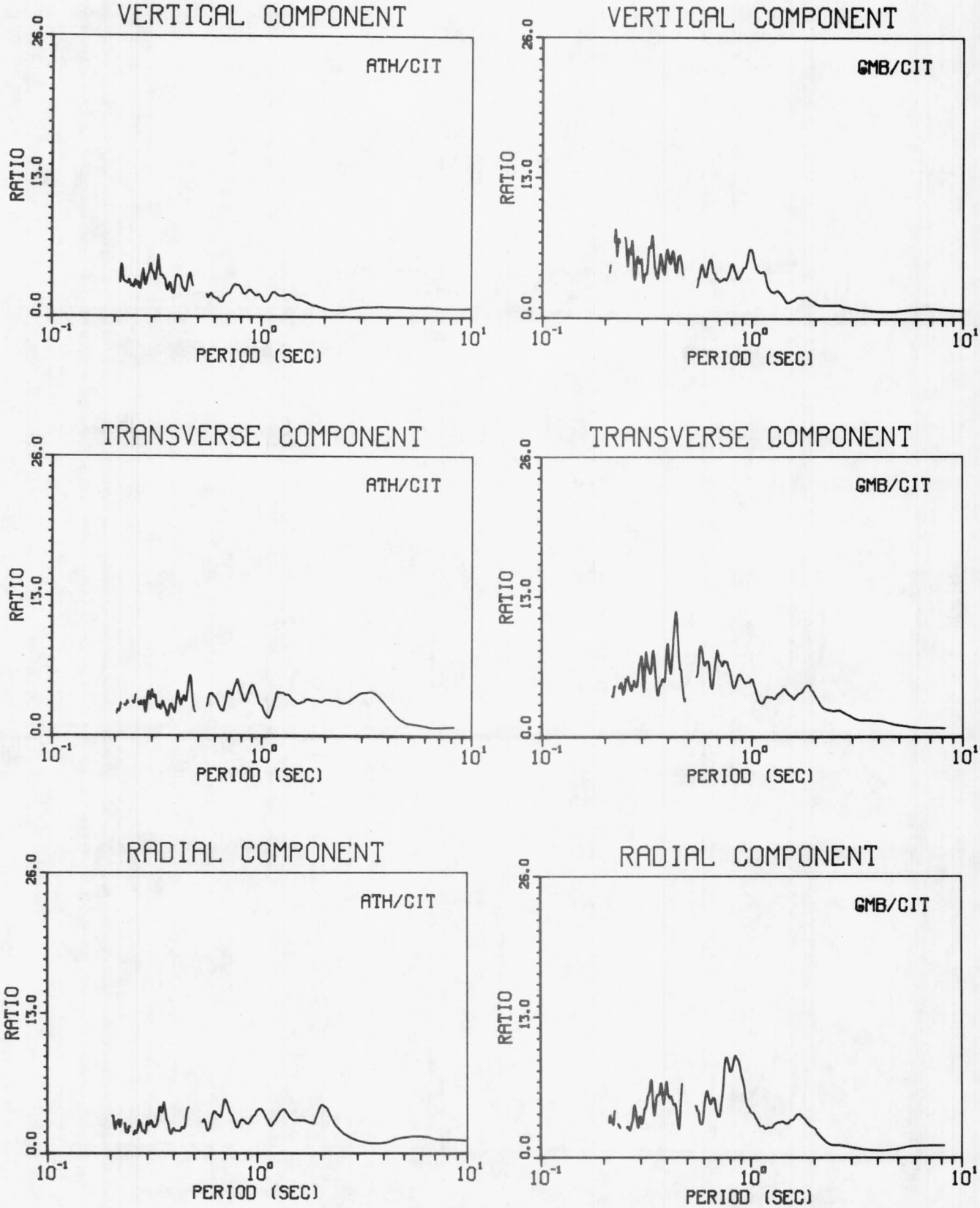

EVENT ICEBERG

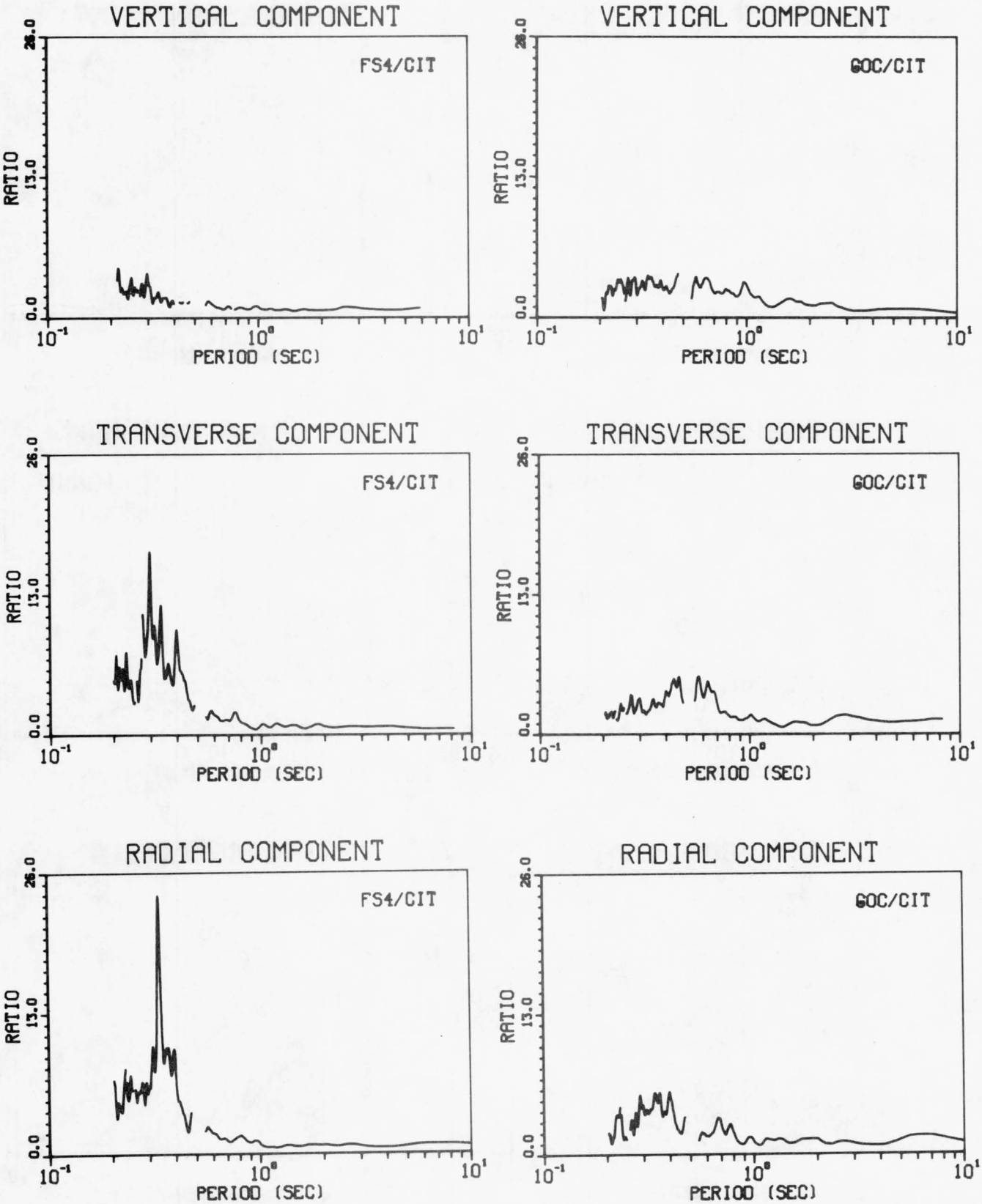

EVENT ICEBERG

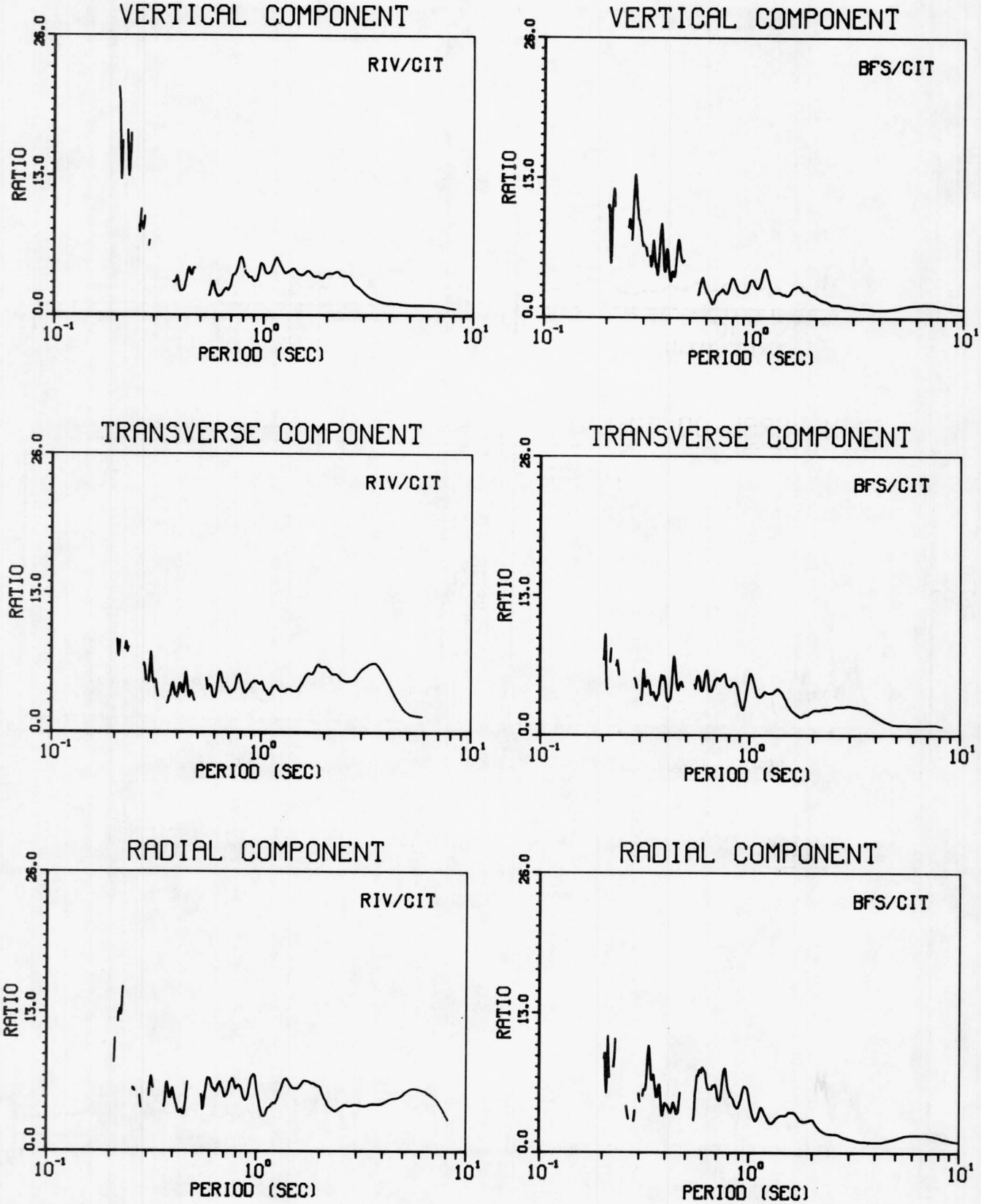

EVENT ICEBERG

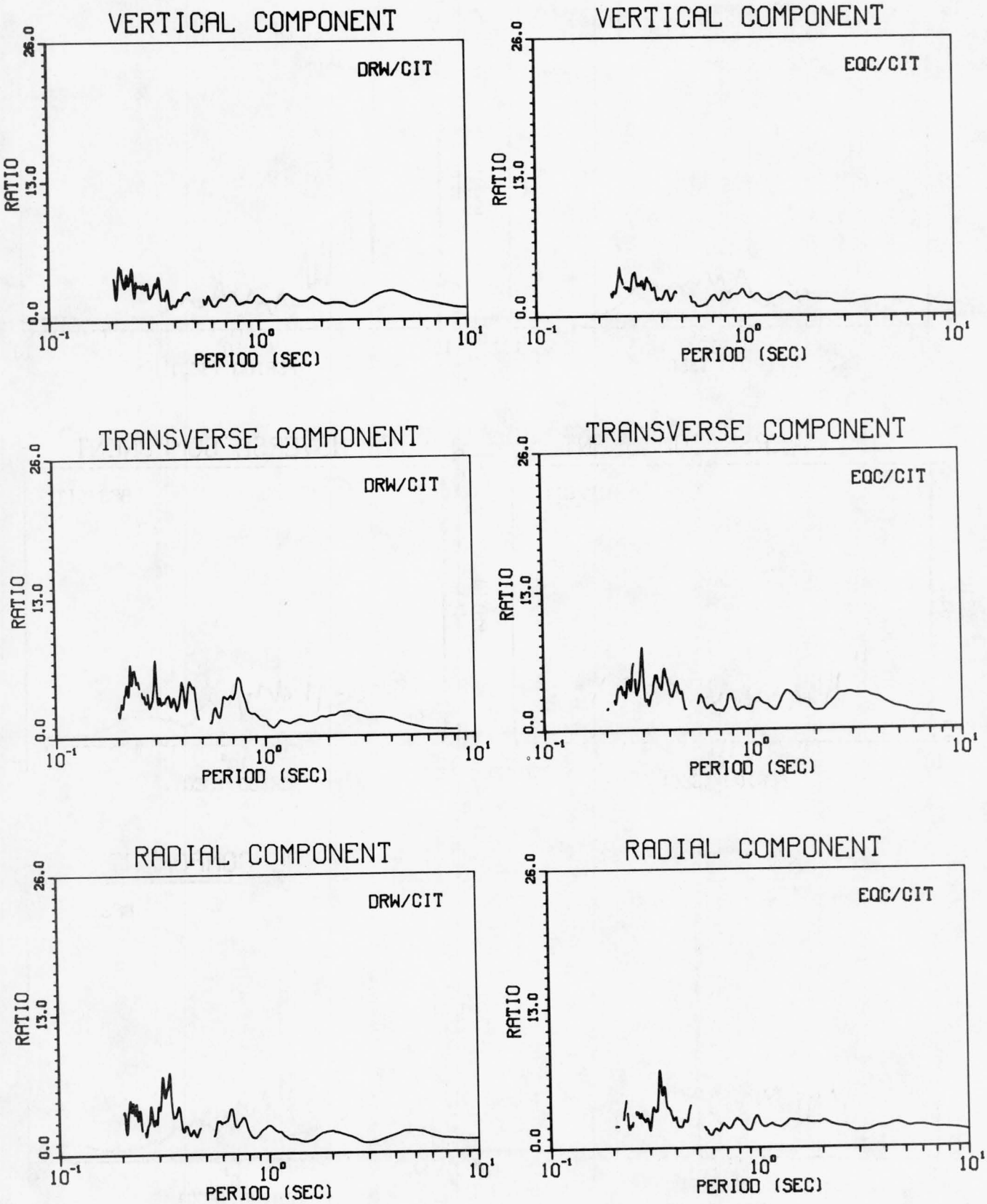

EVENT ICEBERG

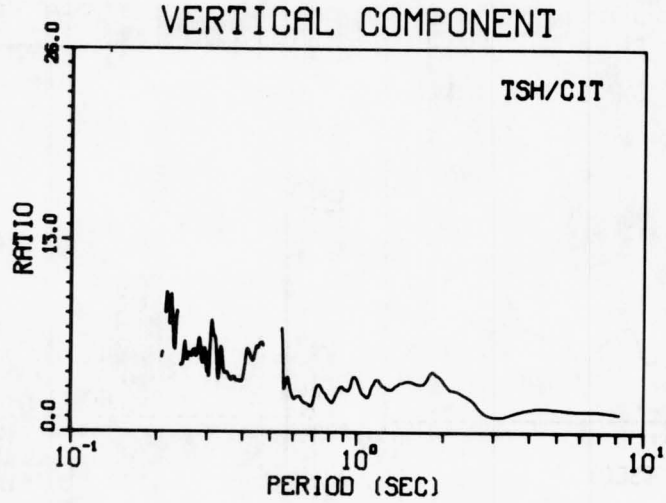

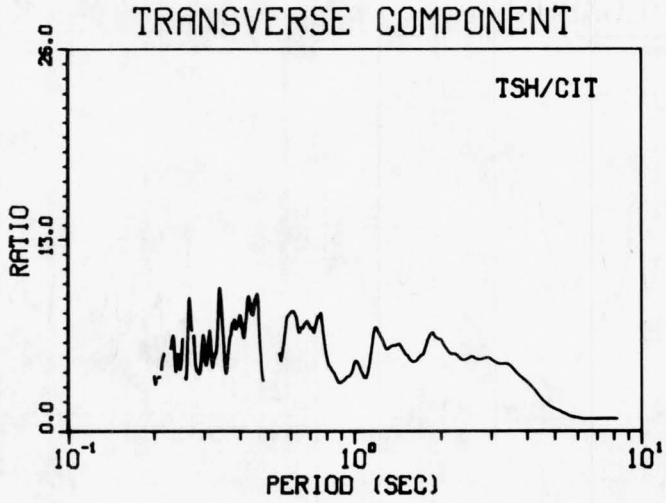

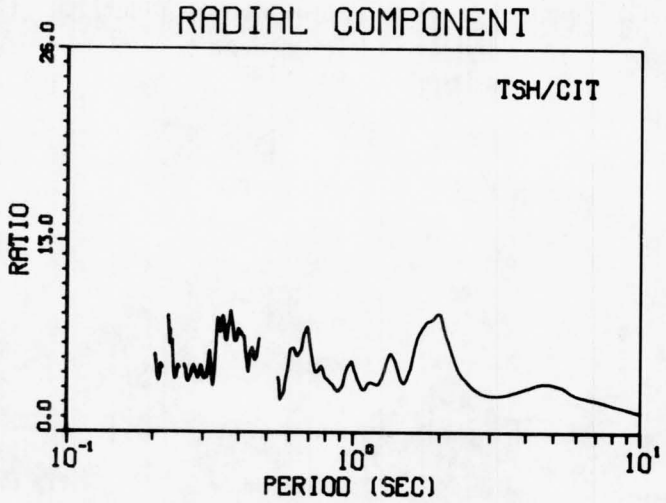

EVENT MAST

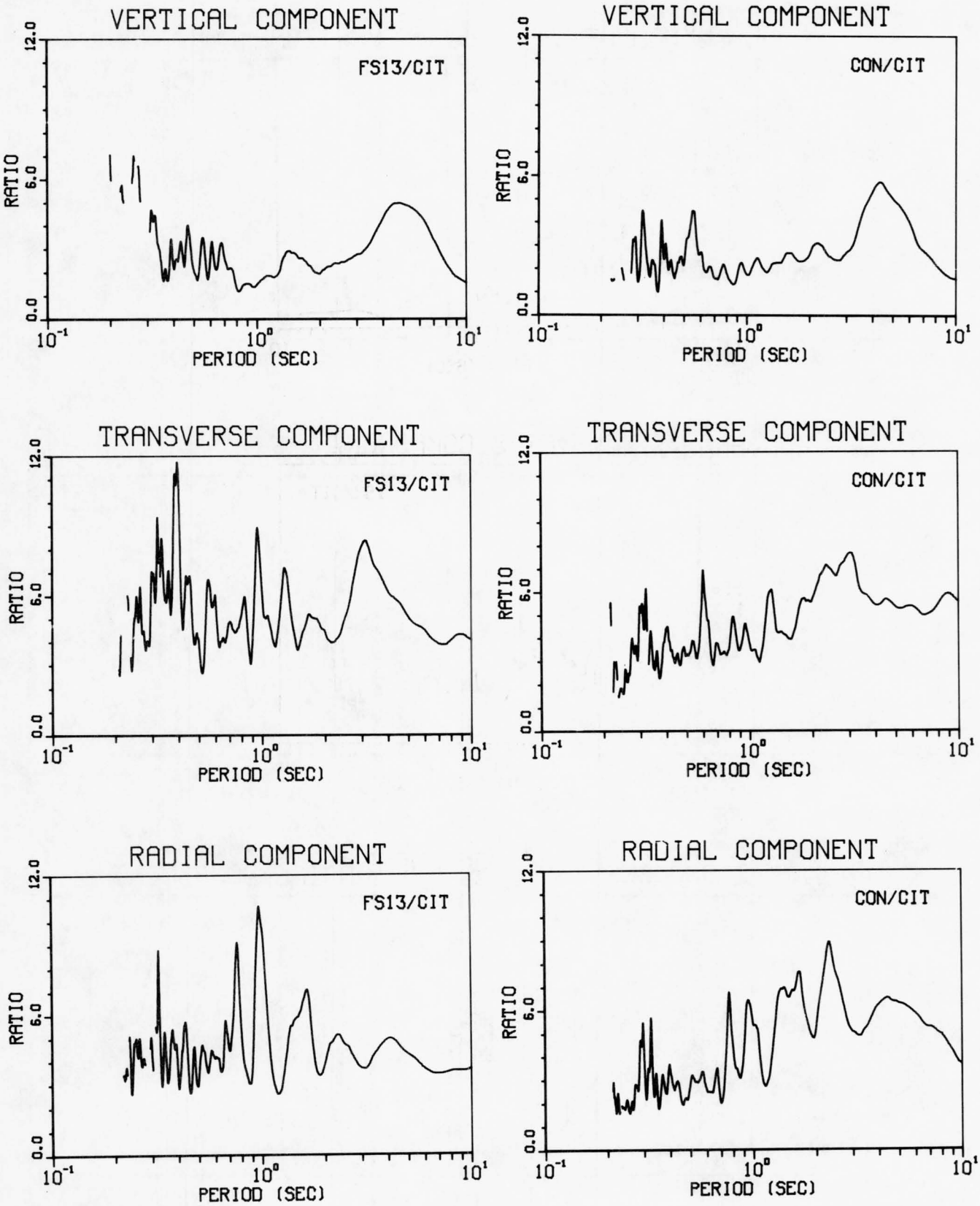
VERTICAL COMPONENT
FS13/CIT
RATIO
12.0
6.0
0.0
10^{-1}
10^{0}
10^{1}
PERIOD (SEC)
VERTICAL COMPONENT
CON/CIT
RATIO
12.0
6.0
0.0
10^{-1}
10^{0}
10^{1}
PERIOD (SEC)
TRANSVERSE COMPONENT
FS13/CIT
RATIO
12.0
6.0
0.0
10^{-1}
10^{0}
10^{1}
PERIOD (SEC)
TRANSVERSE COMPONENT
CON/CIT
RATIO
12.0
6.0
0.0
10^{-1}
10^{0}
10^{1}
PERIOD (SEC)
RADIAL COMPONENT
FS13/CIT
RATIO
12.0
6.0
0.0
10^{-1}
10^{0}
10^{1}
PERIOD (SEC)
RADIAL COMPONENT
CON/CIT
RATIO
12.0
6.0
0.0
10^{-1}
10^{0}
10^{1}
PERIOD (SEC)

EVENT MAST

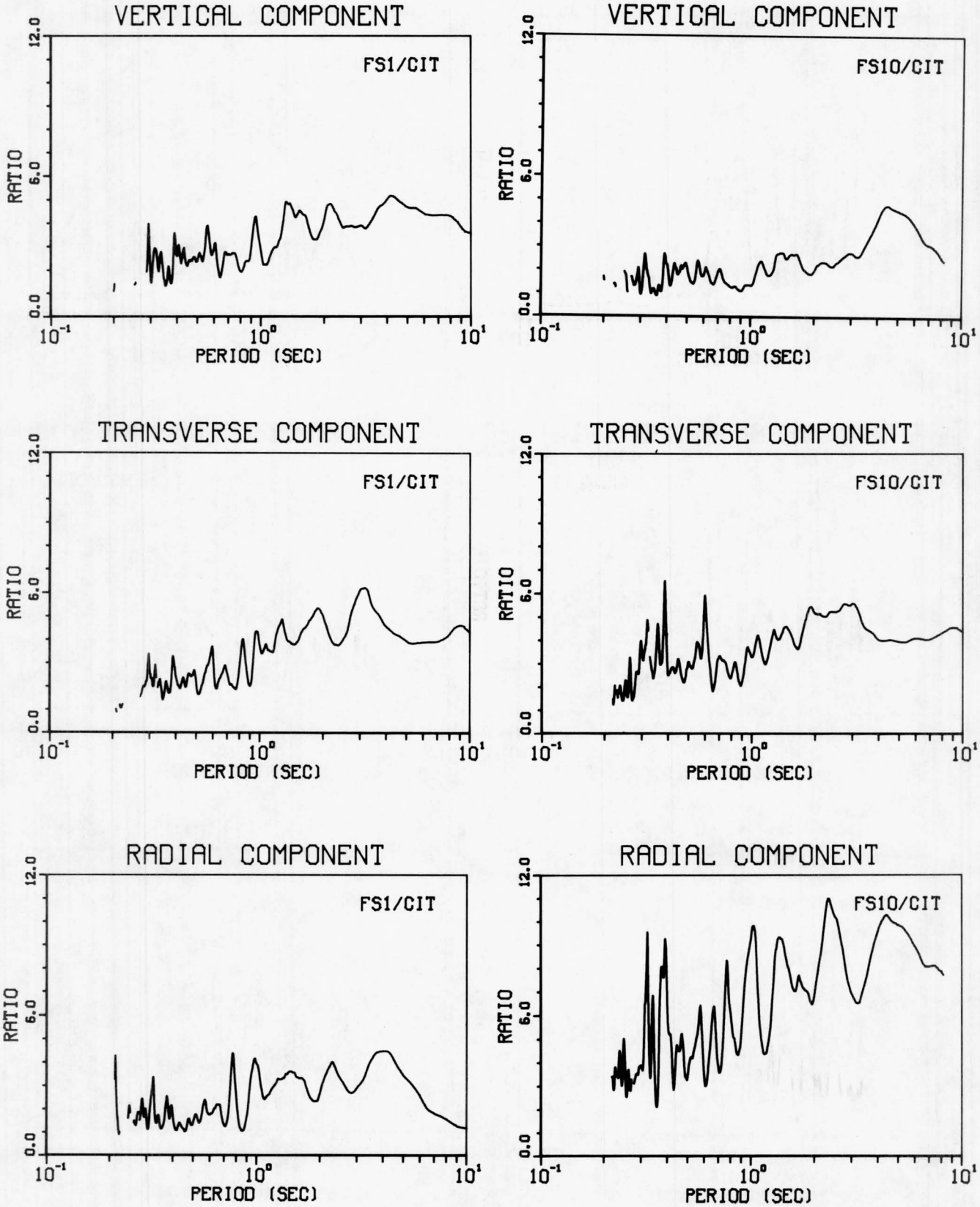
VERTICAL COMPONENT
FS1/CIT
VERTICAL COMPONENT
FS10/CIT
TRANSVERSE COMPONENT
FS1/CIT
TRANSVERSE COMPONENT
FS10/CIT
RADIAL COMPONENT
FS1/CIT
RADIAL COMPONENT
FS10/CIT
RATIO
12.0
6.0
0.0
10^{-1}
10^{0}
10^{1}
PERIOD (SEC)

EVENT MUENSTER

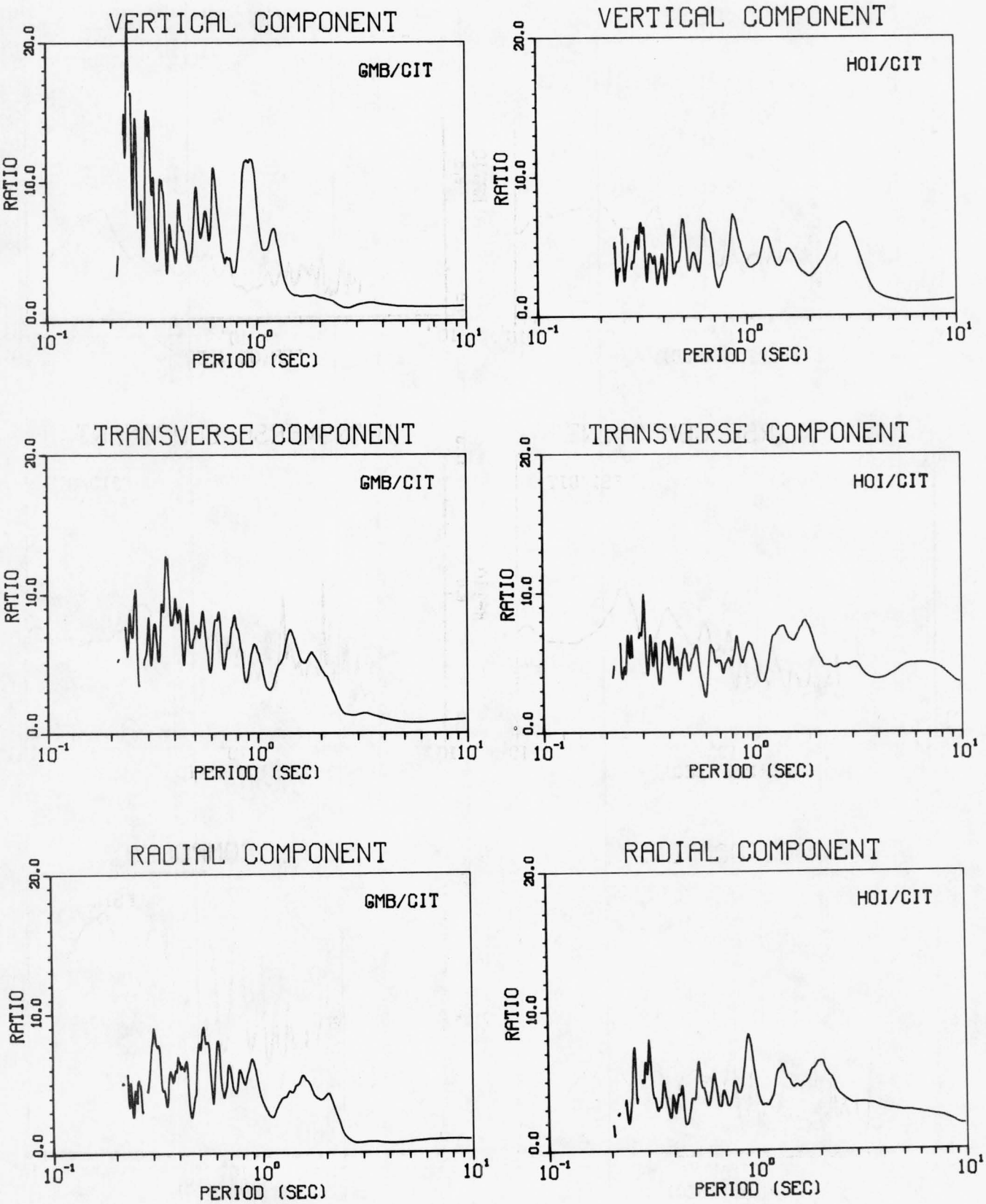

EVENT MUENSTER

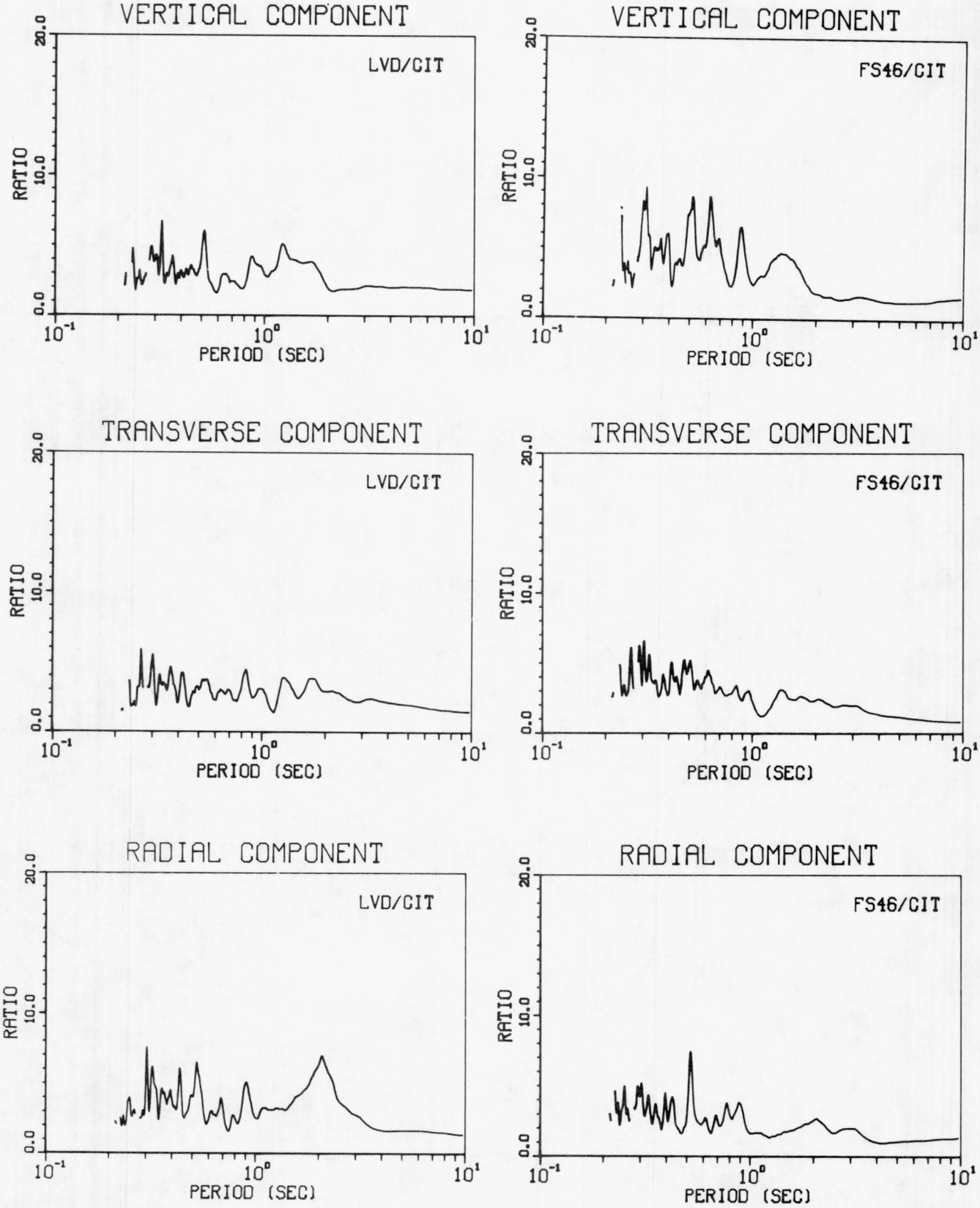

EVENT MUENSTER

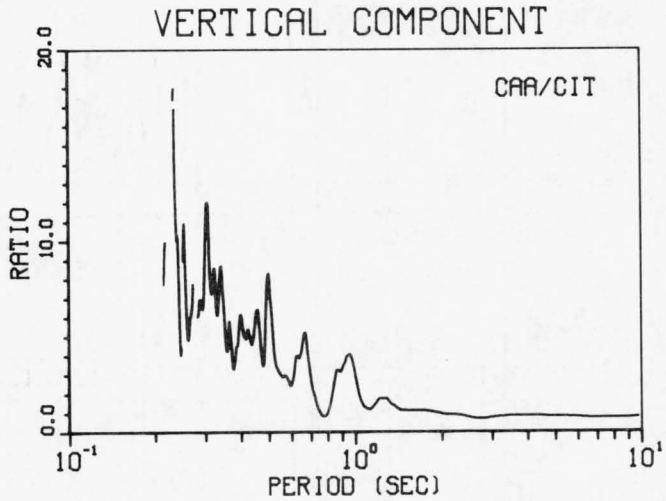

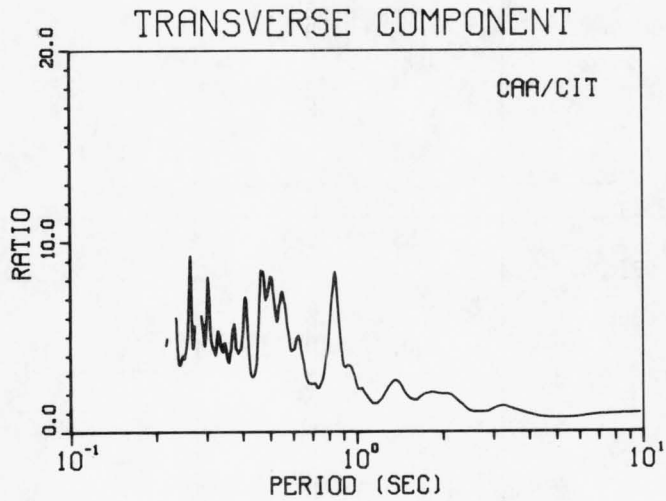

EVENT PEPATO

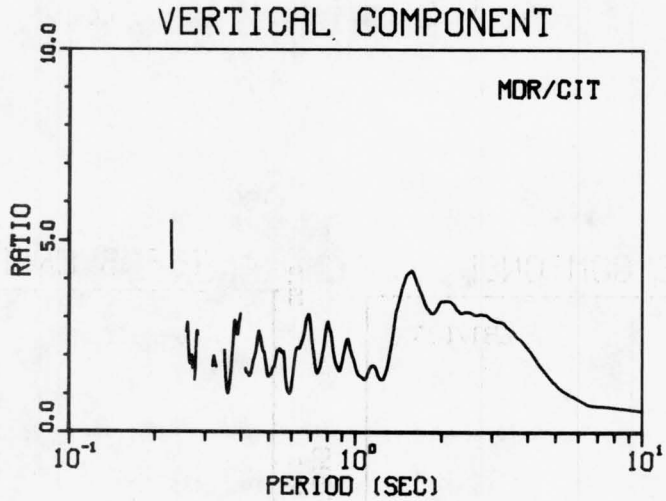

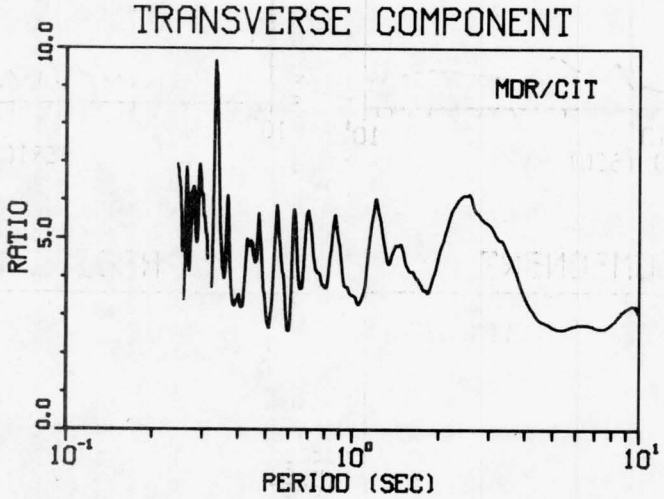

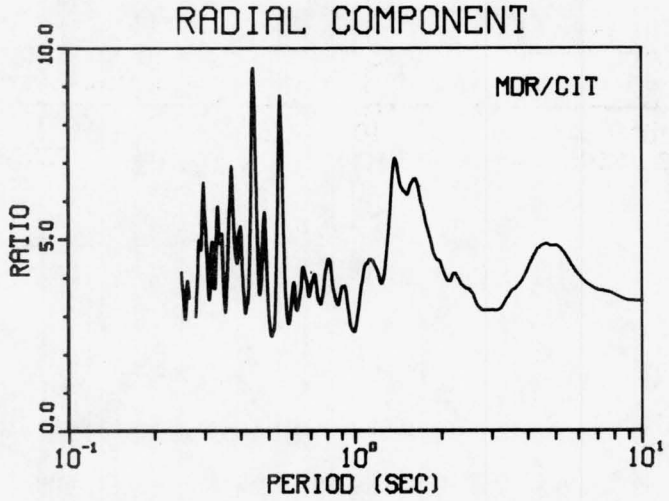

EVENT POOL

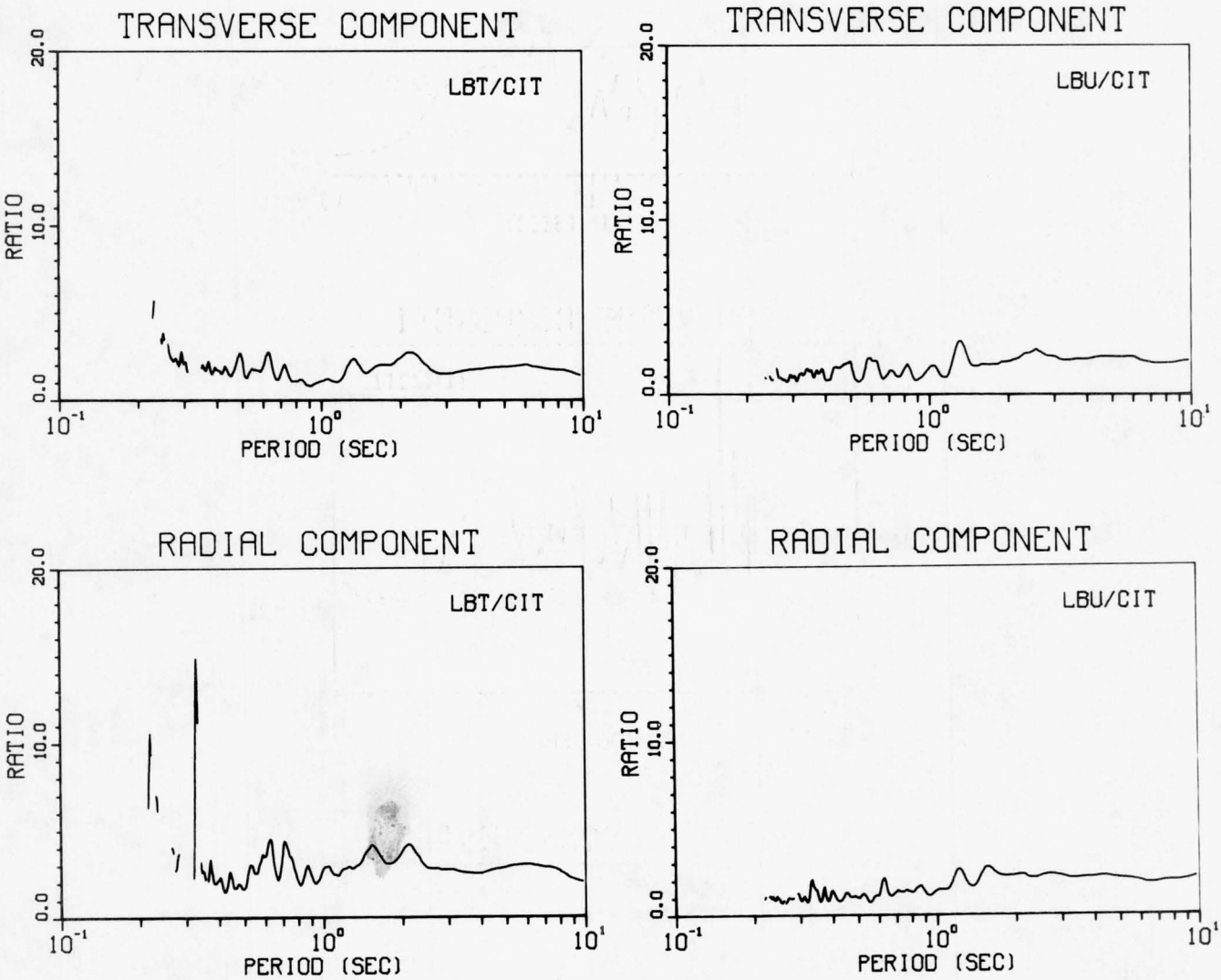
TRANSVERSE COMPONENT
LBT/CIT
RATIO
20.0
10.0
0.0
10^{-1}
10^{0}
10^{1}
PERIOD (SEC)
TRANSVERSE COMPONENT
LBU/CIT
RATIO
20.0
10.0
0.0
10^{-1}
10^{0}
10^{1}
PERIOD (SEC)
RADIAL COMPONENT
LBT/CIT
RATIO
20.0
10.0
0.0
10^{-1}
10^{0}
10^{1}
PERIOD (SEC)
RADIAL COMPONENT
LBU/CIT
RATIO
20.0
10.0
0.0
10^{-1}
10^{0}
10^{1}
PERIOD (SEC)

EVENT POOL

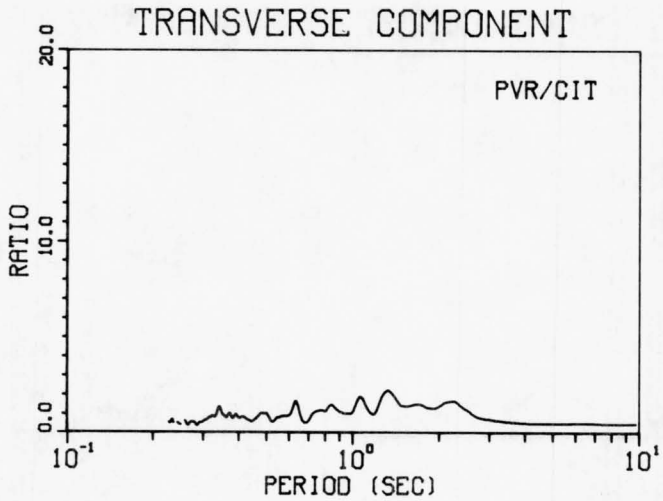
TRANSVERSE COMPONENT
PVR/CIT
RATIO
20.0
10.0
0.0
10^{-1}
10^{0}
10^{1}
PERIOD (SEC)

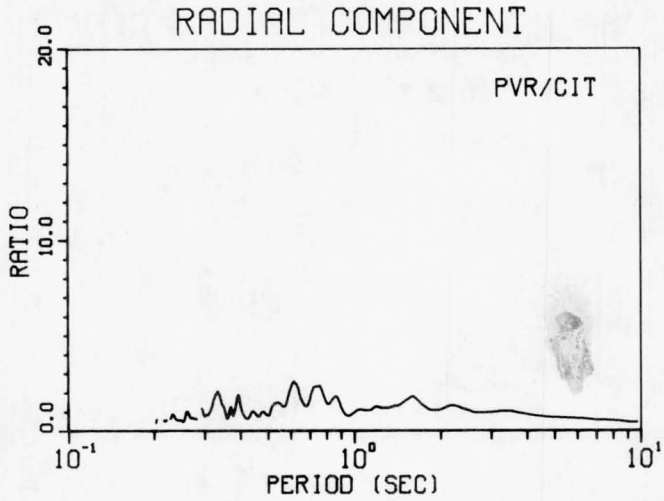
RADIAL COMPONENT
PVR/CIT
RATIO
20.0
10.0
0.0
10^{-1}
10^{0}
10^{1}
PERIOD (SEC)

EVENT RUDDER

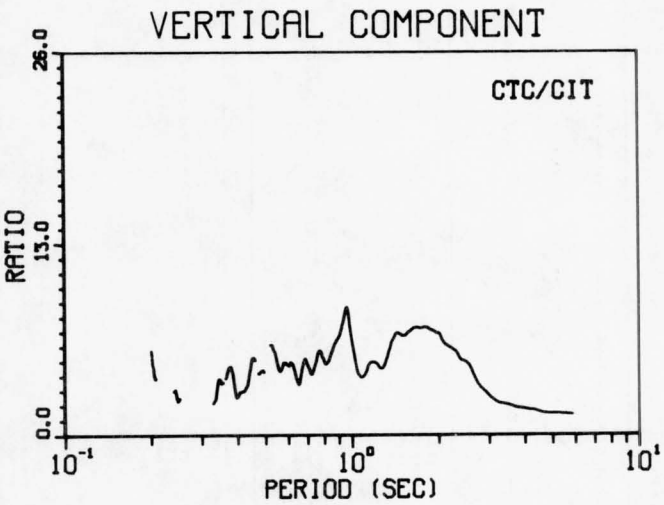

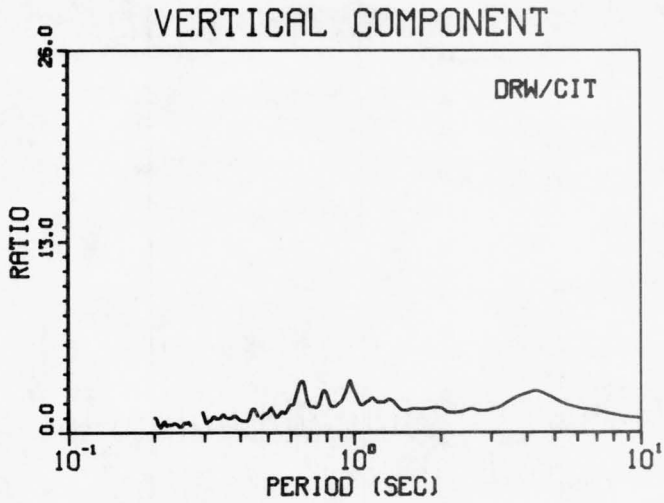

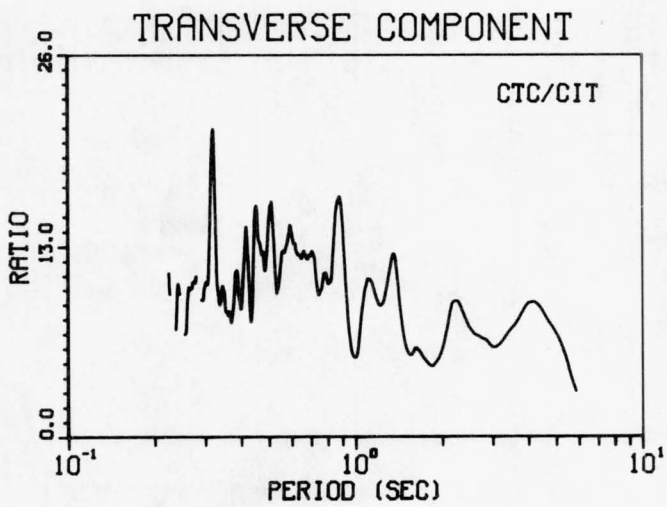

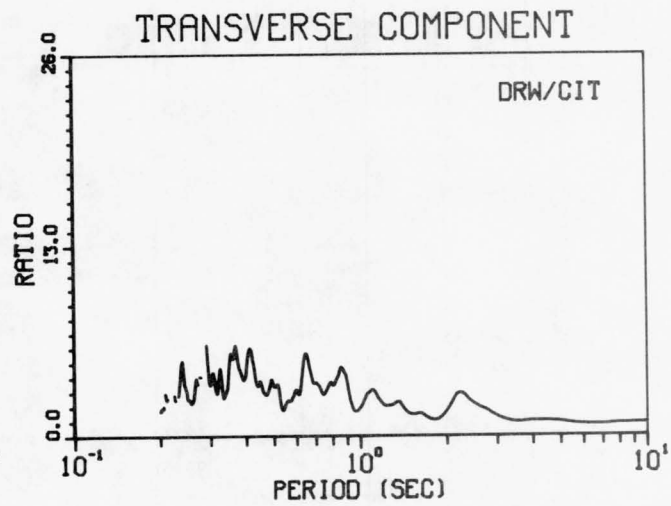

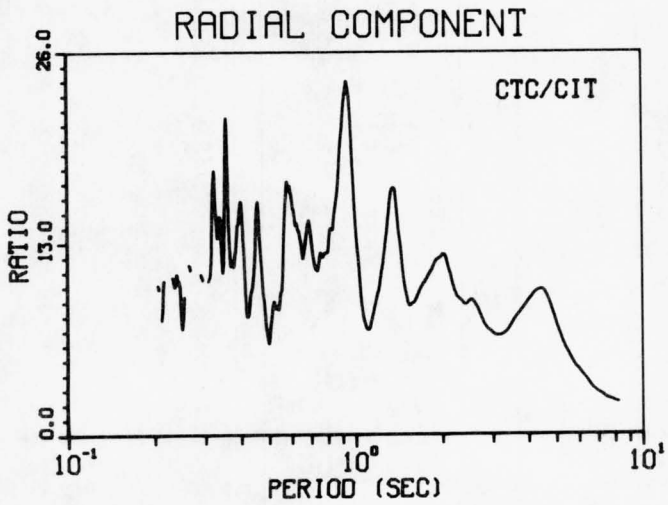

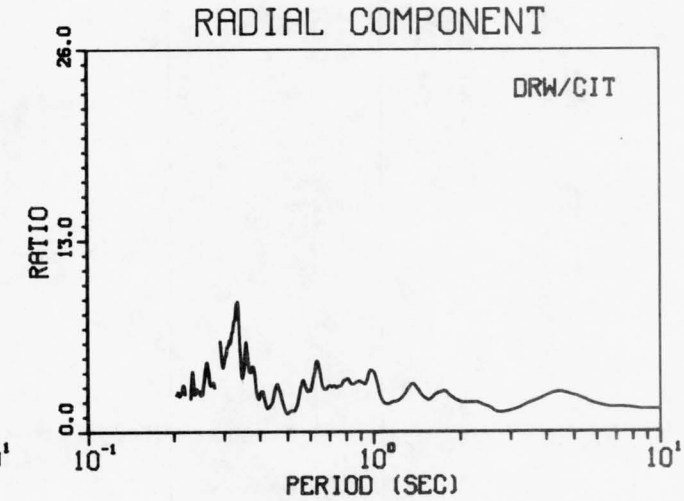

EVENT RUDDER

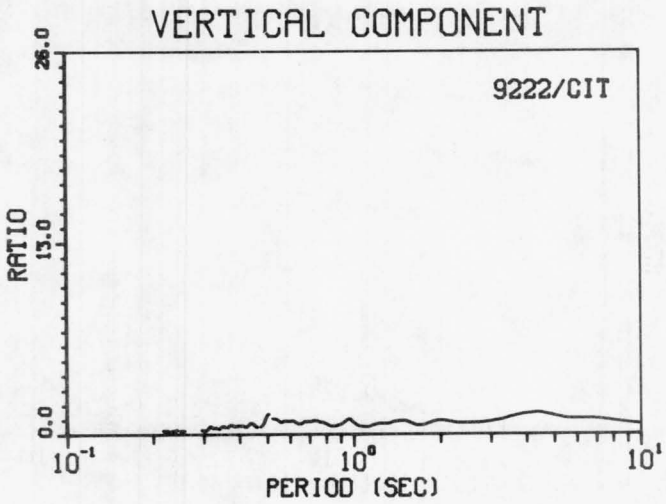

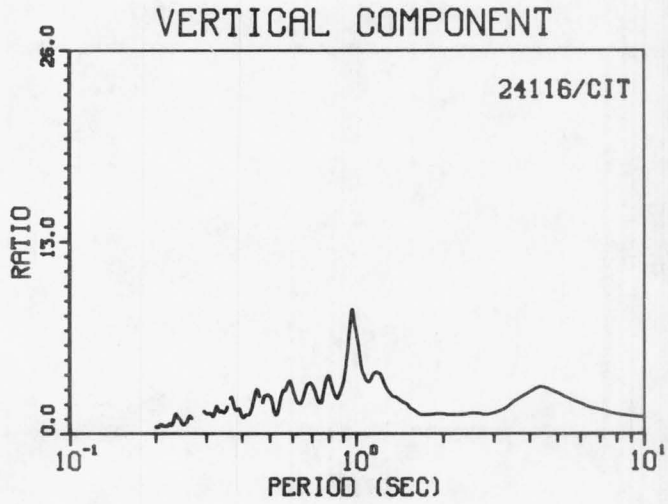

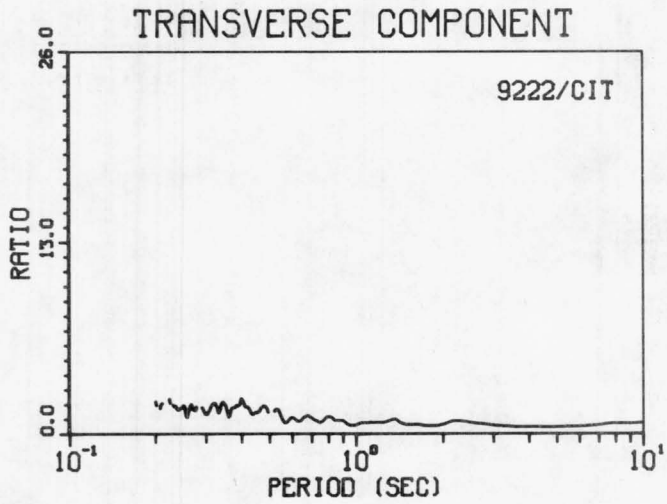

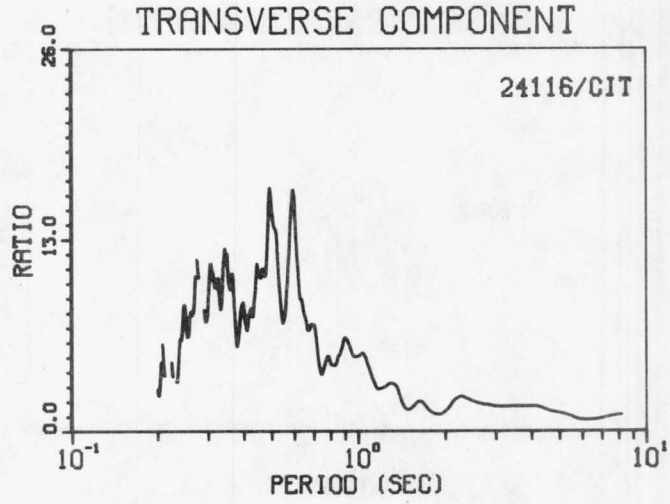

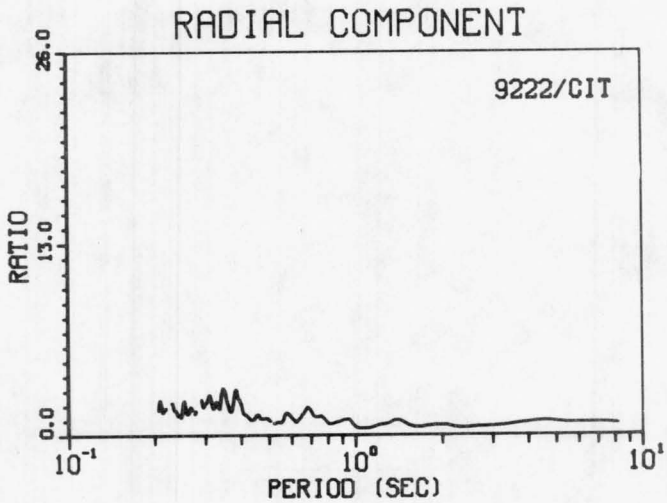

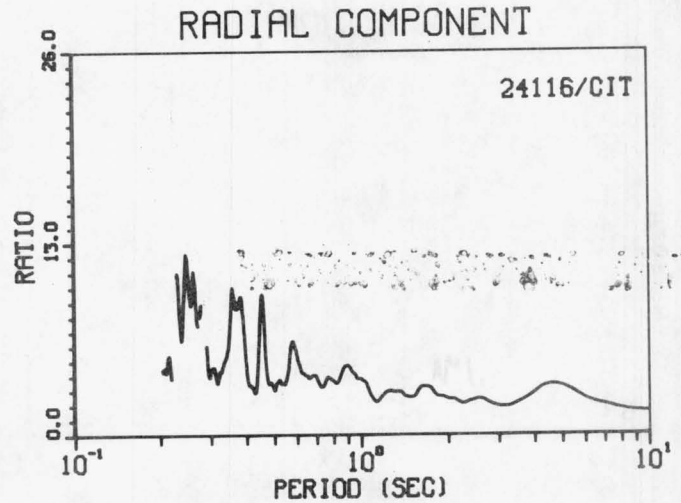

EVENT RUDDER

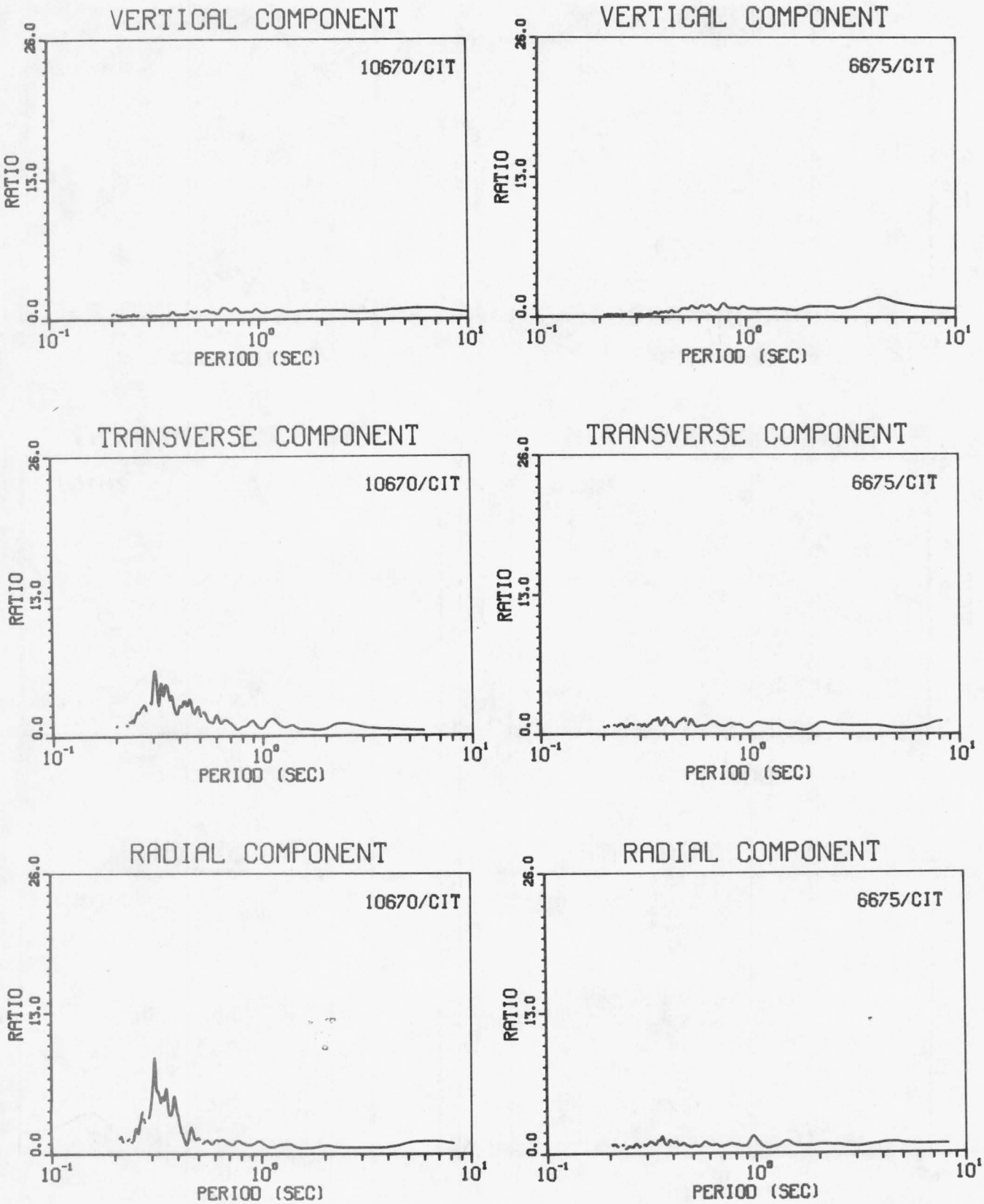

EVENT RUDDER

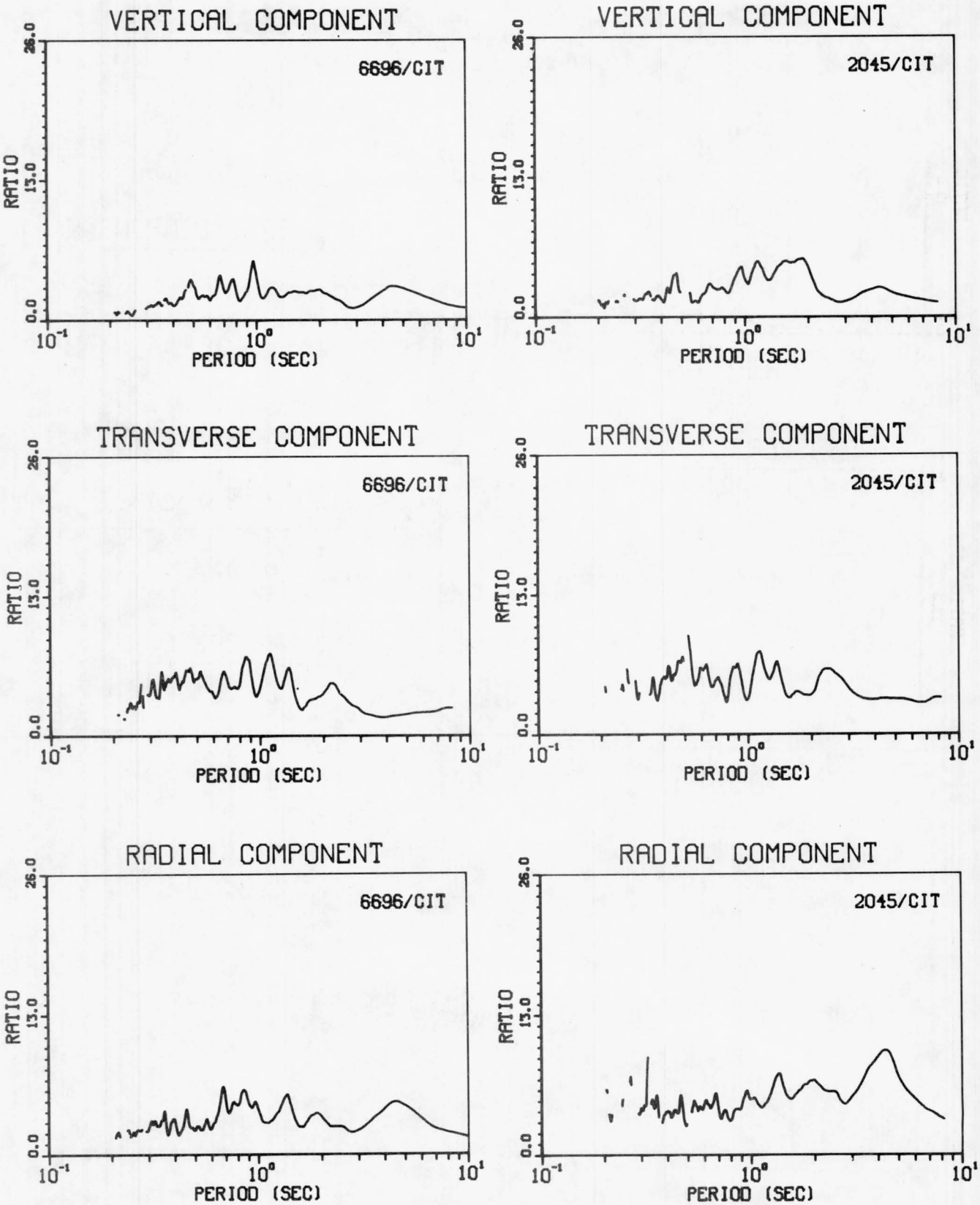

EVENT RUDDER

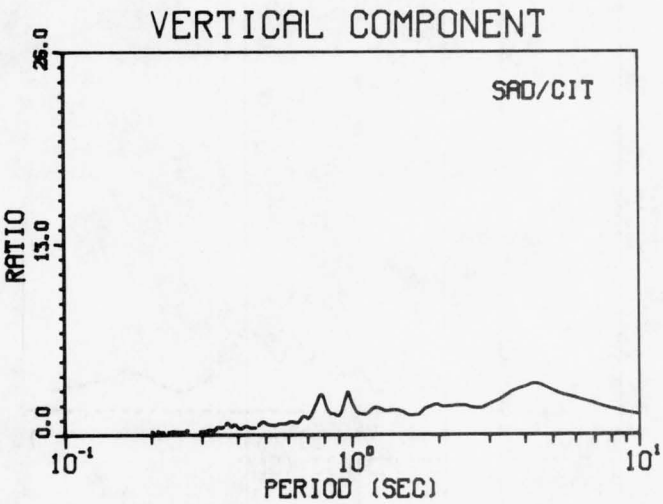

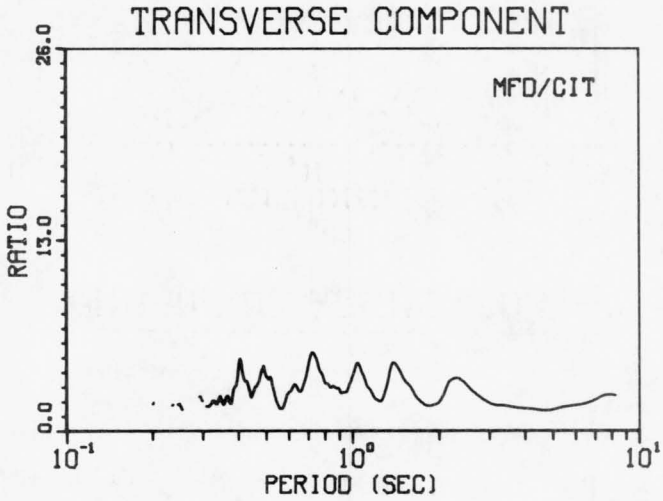

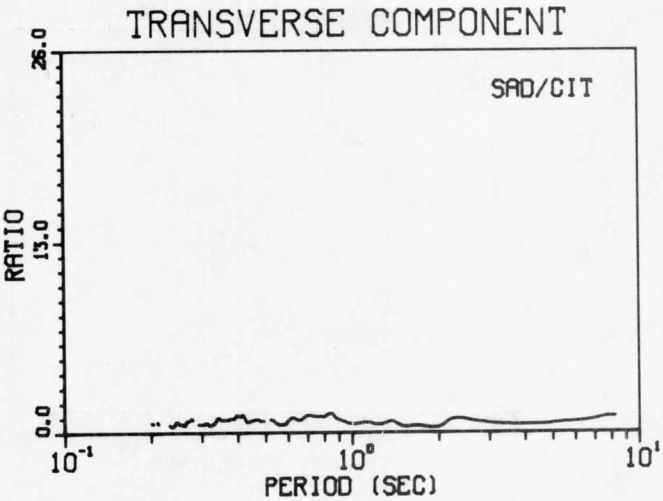

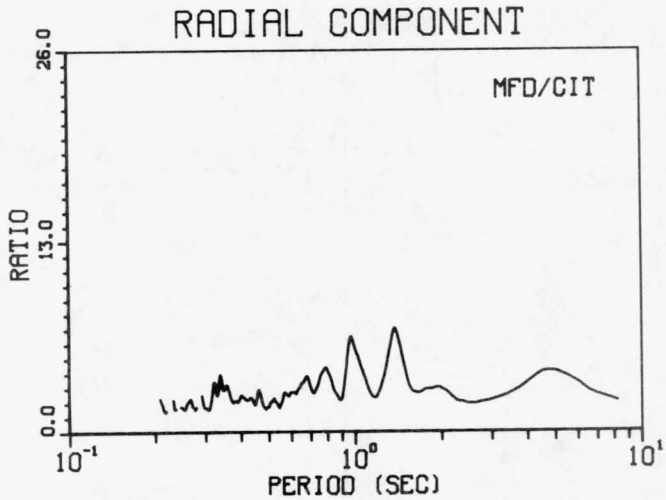

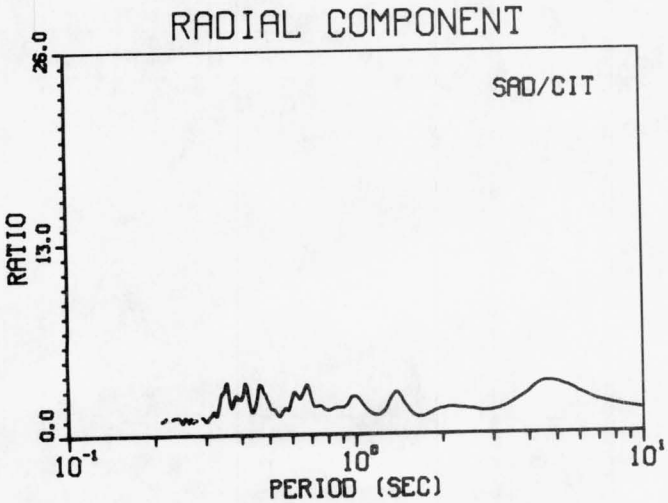

EVENT RUDDER

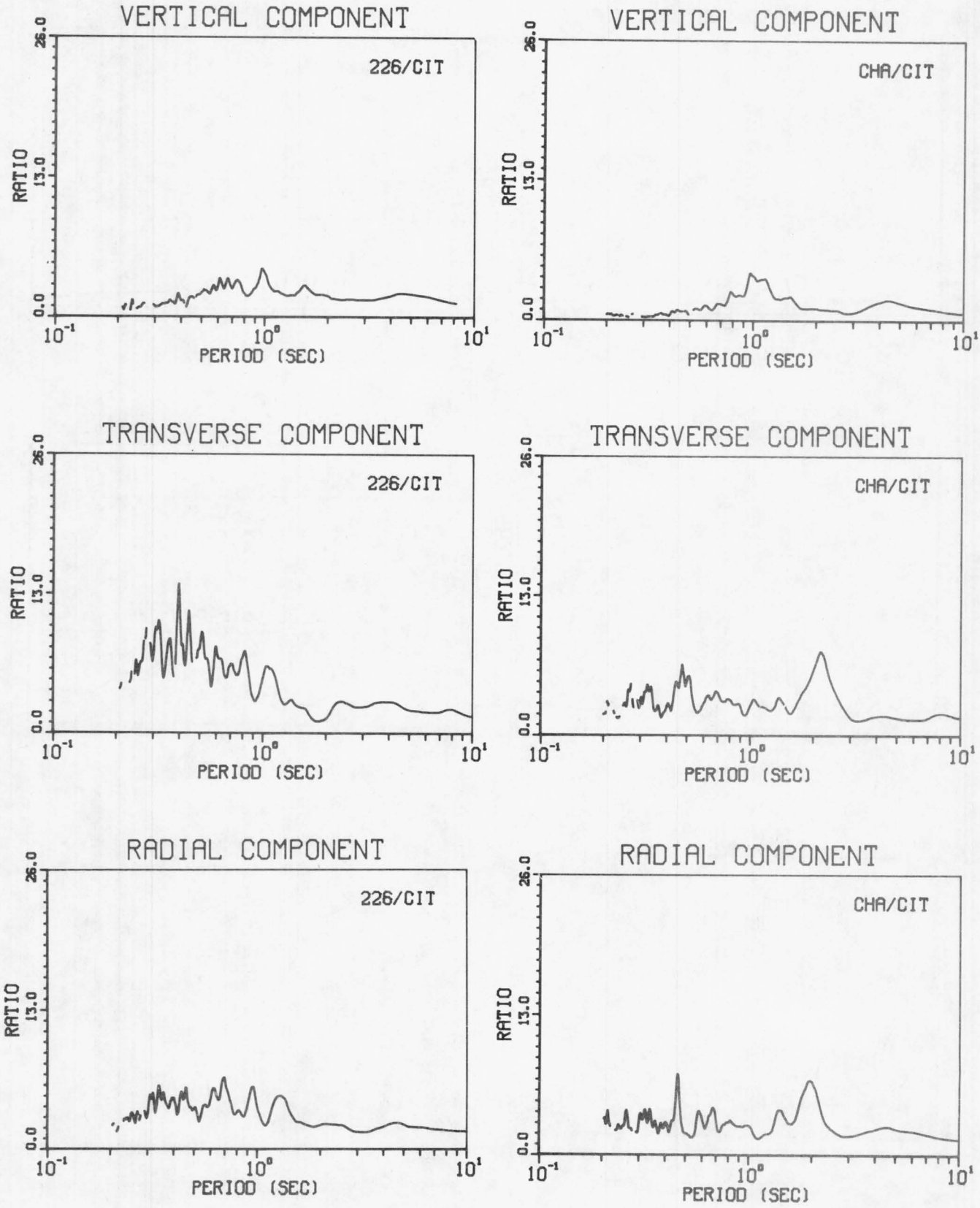

EVENT SCANTLING

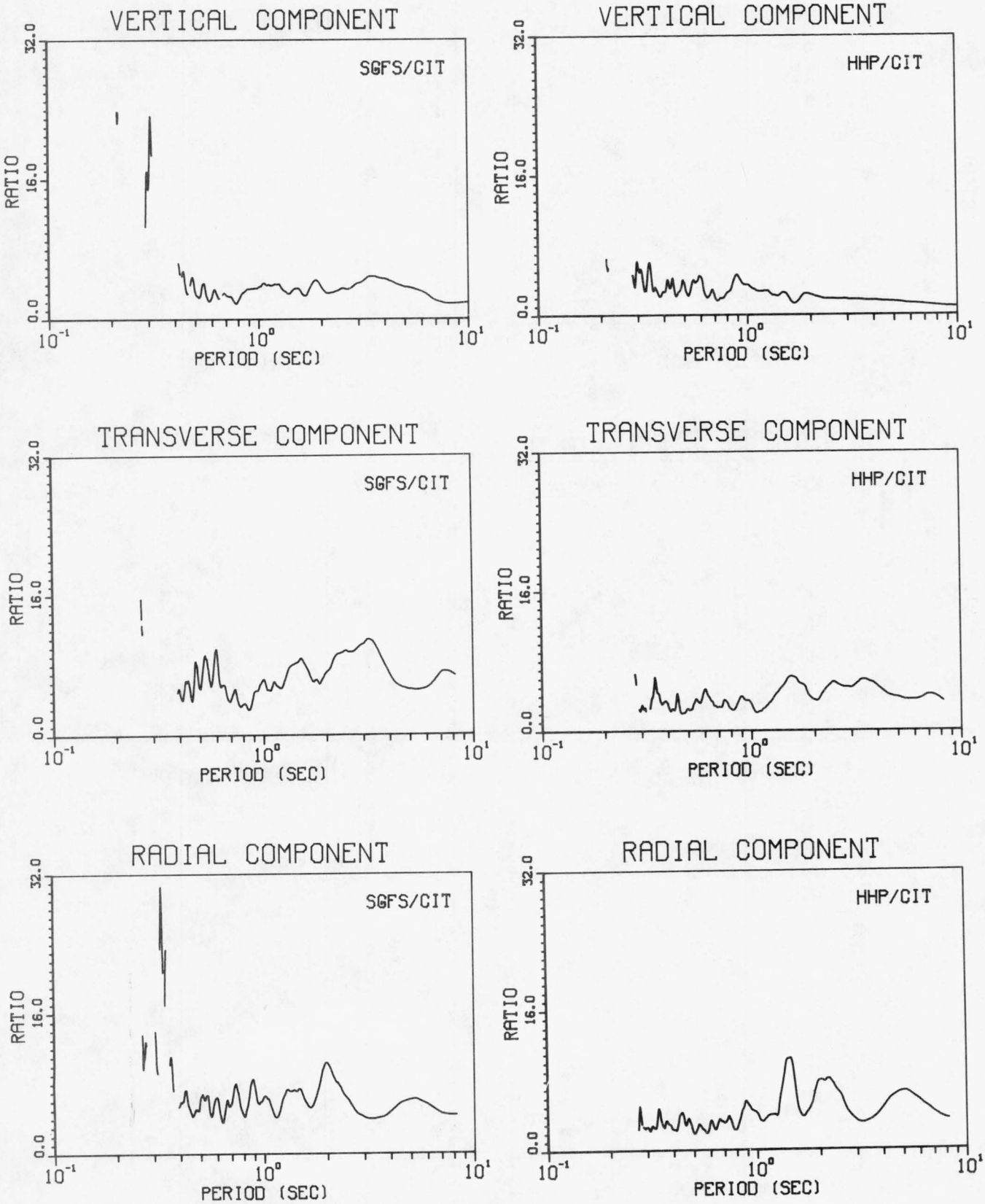

EVENT SCANTLING

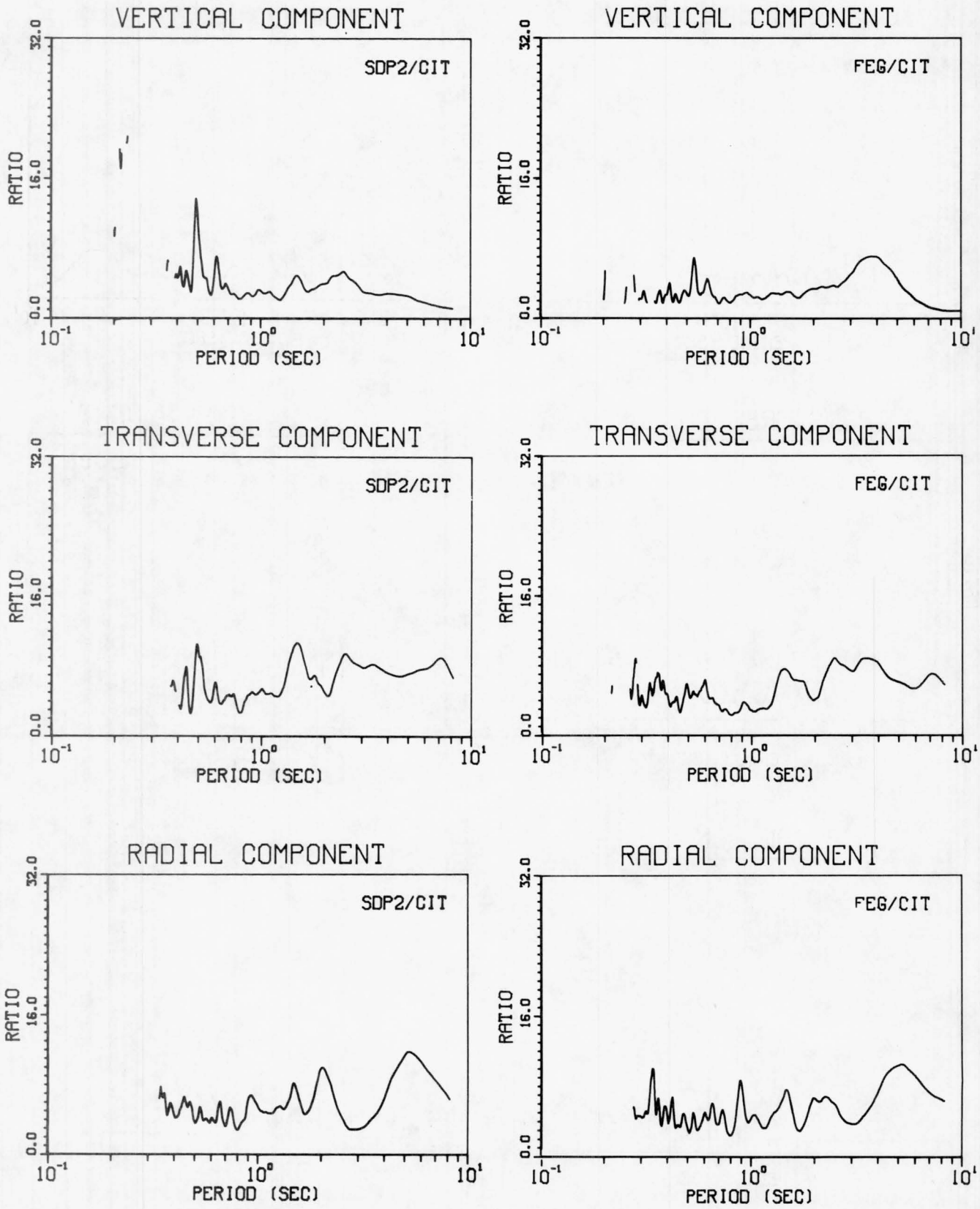

EVENT SCANTLING

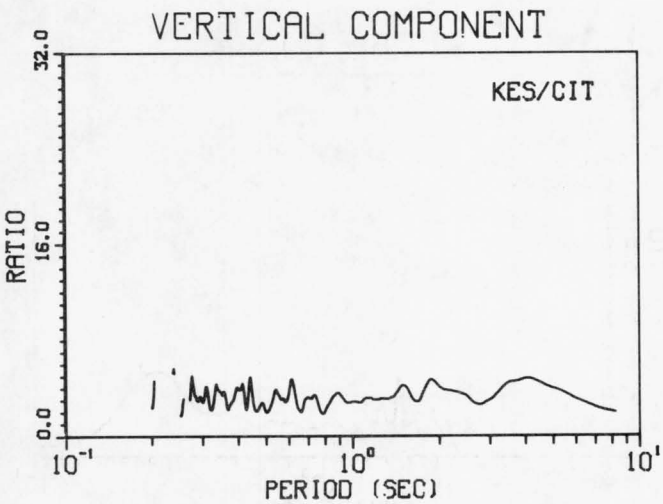

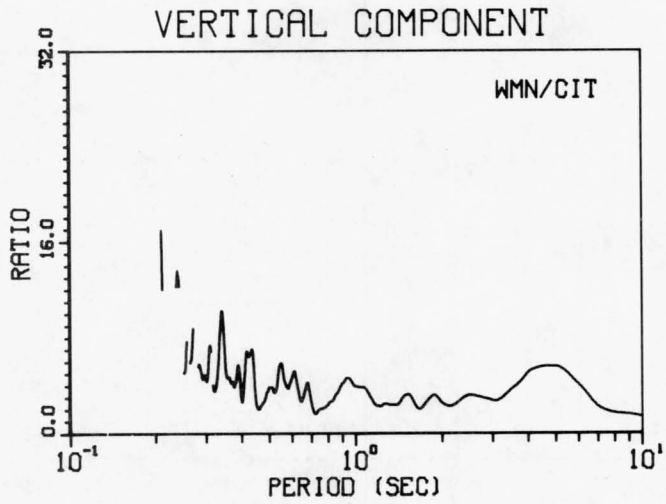

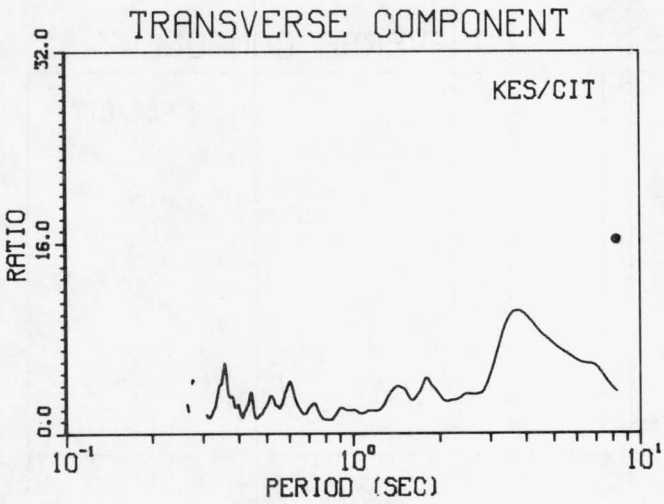

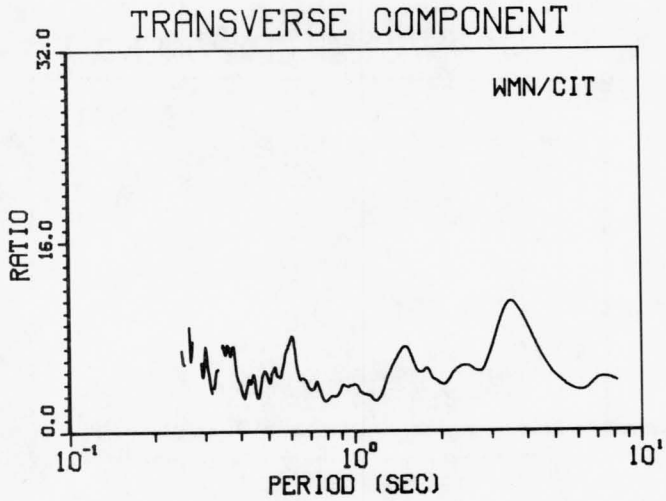

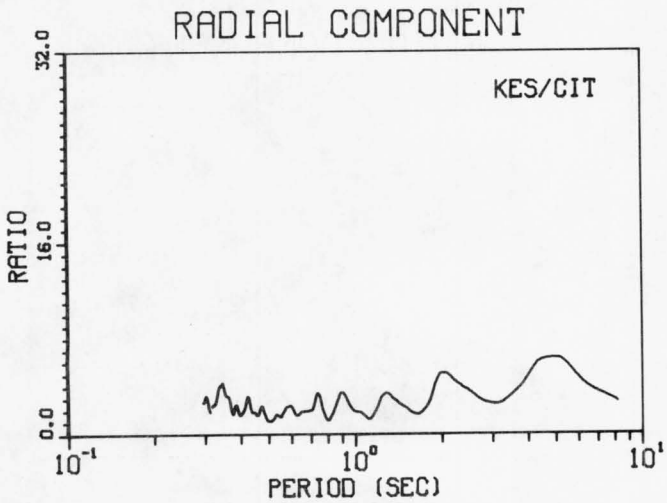

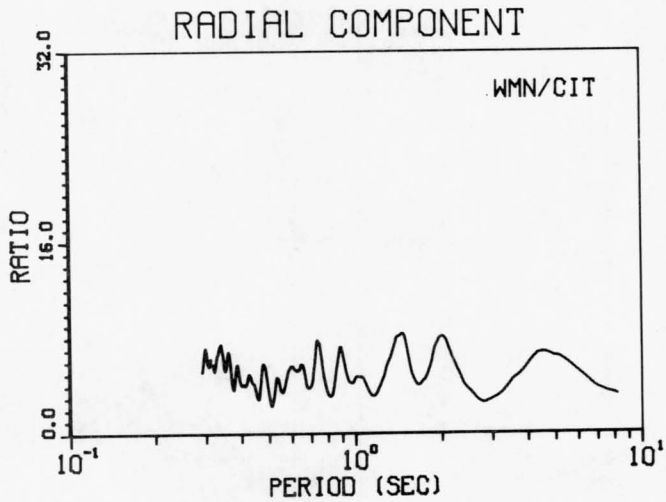

EVENT SCANTLING

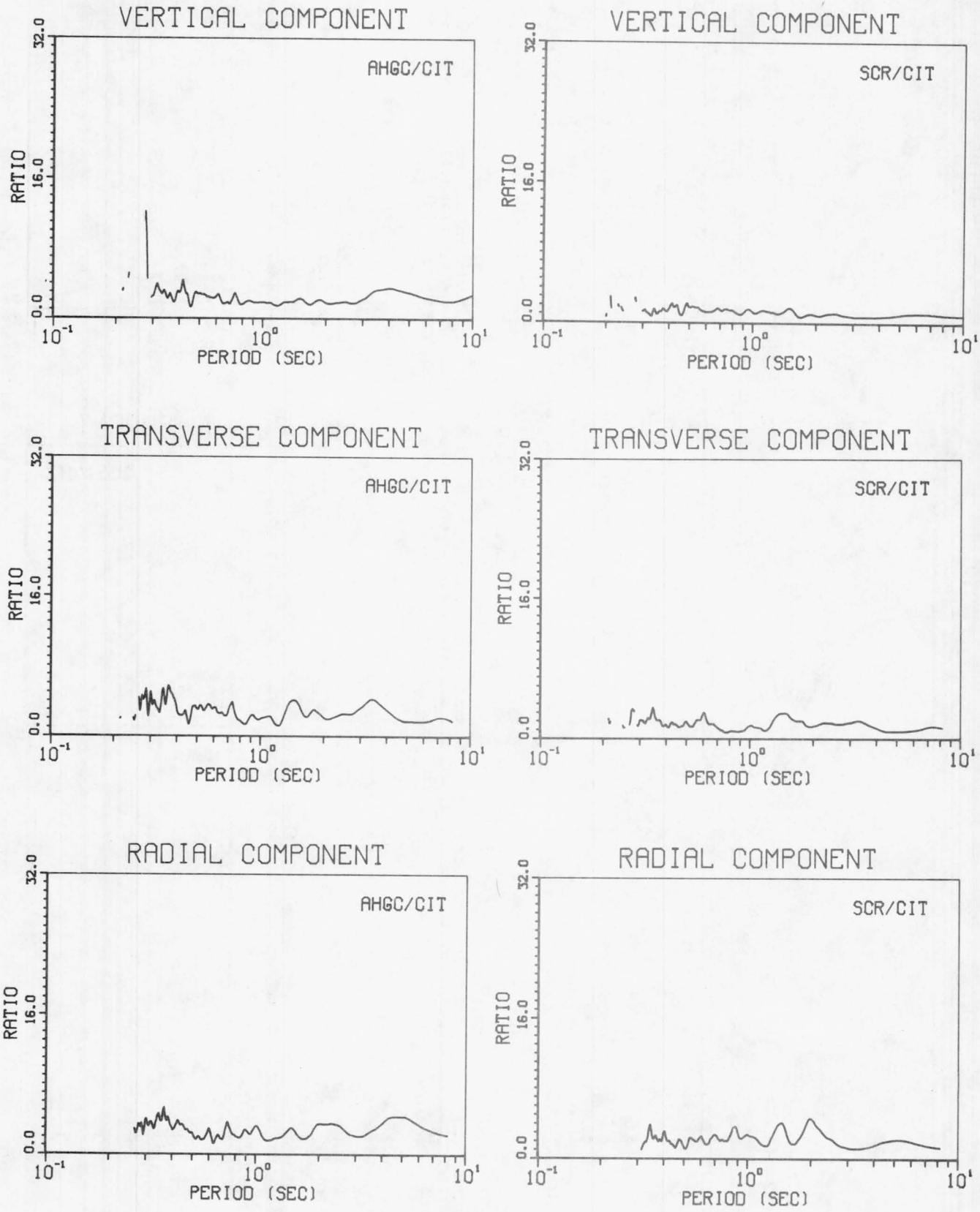

EVENT SCANTLING

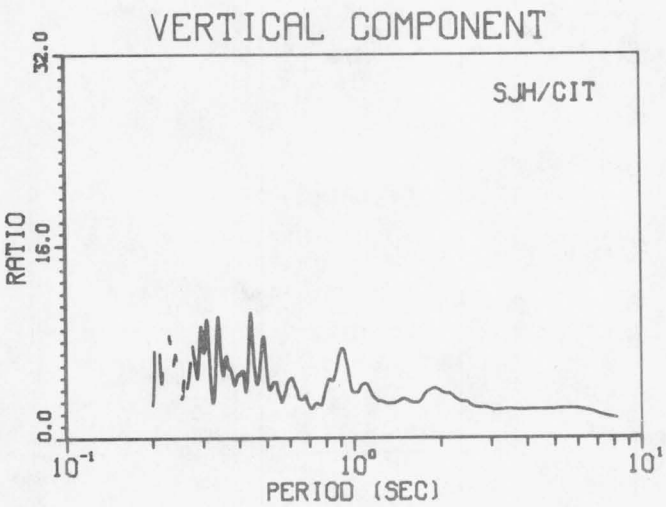

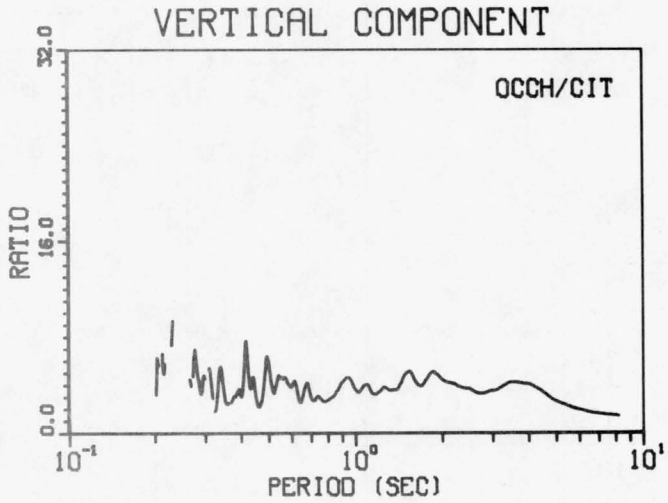

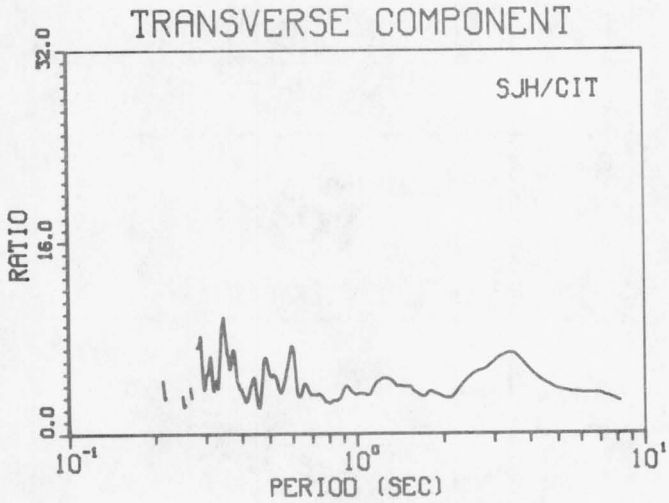

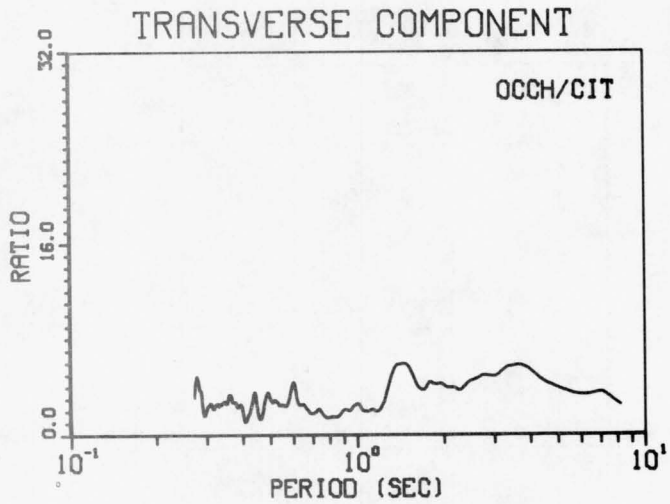

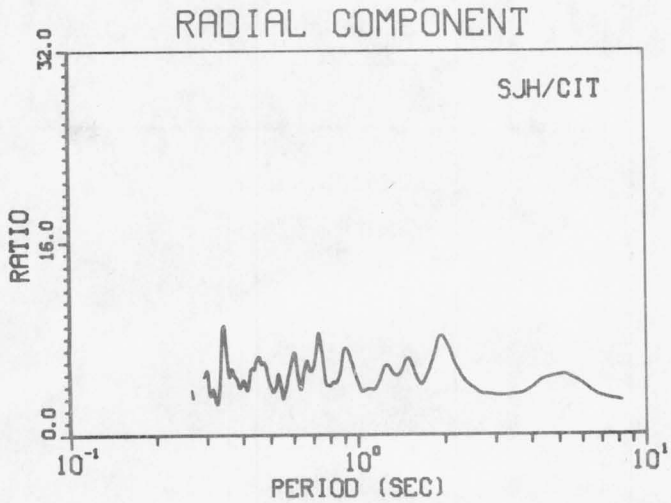

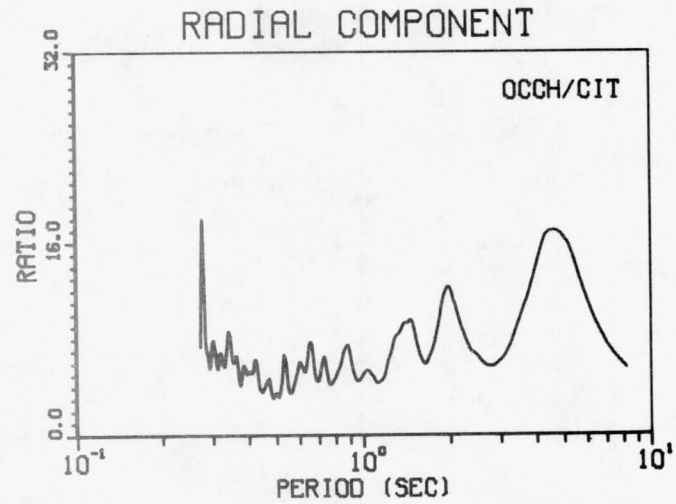

EVENT STRAIT

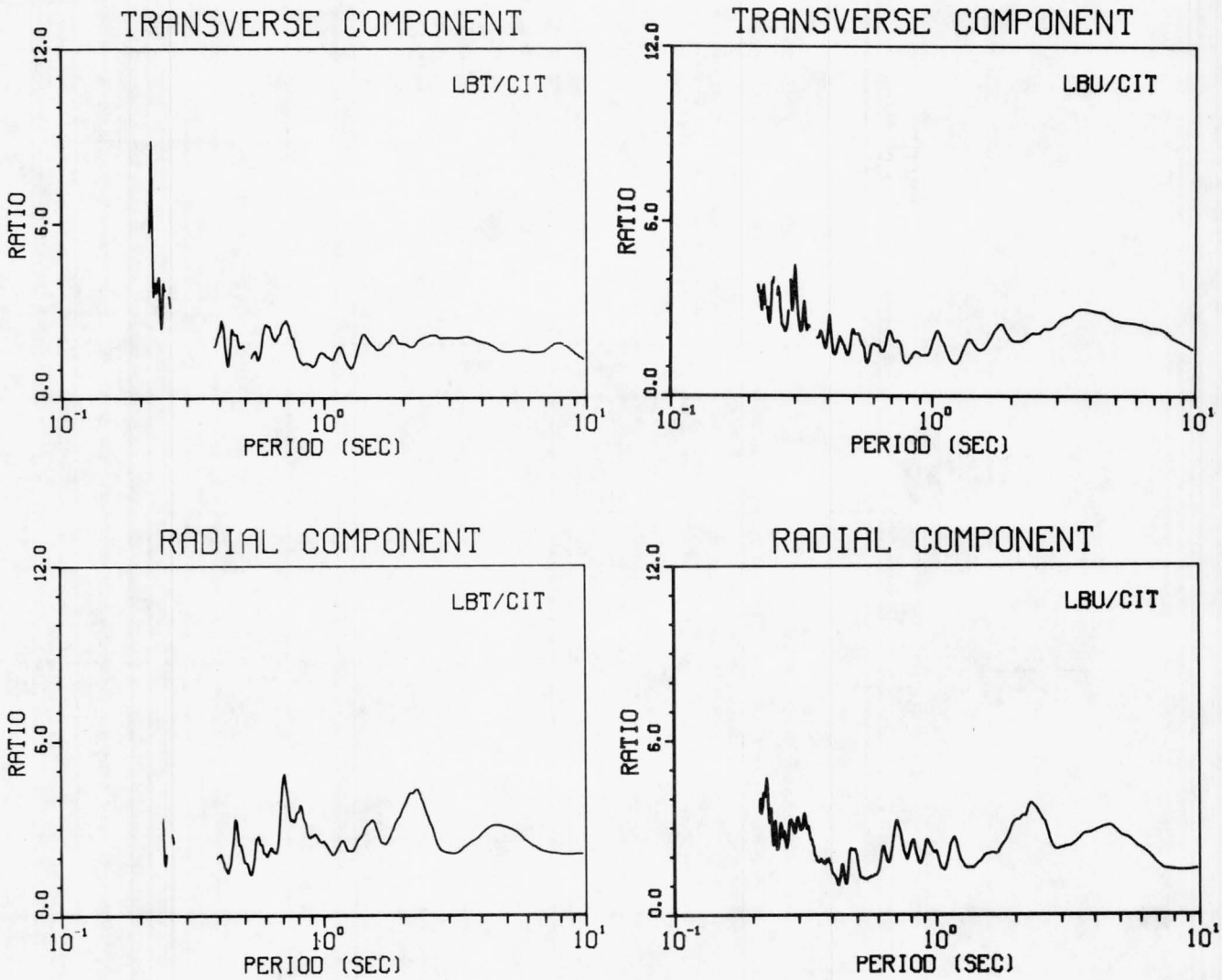

EVENT STRAIT

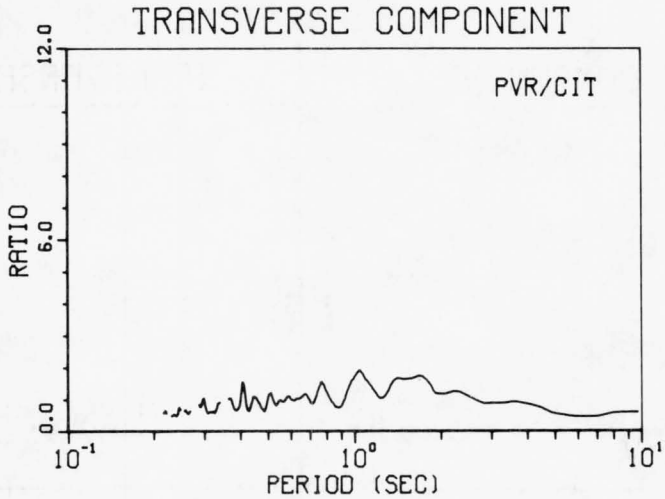

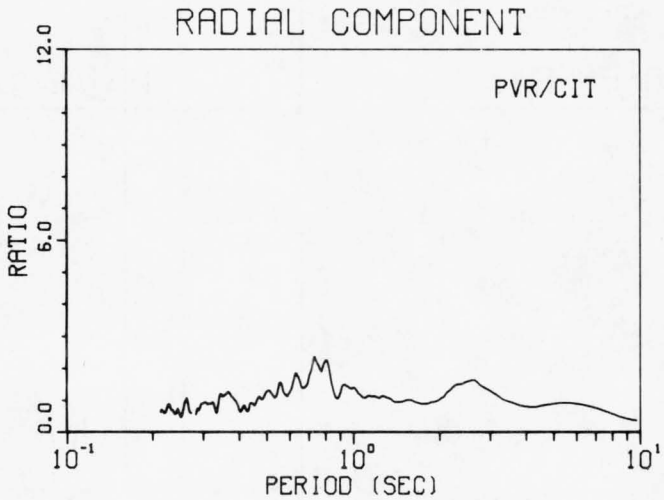

☆ U. S. GOVERNMENT PRINTING OFFICE 1980 - 778-838/241 Reg. 8